RIGID-PLASTIC FINITE ELEMENT ANALYSIS OF SOME METAL FORMING PROCESSES

by

Luis Augusto Pacheco Rodriguez
Ing. Mec., M.Sc. (Manc.)

March, 1980

A thesis submitted for the degree of Doctor of Philosophy of the University of London and for the Diploma of Membership of the Imperial College

Mechanical Engineering Department,
Imperial College,
London, S.W.7

"Two things are to be remembered: that a man whose opinions and theories are worth studying may be presumed to have had some intelligence, but that no man is likely to have arrived at complete and final truth on any subject whatever".

Bertrand Russell. "History of Western Philosophy"

"The mere fact that an author has a Ph.D. - or is even a distinguished professor - does not ensure that he is free from bias, folly, error, or even mild insanity".

John Ziman. "The Force of Knowledge".

To the memory of my Grandfather

SUMMARY

The metal-forming processes basically involve large amounts of plastic deformation; and, due to the complexities of plasticity, the exact analysis of a process is unfeasible in most of the cases.

In this work, finite element techniques, based on the rigid-plastic behaviour assumption, are used in an attempt to elucidate the mechanics of various metal forming processes.

The formulations - penalty function and velocity/pressure - are presented in detail and implemented in the form of computer programs written in FORTRAN IV.

Assessment of the formulations is carried out by analyzing a number of conventional extrusion processes.

The penalty function formulation is then employed to analyze the detailed mechanics of the hydrostatic extrusion of copper-covered aluminium rod. Results are compared with experimental evidence obtained using an existing rig.

The finite element techniques are then extended to deal with non-steady state problems and are employed to analyze simple upsetting and a simple open extrusion-forging process.

The thesis concludes with suggestions for extending the theoretical models to other metal forming problems.

ACKNOWLEDGEMENTS

I wish to express my gratitude to Professor J. M. Alexander for proposing the field of research and for having given me his advice and encouragement during the course of this work.

My thanks go to all my colleagues in the Mechanical Engineering Department; especially to Dr. Juan Damia, who was always willing to listen to my, sometimes, mistaken arguments.

Thanks are also due, in no small measure, to Mr. R. Baxter for his invaluable help with the experimental part of this work.

I am also indebted to Miss Elizabeth Monasterio, whose moral support in times of stress has always provided the uplift needed.

I would also like to express my thanks to my former teacher, Dr. V. G. Wong, who led me into the road of research and opened my eyes to new horizons.

My special thanks go to my parents for their love and patience.

Also many thanks to Mrs. Helen Bastin for careful typing of this thesis.

Finally, I am grateful to "La Universidad del Zulia", Venezuela for providing partial financial assistance.

CONTENTS

NOMENCLATURE

x, y, z	Cartesian coordinates
r, z, θ	Cylindrical coordinates
ξ, η	Natural coordinates
α	Penalty coefficient
α_D	Die semi-angle
δ_{ij}	Kronecker delta
E	Young's modulus
$\dot{\varepsilon}_{ij}$	Strain rate tensor
$\dot{\varepsilon}_x, \dot{\varepsilon}_y, \dot{\varepsilon}_z$	Cartesian normal strain rate components
$\dot{\varepsilon}_r, \dot{\varepsilon}_z, \dot{\varepsilon}_\theta$	Cylindrical normal strain rate components
$\dot{\varepsilon}_v$	Volumetric strain rate
$\dot{\bar{\varepsilon}}$	Equivalent strain rate
$\dot{e}_{ij}$	Deviatoric strain rate tensor
f	Core volumetric fraction
$\Phi, \bar{\Phi}$	Functionals
G	Shear modulus
$\dot{\gamma}_{xy}, \dot{\gamma}_{yz}, \dot{\gamma}_{zx}$	Cartesian engineering shear strain rates components
$\dot{\gamma}_{rz}$	Cylindrical engineering shear strain rate component
H	Height
I_1, I_2, I_3	Deviatoric strain rate tensor invariants
J_1, J_2, J_3	Strain rate tensor invariants
J'_1, J'_2, J'_3	Deviatoric stress tensor invariants
k	Shear yield stress
λ	Lagrange multiplier
m	Friction factor
n	Strain hardening exponent
μ	Viscosity
R, R_{ext}	Extrusion ratio

R_c	Core radius
R_t	Tube radius
σ_{ij}	Stress tensor
σ_x, σ_y, σ_z	Cartesian normal stress components
σ_r, σ_z, σ_θ	Cylindrical normal stress components
σ_m	Hydrostatic or mean stress
σ'_{ij}	Deviatoric stress tensor
$\bar{\sigma}$	Equivalent stress
τ_{xy}, τ_{yz}, τ_{zx}	Cartesian shear stress components
τ_{rz}	Cylindrical shear stress component
u, v	Velocity components in the x and y (or r and z) directions respectively
ν	Poisson's ratio
Y, Y_o	Uniaxial yield stress

Matrices and Vectors

$\underline{B}$	Displacement-strain matrix
$\underline{D}$	Stress-strain matrix
$\underset{\sim}{\dot{\varepsilon}}$	Strain rate vector
$\underset{\sim}{f}$	Loads vector
$[J]$	Jacobian matrix
$\underline{K}$	Stiffness matrix
$\underline{L}$	Differential operator matrix
$\underline{N}$	Shape functions matrix
$\underset{\sim}{P}$	Hydrostatic stress vector
$\underset{\sim}{\sigma'}$	Deviatoric stresses vector
$\underset{\sim}{u}$	Velocities vector

Superscripts

α	Penalty
u	Velocity
p	Pressure
- 1	Inverse
T	Transpose

CHAPTER 1

INTRODUCTION

1.1 General

The working of metals is at least as old as recorded history; the fabrication of objects out of iron goes back more than 3,000 years, and was extremely important for human society, in peace as well as in war. Forging and hammering were known and well-developed by 1500 A.D. Extrusion and drawing of sheet and tube, because of their dependence upon more energy requirements than the former processes, were the result of nineteenth century innovation.

Development of the different processes was initially dependent on accumulated experience and bold experiment and, therefore, fell within the realm of craft rather than science.

The origins of the mathematical theory of plasticity are, within this time scale, relatively recent and can be traced back to Tresca, 1864, who first postulated a yield condition for the continuum problem. Theoretical developments have since then contributed to the transition from craft to technology.

1.2 Analysis of Metal Forming Processes

The analysis of metal forming has been traditionally concerned with the energy requirements of any specific process. Indeed, the majority of the analytical tools developed to study such processes are mainly directed towards calculation of the forces required to carry out a specific deformation.

However, in many practical situations the mode of deformation, together with the associated strain rates and temperature distribution, are of more interest than the actual forces required. Without such stress and deformation analysis, it would be necessary to try to make deductions from properties of the process as a whole. Because these comprise averages over a spacial stress and strain distribution, which can be far from uniform, it is unlikely that criteria embodying any

precision can be deduced in this way.

The calculation of stresses and strains occurring in a component during any forming process is confronted by major mathematical difficulties. In handling problems of actual situations a straight solution of the theoretical plasticity equations can only be obtained by greatly simplifying the presentation of the problem. Solutions obtained by such simplifying methods are the so-called "elementary theory", the slip-line theory and the main-line theory. Fig. 1.1 gives a survey of the possible approximation methods used in tackling theoretical problems of plasticity in metal forming.

The slip-line field theory has provided a powerful technique for the analysis of metal working problems in terms of deformation and local stress distribution, as well as overall forces. The main drawback of this theory is that detailed material properties cannot be included directly in the theoretical solutions.

Most of the other analytical tools require, in general, a closed form solution. Hence, there are a number of approximations associated with these methods which render them inappropriate where accurate analysis is required. They are also less flexible in terms of introducing friction and the work-hardening properties of the material.

With the arrival of computers as an everyday tool, it is becoming no longer necessary to deal with closed solutions only. The present trend, in common with most other fields of engineering, is the application of numerical techniques to the analysis of metal forming problems, trying to avoid as many simplifications as possible. These methods appear to be highly complex and unapproachable, mainly due to the "black-box" attitude with which engineers tend to regard computer based techniques. However, behind the relatively complex computer techniques necessary for the efficient implementation of the

methods, the theoretical principles are conceptually logical and relatively easy to understand.

It is important to point out that numerical methods in no way outdate the more traditional techniques. On the contrary, it is important that the analyst bears in mind the whole spectrum of methods available. In that way, the danger of wasting valuable computer time in seeking a sophisticated solution when a simpler one is more than adequate, can be more easily avoided.

Quantities such as forming strength and forming efficiency can be predicted sufficiently well by the methods of upper and lower bounds (limit analysis). On the other hand, strains and stresses, as a rule, can only be calculated by means of numerical solutions.

1.3 Scope of the Work

The initial aim of this work was to study the extrusion of axisymmetrical bi-metallic rods, with special emphasis on the strain and stress fields developed within the deforming region.

It soon became clear that the use of numerical methods was the best suited tool for obtaining the required information. Among the existing methods the finite element method (FEM) figures prominently as a most efficient engineering tool of analysis. For elastic-plastic problems with relatively large plastic deformation, the FEM has proved useful*. However, despite its numerous advantages, the elasto-plastic FEM has severe drawbacks in terms of computation for the analyses of metal forming processes.

In an attempt to overcome these drawbacks, while keeping the

---

* A detailed review of the subject is given in Chapter 4.

advantages of the FEM, new formulations have been derived. These formulations take advantage of the assumption of the rigid-plastic behaviour of materials, since plastic strains usually outweigh elastic strains in most of the metal forming processes. This assumption allows larger increments of deformation, reduces computational time and still permits reasonable accuracies of solutions required for the analysis.

These rigid-plastic formulations were the ones chosen for this work, in specifically the "matrix method" of Lee and Kobayashi[1.1] and the "penalty function method" developed by Zienkiewicz and co-workers[1.2].

The decision to use FEM changed the character of the work, since it became necessary to develop the pertinent formulation and the corresponding computer programs.

These programs have to be tested against known solutions. Therefore, a number of extrusion problems have been tackled in order to assess the formulations and the techniques developed to include the effects involving the work-hardening characteristics of the material and the boundary conditions.

Once the theoretical analysis had been properly tested it was applied to the problem of extrusion of bi-metallic rods with the aim of obtaining a numerical description of the stress and strain fields in the deforming region. Also, experimental work was carried out to provide supporting evidence to test the theoretical analysis.

It is hoped that the information provided by the numerical model of the process will eventually lead to a better understanding of the mechanisms of the joint deformation of dissimilar metals.

An extension of the method to non-steady problems seems natural. This can be done by modifying the programs accordingly. Again, the numerical model needs to be tested, therefore, simple upsetting problems have been tackled and the numerical solutions

compared with available solutions.

The method of analysis has then been applied to simple open extrusion-forging with the aim of providing information regarding the deformation characteristics of the process under various conditions.

As with any FEM technique, the programs and formulation developed here are not restricted to the problems considered and it is hoped that they can be used to analyse other metal forming processes, such as rolling, asymmetric extrusion, etc.

REFERENCES

1.1 LEE, C. H. and KOBAYASHI, S.
J. of Engng. for Ind., Trans. ASME, Vol. 95, p. 283, (1973).

1.2 ZIENKIEWICZ, O. C.
"The Finite Element Method".
3rd Edition, McGraw-Hill, (1977).

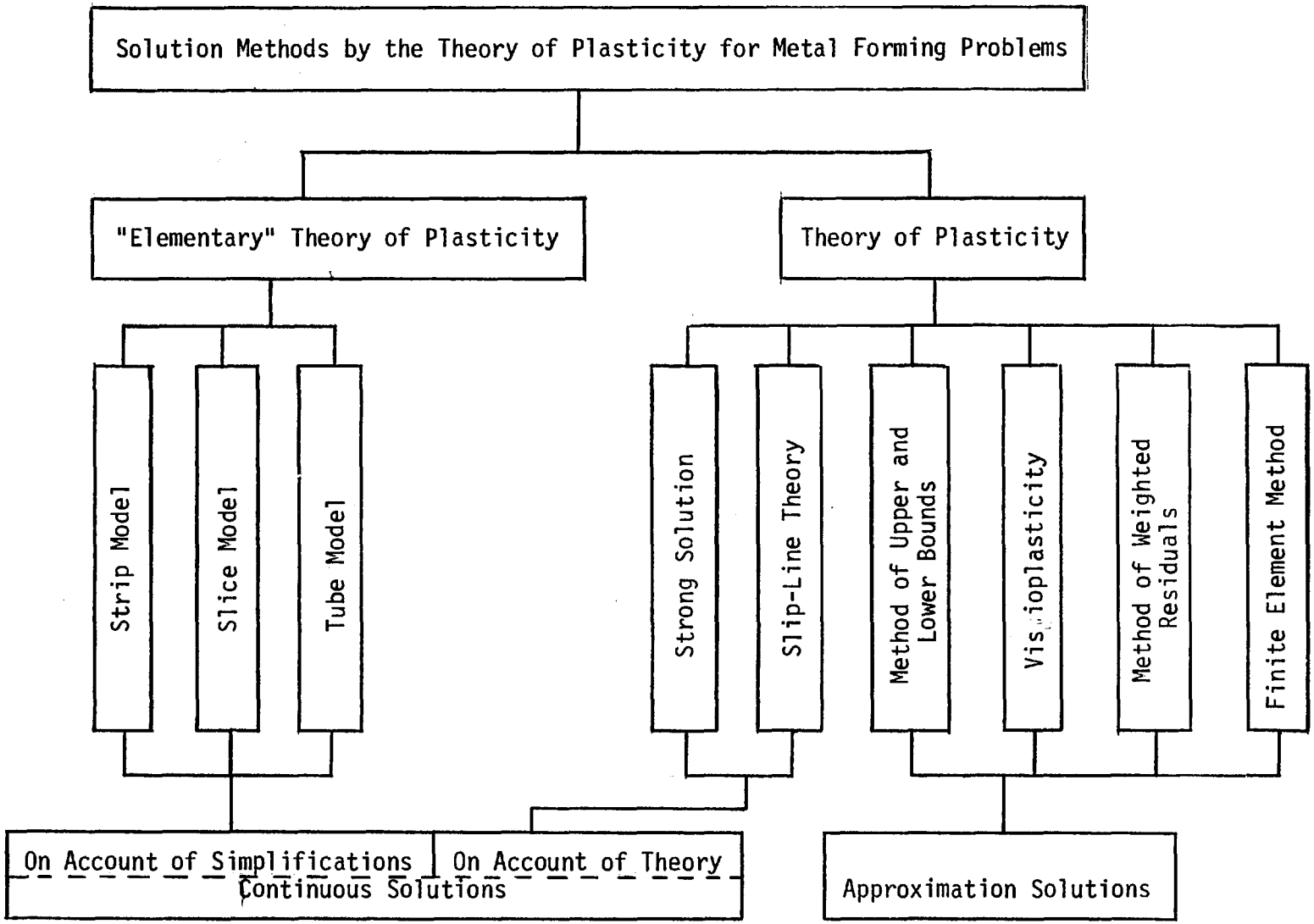

Fig. 1.1 Theoretical possibilities for plasticity solutions in metal forming

CHAPTER 2

BASIC CONCEPTS

2.1 Introduction

This chapter is a brief review of the various concepts and techniques to be used throughout this work. The various properties of stress and strain/strain rate, stress and strain/strain rate constitutive relations and yield conditions as applied to rigid-plastic bodies, are reviewed. Also, variational techniques and the finite element method are summarized. The latter is more fully discussed in a subsequent chapter in the context of the specific problems studied.

2.2 General Considerations on Solid Mechanics

The theories of elasticity and plasticity deal with methods of calculating stress and strain in most engineering solids subjected to deformation, and not, as a literal interpretation suggests, with the physical explanation of the process.

Both theories, as applied to metals and alloys, are based on experimental studies of the relation between strain and stress in a polycrystalline aggregate under simple loading condition. The theory of plasticity, in particular, takes as its starting point certain experimental observations of the macroscopic behaviour of a plastic solid in uniform states of combined stress. The theory sets out to attain two main objectives: first, to construct explicit relations between stress and strain agreeing with the experimental evidence and as general as need be; and second, to develop mathematical techniques for calculating the non-uniform distribution of stress and strain present in bodies permanently distorted.

The theory of plasticity is especially concerned with technological forming process such as extrusion, drawing and rolling, to name but a few. The purpose of the analysis is often to determine external loads, power consumption and the non-uniform strain and hardening due to cold working. One challenging problem of great

interest in metal working processes which is very difficult to solve is that of determining the distribution of residual stress remaining in a body which has suffered plastic deformation. One of the difficulties in applying the theory to practical problems is that technical materials under loads in the plastic range are dependent on their structure. The complete analysis of anisotropic, inhomogeneous solids is too complex to be solved "exactly" by present methods. Even when a material is initially isotropic, the moment it has undergone plastic deformation it becomes anisotropic. So, it must always be borne in mind that, although one can often go a long way assuming idealized solids, the metal structure will intrude sooner or later and lead to behaviour different from that predicted.

It is needless to say that, even in those cases where such difficulties can be overcome and solutions obtained, such solutions do not necessarily represent the true stresses and strains.

The general relation between stress and strain must contain:-

1. Elastic stress-strain relation (generally Hooke's law).

2. Yield criterion, which indicates when yielding starts under a complex state of stress.

3. The plastic stress-strain or incremental stress-strain relations.

This last requirement separates the mathematical theories of plasticity into two types: deformation theories relate the stresses to the strain while flow theories relate the stress to strain rates. Deformation theories utilize an averaging process over the entire deformation history and relate the total plastic strain to the

final strain. This type of theory is only valid when the material is subjected to proportional loading, but is generally considered unsuitable to describe the complete plastic behaviour of a metal[2.1].

Flow theories consider a succession of infinitesimal increments of distortion in which the instantaneous stress is related to the increment of strain rate. Because of this incremental nature of the theory, it is better able to describe large plastic deformations.

2.3 Stress

The state of stress at any point (in cartesian coordinates) can be defined by 9 components of the stress tensor (Cauchy's stress tensor)[2.2]:-

$$\sigma_{ij} = \begin{bmatrix} \sigma_{xx} & \tau_{xy} & \tau_{xz} \\ \tau_{yx} & \sigma_{yy} & \tau_{yz} \\ \tau_{zx} & \tau_{zy} & \sigma_{zz} \end{bmatrix} \qquad (2.1)$$

with the condition $\sigma_{ij} = \sigma_{ji}$ and where σ_{ii} denotes normal stresses and σ_{ik} shear stresses.

For an isotropic plastic material which is defined by the property that the relation between stress and deformation would not change if the body is rotated under a system of stress fixed in space, a "hydrostatic" state of stress:-

$$\sigma_{ij} = \sigma_m \, \delta_{ij} \qquad (2.2)$$

where:-

$$\delta_{ij} = \begin{cases} 1 & \text{if } i = j \\ 0 & \text{if } i \neq j \end{cases} \tag{2.3}$$

denotes the Kronecker delta, would produce a volume dilation only[2.3]. Therefore, the stress tensor may be split off according to:-

$$\sigma'_{ij} = \sigma_{ij} - \sigma_m \delta_{ij} \tag{2.4}$$

where:-

$$\sigma_m = \frac{1}{3} \sum_i \sigma_{ii}$$

Moreover, because $\sigma'_m = 0$, the remaining "stress deviator" would leave the volume unchanged and only deform the shape of the body.

Any tensor has invariants, that is, scalar quantities formed from its components and independent of the selection of axes.

The principal invariants of the σ'_{ij} tensor are given by the expressions:-

$$\left.\begin{aligned} J'_1 &= \sigma'_{ii} = 0 \\ J'_2 &= \frac{1}{2} \sigma'_{ij} \sigma'_{ij} \\ J'_3 &= \text{DET } (\sigma'_{ij}) \end{aligned}\right\} \tag{2.5}$$

At each point in the body the stresses have to satisfy the equilibrium equations:-

$$\left.\begin{aligned} &\frac{\partial \sigma_{ij}}{\partial x_i} + b_j = 0 \qquad \text{at } V \\ &\text{and:-} \\ &\sigma_{ij}\, n_i = T_j \qquad \text{at } S \end{aligned}\right\} \tag{2.6}$$

where S denotes the surface, V the interior (say volume) of the body in question, n_i is a unit vector along the outer normal to the surface, b_j is the body force acting in the direction j and T_j is a specified surface traction.

For the first Equation (2.6) to hold, it has to be assumed that the state of stress depends continuously and in a continuously differentiable manner on the space coordinates x_i (2.2).

2.4 Strain-Rate, Strain

In a Cartesian frame of references the normal strain rates are defined as:-

$$\dot{\varepsilon}_x = \frac{\partial u_x}{\partial x} \quad , \quad \dot{\varepsilon}_y = \frac{\partial u_y}{\partial y} \quad , \quad \dot{\varepsilon}_z = \frac{\partial u_z}{\partial z} \tag{2.7}$$

and the (engineering) strain rates are:-

$$\left.\begin{aligned} \dot{\gamma}_{xy} &= \frac{\partial u_x}{\partial y} + \frac{\partial u_y}{\partial x} \\ \dot{\gamma}_{yz} &= \frac{\partial u_y}{\partial z} + \frac{\partial u_z}{\partial y} \\ \dot{\gamma}_{zx} &= \frac{\partial u_z}{\partial x} + \frac{\partial u_x}{\partial z} \end{aligned}\right\} \tag{2.8}$$

The strain rate tensor is then defined as:-

$$\dot{\varepsilon}_{ij} = \frac{1}{2}\left(\frac{\partial u_i}{\partial x_j} + \frac{\partial u_j}{\partial x_i}\right) \tag{2.9}$$

where $u_i = \dot{x}_i\ (t)$ are the point velocities of the field of moving particle. Therefore, u_i is assumed to be continuous and continuously differentiable with respect to x_i except for some isolated interfaces of discontinuity across which the velocity vector may experience a jump. It will be noted from Equations (2.8) and (2.9) that the engineering shear strain rate is double the tensor shear strain rate.

Strain rates vanish if and only if the volume element moves as a rigid body and, as the stresses, they form a symmetrical tensor.

The three principal invariants of the strain rate tensor $\dot{\varepsilon}_{ij}$ are:-

$$\left.\begin{aligned} J_1 &= \dot{\varepsilon}_{ii} \\ J_2 &= \frac{1}{2}\,\dot{\varepsilon}_{ii}\,\dot{\varepsilon}_{jj} - \frac{1}{2}\,\dot{\varepsilon}_{ij}\,\dot{\varepsilon}_{ij} \\ J_3 &= \det\,(\dot{\varepsilon}_{ij}) \end{aligned}\right\} \tag{2.10}$$

The strain rate tensor can also be expressed in terms of a deviatoric component $\dot{e}_{ij}$ and a hydrostatic one $\dot{\varepsilon}_m\,\delta_{ij}$ as:-

$$\dot{\varepsilon}_{ij} = \dot{e}_{ij} + \dot{\varepsilon}_m\,\delta_{ij} \tag{2.11}$$

where:-

$$\dot{\varepsilon}_m = \frac{1}{3}\,\varepsilon_{ii} \tag{2.12}$$

Note that in metal plasticity, one commonly assumes "incompressibility" of the material which means:-

$$\dot{\varepsilon}_{ij} = \dot{e}_{ij} \tag{2.13}$$

When the strains are small, as is the case in elasticity, a strain tensor ε_{ij} of the same form as Equation (2.9) can be introduced. However, if the deformation becomes finite, this would cause the well-known trouble concerning non-uniqueness and a different formulation is then necessary[2.4].

A basic assumption of the infinitesimal elastic-plastic theory is that strain rate components can be expressed in terms of their elastic and plastic components as:-

$$\dot{\varepsilon}_{ij} = \dot{\varepsilon}^e_{ij} + \dot{\varepsilon}^p_{ij} \tag{2.14}$$

For the cases where the plastic component is large compared with the elastic component, it is usually assumed that elastic behaviour is non-existent, thus simplifying the formulation to:-

$$\dot{\varepsilon}_{ij} = \dot{\varepsilon}^p_{ij} = \dot{e}_{ij} \tag{2.15}$$

From Equation (2.13) and using Equation (2.15) it is possible then to define a tensor $\dot{e}_{ij}$ with its three invariants:-

$$\left.\begin{aligned} I_1 &= \dot{e}_{ii} = 0 \\ I_2 &= \frac{1}{2}\dot{e}_{ij}\,\dot{e}_{ij} \\ I_3 &= \det(\dot{e}_{ij}) \end{aligned}\right\} \qquad (2.16)$$

2.5 Mathematical Theory of Plasticity

2.5.1 Yield Function

In the mathematical theory of plasticity a basic assumption is made in that the material is homogeneous with an isotropic rule of hardening. It is assumed that there exists a scalar function, called a yield function or loading function, and denoted by $f\ (\sigma_{ij}, e^p_{ij}, k)$, which depends on the state of stress and strain and the history of loading, and which characterizes the yielding of the material as follows:-

$f < 0$ no change in plastic deformation (2.17)

$f = 0$ change in plastic deformation (2.18)

No meaning is associated with $f > 0$. The parameter k is called a work-hardening parameter, and it is assumed to depend on the plastic deformation history of the material.

Assuming an isotropic behaviour of the material before and during deformation, the yield condition f depends only on the invariants of stress, strain and strain history[2.2]. If the yield function f is an isotropic function of stress alone, then the theory of plasticity is called an "isotropic stress" theory. In such theories:-

$$f(\sigma_{ij}) = F(J_1, J_2, J_3) - c \qquad (2.19)$$

Furthermore, if the hydrostatic stress is assumed not to influence yielding, Equation (2.19) can be expressed independent of J_1 and in terms of the invariants of the deviatoric stress tensor:-

$$f(\sigma_{ij}) = F(J_2', J_3') - c \qquad (2.20)$$

where F does not depend on the strain history, which only enters through the parameter c.

The two better known yield criteria, Von Mises's[2.5] and Tresca's[2.6] fall within this category.

(i) Von Mises Yield Criterion

This is the simplest form of Equation (2.20) and is given by:-

$$f = J_2' - k^2 = 0$$

or:-

$$f = \frac{1}{2}\sigma_{ij}'\sigma_{ij}' - k^2 = 0 \qquad (2.21)$$

where k is a scalar function depending on plastic strain history. Despite the fact that physical interpretations have been given for this criterion, based on the shear strain energy, they should be merely regarded as formal [2.7].

(ii) Tresca Yield Criterion

In terms of principal stresses σ_1, σ_2, σ_3, where $\sigma_1 > \sigma_2 >$

σ_3, the Tresca yield criterion is expressed by:-

$$f = \sigma_1 - \sigma_3 - 2k = 0 \tag{2.22}$$

This criterion differs from the previous one in that it takes no account of σ_2 and the sign of the stresses has to be taken into consideration.

Experiments give, in general, little support to the hypothesis of isotropic hardening, necessary for the validity of this criterion[2.8,2.9]. The permanent preference for this hypothesis is due to its mathematical simplicity and to the fact that, provided unloading is not performed during the process of deformation, the results are in very good agreement with experiments[2.10].

2.5.2 Equivalent Strain and Equivalent Stress

It is not always possible to determine experimentally the stress-strain relations under conditions similar to the analysis. Use then has to be made of an "effective" stress-strain relationship, and it should be remembered that such relationships cannot, in general, take account of anisotropy or the Bauschinger effect.

The equivalent stress $\bar{\sigma}$ is defined by the expression[2.1]:-

$$\bar{\sigma} = \sqrt{3J_2'} = \sqrt{\frac{3}{2}\,\sigma'_{ij}\,\sigma'_{ij}} \tag{2.23}$$

The equivalent increment of strain $d\bar{\varepsilon}$ is defined, using the expression of plastic work, as:-

$$d\bar{\varepsilon} = \sqrt{\frac{2}{3}\,d\varepsilon^p_{ij}\,d\varepsilon^p_{ij}} \tag{2.24}$$

Drucker[2.11] has proved that the expression (2.24) is reasonably correct for any yield function of the form $f(J_2', J_3') = 0$.

2.6 Stress-Strain, Stress-Strain Rate Relation

2.6.1 Elastic Continuum

For a linear isotropic elastic solid, the stress-strain relations are written as:-

$$\left.\begin{aligned} \sigma_x' &= 2G\, e_x \\ \sigma_y' &= 2G\, e_y \\ \sigma_z' &= 2G\, e_z \\ \tau_{xy} &= G\, \gamma_{xy} \\ \tau_{zx} &= G\, \gamma_{zx} \\ \tau_{yz} &= G\, \gamma_{yz} \end{aligned}\right\} \qquad (2.25)$$

and:-

$$(\sigma_x + \sigma_y + \sigma_z) = 3K\,(\varepsilon_x + \varepsilon_y + \varepsilon_z) \qquad (2.26)$$

where K is related to the Young's modulus (E) and the Poisson's ratio (ν) by:-

$$E = 2G\,(1 + \nu) = 3K\,(1 - 2\nu) \qquad (2.27)$$

and G is the shear modulus.

For incompressible viscous fluid, similar relations between stress and strain rate can be written, using μ (coefficient of

viscosity) instead of G. Viscosity μ is a constant for Newtonian fluids, but for a non-Newtonian fluid is a function of position, velocity gradient and temperature.

2.6.2 Plastic Stress-Strain Relationships

For a material that behaves according to Drucker's postulate[2.11 - 2.13], the general expression for the plastic stress-strain relationship is:-

$$d\varepsilon^p_{ij} = Q \frac{\partial f}{\partial \sigma_{ij}} \frac{\partial f}{\partial \sigma_{RR}} d\sigma_k \qquad (2.28)$$

where Q is a scalar function depending on stresses, strains and loading history.

For a material that hardens isotropically, Equation (2.28) can be written as:-

$$d\varepsilon^p_{ij} = Q \frac{\partial f}{\partial \sigma_{ij}} df$$

or alternatively:-

$$d\varepsilon^p_{ij} = \frac{\partial f}{\partial \sigma_{ij}} \lambda \qquad (2.29)$$

where $\lambda = Q \cdot df$.

If Equation (2.21) is used as the yield function, Equation (2.29) becomes:-

$$d\varepsilon^p_{ij} = \sigma'_{ij} d\lambda \qquad (2.30)$$

or in terms of strain rates:-

$$\dot{\varepsilon}^p_{ij} = \Delta \sigma'_{ij} \tag{2.31}$$

where:-

$$\Delta = \frac{d\lambda}{dt}$$

Equations (2.30) and (2.31) are known as the Levy-Mises equations. The value of Δ can be evaluated by substituting Equation (2.31) in the Von Mises' yield criterion (2.21).

The following expression is then obtained:-

$$\frac{1}{2\Delta^2} \dot{\varepsilon}^p_{ij} \dot{\varepsilon}^p_{ij} = k^2 \tag{2.32}$$

or alternatively as:-

$$I_2 = k^2 \Delta^2 \tag{2.33}$$

where I_2 is the second principal invariant of the plastic strain rate tensor, Equations (2.16).

Finally:-

$$\Delta = \sqrt{I_2} / k$$

and replacing this value in Equation (2.31) we obtain:-

$$\sigma'_{ij} = \frac{k}{\sqrt{I_2}} \dot{\varepsilon}^p_{ij} = \frac{k}{\left(\frac{1}{2} \dot{\varepsilon}^p_{ij} \dot{\varepsilon}^p_{ij}\right)^{1/2}} \dot{\varepsilon}^p_{ij} \qquad (2.34)$$

If the material is assumed rigid-plastic, $\dot{\varepsilon}^p_{ij} = \dot{\varepsilon}_{ij} = \dot{e}_{ij}$ and Equations (2.30) and (2.31) are known as the Levy-Mises equations and Equation (2.34) is its associated "flow rule".

2.6.3 Viscoplastic Behaviour

The relations hitherto discussed are considered within the frame work of classical time-independent plasticity theory. Some attempts to describe the behaviour of materials including time effects assume that the main mechanical properties of the material can be described with a viscoplastic constitutive equation. Since the elastic part of the material is neglected the simplest possible model which may be thought of is a Bingham type constitutive equation of the form[2.14,2.15]:-

$$\dot{\varepsilon}_{ij} = \gamma < \Phi (F) > \frac{\partial Q}{\partial \sigma_{ij}} \qquad (2.35)$$

where F is the description of a yield surface and Q is the definition of a plastic potential.

The symbol < > means that:-

$$< \Phi (F) > \equiv 0 \text{ if } F < 0 \text{ and } < \Phi (F) > \equiv \Phi (F) \text{ if } F \geq 0 \qquad (2.35a)$$

The most common description of viscoplastic flow of metals follows the assumption that both the yield surface and plastic potential surface are identical, and that these depend only on the second stress invariant, i.e.:-

$$F = Q = \sqrt{3}\ \sqrt{J_2'} - Y \tag{2.36}$$

where $J_2' = \frac{1}{2}\ \sigma_{ij}'\ \sigma_{ij}'$ and Y is the uniaxial yield stress. If the plastic strain rate second invariant is defined as:-

$$I_2 = \sqrt{\frac{1}{2}\ \dot{\varepsilon}_{ij}^{p}\ \dot{\varepsilon}_{ij}^{p}} \tag{2.37}$$

the general constitutive equation can be written as:-

$$\dot{\varepsilon}_{ij} = \gamma < \Phi\ (\sqrt{3}\ \sqrt{J_2'} - Y) > \frac{\sqrt{3}}{2\sqrt{J_2'}}\ \sigma_{ij}' \tag{2.38}$$

or alternatively:-

$$\dot{\varepsilon}_{ij} = \frac{1}{2\mu}\ \sigma_{ij}' \tag{2.39}$$

where the viscosity $1/2\mu$ is identified by:-

$$\frac{1}{2\mu} - \gamma < \Phi\ (\sqrt{3}\ \sqrt{J_2'} - Y) > \frac{\sqrt{3}}{2\sqrt{J_2'}} \tag{2.40}$$

and is a function of the stress level.

The similarity between Equation (2.39) and the relation between stress and strain for an isotropic elastic solid (Equations (2.25)) is evident. In order to write an equivalent expression in terms of strain rate, we note from Equations (2.36), (2.37) and (2.39) that:-

$$J_2' = 2\mu^2\ \dot{\varepsilon}_{ij}\ \dot{\varepsilon}_{ij} = 4\mu^2\ I_2^2 \tag{2.41}$$

Substituting in Equation (2.40) we obtain:-

$$\frac{1}{2\mu} = \gamma < \Phi \ (\sqrt{3}\ 2\mu\ I_2 - Y) > \frac{\sqrt{3}}{4\mu\ I_2} \tag{2.42}$$

Hence:-

$$I_2 = \gamma < \Phi \ (\sqrt{3}\ 2\mu\ I_2 - Y) > \frac{\sqrt{3}}{2\ I_2} \tag{2.42a}$$

from which μ can be found for any strain rate function.

For an exponential type law, Equation (2.38) takes the form:-

$$\dot{\varepsilon}_{ij} = \gamma < (\sqrt{3}\ \sqrt{J_2'} - Y)^n > \frac{\sqrt{3}}{2\sqrt{J_2'}} \tag{2.43}$$

and we can evaluate μ explicitly from Equation (2.42a) as:-

$$\mu = \frac{Y + \left[\frac{2\ I_2}{\gamma\ \sqrt{3}}\right]^{1/n}}{2\ .\ \sqrt{3}\ I_2} \tag{2.44}$$

Ideally plastic plastic material with a fixed yield point is simply obtained by taking $\gamma = \infty$ and gives:-

$$\mu = \frac{Y}{2\ \sqrt{3}\ I_2} \tag{2.45}$$

Substituting Equation (2.45) in Equation (2.39) we obtain the stress-strain rate relation as:-

$$\sigma'_{ij} = \frac{Y}{\sqrt{3}\, I_2} \dot{\varepsilon}_{ij} \qquad (2.46)$$

It is evident that this equation is the same as Equation (2.34), namely, the associated flow rule for a material obeying the Mises Yield criterion.

2.7 Variational Principles

The calculus of variations is a branch of mathematics, wherein the stationary property of a function of functions, namely, a functional is studied.

The calculus of variations has a wide field of application in mathematical physics. This is due to the fact that the problems encountered can be, in general, specified in two ways. In the first, differential equations governing the behaviour of an infinitesimal region are given. In the second, a variational, extremum, principle, valid over the whole region is postulated and the correct solution is one of minimizing a "functional".

Here, we will confine ourselves to state the variational principles directly related to this work. A more "in-depth" discussion of the subject can be found in[2.16,2.17].

We shall consider the variational principles for a body comprised of rigid-plastic material under the assumption that the entire body is plastic and in the absence of body forces.

The problem is defined as follows:-

(i) Equilibrium equations

$$\frac{\partial \sigma'_{ij}}{\partial x_j} = 0 \qquad (2.47)$$

(ii) Yield condition

$$\sigma'_{ij}\,\sigma'_{ij} = 2k^2 \tag{2.48}$$

(iii) Stress-strain rate relations

$$\sigma'_{ij} = \frac{k}{\frac{1}{2}\,(\dot{\varepsilon}_{k\ell}\,\dot{\varepsilon}_{k\ell})^{1/2}}\,\dot{\varepsilon}_{ij} \tag{2.49}$$

(iv) Strain rate-velocity relations

$$2\,\dot{\varepsilon}_{ij} = \frac{\partial u_i}{\partial x_j} + \frac{\partial u_j}{\partial x_i} \tag{2.50}$$

(v) Condition of incompressibility

$$\dot{\varepsilon}_{ii} = 0 \tag{2.51}$$

(vi) Boundary conditions

$$\left.\begin{aligned} \sigma'_{ij}\,n_j &= \bar{F}_i \qquad \text{on } S_1 \\ u_i &= \bar{u}_i \qquad \text{on } S_2 \end{aligned}\right\} \tag{2.52}$$

There results two variational principles[2.16]. The first one, called Markov's principle[2.18] may be stated as follows.

Among admissible solutions which satisfy the conditions of compatibility and incompressibility, as well as the geometric boundary conditions on S_2, the actual solution (except perhaps for a possible indeterminate uniform hydrostatic pressure) renders:-

$$\pi = \sqrt{2}\, k \int_V \sqrt{\dot{\varepsilon}_{ij}\, \dot{\varepsilon}_{ij}}\, dv - \int_{S_1} \bar{F}_i\, u_i\, ds \tag{2.53}$$

an absolute minimum.

The second principle may be stated as follows.

Among admissible solutions which satisfy the equations of equilibrium and the mechanical boundary conditions on S_1, the actual solution renders:-

$$\pi_c = - \int_{S_2} \sigma'_{ij}\, n_j\, \bar{u}_i\, ds \tag{2.54}$$

an absolute minimum.

This is equivalent to Hill's principle[2.1] of maximum plastic work, which states that among admissible solutions, the actual solution renders:-

$$\int_{S_2} \sigma'_{ij}\, n_j\, \bar{u}_i\, ds \tag{2.55}$$

an absolute minimum.

2.8 Finite Element Method

Although the label "finite element method" first appeared in 1960, when it was used by Clough[2.18] in a paper on plane elasticity problems, the ideas of finite element analysis date back much further. In fact, some authors can trace three different origins, depending on whether one is interested in the mathematics, the physics or the engineering applications of the method.

A complete history is outside the scope of this work, the interested reader will find that many of the excellent books available will fill this gap[2.20 - 2.22].

In a continuum problem of any size the field variable (whether it is pressure, temperature, displacement, or some other quantity) possesses infinitely many values because it is a function of each generic point in the body or the region of the solution. The discretization nature of the finite element reduces the problem to one of a finite number of unknowns by dividing the solution region into elements and by expressing the unknown field variable in terms of assumed approximating functions within each region.

These approximating functions are defined in terms of the values taken by the field variable in question at specified locations within the elements called nodes or nodal points. Nodes usually lie on the element boundaries and adjacent elements are considered to be connected only at these points.

The kinds of continuum problems that we wish to solve are usually formulated in general terms as follows. Consider some domain D bounded by the surface Σ. Let Φ be a scalar function defined in the interior of D such that the behaviour of Φ in D is given by:-

$$L(\Phi) - f = 0 \qquad (2.56)$$

where f is a known scalar function of the independent variables and L is a linear or non-linear differential operator.

The general problem is then to find the unknown function Φ that satisfies Equation (2.56) and some associated boundary conditions specified on Σ.

The finite element process, being one of approximation, will seek the solution in the approximate form:-

$$\Phi \simeq \tilde{\Phi} = \sum_{1}^{r} N_i \, a_i \tag{2.57}$$

where N_i are shape functions prescribed in terms of independent variables (such as the coordinates) and all or some of the parameters a_i are unknown. The shape functions are usually defined locally for elements or subdomains. Therefore, Equation (2.57) can be rewritten for an element, using matrix notation as:-

$$\Phi \simeq \hat{\Phi}^e = \Sigma \, N_i \, a_i^e = \begin{bmatrix} N_i, & N_j, & \ldots \end{bmatrix} \begin{Bmatrix} a_i \\ a_j \\ . \\ . \\ . \\ . \end{Bmatrix} = \underset{\sim}{N}^e \, \underset{\sim}{a}^e \tag{2.58}$$

where i, j, m, etc. are the nodes defining the element or subdomain in question.

If we assume that the field variable Φ is thus completely represented in the solution domain in terms of a collection of nodal values, the problem of finding an approximation to Φ would be solved once these discrete values were found.

Clearly, the nature of the solution and the degree of approximation used depend upon the size and number of elements used and the nature of the chosen interpolation function[2.21].

2.8.1 Element Equations

These are basically four different approaches in which one can formulate the properties of individual elements: direct approach, variational principle, weighted residuals and energy balance.

The Direct Approach

The origin of this approach is directly traceable to the

direct stiffness method of structural analysis. Although this approach is limited in its application to relatively simple problems, it is the easiest to understand when meeting the method for the first time.

Variational Approach

This approach relies on the calculus of variations and involves extremizing a functional. This extends the method to problems with a known function or variational statements. For problems in solid mechanics, the functional turns out to be the potential energy, the complementary potential energy or some derivative of these[2.16].

Weighted Residuals

This is an even more versatile approach and it has its basis in mathematics. It begins with the governing equation of the problem and proceeds without relying on a functional or variational statement. This enables the method to attack problems without a known functional.

Energy Balance

This approach relies on the balance of thermal and/or mechanical energy of a system. Like the weighted residuals it requires no variational statement and hence broadens considerably the range of possible applications of the method.

Regardless of the approach used to find the element properties, the solution of a continuum problem by the finite element method always follows an orderly step by step process. These steps will be succintly summarized now; they will be developed in detail in a following chapter.

(i) Idealization

The continuum is divided into an assemblage of discrete elements.

(ii) Evaluation of element characteristics

Nodes are assigned to each element and the interpolation functions chosen so that the element properties can be evaluated with one of the four approaches just mentioned.

(iii) Assembly and solution of the system of equations

The properties of the overall system modelled by the network of elements are found by assembling all the elemental properties. The matrix equations so found have the same form as the elemental equations. Before solving this system of equations, they must be modified to account for the boundary conditions of the problem.

2.8.2 Numerical Integration

Since closed form integrations are seldom possible, the use of numerical techniques for the integration of the expressions resulting from a finite element formulation becomes necessary. For example, in two dimensions:-

$$\int_{-1}^{1}\int_{-1}^{1} f(\xi, \eta)\, d\xi\, d\eta = \sum_{i=1}^{n}\sum_{u=1}^{n} H_i\, H_j\, f(a_j, b_i) \qquad (2.59)$$

where i, j are the sampling points, $f(a_j, b_i)$ is the value of the function at a particular sampling point (a_j, b_i), $H_i\, H_j$ are the weighting coefficients and n is the number of sampling points in one direction. In finite element analysis the Gauss-Legendre quadrature

rule is the most often used for such evaluations[2.20].

REFERENCES

2.1 HILL, R.
"Mathematical Theory of Plasticity".
Oxford University Press, (1950).

2.2 FUNG, Y. C.
"Foundations of Solid Mechanics".
Prentice Hall Inc., (1965).

2.3 LIPPMANN, H.
"Engineering Plasticity : Theory of Metal Forming Processes".
Vol. 1, Springer-Verlag, (1977).

2.4 JOHNSON, W. and MELLOR, P. B.
"Engineering Plasticity".
Van Nostrand Reinhold, (1973).

2.5 MISES, v. R.
"Göttinger Nachrichten".
Math-Phys., Kl, 852, (1913).

2.6 TRESCA, H.
C. r. Acad. Sci., Paris, 59, 754, (1864).

2.7 FORD, H. with ALEXANDER, J. M.
"Advanced Strength of Materials".
2nd Edition, Ellis Horwood, (1977).

2.8 PHILLIPS, A. and LAECHELE, L.
"Combined Stress Test in Plasticity".
ASME Ann. Meeting, Chicago, Paper 55-A-15, (1955).

2.9 IVEY, H. J.
J. Mech. Engng. Sci., 3, (1), pp. 15-31, (1961).

2.10 TAYLOR, G. I. and QUINNEY, H.
"The Plastic Deformation of Metals".
Phil. Trans., R. Soc. A., 230, 323, (1931).

2.11 DRUCKER, D. C.
"On Uniqueness in the Theory of Plasticity".
Quart. Appl. Math., 14, pp. 35-42, (1956).

2.12 DRUCKER, D. C.
"Some Implications of Work Hardening and Ideal Plasticity".
Quart. Appl. Math., 7, pp. 111-418, (1950).

2.13 DRUCKER, D. C.
Proc. 1st Nat. Congr. Appl. Mech., ASME, pp. 487-491, (1951).

2.14 PERZYNA, P.
"Fundamental Problems in Visco-Plasticity".
Recent Advances in Applied Mechanics, Academic Press,
Chapter 9, 243-377, (1966).

2.15 ZIENKIEWICZ, O. C. and CORMEAU, I. C.
"Viscoplasticity, Plasticity and Creep in Elastic Solids : A Unified Numerical Approach".
Int. J. Num. Meth. Engng., 8, pp. 821-845, (1974).

2.16 WASMIZU, K.
"Variational Methods in Elasticity and Plasticity".
2nd Edition, Pergamon Press, (1975).

2.17 LANCZOS, C.
"Variational Principles of Mechanics".
3rd Edition, University of Toronto Press, Canada, (1966).

2.18 MARKOV, A. A.
Prikl. Mat. i. Mekh., 11, p. 338, (1947).

2.19 CLOUGH, R. W.
"The Finite Element Method in Plane Stress Analysis".
Proc. of 2nd A.S.C.E. Conf. on Elect. Comp., Pittsburg, September, (1960).

2.20 ZIENKIEWICZ, O. C.
"The Finite Element Method".
3rd Edition, McGraw-Hill, (1977).

2.21 HUEBNER, K. H.
"The Finite Element Method for Engineers".
John Wyley, (1975).

2.22 ODEN, J. T.
"Finite Elements of Non-Linear Continua".
McGraw-Hill, (1972).

CHAPTER 3

EXPERIMENTAL WORK

3.1 Introduction

The general aim of the experimental work described here was to obtain a composite rod of copper and aluminium by means of an existing apparatus for conventional hydrostatic extrusion.

The main purpose was to design an adequate composite specimen, suitable for being hydrostatically extruded in the available equipment, and to gather relevant data for the validation or otherwise of the theoretical model developed to describe the stress fields and kinematical characteristics of the process.

3.2 Experimental Equipment

3.2.1 Hydraulic Press

Hydrostatic extrusion of the bi-metal specimens was carried out on a 250 ton Universal Avery testing machine.

The press has two main columns which have locating holes at regular distances along their length. The stationary cross-head can be located at any of these holes and secured to the main columns by two shear pins. The moving cross-head is directly attached to the hydraulic ram which exerts the operating force in its upward stroke. The downward stroke is not power assisted.

Loading and unloading is achieved by two valves located on the control console. There are four capacity ranges on the chart, and the capacity of the press is controlled by a wheel located below the chart (see Plate 3.1).

3.2.2 High Pressure Container

The high pressure container used consists of an outer container with a central bore, and tapered with a 2^{o} included angle. An inner container with a bore diameter of 44.45 cm (1.75"), 279.4 mm

(11") long and a matching exterior, fits into the outer container. A thin sheet of lead is interposed between the two containers so that friction can be reduced.

The material used for the container was EN30B steel having an ultimate tensile strength (UTS) of 1544 MN/m^2 and a tensile yield stress of 1389.6 MN/m^2, hardened and tempered to 52 HRC.

The bore of the container is sealed at the bottom by a plug which has provisions for taking the high pressure electrical leads out of it.

The container is attached to a tubular support which is secured at its base plate to the moving cross-head of the press. A 2 inch (50.8 mm) wide longitudinal slot is machined out of the tubular support; this ensures easy access to the bottom of the container base. Details of the apparatus are shown in Plate 3.1 and Fig. 3.1.

3.3 Extrusion Fluid

The main characteristics of an appropriate extrusion fluid must be: (i) a good lubricant and (ii) not to "freeze" at the high pressures used in the process[3.1]. It is worth noting that fluids reduce their volumes in a 30% - 50% range at the usual working pressures developed during hydrostatic extrusion.

Due to the important increase in viscosity of fluids at high pressures, not all lubricants are suitable for being used in this process. A comparative analysis of the ones more commonly used is presented by Lowe and Goold[3.2] and Pugh[3.1]. An illustrative plot relevant to fluid behaviour is presented in Fig. 3.2.

One of the more "efficient" fluids for transmitting the load acting on the plunger to the whole fluid volume and to convert it into hydrostatic pressure, at the highest working pressures, is Castor Oil. This was the fluid chosen for this work. However, the

addition of 10% methanol was necessary to avoid "freezing".

3.4 Billet Lubricant

All the specimens were coated with a colloidal graphite emulsion so as to enhance the lubrication at the billet/die interface. The choice of lubricant is important since it has been found that certain combinations of fluid and lubricant are incompatible, e.g. glycerine and glycol liquid with Evostik and methylethylketone[3.3].

3.5 Pressure Measurement

The pressure in the high pressure vessel is measured by the change in electrical resistance of a 100 Ω manganin coil made of 42 S.W.G. wire (0.1016 mm diameter); manganin is an alloy (roughly 84% Cu, 12% Mn, and 4% Ni) which was developed for the production of precision resistors.

The coil has to be wound non-inductively and must be thoroughly seasoned to remove the strains that are present. The coil is connected as an arm of a Wheatstone bridge and the pressure changes are measured as changes in the output of the bridge (see Fig. 3.3).

Any version of the Wheatstone bridge will give acceptable accuracy; however, most investigators use d.c. bridges since generally speaking they are more precise than a.c. bridges.

The output of the bridge is fed to an Ultraviolet Recorder S.E. Type 3006, with a galvanometer type A-100 (0.130 mv/cm sensitivity). For the calibration of the recorder a calibration resistor is used. This resistor, when connected to the bridge, produces a displacement from equilibrium equivalent to the effect of 772 MN/m^2 pressure acting on the manganin coil.

3.6 Dies

The dies used were made of K.E.A. 180 steel (12% Cr, 1.55% C)

hardened to 62 RC and with a yield strength of 2316 MN/m^2. Two sets of dies were used having included angles of 90^o and 40^o and with (outside) exit diameters of 0.5 in (11 mm), 0.312 in (69 mm) and 0.408 in (9 mm).

These dies did not have the facility for their removal after the extrusion was completed and some difficulty was experienced in this connection. Plate 3.3 shows the dies used.

3.7 Metals and Billet Characteristics

Commercially pure copper and aluminium were the materials chosen for the billets. Their chemical composition was as follows:-

Aluminium

99.61% Al : 0.27% Fe : 0.01% Cu : 0.11% Si : Trace of Mn

Copper

99.9% Cu : 0.001% Bi : 0.001 Pb

The stress-strain curves for both materials, shown in Fig. 3.4, were constructed with a mixture of data obtained in this work and that obtained by Whitfield[3.4].

3.7.1 Billet Preparation

Several techniques for billet preparation are mentioned in the literature. Ziemek[3.5] mentions a process employed at Kabbel Metale in which an aluminium rod, after being cleaned and brushed, is continuously wrapped with a copper strip similarly treated. This process employs no heat treatment. The interfacial bond is developed

through reduction.

The Texas Instruments method[3.6] uses two separate strips for wrap-up instead of one, with bonding taking place in two spots.

Dion and Hagarman[3.7] describe a method of roll bonding of two copper strips upon aluminium. In the method described by Yamaguchi et al[3.8] welding in a reducing atmosphere, followed by drawing is used to bring about the bonding. An explosive cladding operation is described by Dalrymple and Johnson[3.9]. Bedroud et al[3.10] also describe the use of implosive welding for the fabrication of mono- and bi-metallic arrays of rods.

Ahmed[3.11] uses a process in which a cleaned and brushed aluminium rod is introduced into a copper sleeve similarly treated. A compressive load is applied to the aluminium billet until both aluminium and copper experience plastic deformation. Upon release of the load both core and sleeve relax elastically and since the relaxation of the copper is higher, the sleeve grips firmly the aluminium rod. Thereafter both rod and sleeve are drawn. Matsuura and Takase[3.12] describe a method whereby a steel rod is enclosed with molten aluminium.

The method described by Alexander and Hartley[3.13] was chosen in this work because of its simplicity.

The composite billets were prepared by drilling out a copper billet to accept a cylindrical aluminium core. The cores were machined to achieve a light interference fit with the copper sleeve. All the billets were machined with a nose tapered 4^{o} less than the included angle of the dies; this, as reported by Pugh[3.1], contributes to the reduction of the height of the initial peak in the pressure characteristic and minimizes stick-slip.

The billets were 4.75 in (99.1 mm) long and 0.875 in (19.3 mm) in diameter circular cross-section, terminating in a butt threaded 1 in.

B.S.F. A shoulder of 0.125 in (2.8 mm) was machined in the junction between the tapered nose and the straight shank.

A hole was drilled on the nose of the billets and threaded 4 in; this was used for initial sealing arrangements.

Core diameters were 0.750 in (16.5 mm) and 0.500 in (11 mm), giving aluminium fractions of 0.7347 and 0.327. Fig. 3.5 shows a sketch of a typical specimen.

3.8 Experimental Procedure

Prior to assembly both the cores and sheaths are thoroughly degreased and heat treated. Aluminium cores were annealed for one hour in air at 360^{0} C , and the copper sheaths were annealed for one hour in 1/2 atm of oxygen free nitrogen at 600^{0} C. After the annealing process the sheaths and cores were once again degreased using Methyltetrachlorene and then assembled.

The threaded butt of the sheath is wrapped with P.T.F.E. tape before being threaded into the damping block. This prevented the pressurizing fluid reaching the core sheath interface. The damping block was made of mild steel, 1.75 in (38.5 mm) diameter and 1.25 in (27.5 mm) long. This block preserved axial alignment of the billet and reduced the magnitude of pressure fluctuations, due to stick-slip, when they occurred.

All billets were then prelubricated with a thin coating of D.A.G. (suspension of colloidal graphite in water).

The specimen nose is then lapped against the die and a screw threaded into the nose allows the application of a small load in order to create an initial seal. This assembly is put (see Plate 3.4) into the container which has been previously filled with the pressurizing fluid. The container is then raised up to the point where contact is made with a plunger. This operation, together with the small

pulling load applied through the nose, creates an initial sealing. Once this initial sealing is obtained, the small pulling load is removed.

Pressure in the container is then increased by raising the container further so as to allow the die to travel inside it and the extrudate to emerge upwards through the hollow core of the plunger. The high pressure so induced is recorded in the U.V. recorder.

Extrusion was terminated when a sudden increase in the chamber pressure indicated that the butt had reached the die.

The experimental results together with their theoretical counterparts are presented in another chapter.

REFERENCES

3.1 PUGH, H. Ll. D.
"The Mechanical Behaviour of Materials Under Pressure".
Elsevier, (1970).

3.2 LOWE, B. W. H. and GOOLD, D.
High Pressure Engineering Conf., Proc. Inst. Mech. Eng.
London, 182 (3c), 197, (1968).

3.3 PUGH, H. Ll. D.
"Recent Developments in Cold Forming".
Bulleid Memorial Lectures, University of Nottingham, England, (1966).

3.4 WHITFIELD, E.
"Stress/Strain Curves for Selected Steels and Non-Ferrous Metals Under Large Compressive Strains".
N.E.L. Report No. 325, (1967).

3.5 ZIEMEK, G.
Wire Jnl., March, pp. 47-52, (1973).

3.6 POLLEYS, W. V.
Wire and Wire Products, May, p. 116, (1971).

3.7 DION, P. A. and HAGARMAN, P. O.
U.S. Patent No. 3,714,701, February 6, (1923).

3.8 YAMAGUCHI, T., TAKAYAMA, T. and HIDERITA, M.
U.S. Patent No. 3,854,194, December 17, (1974).

3.9 DALRYMPLE, D. G. and JOHNSON, W.
Int. Jnl. Mach. Tool Des. Res., 7, pp. 257-267, (1968).

3.10 BEDROUD, Y., EL-SOBKY, H. and BLAZINSKY, T. Z.
"Implosive Welding of Mono- and Bi-Metallic Arrays of Rods".
Metals Technology, 3, p. 21, (1976).

3.11 AHMED, N.
Jnl. of Mechanical Work Tech., 2, pp. 19-32, (1978).

3.12 MATSUURA, Y. and TAKASE, K.
Report of the Castings Research Laboratory, Waseda University, No. 27, (1976).

3.13 ALEXANDER, J. M. and HARTLEY, C. S.
"On the Hydrostatic Extrusion of Copper Covered Aluminium Rods".
Int. Conf. on Hydrostatic Extrusion, University of Stirling, Scotland, (1973).

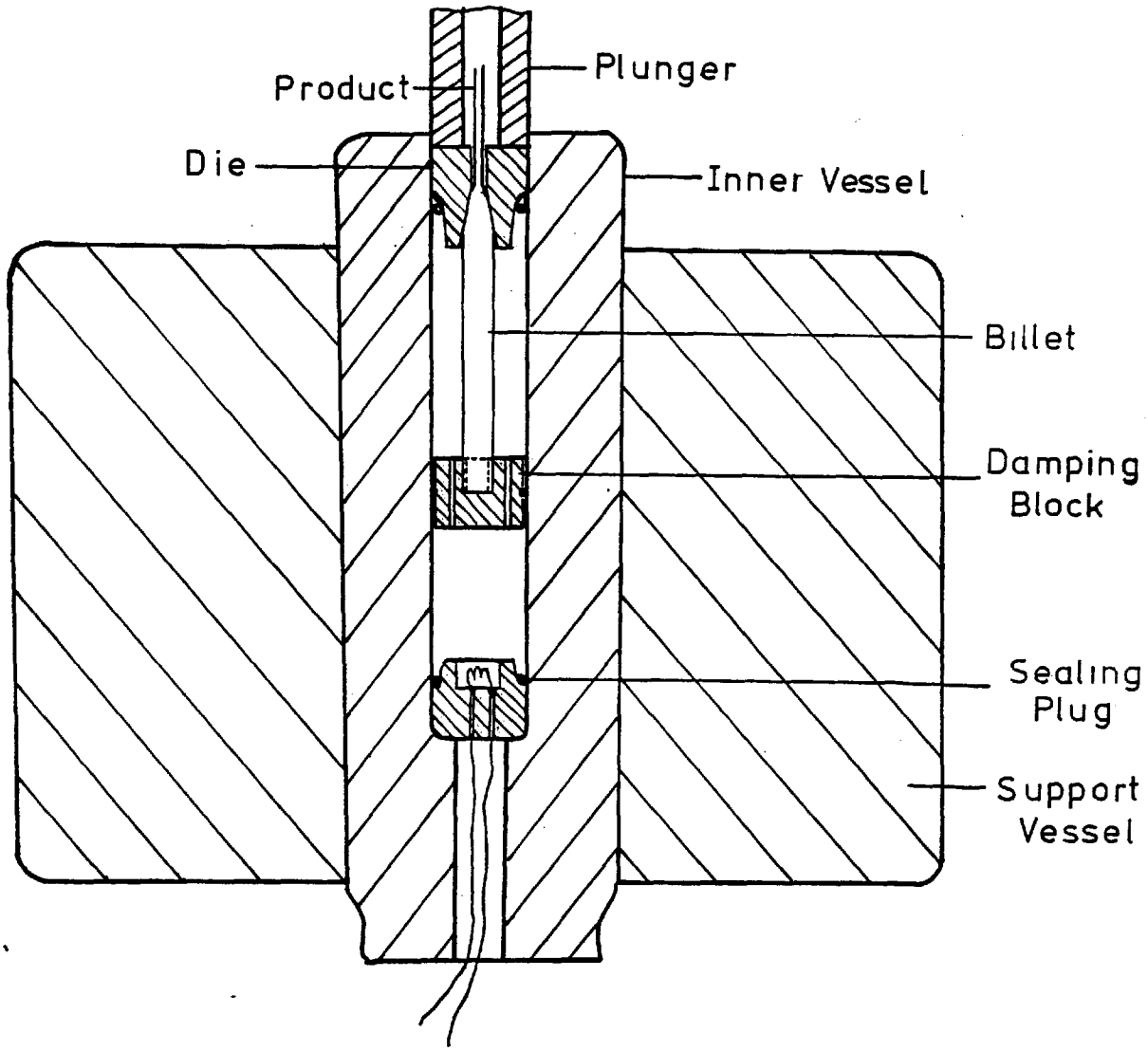

Figure 3.1: Schematic description of the extrusion container

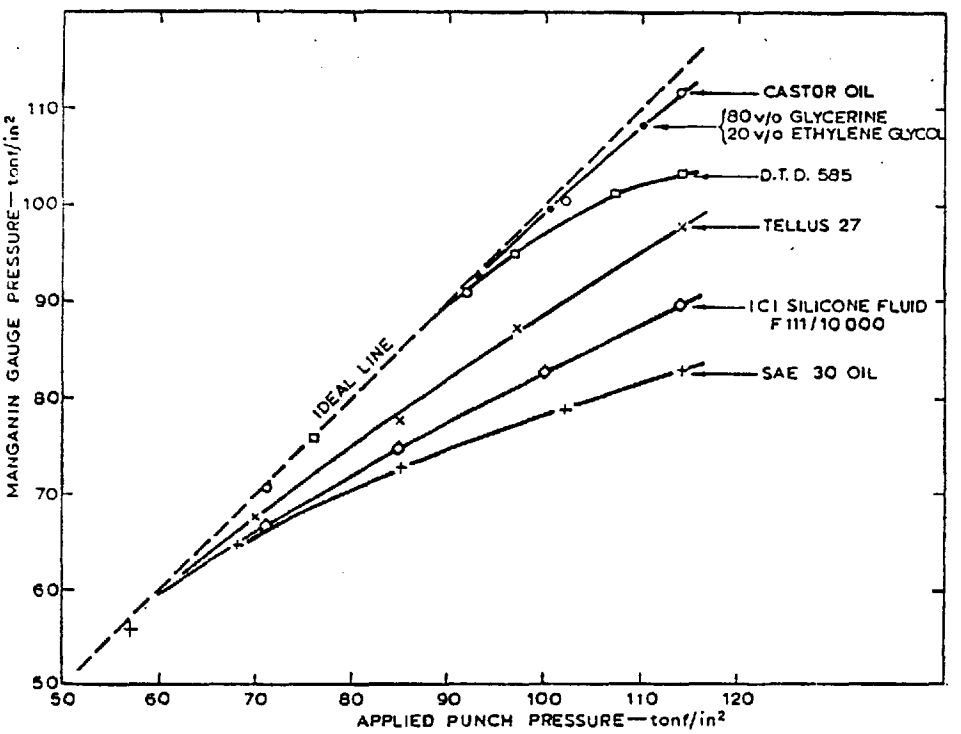

Behaviour of various pressure-transmitting fluids

Figure 3.2: After Ref. 3.2.

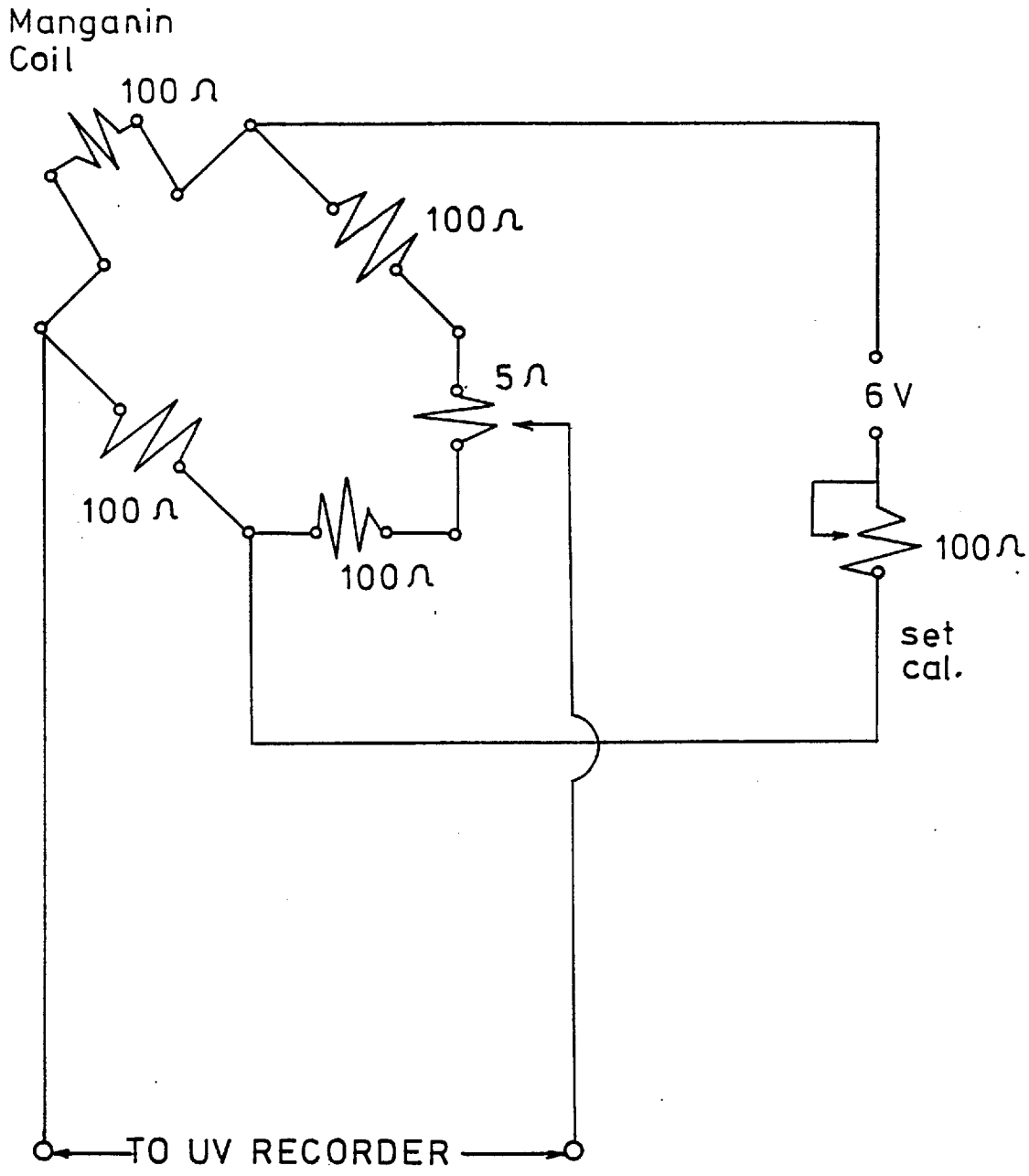

Figure 3.3: Pressure measurement circuit

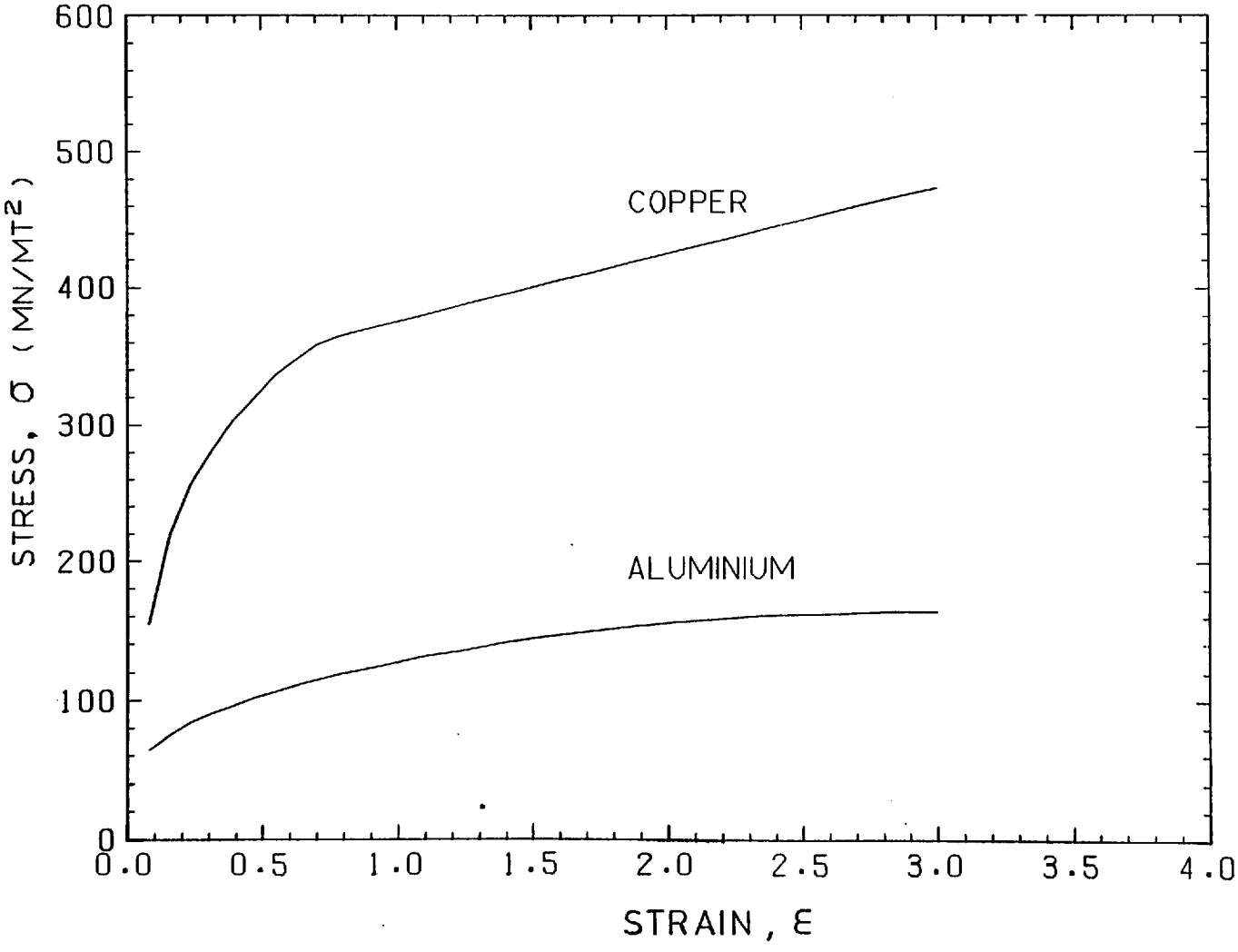

Figure 3.4: Stress-Strain curves

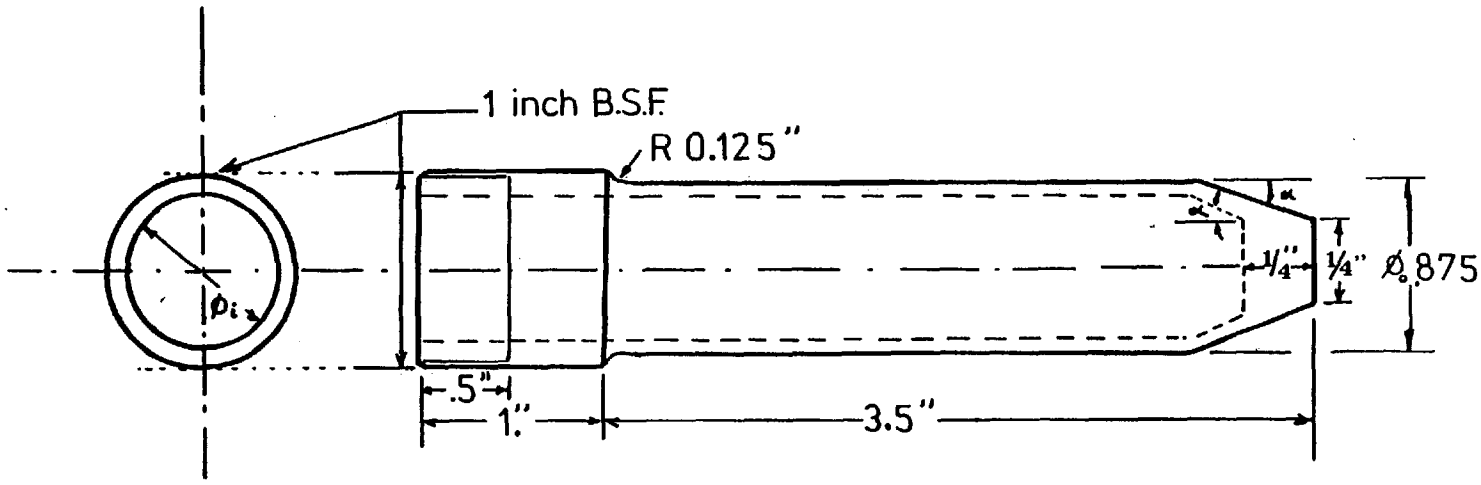

Figure 3.5: Schematic description of a typical specimen

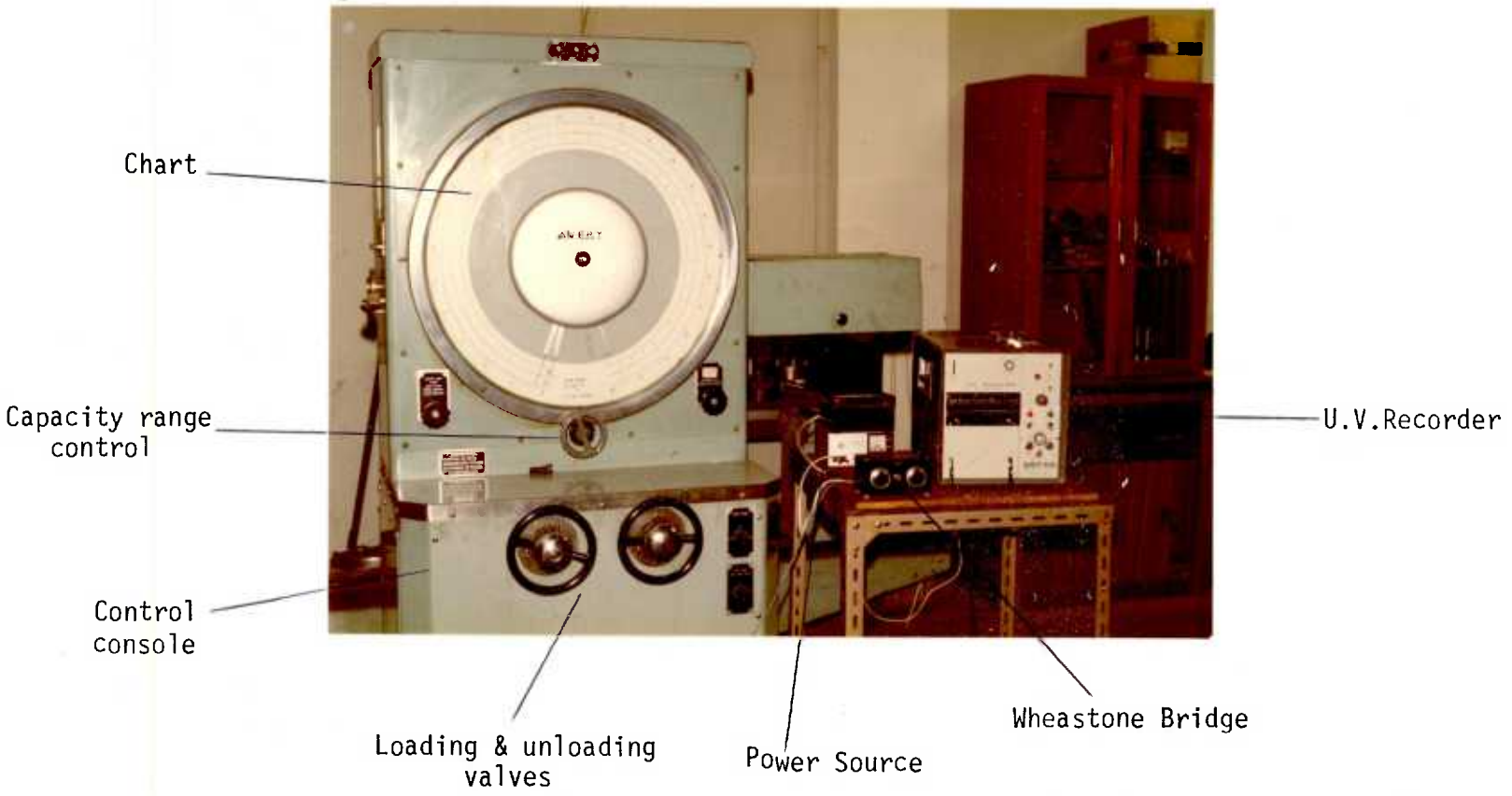

Plate 3.1: Details of instrumentation.

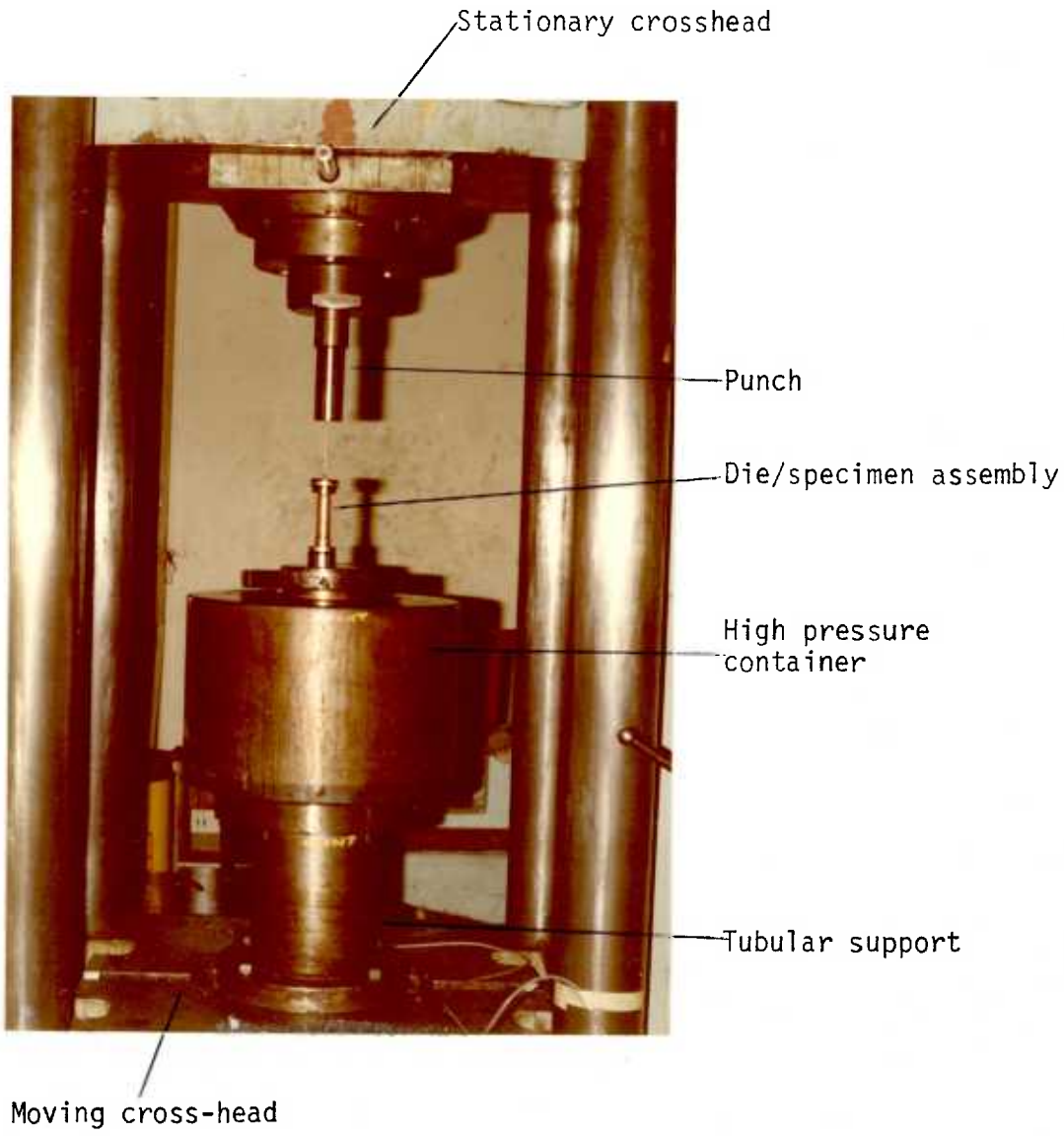

Plate 3.2: Hydrostatic extrusion set-up.

Plate 3.3: Dies,seals and damping blocks.

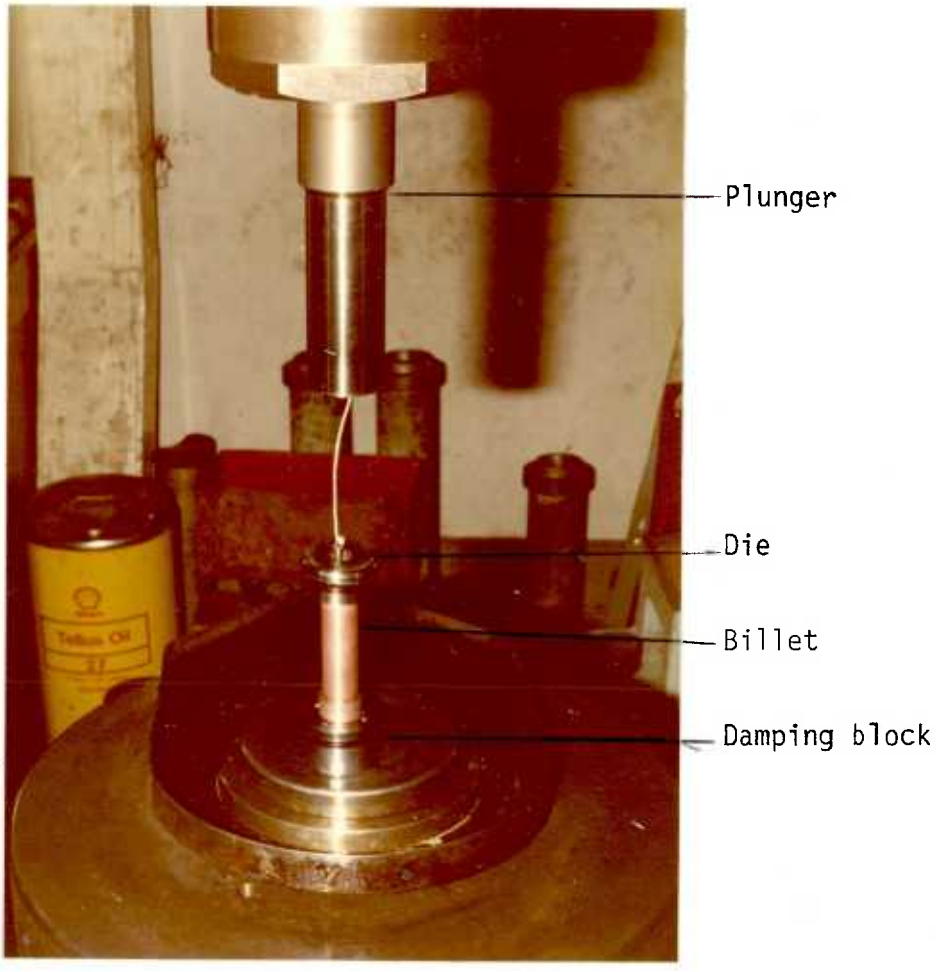

Plate 3.4: Specimen-Die assembly.

CHAPTER 4

FINITE ELEMENT ANALYSIS IN METAL FORMING

4.1 Introduction

The finite element method is now widely accepted as a very powerful method in stress analysis. Progress has been made on three fronts, all of which contribute to the strength of the method. First of all, a mathematical foundation of the method has now been well established[4.1]. Secondly, the search for and development of the many consistent elements has given it a wide area of application. Finally, extension of the method to the study of non-linear behaviour has resulted in more realistic models.

Here we shall be concerned with the literature in the area of non-linear behaviour as it applies to metal forming problems.

4.2 Review of Elastic-Plastic Formulations

Application of the finite element method to plasticity problems started immediately after its success in the solution of linear elasticity problems. This was done resorting to various computational procedures, mainly, the "Thermal strain" or "Initial strain" approach, and the "tangent modulus" or "direct incremental approach".

In the "thermal strain" approach the elastic equations of equilibrium were modified to compensate for the fact that the inelastic strains do not cause any change in stress. This idea was originally proposed by Mendelson and Mason[4.2] in 1959. Soon after the above work was reported, Gallagher and co-workers[4.3,4.4] adapted the method to the finite element method by calculating the so-called initial force vector.

Subsequent applications of the method in the area of plane solids were made by Percy et al[4.5], Argynis et al[4.6] and Jensen et al[4.7]. Parallel to the development of this approach, the method known as the "tangent modulus" was being developed. In this approach,

the stress-strain relationship is adjusted in every load increment to take into account the history of plastic deformation. The problem being then treated in a piecewise linear manner.

The equations for the "tangent modulus" approach were developed by Pope[4.8] and Swedlow and Young[4.9]; these authors being mainly concerned with structural problems.

Marcal and King[4.10] introduced a partial stiffness concept and applied the tangent modulus technique to the thick walled cylinder problem. They compared finite element solutions with known solutions obtained by other methods or with known experimental results.

Although good agreement was obtained in general, the analysis of the deformation had to be interrupted at some stage because negative strains were obtained.

Yamada et al[4.11,4.12] modified Marcal's algorithm and used it to predict collapse conditions in certain categories of problems. Again, the procedure had limited application because of the development of negative strains. Nevertheless, this work by Yamada influenced several workers and a stream of papers, using this particular approach, were published. Iwata et al[4.13] carried out the analysis of hydrostatic extrusion and obtained detailed information of the process. Nagamatsu et al[4.14] analyzed plane strain upsetting, including the effect of friction. An extensive application of the method to metal forming problems is due to Lee and Kobayashi[4.15 - 4.19]. They analyzed the problems of flat punch indentation, Brinell hardness test, upsetting, side pressing and extrusion. They not only followed the path of deformation to obtain information on the development of the plastic zone, stress and strain distributions and geometrical changes of the workpiece, but also examined unloading and calculated the residual stresses involved. However, these were exploratory applications, and doubts existed as to the real accuracy of the

solutions obtained, especially where large strains were present.

Parallel to these developments, Zienkiewicz et al[4.20] introduced what they called the "initial stress approach" to try to overcome the computing difficulties of the tangent modulus approach and the limitations imposed in the thermal strain approach by nearly perfect plasticity. To show the capabilities of the method, they presented results for some stress concentration problems in coil engineering.

A subsequent work by Nayak and Zienkiewicz[4.21] expands on the subject and condenses a series of results obtained by Nayak[4.22] in the analysis of pressure vessels, plane strain extrusion and indentation. In the case of extrusion, both Von Mises and Tresca criteria were considered.

More recently, Hartley and co-workers[4.23] have used the tangent modulus approach to solve problems of extrusion and ring upsetting. A. Najafi-Sani[4.24] has looked at the problem of clamp design in the continuous hydrostatic extrusion and M. Najafi-Sani[4.25] has solved the problem of blanking.

Wong and Das[4.26] tried to analyze cropping, but their results were constrained by the nature of the small deformation formulation they used. Odell[4.27] has looked into the problem of wall ironing, but strangely enough, he did not take advantage of the method and still solved the problems with the traditional plane strain assumption.

Most of the literature reviewed so far is concerned with small strain plasticity. Therefore, it is strictly concerned with predicting the onset of yielding and the early spreading of the plastic zone. Large strains can either not be tackled or require a very heavy penalty in terms of computer time.

Most of the computational schemes are based on the calculation

of changes in geometry and stress distribution, in a finite element net, associated with small increments of deformation. The frame of reference is a Lagrangian one, that is, the network is considered to be attached to the particles of the continuum at the nodal points. The analysis of the sequence of the small increments allows the total deformation and stress distribution to be determined, and this can result in large (finite) deformation.

Lee[4.28] has pointed out that such formulations are not suitable to solve metal forming problems, especially those that require that a steady state mode be analyzed, e.g. extrusion, rolling.

Quite apart from this limitation, Rice[4.29] and McMeeking and Rice[4.30] have pointed out errors in the formulation of many existing elastic-plastic problems.

One source of error is a lack of preciseness in defining increments of stress and strain. They stress the fact that care must be taken in the selection of stress definitions and stress-rate and strain-rate expressions, particularly in the common circumstance that the tangent modulus in plastic flow is of the order of the stress. They also point out that the error incurred when selecting the "wrong" definition is independent of the size of the increment used and, therefore, the common small strain assumptions are not valid for large strain problems, even when small increments in strain are used.

There are available various formulations dealing with elastic-plastic problems which include large strains and/or large displacements considerations.

Marcal[4.31] used incremental equations to form the basis for a general purpose program for non-linear analysis. Hibbit et al[4.32] use Marcal's work as the basic material to propose a formulation for large strains and large displacements, though restricted to isotropic material behaviour, in a Lagrangian frame of

reference. The overall stiffness matrix is obtained as a linearization of element equilibrium defined by virtual velocity equations. A similar approach is presented by Gordon and Weinstein[4.33]; they examine plane sheet drawing, considering both smooth and friction conditions. Blass[4.34] also uses a similar approach to solve the problem of radial upsetting.

Kitagawa et al[4.35] analyze the problem of a finite element formulation similar to the one presented in Ref. [4.32], but referred to the current configuration of the continuum. They use a convected coordinate system embedded in the body.

Osias[4.36 - 4.38] also contributes to the subject and expands previous work for infinitesimal strains by Swedlow[4.39,4.40]; the formulation uses an Eulerian frame of reference, places no restriction on the amount of deformation and assumes an isotropic work hardening material. A number of problems were considered: simple extension, simple rotation, and combined extension and rotation of prismatic volume elements. The problem of necking was also considered.

Gunasekera and Alexander[4.41] employ a formulation which is very similar to that of Hibbit et al, being, however, described in terms of the instantaneous frame of reference. They solve the problem of elastic-plastic expansion of a hole in a plate. This particular formulation is essentially only applicable to the small strain range, for, as already pointed out in Ref. [4.30], no objective definition for the stress increments is considered.

McMeeking and Rice[4.30] produced an apparently simpler formulation than the Lagrangian one proposed in Ref. [4.32], and much more so than the Eulerian approach proposed by Kitagawa et al[4.35]. The authors use the current configuration of the continuum as the frame of reference for the deformation increments, that is, an up-

dated Lagrangian frame of reference. They consider the problem of necking in the tensile test, and compare their result very favourably with Osias'[4.36 - 4.38].

Lee and co-workers[4.42 - 4.44] used this formulation to predict the steady state force and residual stresses in extrusion and sheet drawing, being able to achieve deformations well beyond those achieved by Iwata et al[4.13].

Oh et al[4.45] solved the problems of a void growth model, and, in conjunction with solutions to drawing and extrusion problems, attempt to define a formability criterion.

Yamada and Hirakawa[4.46] have also developed an updated Lagrangian formulation and used it to solve the problem of plane extrusion through a doubly curved die.

Derbalian et al[4.47] discuss the advantages of using an Eulerian scheme, as opposed to an updated Lagrangian scheme, in the solution of steady-state problems. They propose to use an Eulerian type of mesh fixed in space and employ the McMeeking and Rice formulation[4.30] to find the incremental displacements and stresses. The difference stems from the fact that the mesh points are not updated to follow material points and the stresses in the fixed mesh are, therefore, found by adding the incremental stresses, obtained for a forward Lagrangian step, to a set of interpolated stresses. In this way they claim to combine the best of the Eulerian and Lagrangian formulations. However, they only present a solution for a very idealized problem and comment on the still "unjustifiably high cost" of solving a more realistic problem.

Yamada et al[4.48] use another approach. They solve the unsteady elastic-plastic problem by first applying finite element procedures of elasto-plasticity. Then, using this solution as a first approximation and following the change of mechanical state of

material elements along assumed streamlines, pursue the steady state iteratively.

A very important report, worth noting, is that of Nagtegaal et al[4.49]. They study the over-stiffening effect of finite element solutions in the fully plastic range. They suggest that this is due to the excessive kinematic constraints imposed on the modes of deformation by the element types commonly used in two- and three-dimensional analysis. They propose using special arrangements of elements to alleviate the problem. However, only one of such arrangements has been found to date: a quadrilateral formed by four (4) constant strain triangles (CST).

Argyris et al[4.50] also discuss the difficulties found when using displacement finite elements to solve problems with an incompressible or nearly incompressible material.

It is interesting to note that despite this highlighting of the problems encountered with simpler elements, some authors have continued to use CSTs without taking proper care as to the way they are arranged.

Zienkiewicz[4.51] states that this problem of over-constraint can also be alleviated by using higher order elements with reduced order of integration.

In a recent work, Argyris et al[4.52] propose a method to modify the simpler elements so that they can be used in the incompressible regime. They use separate models for the dilatational and deviatoric strain energies. The method is based on a physical rather than a mathematical reasoning and, unlike reduced integration, it does not create problems due to spurious mechanisms and loss of rank.

4.3 Review of Rigid-Plastic Formulations

A very interesting situation has developed recently in the

field of numerical methods in metal forming. When the methods first appeared, they were heralded as the end of the assumption of rigid-plastic behaviour necessary for almost all of the traditional theories: slip-line field theory, upper-bounds, visioplasticity, etc. However, after the initial success, researchers started to realize that the implementation of elastic-plastic formulations, from the point of view of computer coding, was becoming highly complex, and that a realistic solution required "too much" computer time.

It was then realized that the rigid-plastic behaviour assumption was not as bad as it was made out to be in the first place, and it was re-adopted as a fair assumption, and a number of formulations for the finite element method based on this assumption have come to the fore in recent years.

This section will be concerned with a brief review of the formulations available to-day. A more "in-depth" discussion of the formulations used in this work will be left for the next section.

Although the various formulations are widely different as to the inclusion of kinematical constraints and the handling of rigid regions, all of them stem from the same constitutive relations between stress and strain increment, namely, the equations of Levy-Mises which can be written as follows:-

$$d\varepsilon_{ij} = \sigma'_{ij}\, d\lambda \tag{4.1}$$

where $d\varepsilon_{ij}$ represents only the increments in plastic strain. This equation can be differentiated with respect to time to produce:-

$$\sigma'_{ij} = 2\eta\ \dot{\varepsilon}_{ij} \tag{4.2}$$

This equation is called a "viscous flow" type of equation because of

its similarity with the equation for a viscous fluid. This fact has been the main catalyst in the recent development of computer codes for the solution of problems involving rigid-plastic materials.

Most formulations derive the finite element equations by minimizing the total internal work (or work rate) given particular boundary conditions. This has been done, in general, by using the virtual work principle, although, as it will be shown in subsequent paragraphs, other equivalent variational statements have been used leading to the same equations.

Neither of the variational principles used to derive the elemental equations provides for enforcing the incompressibility constraint, even though this is a necessary assumption. Several possibilities for enforcing this constraint have been presented and they provide the mark of identity of each different formulation.

4.3.1 The Stream Function Approach

This is the most usual procedure of describing incompressible velocity fields in the traditional fluid mechanics literature and it was originally suggested by Goon[4.53], who used mapping techniques to obtain solutions, for metal flow problems.

The finite element implementation for metals was done by Godbole[4.54] and Zienkiewicz and Godbole[4.55] who treated the plastic and visco-plastic flow of metals as a special case of non-Newtonian fluids. They solved different cases of extrusion and the non-steady state problem of punch indentation.

The procedure is based on the introduction of a stream function in two-dimensional problems or by introduction of a vector potential in three dimensions.

Confining our attention to plane flow with u and v velocity components in the x and y directions, we can write:-

$$u = -\frac{\partial \psi}{\partial y} \quad , \quad v = \frac{\partial \psi}{\partial x} \tag{4.3}$$

and thus:-

$$\dot{\varepsilon}_v = \dot{\varepsilon}_x + \dot{\varepsilon}_y = \frac{\partial u}{\partial x} + \frac{\partial v}{\partial y} = 0 \tag{4.4}$$

For the axisymmetric case:-

$$u = -\frac{1}{r}\frac{\partial \psi}{\partial y} \quad , \quad v = \frac{1}{r}\frac{\partial \psi}{\partial x} \tag{4.5}$$

and thus incompressibility is again obtained.

The finite element equations are found using the principle of virtual work (see Ref.(4.54)). In the finite element code, three nodal variables must be found at each node if ψ is to be found throughout the body; in addition, elements whose shape functions have C^1* continuity, are required. While in two-dimensional problems the use of such elements presents little difficulty, in three dimensions no satisfactory element has yet been devised. This, coupled with the fact that boundary conditions are difficult to define unless the velocities are entirely prescribed on all the boundaries, has stopped this particular approach from being more widely used.

4.3.2 Lagrange Multiplier/Velocity and Pressure Fields

The application of this formulation to metal flow problems can be traced to three different, and apparently independent sources.

In 1972, M. Lung(4.56) published a very short article, in German, where he outlined the method. He implemented it using

---

* Continuity of nodal variable and its first derivatives.

triangular elements and presented the solution of a plane strain extrusion problem. In the same year, C. H. Lee and S. Kobayashi[4.51] presented a very similar formulation but this time implemented it using bilinear rectangular elements; they also proposed a linearization of the resulting equations by use of a simple perturbation method. They not only presented a solution to the problem of simple upsetting, but also used the method to smooth errors from visioplasticity analysis of the extrusion problems.

Parallel with these developments, Godbole[4.54] proposed a similar formulation; however, his starting point was not an upper bound theorem, as in the previous two, but an extension of his work on the analogy of flow of viscous fluids and metal flow. This formulation was later extensively used by Jain[4.58].

Lung and co-workers[4.59 - 4.61] have subsequently used this approach for solving the drawing problem under various conditions of friction in both plane-strain and axisymmetric conditions, upsetting of a trapeze in plane strain and axisymmetric upsetting of hardening and non-hardening materials.

Lee and Kobayashi[4.62] presented a more detailed formulation of the approach, which they christened "the Matrix Method" and used it to obtain new solutions in cylinder compression with regard to different parameters. In plane stress problems the planar anisotropy was taken into account and new solutions were found for non-axisymmetric hole expansion and "easing" in flange drawing. Shah, Lee and Kobayashi[4.63] modified the method so that it could handle efficiently the rigid regions and applied it to the problem of compression of tall cylinders. Shah and Kobayashi[4.64] analyzed the problem of cold heading, and Lee and Kobayashi[4.65] solved the problem of bore expanding and flange drawing of anisotropic sheet metals, being able to predict the development of "earing".

Shah and Kobayashi subsequently went on to solve the problem of axisymmetric piercing and extrusion[4.66]. This work was later extended by Chen et al[4.67] who not only solved the problem of extrusion and drawing, but also combined these results with experimental data and a void growth model and tried to define workability and fracture criteria for the process.

Matsumoto et al[4.68] improved upon the formulation by introducing means to handle friction conditions on surfaces whose direction of flow is not known a priori; this new procedure was applied to the problem of ring upsetting. Chen and Kobayashi[4.69] extended this new feature and carried out a comprehensive analysis of the ring upsetting problem comparing their solutions with known upper-bounds and published experimental results.

Gotoh and Ishire[4.70] introduced a local system of convected co-ordinates into each element so that geometrical non-linearity could be taken into consideration. They also included the effect caused by the rotation of the principal axes of orthotropy of the material. This approach was used to tackle the problem of deep drawing of the flange. Unlike Lee and Kobayashi[4.62], the system of equations is not linearized but contrived to be solved by a repeated calculation.

Tomita and Sowerby[4.71] used the Lagrange multiplier approach for analyzing the plane strain deformation of rate sensitive materials, the actual process considered was frictionless, plane-strain side extrusion.

As can be seen from the named literature, this particular approach has been widely explored especially by Professor Kobayashi and co-workers at the University of California, Berkeley. However, some difficulties are associated with this method. Firstly, more than two variables per node have to be found, increasing the core and computer time needed to get a solution; secondly, zeros are

introduced into the leading diagonal of the stiffness matrix which may mean that standard solution techniques cannot be used. Experience has shown, however, that with a proper order of elimination this last difficulty can be overcome.

4.3.3 The Penalty Function Approach

Penalty functions are traditionally used to modify variational principles in the finite element analysis to enforce constraint. The problem of flow of a rigid-plastic material can be viewed as a problem of constrained minimization of a functional.

This approach is based on the application of a penalty to the square of the error, in this case the square of the compressibility value. Thus, when the functional is minimized, the compressibility will be forced to be close to zero. Therefore, the penalty approach in solid mechanics amounts to approximating an incompressible medium by a slightly compressible one.

This approach was originally established by Zienkiewicz[4.72] and subsequently used by Zienkiewicz and Godbole[4.73] for problems of creeping flow in which they include some extrusion problems as well as problems involving large surface deformations.

Zienkiewicz and Godbole[4.74] have stated that the use of a penalty is identical to the use of a Poisson's ratio close to 0.5 in elasticity problems.

Because of its simplicity of implementation, this approach has become widely popular and its application is under continuous increase.

Sharman[4.76] applied it to the problem of hot extrusion; Connfield and Johnson[4.77] tackled the problem of hot rolling and studied the effect of various temperature distributions. Turner[4.78] and Alexander and Turner[4.79] solved the problem of hot dieless

drawing; they reported some success on the prediction of the deformed shape, but some oscillations in stresses were also found and this was attributed to the use of simplex elements. Price and Alexander[4.80,4.81] presented solutions for various problems of isothermal forming; they use serendipity quadratic elements and devised a method for calculating the mean stress, being able then to calculate the stress distribution.

Jain[4.58] and Zienkiewicz et al[4.82] extended further the application to various problems of extrusion, introducing a special element to account for the friction effects and presenting some comparisons with results obtained using the Lagrange multiplier approach.

Zienkiewicz et al[4.83] and Zienkiewicz and Oñate[4.84] used the penalty function together with an analysis of the energy dissipation to solve the problem of coupled thermal flow in extrusion and hot rolling. They also extended the flow approach to problems of sheet forming. Kanazawa and Marcal[4.85] have introduced a special element to include the effect of spread in the analysis of rolling using penalty function.

The penalty function approach is the simplest to implement since, at its most basic form, it only involves a simple modification of existing elastic codes. Recent investigations (see Refs.[4.86,4.87]) have given mathematical formality to the approach and to its particular form of numerical integration. The method is also being used in other areas; worth noting is the work by Hughes et al[4.88], where a comprehensive account of the theory behind the method is presented together with computational techniques referred to the fluid mechanics context.

The penalty function and the Lagrange multiplier approach were selected for the investigation reported in this work and a more detailed discussion of the formulations is presented in a following

section.

At this point, the author would like to call attention to some points of method which have become apparent during the research for this review.

It has become evident that there is a lack of feedback between the people that develop the methods and the people that actually use them. This gap in the communication network, contributes to the continuous application by the "users" of tools that have been found to be unsuitable by the "developers". On the other hand, the pace at which new formulations come about does not allow for existing formulations to be fully tested under "real life" conditions, creating confusion as to the advantages or drawbacks of any specific approach.

Also, the character of the finite element method has changed in the last few years. From being an engineering tool, developed by engineers, it has become a focus of attraction, and rightly so, for mathematicians. This has meant, however, that the language of presentation has changed and, in the opinion of this author, it is sometimes so esoteric as to be meaningless for everybody except other mathematicians, having as a consequence that potential users simply shy away.

Fortunately, this tendency is not universal and it is still possible to find workers writing within the limits imposed by the mathematical working knowledge of the average engineer.

4.4 General Formulation

In the preceding sections, most of the existing formulations for plasticity problems have been reviewed. Both elastic-plastic and rigid-plastic formulations have advantages and drawbacks, hence, the choice of any specific formulation is by no means a straightforward one, let alone a logical one.

In this context, any choice has to be regarded as an arbitrary one, and only its later success in tackling the specific problems in hand will justify, or otherwise, the wisdom of the selection.

From an engineering point of view, simplicity of formulation is generally felt to be an asset, although this has to be weighed against the number of assumptions made. Nevertheless, this simplicity is a relative one since any numerical method will, in general, involve more complexity than any non-numerical approach. Therefore, the choice is in degree of complexity rather than between a simple approach or a complex one.

Of the existing approaches, the rigid-plastic one affords the inclusion of most of the parameters involved in metal forming, and at the same time renders a formulation that is relatively simple to handle on the computer.

Therefore, rigid-plastic approaches, namely, velocity and pressure and penalty function formulation, were chosen as the ones to be used in this work.

4.4.1 Method of Analysis

The equations for both formulations turn out to be identical except for the introduction of the compressibility constraint, thus, a general statement of the problem will first be made and the differences will be introduced as variations in a theme.

The formulations can be derived from either considerations of solid mechanics[4.73] or fluid mechanics[4.88]. In this work the former will be chosen for the sake of consistency with the rest of the contents.

4.4.2 Formal Statement of the Problem

Consider a body, V, whose surface, S, consists of S_u and S_t.

The body is composed of a rigid-plastic material which obeys the Von Mises yield criterion and its associated flow rule, under the boundary conditions, such that the entire body is deforming plastically. Body forces are assumed to be absent in the region V. Then, according to an extremum principle (see Ref. (4.16)) the functional (4.6) takes an absolute minimum value for the actual solution with respect to a kinematically admissible velocity field:-

$$\Phi = \int_V \sigma'_{ij}\, \dot{\varepsilon}_{ij}\, dv - \int_{S_T} F_i\, u_i\, ds \qquad (4.6)$$

This functional can be rewritten as(4.62):-

$$\Phi = \int_V \bar{\sigma}\, \dot{\bar{\varepsilon}}\, dv - \int_{S_T} \underset{\sim}{F}^T\, \underset{\sim}{U}\, ds \qquad (4.7)$$

where $\dot{\bar{\varepsilon}}$ is the effective strain rate; $\bar{\sigma}$ is the equivalent stress; $\underset{\sim}{F}$, the traction vector specified at boundary S_T.

It is obvious that the functional Φ does not include the effect of the incompressibility constraint; therefore, it is necessary to introduce it. This can be done in various ways. Here we will limit the discussion to the Lagrange multiplier and the penalty function approaches.

4.4.3 Lagrange Multiplier. Velocity and Pressure Formulation

In general, the problem is one of obtaining stationality of a functional π with a set of constraints $\underline{C}\ (u_i) = 0$.

This constraint can be introduced by forming another functional:-

$$\overline{\pi} = \pi + \int_{\Omega} \lambda \, \underline{C} \, (u_i) \, d\Omega \tag{4.8}$$

in which λ is some function (or set of functions) of the independent coordinates in domain Ω known as the Lagrange multiplier.

Considering the specific problem under our consideration (Equation (4.7)), we can form a new functional as:-

$$\overline{\Phi} = \Phi + \int_{V} \lambda \, \dot{\varepsilon}_v \, dv \tag{4.9}$$

The problem is then identified as one of minimization of potential energy defined in terms of distortional strain energy and the incompressibility constraint. After some standard manipulation[4.51], the Lagrange multiplier can be identified as the hydrostatic pressure or mean stress:-

$$\lambda \equiv \sigma_m \tag{4.10}$$

This constrained variational principle was first identified by Hermann[4.89] in the context of elastic stress analysis of incompressible media.

It will be observed that in a problem formulated in the above manner the constraint introduces a new variable to the problem, namely, the hydrostatic stress, thus increasing the computer requirements when the discretization is carried out.

Application of the stationary condition to functional (4.8) leads to:-

$$\left.\begin{aligned} \frac{\partial \overline{\Phi}}{\partial \underset{\sim}{U}} &= 0 \\ \frac{\partial \overline{\Phi}}{\partial \lambda} &= 0 \end{aligned}\right\} \qquad (4.11)$$

which lead directly to discretization.

4.4.4 Penalty Function

In this approach, which stems originally from optimization literature[4.72], the constraint is introduced by imposing a penalty on the integral of the square of the error, in this case the value of compressibility.

Therefore, functional (4.7) can now be written as:-

$$\int_V \underline{\sigma}\, \dot{\underline{\varepsilon}}\, dv - \int_{S_T} \underset{\sim}{F}^T \underset{\sim}{U}\, ds + 2\alpha \int_V \dot{\varepsilon}_v^{\,2}\, dv$$

or:-

$$\overline{\Phi} = \Phi + 2\alpha \int_V \dot{\varepsilon}_v^{\,2}\, dv \qquad (4.12)$$

where $\alpha > 0$ is the penalty number and requires the stationality for the constrained solution. The solution obtained from functional (4.12) will satisfy the constraint only approximately. The larger the value of α the better the constraints will be achieved.

It is worth noticing that this formulation does not introduce any additional unknown parameters.

Examination of functionals (4.12) and (4.9) shows that the penalty approach is equivalent to elimination of the variable σ_m

from integral (4.9) by writing the constitutive relation (4.13):-

$$\sigma_m = \alpha \dot{\varepsilon}_v \tag{4.13}$$

Indeed, the penalty approach has been shown recently, provided certain considerations related to problems of over-constraint are taken into account, to be "equivalent" to a mixed formulation (velocity-pressure), (4.86,4.89).

Application of the stationary condition leads directly to discretization. This together with the problems arising from over-constraint will be discussed below.

4.4.5 Matrix Problem. Discretization

The domain V is discretized into $\underline{M}$ non-overlapping elements connected at $\underline{N}$ nodal points. If $\overline{\phi}^{(m)}$ is the value of the functional $\overline{\Phi}$ evaluated over the m^{th} element, then:-

$$\overline{\Phi} = \sum_{m=1}^{M} \overline{\phi}^{(m)} \tag{4.14}$$

The approximation of the functional $\overline{\Phi}$ by a functional ψ is performed on the elemental level by replacing $\underset{\sim}{U}^{(m)}$ with a kinematically complete distribution given by:-

$$\underset{\sim}{U}^{(m)} = \sum_{i=1} N_i^u u_i = \underline{N}^u \underline{u}^{(m)} \tag{4.15}$$

where $\underline{N}$ is the interpolation function and $\underset{\sim}{u}$ is the vector of nodal points velocities. Similarly, if the pressure is one of the variables involved:-

$$P = \underline{N}^p \underline{p}^{(m)} \tag{4.16}$$

Let u, v and w describe the three cartesian components of velocity vector $\underset{\sim}{U}$. The strain rate vector $\dot{\underset{\sim}{\varepsilon}}^{(m)}$ is then related to the velocities by:-

$$\dot{\underset{\sim}{\varepsilon}}^{(m)} = \underline{L}\ \underset{\sim}{U}^{(m)} \tag{4.17}$$

where:-

$$\dot{\underset{\sim}{\varepsilon}}^{(m)T} = \left[\dot{\varepsilon}_x,\ \dot{\varepsilon}_y,\ \dot{\varepsilon}_z,\ \dot{\gamma}_{xy},\ \dot{\gamma}_{yz},\ \dot{\gamma}_{zx}\right] \tag{4.18}$$

The operator $\underline{L}$ is defined as:-

$$\underline{L} = \begin{bmatrix} \frac{\partial}{\partial x} & 0 & 0 \\ 0 & \frac{\partial}{\partial y} & 0 \\ 0 & 0 & \frac{\partial}{\partial z} \\ \frac{\partial}{\partial y} & \frac{\partial}{\partial x} & 0 \\ 0 & \frac{\partial}{\partial z} & \frac{\partial}{\partial y} \\ \frac{\partial}{\partial z} & 0 & \frac{\partial}{\partial x} \end{bmatrix} \tag{4.19}$$

The incompressibility constraint takes the form:-

$$\dot{\varepsilon}_v^{(m)} = \dot{\varepsilon}_x^{(m)} + \dot{\varepsilon}_y^{(m)} + \dot{\varepsilon}_z^{(m)} = \underline{M}^T\ \dot{\underset{\sim}{\varepsilon}} = 0 \tag{4.20}$$

where:-

$$\underline{M}^T = \left[1,\ 1,\ 1,\ 0,\ 0,\ 0\right]$$

The effective strain rate and effective stress are defined, respectively, as*:-

$$\dot{\bar{\varepsilon}} = \left(\frac{2}{3}\,\underset{\sim}{\dot{\varepsilon}}^T\,\underline{D}_o\,\underset{\sim}{\dot{\varepsilon}}\right)^{1/2} \tag{4.21}$$

and:-

$$\bar{\sigma} = \left(\frac{3}{2}\,\underset{\sim}{\sigma'}^T\,\underline{D}_o\,\underset{\sim}{\sigma'}\right)^{1/2} \tag{4.22}$$

where $\underset{\sim}{\sigma'}$ is the deviatorial stress vector, which is related to $\underset{\sim}{\dot{\varepsilon}}$ according to the Levy-Mises equations by:-

$$\underset{\sim}{\sigma'} = \frac{2}{3}\,\frac{\bar{\sigma}}{\dot{\bar{\varepsilon}}}\,\underline{D}_o\,\underset{\sim}{\dot{\varepsilon}} \tag{4.23}$$

in which $\underline{D}_o$ is a diagonal matrix defined as:-

$$\begin{bmatrix} 1 & & & & & \\ & 1 & & & & \\ & & 1 & & & \\ & & & 1/2 & & \\ & & & & 1/2 & \\ & & & & & 1/2 \end{bmatrix} \tag{4.24}$$

---

* In this and the following sections all quantities are at the elemental level, but for convenience, the superscript (m) is dropped unless otherwise specified.

Noting relations (4.15) to (4.23), the functionals (4.9) and (4.12) can now be rewritten as:-

$$\int_{v(m)} \bar{\sigma} \left(\frac{2}{3} \underset{\sim}{u}^T \underline{B}^T \underline{D}_o \underline{B} \underset{\sim}{u}\right)^{1/2} dv - \int_{S_T(m)} (\underline{N}^u \underset{\sim}{u})^T \underset{\sim}{F} ds + \int_{v(m)} (\underline{M}^T \underline{B} \underset{\sim}{u})^T \underline{N}^p \underset{\sim}{p} dv \tag{4.25}$$

and:-

$$\int_{v(m)} \bar{\sigma} \left(\frac{2}{3} \underset{\sim}{u}^T \underline{B}^T \underline{D}_o \underline{B} \underset{\sim}{u}\right)^{1/2} dv - \int_{S_T(m)} (\underline{N}^u \underset{\sim}{u})^T \underset{\sim}{F} ds + \int_{v(m)} (\underline{M}^T \underline{B} \underset{\sim}{u})^T 2\alpha(\underline{M}^T \underline{B} \underset{\sim}{u}) dv \tag{4.26}$$

where:-

$$\underline{B} = \underline{L}\, \underline{N}^u \tag{4.27}$$

Applying the stationary condition to functional (4.26), when the yield stress is independent of the strain rate, leads to:-

$$\frac{\partial \psi^{(m)}}{\partial \underset{\sim}{u}^{(m)}} = \int_{v(m)} \underline{B}^T \underline{D} \underline{B} \underset{\sim}{u} dv + \int_{v(m)} (\underline{M}^T \underline{B})^T \underline{N}^p \underset{\sim}{p} dv - \int_{S_T(m)} \underline{N}^{u^T} \underset{\sim}{F} ds = 0 \tag{4.28}$$

and:-

$$\frac{\partial \psi^{(m)}}{\partial \underset{\sim}{p}^{(m)}} = \int_{v(m)} \underline{N}^{p^T} \underline{M}^T \underline{B} \underset{\sim}{u} dv = 0 \tag{4.29}$$

where:-

$$\underline{D} = \frac{2}{3}\frac{\bar{\sigma}}{\bar{\varepsilon}}\, D_o \tag{4.30}$$

This results in a simple set of equations which can be written as:-

$$\begin{bmatrix} \underline{K}^u & \underline{K}^p \\ \underline{K}^{p^T} & 0 \end{bmatrix} \begin{pmatrix} \underset{\sim}{u} \\ \underset{\sim}{p} \end{pmatrix} + \begin{pmatrix} \underset{\sim}{f}^u \\ 0 \end{pmatrix} = 0 \tag{4.31}$$

or:-

$$\underline{K}\ \underset{\sim}{a} + \underset{\sim}{f} = 0 \tag{4.32}$$

where:-

$$\left.\begin{aligned} \underline{k}^u_{ij} &= \int_v \underline{B}_i^T\, \underline{D}\, B_J\, dv \\ \underline{k}^p_{ij} &= \int_v (M^T B_i)^T N^p_J\, dv \\ \underset{\sim}{f}^u_i &= -\int_S \underline{N}_i^{u^T}\, \underset{\sim}{F}\, ds \end{aligned}\right\} \tag{4.33}$$

where i and j are element ("local") node numbers.

Analagously, the stationary condition applied to functional (4.27) leads to:-

$$\frac{\partial \psi^{(m)}}{\partial \underset{\sim}{u}^{(m)}} = \int_{v(m)} \underline{B}^T \underline{D} \underline{B} \underset{\sim}{u} \, dv - \int_{S_T(m)} \underline{N}^{u^T} \underset{\sim}{F} \, ds + \int_{v(m)} \underline{B}^T \underline{M} \alpha \underline{M}^T \underline{B} \underset{\sim}{u} \, dv = 0 \tag{4.34}$$

Again this results in a simple set of equations of the form:-

$$\underline{K} \underset{\sim}{u} + \underset{\sim}{f} \equiv (\underline{K}^u + \underline{K}^\alpha) \underset{\sim}{u} + \underset{\sim}{f} = 0 \tag{4.35}$$

where:-

$$\left.\begin{aligned} \underline{k}^u_{ij} &= \int_v \underline{B}_i^T \underline{D} \underline{B}_J \, dv \\ \underline{k}^\alpha_{ij} &= \int_v \underline{B}_i^T \underline{M}\alpha \underline{M}^T \underline{B}_J \, dv \\ \underset{\sim}{f}^u_i &= - \int \underline{N}_i^{u^T} \underset{\sim}{F} \, ds \end{aligned}\right\} \tag{4.36}$$

This process is formally identical to that of solving an elastic solid problem with a high Poisson's ratio $\nu \to 0.5$.

A comparison with Equations (4.33) stresses the advantages of the penalty function; the only variables involved are the velocities and use of the constitutive Equation (4.13) renders the pressure variable which is then used to find the complete stress distribution. In coding terms this leads to considerable simplification.

4.4.6 Element Matrices

Examination of Equations (4.33) and (4.36) shows that elements with C^0 continuity are required for the velocity field but

discontinuous functions can be used to describe the pressure field in the velocity/pressure formulation. Indeed, practitioners[4.51] have found that, generally, a lower order of interpolation of the pressure field compared with that of the velocity field is desirable to avoid over-constraints.

The element used for the present investigation is the 4-node, bi-linear, isoparametric quadrilateral element. This element has proved to be the simplest effective one for use in both the mixed and the penalty function formulation[4.62,4.88].

For convenience of calculation it is usual practice to transform the actual coordinate system into a natural coordinate system, see Fig. 4.1*.

Thus, the following relationship may be written:-

$$r(\xi, \eta) = \sum_{i=1}^{4} N_i \, r_i \quad \text{and} \quad z(\xi, \eta) = \sum_{i=1}^{4} N_i \, z_i \tag{4.37}$$

where the shape functions, N_i, are expressed as[4.51]:-

$$N_i = \frac{1}{4} (1 + \xi \, \xi_i) \, (1 + \eta \, \eta_i) \tag{4.38}$$

and (r_i, z_i) and $(\xi_i \, \eta_i)$ are the coordinates of the nodal points in actual and natural coordinate systems respectively.

The (ξ, η) system shown in Fig. 4.1 is defined such that ξ and η vary from - 1 to + 1 within each element.

The velocity components u and v in the radial (r) and axial (z) directions respectively are assumed to be:-

---

* In this section all the derivation shall be made for the axi-symmetric case. Plane strain matrices can be found by deleting the appropriate terms.

$$u(\xi, \eta) = \sum_{i=1} N_i u_i \quad \text{and} \quad v(\xi, \eta) = \sum_{i=1} N_i v_i \tag{4.39}$$

If the velocity vector is noted as $\underset{\sim}{U}^T = \{u, v\}$ and the nodal point velocity vector as $u^T = \{u_1, v_1, u_2, v_2, u_3, v_3, u_4, v_4\}$, then according to Equation (4.15) the interpolation matrix $\underline{N}^u$ is given by:-

$$\underline{N}^u = \{\underline{N}_1, \underline{N}_2, \underline{N}_3, \underline{N}_4\} \tag{4.40}$$

where:-

$$\underline{N}_i = \begin{bmatrix} N_i & 0 \\ 0 & N_i \end{bmatrix} \tag{4.41}$$

Similarly, the operator matrix $\underline{L}$ can be defined as:-

$$\underline{L} = \{\underline{L}_1, \underline{L}_2, \underline{L}_3, \underline{L}_4\} \tag{4.42}$$

where:-

$$\underline{L}_i = \begin{bmatrix} \frac{\partial}{\partial r} & , & 0 \\ 0 & , & \frac{\partial}{\partial z} \\ 1/r & , & 0 \\ \frac{\partial}{\partial z} & , & \frac{\partial}{\partial r} \end{bmatrix} \tag{4.43}$$

Therefore, matrix $\underline{B}$ in Equation (4.28) can be expressed as:-

$$\underline{B} = \left[\underline{B}_1, \underline{B}_2, \underline{B}_3, \underline{B}_4\right] \tag{4.44}$$

where:-

$$\underline{B}_i = \begin{bmatrix} \dfrac{\partial N_i}{\partial r} & 0 \\ 0 & \dfrac{\partial N_i}{\partial z} \\ \dfrac{N_i}{r} & 0 \\ \dfrac{\partial N_i}{\partial z} & \dfrac{\partial N_i}{\partial r} \end{bmatrix} \tag{4.45}$$

To evaluate such matrices, two transformations are necessary. In the first place as N_i is defined in terms of local coordinates it is necessary to devise some means of expressing the global derivatives of Equation (4.44) in terms of local coordinates.

Secondly, the element volume over which the integrations are to be carried out needs to be expressed in terms of the local co-ordinates. Noting that:-

$$\begin{pmatrix} \dfrac{\partial N_i}{\partial \xi} \\ \dfrac{\partial N_i}{\partial \eta} \end{pmatrix} = \begin{pmatrix} \dfrac{\partial r}{\partial \xi} & \dfrac{\partial z}{\partial \xi} \\ \dfrac{\partial r}{\partial \eta} & \dfrac{\partial z}{\partial \eta} \end{pmatrix} \begin{pmatrix} \dfrac{\partial N_i}{\partial r} \\ \dfrac{\partial N_i}{\partial z} \end{pmatrix} = \left[J\right] \begin{pmatrix} \dfrac{\partial N_i}{\partial r} \\ \dfrac{\partial N_i}{\partial z} \end{pmatrix} \tag{4.46}$$

the derivatives in Equation (4.44) can be written as:-

$$\begin{pmatrix} \frac{\partial N_i}{\partial r} \\ \\ \frac{\partial N_i}{\partial z} \end{pmatrix} = \left[J\right]^{-1} \begin{pmatrix} \frac{\partial N_i}{\partial \xi} \\ \\ \frac{\partial N_i}{\partial \eta} \end{pmatrix} \tag{4.47}$$

in which $\left[J\right]$ is the Jacobian matrix which can be easily evaluated numerically.

Similarly:-

$$\left.\begin{aligned} dv &= |J|\ d\xi\ d\eta\ 2\pi\ r \\ \text{and:-} & \\ ds &= |J|\ d\xi\ d\eta \end{aligned}\right\} \tag{4.48}$$

The stress strain rate relationship, matrix $\underline{D}^o$ in Equation (4.30), is given by:-

$$\underline{D}^o = \begin{bmatrix} 1 & & & \\ & 1 & & \\ & & 1 & \\ & & & 1/2 \end{bmatrix} \tag{4.49}$$

noticing that:-

$$\underset{\sim}{\sigma}'^T = \left[\sigma'_r,\ \sigma'_z,\ \sigma'_\theta,\ \tau_{rz}\right]$$

and:-

$$\dot{\underset{\sim}{\varepsilon}}^T = \left[\dot{\varepsilon}_r, \dot{\varepsilon}_z, \dot{\varepsilon}_\theta, \dot{\gamma}_{rz}\right]$$

The $\underline{M}$ matrix is expressed as:-

$$\underline{M}^T = \left[1, 1, 1, 0\right] \tag{4.50}$$

For the element considered the pressure field is taken as constant within the element, hence:-

$$P = \underline{N}^p \, \underset{\sim}{p}^{(m)} = \sigma_m \tag{4.51}$$

Assuming that the inverse of $\left[J\right]$ can be found, the evaluation of the element properties is reduced to finding integrals of the following form:-

$$\int_{-1}^{1}\int_{-1}^{1} |J| \; f(\xi, \eta) \; 2\pi \; . \; r(\xi, \eta) \; d\xi \; d\eta \tag{4.52}$$

This is usually done using Gaussian quadrature, thus, Equation (4.51) is transformed to:-

$$\sum_{i=1}^{n}\sum_{j=1}^{n} W_i \; W_j \; f(\xi_i, \eta_j) \tag{4.53}$$

where W_i and W_j are weight coefficients and $f(\xi_i, \eta_j)$ is the value of the function to be integrated at the n^{th} point of integration.

4.4.7 Locking Effects in the Penalty Function Formulation

The penalty function formulation leads to a system of equations of the form:-

$$\underline{K}\,\underset{\sim}{u} + \underset{\sim}{f} \equiv (\underline{K}^{u} + \underline{K}^{\alpha})\,\underset{\sim}{u} + \underset{\sim}{f} = 0 \qquad (4.54)$$

In this system the matrices $\underline{K}^{u}$ and $\underline{K}^{\alpha}$ are finite, and a solution is sought when α (penalty number) $\rightarrow \infty$.

It is apparent that if $\underline{K}^{\alpha}$ is non-singular, then $\underset{\sim}{u} \rightarrow 0$ as $\alpha \rightarrow \infty$.

This illustrates a problem of over-constraint which causes the mesh to lock, resulting in worthless results. This problem of over-constraint of elements in the isochoric regime has been extensively discussed by Hughes et al[4.90], Fried[4.91], Malkus and Hughes[4.86] and Nagtegaal et al[4.49].

To alleviate this condition, $\underline{K}^{\alpha}$ must be made singular so that:-

$$\underline{K}^{\alpha}\,\underset{\sim}{u} = 0 \quad \text{but} \quad \underset{\sim}{u} \neq 0 \qquad (4.55)$$

The singularity (or its absence) is a function of the number of independent relations used at each integrating point. Zienkiewicz[4.51] states the condition for the presence of singularity in the following words: "If the number of such relations introduced at all the integrating points is less than that of the degrees of freedom available, then the singularity must exist" (op. cit, p. 288).

It is interesting to note that the wording of this statement is in the context of the existence of the singularity, for, as Zienkiewicz readily admits, the non-singularity is more difficult to prove.

It turns out that virtually all the commonly used conforming elements result in non-singular $\underline{K}^{\alpha}$ when "exact" numerical integration is performed. It is then possible to show[4.92] that singularity of $\underline{K}^{\alpha}$ is introduced for bi-linear quadrilaterals with a single point

integration.

Malkus and Hughes[4.86] have used an heuristic theory to predict the behaviour of elements and integration schemes. Briefly, the theory suggests that the most effective elements in applications of the type considered here are the so-called "Lagrange" isoparametric elements with appropriate selective-integration schemes. Triangular elements and "serendipidity" quadrilaterial elements are predicted to exhibit inferior behaviour, which has been confirmed numerically[4.49].

Thus, for the bi-linear quadrilateral element used in this work, one point integration is used to evaluate $\underline{K}^{\alpha}$. The 2 x 2 integration is retained on $\underline{K}^{u}$ so as to ensure non-singularity of $\underline{K}$ in Equation (4.54).

When this element is used in axisymmetric analysis, the property of "incompressibility in the mean", introduced by the under-integration, is lost. Nevertheless, the element is still convergent[4.88].

Recently, Bicanic and Hinton[4.93] have reported that reduced integration introduces extra zero energy modes. These extra modes can combine into either mechanisms, leading to singular stiffness matrices, or into near mechanisms which are spurious low energy modes which mask the solution. These zero energy modes on the element level combine into the well-known "hour-glassing" or "keystoning" mode for the 4-noded element and into the so-called "Escher" mode for the 2-noded element. In meshes formed from 8-noded elements these near mechanisms do not exist. They also found that elimination of the overall matrix singularity does not suppress the influence of the modes completely. If the modes are excited they can completely destroy the solution.

4.4.8 Solution Procedure

It is obvious that the systems of Equations (4.31) and (4.35) are non-linear and that an iterative mode of solution is needed.

In general, the most simple and direct solution procedure is a direct iteration which starts from the form:-

$$\underset{\sim}{K}\,\underset{\sim}{u} + \underset{\sim}{f} = 0 \tag{4.56}$$

in which:-

$$\underset{\sim}{K} = K\,(\dot{\underset{\sim}{\varepsilon}})$$

If initially a value of $\dot{\underset{\sim}{\varepsilon}} = \dot{\underset{\sim}{\varepsilon}}^{o}$ is assumed, an improved approximation is obtained as:-

$$\underset{\sim}{u}^{1} = -\,(\underset{\sim}{K}^{o})^{-1}\,f \tag{4.57}$$

where:-

$$\underset{\sim}{K}^{o} = \underset{\sim}{K}\,(\dot{\underset{\sim}{\varepsilon}}^{o})$$

Repetition of this process can be written as:-

$$\underset{\sim}{u}^{n} = -\,(\underset{\sim}{K}^{n-1})^{-1}\,\underset{\sim}{f} \tag{4.58}$$

and the process is terminated when the error is sufficiently small.

This system of solution has been applied successfully to metal forming problems[4.75,4.80] and gives very rapid convergence, provided the forcing function is specified as velocities.

4.4.8.1 Sequence of Operation

We start from a prescribed initial effective strain rate distribution, namely, a uniform distribution. The system of

equations is then solved and the velocities thereof computed are used to evaluate a new strain rate distribution which modifies the system of equations accordingly.

Iterations of the type described in Equation (4.58) are then performed. For the analysis of non-steady state processes, the problem is analyzed in a step-by-step manner by treating it quasi-linearly during each step of incremental deformation. A proper increment size is chosen to justify this approximation.

The convergence is measured by the quantity $||\Delta\underset{\sim}{u}||/||\underset{\sim}{u}||$, where the euclidean vector norm is defined by:-

$$||\underset{\sim}{u}|| = \sqrt{\sum_{i=1}^{N} \{(u_r)_i^2 + (u_z)_i^2\}} \qquad (4.59)$$

The solution with a reasonable accuracy is accepted as the final velocity distribution. At this stage the new geometry of the deformed material is determined by adding the nodal point velocities incrementally to the current coordinates of the nodal points.

In the steady-state process, since the velocity solution for the current geometry is also the solution for the subsequent steps, the process of incremental addition of the velocity distribution for the determination of the new geometry is not required.

Computer programs based on the formulations developed in this chapter are presented in Appendix 2.

REFERENCES

4.1 ODEN, T. J. and REDY, J.
"Mathematics of the Finite Element Method".

4.2 MENDELSON, A. and MANSON, S. S.
"Practical Solutions of Plastic Deformation Problems in the Elastic-Plastic Range".
NASA TR R28, (1959).

4.3 GALLAGHER, R. H., PADLOY, J. and BIJLAARD, P. P.
"Stress Analysis of Heated Complex Shapes".
ARS Journal, May, pp. 700-707, (1962).

4.4 PADLOG, J., HUFF, R. D. and HOLLOWAY, G. F.
"The Unelastic Behaviour of Structures Subjected to Cyclic, Thermal and Mechanical Stressing Conditions".
Bell Aerosystems Company, Report WPADD TR60-271, (1960).

4.5 PERCY, J. H., LODEN, W. A. and NAVARATNA, D. R.
"A Study of Matrix Analysis Methods for Inelastic Structures".
RTD-TDR-63-4032, October, (1963).

4.6 ARGYRIS, J. H., KEBEY, S. and KAMEL, W. H.
"Matrix Methods of Structural Analysis. A Precis of Recent Development".
Proc. 14th Meeting of Structures and Materials Panel, AGARD, (1963).

4.7 JENSEN, W. R., FALBY, W. E. and PRINCE, N.
"Matrix Analysis Methods for Anisotropic Inelastic Structures".
AFFDL-TR-65-220, (1966).

4.8 POPE, G. G.
"A Discrete Element Method for the Analysis of Plane Elastic-Plastic Stress Problems".
Royal Aeronautical Establishment, TR 65028, (1965). Later Published in The Aer. Quarterly, 17, pp. 83-104, (1966).

4.9 SWEDLOW, J. L. and YANG, W. H.
"Stiffness Analysis of Elastic-Plastic Plates".
Graduate Aeronautical Laboratory, California Institute of Technology, SM65-10, (1965).

4.10 MARCAL, P. V. and KING, I. P.
"Elastic-Plastic Analysis of Two-Dimensional Stress Systems by the Finite Element Method".
Int. Jnl. of Mechanical Sciences, Vol. 9, No. 3, (1967).

4.11 YAMADA, Y., YOSHIMURA, N. and SAKURAI, T.
"Plastic Stress-Strain Matrix and its Application for the Solution of Elastic-Plastic Problems by the Finite Element Method".
Int. Jnl. of Mech. Sci., Vol. 10, pp. 343-354, (1968).

4.12 YAMADA, Y., YOSHIMURA, N., KAWAI, T. and SAKURAI, T.
"Analysis of the Elastic-Plastic Problems by the Matrix Displacement Method".
Proc. 2nd Conf. on Matrix Methods in Structural Mechanics, Airforce Institute of Technology, pp. 1271-1299, (1968)

4.13 IWATA, K., OSAKADA, K. and FUJINO, S.
"Analysis of Hydrostatic Extrusion by the Finite Element Method".
Trans. ASME, J. of Engng. for Ind., Vol. 84, pp. 697-703, (1972).

4.14 NAGAMATSU, A., MUROTA, T. and JIMMA, T.
"On the Non-Uniform Deformation of a Block in Plane-Strain Caused by Friction".
Bull. of the JSME, 13, pp. 1385-1402, (1970) and 14, pp. 314-330, (1971).

4.15 LEE, C. H. and KOBAYASHI, S.
"Analyses of Axisymmetric Upsetting and Plane-Strain Side Pressing of Solid Cylinders by the Finite Element Method".
Trans. of ASME, J. of Engng. for Ind., Vol. 93, pp. 445-454, (1971).

4.16 LEE, C. H. and KOBAYASHI, S.
"Elastoplastic Analysis of Plane-Strain and Axisymmetric Flat Punch Indentation by the Finite Element Method".
Int. J. Mech. Sci., Vol. 12, pp. 349-370, (1970).

4.17 LEE, C. H., IWASAKY, H. and KOBAYASHI, S.
"Calculation of Residual Stresses in Plastic Deformation Processes".
Trans. ASME, J. of Engng. for Ind., Vol. 95, pp. 283-291, (1973).

4.18 LEE, C. H., MASAKI, S. and KOBAYASHI, S.
"Analysis of Ball Indentation".
Int. J. Mech. Sci., Vol. 14, pp. 417-426, (1972).

4.19 LEE, C. H.
"Numerical Analysis of the Mechanics of Plastic Deformation Problems".
Ph.D. Dissertation, University of California, Berkeley, (1970).

4.20 ZIENKIEWICZ, O. C., VALLIAPAN, S. and KING, J. P.
"Elasto-Plastic Solutions of Engineering Problems, 'Initial Stress' Finite Element Approach".
Int. J. Num. Meths. Engng., 1, pp. 75-100, (1969).

4.21 NAYAK, G. C. and ZIENKIEWICZ, O. C.
"Elasto-Plastic Stress Analysis : A Generalization for Various Constitutive Relations, Including Strain Softening".
Int. J. Num. Meths. Engng., 5., pp. 113-135, (1972).

4.22 NAYAK, G. C.
"Plasticity and Large Deformation Problems by the Finite Element Method".
Ph.D. Thesis, University of Wales, Swansea, (1971).

4.23 HARTLEY, P., STURGESS, C. E. N. and ROWE, G. W.
"Friction in Finite-Element Analyses of Metal Forming Processes".
Int. J. Mech. Sci., Vol. 21, p. 301, (1979).

4.24 NAJAFI-SANI, A.
Ph.D. Thesis (to be submitted), Imperial College, University of London.

4.25 NAJAFI-SANI, M.
Ph.D. Thesis (to be submitted), Imperial College, University of London.

4.26 WONG, V. G. and DAS, M. K.
"Analysis of Stresses in Bar Cropping".
15th Int. M.T.D.R. Conf., Birmingham, (1974). See also: AHMED, M. H. M. and DAS, M. K. "A Study of Stresses in the Double Cropping Process", 18th Int. M.T.D.R. Conf., London, (1977).

4.27 ODELL, E. I.
"A Study of Wall Ironing by the Finite Element Technique".
Trans. of ASME, J. of Engng. Ind., Vol. 10, pp. 31-36, (1978).

4.28 LEE, E. H.
"Stress Analysis of Metal Forming Problems".
Engineering Plasticity : Theory of Metal Forming Processes, Vol. 1, Editor: H. Lippmann, Springer-Verlag, (1977).

4.29 RICE, J. R.
"A Note on the 'Small Strain' Formulation for Elastic-Plastic Problems".
Technical Report N00014-67-A0191-0003/8, Division of Engineering, Brown University, (1970).

4.30 McMEEKING, R. M. and RICE, J. R.
"Finite Element Formulations for Problems of Large Elastic-Plastic Deformation".
Int. J. Solids Structures, 11, pp. 601-616, (1975).

4.31 MARCAL, P. V.
"Finite Element Analysis of Combined Problems of Non-Linear Material and Geometric Behaviour".
Proc. ASME Joint Computer Conf. on Computational Approach to Applied Mechanics, pp. 133-147, Chicago, (1969).

4.32 HIBBIT, D. H., MARCAL, P. V. and RICE, J. R.
"A Finite Element Formulation for Problems of Large Strain and Large Displacements".
Int. J. Solids Structures, 6, pp. 1069-1086, (1970).

4.33 GORDON, J. L. and WEINSTEIN, A. S.
"A Finite Element Analysis of the Plane-Strain Drawing Problem".
Proc. 2nd N.A.M.R.C., pp. 194-208, (1974).

4.34 BLASS, A.
"A Finite Element Approach in Metalworking and its Application to the Radial Upsetting Process".
Ph.D. Thesis, Imperial College, London, (1976).

4.35 KITAGAWA, H., SEGUCHI, Y. and TOMITA, Y.
"An Incremental Theory of Large Displacements and its Finite Element Formulation".
Ing. Archiv., 41, pp. 213-224, (1972).

4.36 OSIAS, J. R.
"Finite Deformation of Elasto-Plastic Solids".
NASA CR-2199, (1973).

4.37 OSIAS, J. R. and SWEDLOW, J. L.
"Finite Elasto-Plastic Deformation, I - Theory and Numerical Examples".
Int. J. Sols. Struct., 10, pp. 321-339, (1974).

4.38 OSIAS, J. R. and SWEDLOW, J. L.
"Finite Elasto-Plastic Deformation, II - Necking in Tensile Bars".
Report SM-73-4, Dept. Mech. Eng., Carnegie Mellon University, (1973).

4.39 SWEDLOW, J. L.
"Approaches to Non-Linear Problems: The Example of Plasticity".
Proc. ASME Joint Computer Conf. on Computer Approach to Appl. Mech., pp. 191-199, Chicago, (1969).

4.40 SWEDLOW, J. L.
"Character of the Equations of Elastic-Plastic Flow in Three Independent Variables".
Int. J. Non-Linear Mech., 3, pp. 325-336, (1968).

4.41 GUNASEKERA, J. S. and ALEXANDER, J. M.
"Matrix Analysis of the Large Deformation of an Elastic-Plastic Axially Symmetric Continuum".
Symp. on Foundations of Plasticity, (edited by A. Sawczuk), pp. 125-146, Noordhoff, Leyden, (1973).

4.42 LEE, E. H., MALLET, R. L. and YANG, W. H.
"Stress and Deformation Analysis of the Metal Extrusion Process".
Comp. Meths. Appl. Mech. Eng., 10, pp. 339-353, (1977).

4.43 LEE, E. H., MALLET, R. L. and McMEEKING, R. M.
"Stress and Deformation Analysis of Metal Forming Processes".
Numerical Modelling of Manufacturing Process, Editors - R. F. Jones, Jnr., H. Armen and J. T. Fong, ASME, New York, pp. 19-33, (1977).

4.44 LEE, E. H. and MALLET, R. L.
"Determination of the Mechanical State of a Cold Worked Structural Component".
Trans. 4th Int. Conf. on Structural Mechanics of Reactor Technology, Vol. L, Paper L1/7, pp. 1-9, (1977).

4.45 OH, S. I., CHEN, C. C. and KOBAYASHI, S.
"Ductile Fracture in Axisymmetric Extrusion and Drawing. Part 2 - Workability in Extrusion and Drawing".
Trans. ASME, J. Engng. Ind., Vol. 101, pp. 36-44, (1979).

4.46 YAMADA, Y and HIRAKAWA, H.
"Large Deformation and Instability Analysis in Metal Forming Processes".
Application of Numerical Methods to Forming Processes, Editors - H. Armen and R. F. Jones, Jnr., ASME, New York, pp. 27-38, (1978).

4.47 DERBALIAN, K. A., LEE, E. H., MALLET, R. L. and McMEEKING, R. M.
"Finite Element Metal Forming Analysis with Spacially Fixed Mesh".
Ibid., pp. 39-47.

4.48 YAMADA, Y., ITO, K. YOKOUCHI, Y., TAMANO, T. and OHTSUBO, T.
"Finite Element Analysis of Steady Fluid and Metal Flow".
Finite Elements in Fluids, Vol. 1, John Wiley & Sons, p. 73, (1975).

4.49 NACTEGAAL, J. C., PARKS, D. M. and RICE, J. R.
"On Numerically Accurate Finite Element Solutions in the Fully Plastic Range".
Comp. Meth. Appl. Mech. Eng., 4, pp. 153-178, (1974).

4.50 ARGYRIS, J. H., DUNNE, P. C., ANGELOPOULOS, T. and BICHAT, B.
"Large Natural Strains and Some Special Difficulties due to Non-Linearity and Incompressibility in Finite Elements".
Comp. Meth. Appl. Mech. Eng., 4, p. 210, (1974).

4.51 ZIENKIEWICZ, O. C.
"The Finite Element Method".
3rd Edition, McGraw-Hill, p. 469, (1977).

4.52 ARGYRIS, J. H., DUNNE, P. C. and MÜLLER, M.
"Isochoric Constant Strain Finite Elements".
Comp. Meths. Appl. Mech. Eng., Vol. 13, pp. 245-278, (1978).

4.53 GOON, G. Y.
"Conformal Mapping and Variational Methods in Metal Flow Problems".
Internal Report, University of Aston, (1972).

4.54 GODBOLE, P. N.
Ph.D. Thesis, University College of Swansea, (1974).

4.55 ZIENKIEWICZ, O. C. and GODBOLE, P. N.
"Flow of Plastic and Visco-Plastic Solids with Special Reference to Extrusion and Forming Processes".
Int. J. Num. Meth. in Eng., 8, pp. 3-16, (1974).

4.56 LUNG, M.
"Anwending der Methode der Finite Elemente zur Untersuchung stationärer Umformverfahren".
Z. Angew. Math. Mech., Vol. 52, No. 4, pp. 63-65, (1972).

4.57 LEE, C. H. and KOBAYASHI, S.
"A Matrix Method of Analysis for Plastic Deformation Mechanics and its Application to Viscioplasticity".
Presented at the 22nd General Assembly of International Institution of Production Engineering Research, Stockholm, Sweden, August, (1974).

4.58 JAIN, P. C.
Ph.D. Thesis, University of Wales, October, (1976).

4.59 LUNG, M. and MAHRENHOLTZ, O.
"A Finite Element Procedure for Analysis of Metal Forming Processes".
Transactions of the CSME, Vol. 2, pp. 32-36, (1973-1974).

4.60 MAHRENHOLTZ, O. and KLLE, W.
"Plane and Axisymmetric Rigid-Plastic Deformation Using the Finite Element Method".
Proc. of the 5th Canadian Congress of Applied Mechanics, pp. 95-96, (1975).

4.61 ROLL, K.
"Calculation of Metal Forming Processes by Finite Element Methods".
Presented at CIRP Meeting, (1978).

4.62 LEE, C. H. and KOBAYASHI, S.
"New Solutions to Rigid Plastic Deformation Problems Using a Matrix Method".
Trans. ASME, J. of Engng. for Ind., Vol. 95, pp. 865-873, (1973).

4.63 SHAH, S. N., LEE, C. H. and KOBAYASHI, S.
"Compression of Tall, Circular, Solid Cylinders Between Parallel Flat Dies".
Proc. Int. Conf. Prod. Engng., Tokyo, pp. 295-300, (1974).

4.64 SHAH, S. N. and KOBAYASHI, S.
"Rigid-Plastic Analysis of Cold Heading by the Matrix Method".
Proc. 15th Int. MTDR Conf., pp. 603-610, (1974).

4.65 LEE, S. H. and KOBAYASHI, S.
"Rigid Plastic Analysis of Bore Expanding and Flange Drawing with Anisotropic Sheel Metals by Matrix Method".
Ibid., p. 561.

4.66 SHAH, S. N. and KOBAYASHI, S.
"A Theory on Metal Flow in Axisymmetric Piercing and Extrusion".
J. Prod. Eng., Vol. 1, pp. 73-108, (1977).

4.67 CHEN, C. H., OH, S. I. and KOBAYASHI, S.
"Ductile Fracture in Axisymmetric Extrusion and Drawing. Part 1 : Deformation Mechanics of Extrusion and Drawing".
Trans. ASME, J. of Engng. for Ind., Vol. 101, pp. 23-35, (1979).

4.68 MATSUMOTO, H., OH, S. I. and KOBAYASHI, S.
"A Note on the Matrix Method for Rigid-Plastic Analysis of Ring Compression".
Proc. of the 18th MTDR Conf., London, pp. 3-9, (1977).

4.69 CHEN, C. C. and KOBAYASHI, S.
"Rigid Plastic Finite Element Analysis of Ring Compression".
Application of Numerical Methods to Forming Processes, AMD - Vol. 28, pp. 163, 174, ASME, New York, (1978).

4.70 GOTOH, M. and ISHUE, F.
"A Finite Element Analysis of Rigid-Plastic Deformation of the Flange in a Deep Drawing Process Based on a Fourth Degree Yield Function".
Int. J. Mech. Sci., Vol. 20, pp. 423-435, (1978).

4.71 TOMITA, Y. and SOWERBY, R.
"An Approximate Analysis for Studying the Plane Strain Deformation of Strain Rate Sensitive Materials".
To be published.

4.72 ZIENKIEWICZ, O. C.
"Constrained Variational Principles and Penalty Function Methods in the Finite Element Analysis".
Lecture Notes in Mathematics, No. 363, Springer-Verlag, pp. 207-214, (1974).

4.73 ZIENKIEWICZ, O. C. and GODBOLE, P. N.
"Penalty Function Approach to Problems of Plastic Flow of Metals with Large Surface Deformation".
J. Strain Analysis, Vol. 10, pp. 180-183, (1975).

4.74 ZIENKIEWICZ, O. C. and GODBOLE, P. N.
"Viscous Incompressible Flow with Special Reference to Non-Newtonian (Plastic) Flow".
Finite Elements in Fluids, (Editors - J. T. Oden, O. C. Zienkiewicz, R. H. Gallagher and C. Taylor), Vol. I, Ch. 2, pp. 25-71, (1975).

4.75 ALEXANDER, J. M. and PRICE, J. W. H.
"Finite Element Analysis of Hot Metal Forming".
Proc. 18th Int. MTDR Conf., pp. 267-274, London, (1977).

4.76 SHARMAN, F. W.
Electricity Council Report R581, (1975).

4.77 CORNFIELD, G. C. and JOHNSON, R. H.
"Theoretical Prediction of Plastic Flow in Hot Rolling Including the Effect of Various Temperature Distributions".
J. of Iron and Steel Institute, 211, pp. 567-573, (1973).

4.78 TURNER, T. W.
Ph.D. Thesis, University of London, (1973).

4.79 ALEXANDER, J. M. and TURNER, T. W.
"A Preliminary Investigation of the Dieless Drawing of Titanium and Some Steels".
Proc. of the 15th Int. MTDR Conf., (1975).

4.80 PRICE, J. W. H. and ALEXANDER, J. M.
"A Study of Isothermal Forming or Creep Forming of a Titanium Alloy".
4th NAMRC, Batelle, Columbus, Ohio, (1976).

4.81 PRICE, J. W. H. and ALEXANDER, J. M.
"The Finite Element Analysis of Two High Temperature Metal Deformation Processes".
2nd Int. Symp. on Finite Elements in Flow Problems, Santa Margherita, Ligure, Italy, (1976).

4.82 ZIENKIEWICZ, O. C., JAIN, P. C. and OÑATE, E.
"Flow of Solids During Forming and Extrusion Some Aspects of Numerical Solutions".
University College of Swansea, Report C/R/283/76, (1976).

4.83 ZIENKIEWICZ, O. C., OÑATE, E. and HEINRICH, J. C.
"Plastic Flow in Metal Forming, I - Coupled Thermal Behaviour in Extrusion, II - Thin Sheet Forming".
Applications of Numerical Methods to Forming Processes, AMD - Vol. 28, ASME, New York, (1978).

4.84 ZIENKIEWICZ, O. C. and OÑATE, E.
"Finite Element Solutions of Metal Forming Using the Plastic Flow Approach".
Presented at the Int. Cong. Num. Meths. Engng., Paris, November, (1978).

4.85 KANAZAWA, K. and MARCAL, P. V.
"Finite Element Analysis of the Steel Rolling Process".
Applications of Numerical Methods to Forming Processes, AMD - Vol. 28, ASME, New York, (1978).

4.86 MALKUS, D. S. and HUGHES, T. J. R.
"Mixed Finite Element Methods - Reduced and Selective Integration Techniques : A Unification of Concepts".
Comp. Meths. in Appl. Mech. Engng., Vol. 15, pp. 63-81, (1978).

4.87 ODEN, J. T.
Computers and Structures, Vol. 8, pp. 445-449, (1978).

4.88 HUGHES, T. J. R., LIU, W. K. and BROOKS, A.
"Finite Element Analysis of Incompressible Viscous Flow by the Penalty Function Formulation".
J. of Comp. Physics, Vol. 30, pp. 1-60, (1979).

4.89 ODEN, J. T.
Computers and Structures, Vol. 8, pp. 445-449, (1978).

4.90 HUGHES, T. J. R., TAYLOR, R. L. and LEVY, J. E.
"A Finite Element Method of Incompressible Flow".
Proc. Conf. Finite Element Methods in Flow Problems, pp. 1-16, Sta. Margherita, Italy, (1976).

4.91 FRIED, I.
"Finite Element Analysis of Incompressible Materials by Residual Energy Balancing".
Int. J. Sol. Struct., 10, pp. 993-1000, (1976).

4.92 ZIENKIEWICZ, O. C. and HINTON, E.
"Reduced Integration, Function Smoothing and Non-Conformity in Finite Element Analysis".
J. Franklin Inst., 302, pp. 443-461, (1976).

4.93 BICANIC, N. and HINTON, E.
"Spurious Modes in Two Dimensional Isoparametric Elements".
Int. J. Num. Meths. Engng., Vol. 14, p. 1545, (1979).

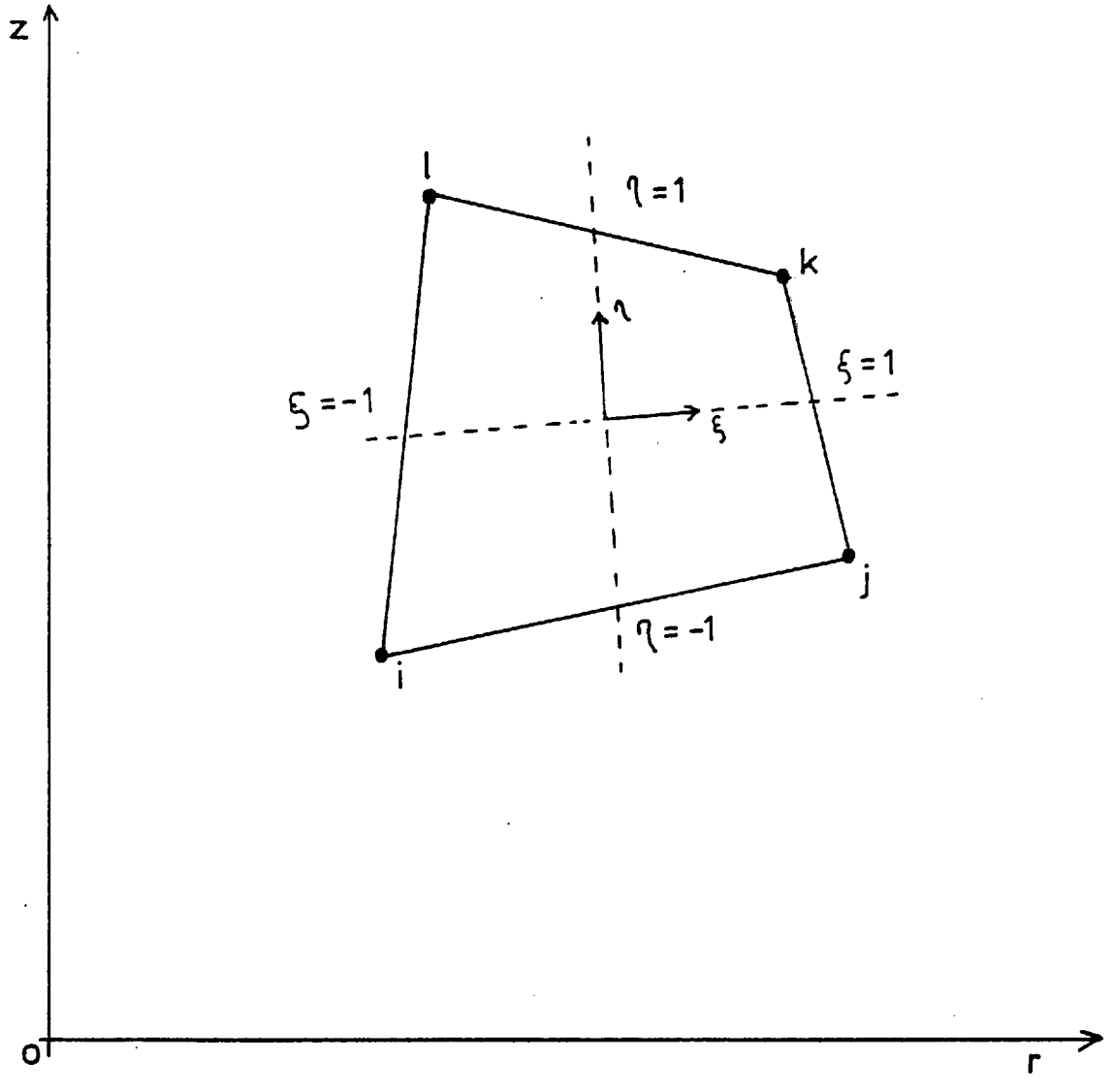

Figure 4.1: Bilinear Isoparametric Element

CHAPTER 5

EXTRUSION

5.1 Introduction

Extrusion is believed to be one of the more recently developed metal forming processes, and was probably first used at the end of the 18th century for the manufacture of lead pipes. The book by Pearsons and Parkins[5.1] gives a survey of the subject and provides a good account of the historical development of the process.

In the actual operation, whether it be conducted by the direct, indirect or hydrostatic method, the billet is compressed as it is forced through the die which is shaped to give the required cross-section, thereby reducing the area of the cross-section and increasing the length of the workpiece (see Fig. 5.1).

The important parameters of the process are: the amount of reduction, friction along the die and container walls, the work hardening properties of the material and the semi-cone angle of the dies (in the case of axisymmetrical extrusion).

The complex inter-relation of all these variables makes an analysis of the detailed mechanics of the process very difficult, although a number of approximate analyses have been carried out.

The finite element technique has the capability of analyzing the process in a detailed way, giving not only information on the power requirements of the process, but also information on the complex mechanics of the process.

The object of this chapter is twofold. Firstly, it will present solutions to some extrusion problems using the computer codes developed following the theory outlined in the previous chapter (see Appendix 2), stressing the comparative performance of the "penalty function" and the "velocity-pressure" formulation. Secondly, the problems are chosen so that techniques for dealing with boundary conditions and introduction of work-hardening can be assessed. At the same time, results are compared with known solutions, when available.

5.2 Previous Work

For the purpose of this work, we will only consider a limited selection of the extensive literature available in order to illustrate the range of theoretical methods.

The first rational relationship between the extrusion pressure and reduction in area was developed by Siebel and Fauymeien[5.2] in 1931, using a deformation energy approach. Since then, many valuable contributions have been made to research in the field of extrusion. However, until recently, attention has been traditionally focussed mainly on predicting the extrusion pressure, indeed, research in this direction is all but exhausted.

The free body equilibrium approach, i.e. the slab or force balance technique, has been favoured by a number of workers in the analysis of direct extrusion[5.3]. This technique is simple to apply and gives useful results. However, by virtue of ignoring the effects of redundancy on the one hand and of the pattern of flow on the other, it gives an oversimplified view of the mechanics of the process.

The upper bound approach for both plane strain and axisymmetric direct and indirect extrusion has been treated by Johnson and Kudo[5.4] for a variety of solutions for different conditions. The work of Avitzur[5.5] describes the application of the upper method to axisymmetric direct, indirect and hydrostatic extrusion. The method can provide reasonable agreement with experimental data when assessing the effect of the different parameters of the process on the extrusion pressure. Avitzur, op. cit. and Ref.[5.23] has also tried to extend the technique to predict the range of parameters over which the most common extrusion defects, such as "chevroning" and the formation of "dead metal zones", are most likely to occur.

The upper bound approach does not, in general, predict stress distribution and, therefore, does not give an insight into the

mechanics of the process, excepting the assumed kinematically acceptable velocity field. The likelihood of a process occurring is determined on the basis of the energy consumed which in itself is dependent on the accuracy of the assumed velocity field.

The slip-line theory[5.6] has been extensively applied to plane extrusion problems and results are found to agree fairly well with experiments. A survey of the modern literature up to 1969 is provided in the book by Johnson et al. Recently, matrix techniques for the construction of slip-line fields[5.7] have come to the fore and have been employed to tackle the problem of asymmetric plane extrusion[5.8].

The visioplasticity technique[5.9,5.10] is particularly well adapted to the needs of the extrusion problem and has, therefore, become a major analytical tool in the study of the pattern of flow and the determination of redundant deformation. However, it should be regarded as an aid for interpreting experimental data rather than for prediction.

Extrusion problems have also received attention from finite element workers. A survey of that work is given in the preceding chapter and will not be repeated here except when required.

5.3 Plane Strain Extrusion Through a Square Die, Reduction = 0.5

This problem has attracted great interest in the past[5.11]. Here we consider a steady-state, plane, ideally plastic metal extrusion through a square die with 50% reduction in area.

The walls of the container and die are assumed to be frictionless and the product is moving in a parallel stream. The reason for including this problem is that a slip-line solution exists[5.6] and comparison with the two finite elements techniques used in this work can be readily made.

Computational Conditions

The dimensions of the problem, together with the mesh and boundary conditions used are shown in Fig. 5.2. A constant yield stress value of 120 MN/m^2 was used.

A cut-off value for the rigid regions of $\gamma = 10^9$, where $\gamma = 2/3\ (\bar{\sigma}/\dot{\bar{\varepsilon}})$, was specified.

The extrusion pressure and the distribution of velocity at the die exit were chosen as the main indicators of the accuracy of the solution.

The problem was first solved using the "velocity-pressure" formulation and dealing with the singularity at point A (Fig. 5.2) in two different ways. Firstly, point A was taken as belonging to the die and the boundary condition specified accordingly. Secondly, the mesh was made singular at this point; this was carried out by making collapse the element at the die exit as shown in Fig. 5.2b. A comparison of the results is made in Table 5.1.

TABLE 5.1

	No singularity	Singularity
P/2k	1.52	1.40
U*	2.16	2.04

Slip line solution (after Johnson[5.6])

P/2k = 1.29

P = Extrusion pressure

U* = Velocity at exit (cm/sec) at x = 19 cm

It is evident that the mesh with the singularity at the die corner gives a better solution, particularly with respect to the velocity distribution at the exit.

Next, the problem was solved using the singular mesh with the penalty function formulation and varying the value of the penalty parameter (α) to assess its influence. For this study, the hydrostatic stress distributions, calculated directly in the u/p formulation and by using $\sigma_m = \alpha \dot{\varepsilon}_v$ in the penalty-function, were compared to assess the level of equivalence between the two methods. The results are shown in Fig. 5.3 and Table 5.2.

It is clearly seen that a low value of α renders useless results, due to the fact that too great an error is introduced in the compressibility. This is reflected in the values of the velocity at the exit. An increase of the value of α results in a noticeable improvement not only in the extrusion pressure and exit velocity but also in the hydrostatic stress. For a value of $\alpha = 10^8$ the results of both methods are practically equal and compare favourably with the slip-line results.

Fig. 5.4 shows the velocity distribution and the flow lines calculated in comparison with the slip-line field. It is clear that this also compares very well. Worth mentioning is the fact that the velocities in the dead zone (predicted by the slip-line theory) are indeed very small, and that the velocity vectors at the exit are in fact parallel to the horizontal plane.

5.4 Plane Strain Extrusion Through a Wedge Shaped Die, $R = 0.5$, $\alpha_D = 45^o$

This problem was chosen for two main reasons. First to check the capability of the computer code to deal with skewed boundaries, and second, because it has a known slip-line solution and presents

another chance of comparing the "velocity-pressure" and "penalty function" formulations. Moreover, similar problems to these have been previously solved with finite elements using various different approaches[5.12,5.15,5.16] so comparisons can be readily made.

The continuum to be discretized and boundary conditions are shown in Fig. 5.5.

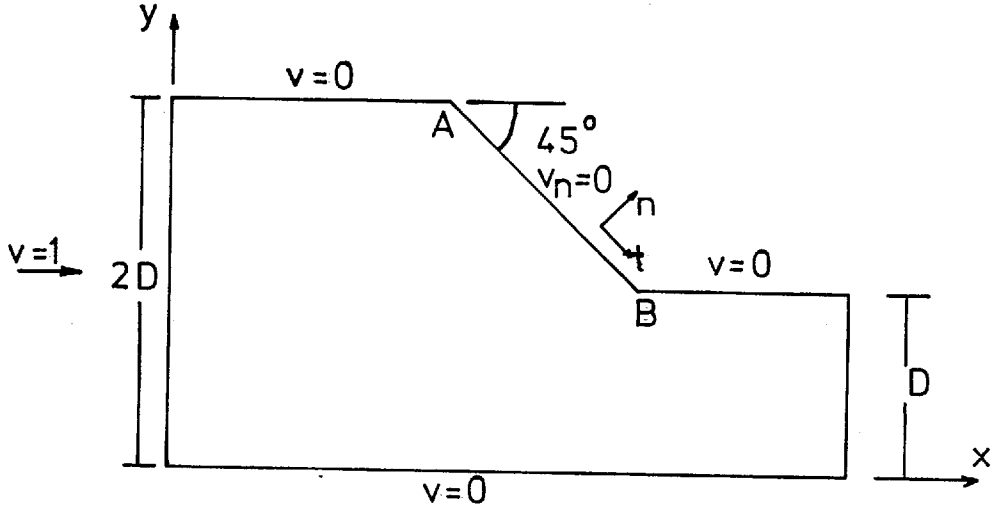

Fig. 5.5

The problem was initially solved using the velocity-pressure formulation and taking singularity points A and B as part of the die face, i.e. the velocities parallel to it. Again a constant yield stress of 120 MN/m^2 and a cut-off factor (γ) equal to 10^9 were selected.

The results obtained, although giving a satisfactory velocity distribution showed a gross over-evaluation of the extrusion pressure when compared with the slip-line solution as given by Ref.[5.12]. An increase in the number of elements produced a slight improvement in the results. Table 5.3 gives the results for various meshes and Fig. 5.6 shows the finest mesh used together with the calculated velocity

distribution.

TABLE 5.3

No. of Elements	P/2k
84	1.080
120	1.030
156	0.994
300	0.985
Slip-line*	0.950

$$k = Y/\sqrt{3}$$

The problem was then solved using the "penalty function" formulation and similar results were obtained.

It appeared, then, that the bi-linear quadrilateral element was inadequate for this kind of problem, especially in view of the results reported by Godbole[5.12] for the same problem using the "penalty function" and under-integrated quadratic elements.

It was then decided to implement the aforementioned elements within the existing program (penalty-function). The mesh was the same as the one used in Ref.[5.12], and with the same boundary conditions as before, see Fig. 5.7.

The solution, shown in Fig. 5.8, was completely different from the one presented by Godbole (see Fig. 5.9) or the one

---

* This value for the slip-line solution is given in Ref.[5.12] and it was wrongly taken, as it will be shown, as the standard to compare our initial solution.

(apparently misprinted) in Refs.[5.13,5.14].

A closer look into Godbole's solution suggests that he used a different boundary condition, namely, assuming the direction of the velocity at the exit singularity to be horizontal. This, of course, is no more than an educated guess since the treatment of the die corners is not explicitly stated in his work. This boundary condition was implemented and the results are shown in Fig. 5.10. The velocity distributions compare now very well but the load is still far from close.

This failure to duplicate previous work led to a careful examination of the computer code. This examination revealed no apparent errors; indeed, solution of the problem discussed in the previous section, using quadratic elements, produced an identical solution to that of Jain[5.15] who used a computer code similar to that of Godbole.

On the other hand, a careful analysis of Godbole's work revealed that his results reported as slip-line solution were, in fact, wrong, when compared to the ones reported in Johnson's definitive work[5.17]. The slip-line solution of the problem was then recalculated and the result confirmed that of Johnson (see Table 5.4).

TABLE 5.4

	P/2k
Godbole[5.12]	0.950
Johnson[5.16]	0.900
Our solution	0.903

Slip-line Solutions

This mis-quotation (or mis-calculation, as the case may be) in Godbole's work was traced back to an earlier paper by Nayak and Zienkiewicz[5.15]. Furthermore, Godbole's results converged to his slip-line solution from below, whereas the rest of his solution to other extrusion problems converged from above, showing an inconsistency that was not explained. All this casts doubts over Godbole's reported solution of this specific problem, or at least, what boundary conditions were used.

Thus, there is still a problem to be solved and ways to improve the solution will now be discussed.

5.4.1 Boundary Conditions at the Entry and Exit Corners

In the previous section, we have seen how a change in the boundary condition at the exit corner caused the estimated extrusion pressure to be reduced. This suggests that these conditions play a major part (apparently not previously considered) in the solution of the extrusion problem.

Of course, it is not feasible to try and obtain an identical solution to that of the slip-line field because of the basic difference between that theory and the finite element method. Nevertheless, some improvement in the solution by finite elements is possible and, indeed, desirable.

The initial choice of boundary conditions at points A and B (see Fig. 5.5) stems from the finite element elasto-plastic solutions of similar problems (see Refs.[5.15,5.16].

These solutions solve the problem in a "Lagrangian" frame of reference, i.e. the elements are part of a continuum and deform with it. On the other hand, the formulation used in this work is an "Eulerian" description, that is, the elements are fixed in space. This basic difference seems to be the cause of the failure of the boundary

conditions.

To understand more fully the mechanics of the process let us look in more detail at a region close to the entry corner (see Fig. 5.11).

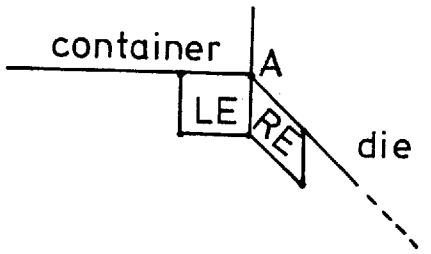

Fig. 5.11

To facilitate the discussion let us assume that both the container and the die are frictionless.

It can be safely assumed that material close to the outermost boundary is moving parallel to the container just before A. Equally, material after A is moving parallel to the die. However, the direction of flow at point A is far from known a priori, indeed, the slip-line theory predicts a singularity at this point.

In a Lagrangian frame of reference it could be assumed that when material comes into contact with the die it slides along it. However, in the Eulerian frame such an assumption would involve the velocity at that point being parallel to the die and this will have an entirely different physical meaning which now will be discussed.

If it is assumed that the direction of flow at the point A is parallel to the container, what this actually implies, in the finite element context, is that material does not begin to distort until it has crossed into the region represented by element RE

(Fig. 5.11). Consequently, the redundant strain at the die corner is being under-estimated, and the extrusion pressure will be accordingly under-estimated.

On the other hand if material at point A is assumed to be moving parallel to the die, the opposite will occur: material will begin to shear when entering the region represented by element LE, resulting in a corresponding over-estimation of the redundant strain and extrusion load.

Obviously, one simple way of reducing the problem will be to use a finer mesh around the corner A. This seems to be a rather simplistic way of solving the problem because of the corresponding complication of the strain rate integration procedure (this will be discussed in another section), and the boundary condition at the point will still have to be chosen arbitrarily.

Another more formal way is to introduce the singularity into the formulation. This has been done by Shen et al[5.18] for fluid problems using a special element whose trial functions are only the corner eigenfunctions. This seems an unnecessary complication to solve a problem which, although theoretically predicted, does not necessarily occur in "real-life" problems.

Problems, in practice, seldom present sharp cornered dies which will impose the mathematical singularity present in the slip-line field solution. More often than not, the transition of flow is a "smooth" one and this is up to a point, what the above analysis of the flow around the corner suggests. It would seem that a boundary condition somewhere between the two extremes discussed would be more realistic and this condition could be chosen on an ad hoc basis for each problem. However, this would obviously be as arbitrary as the original choice and a more formal argument is then required.

5.4.1.1 Modification of Boundary Conditions

Case A

Let us consider a stream-line J sufficiently close to the die and container walls as to justify the assumption that it is straight before and after the die corner.

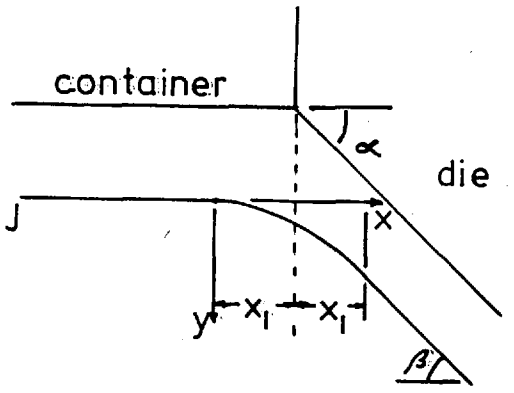

Fig. 5.12

The slip-line solution predicts discontinuities in the velocity field. In real metals, of course, such a discontinuity is not present and the "velocity jump" occurs in a narrow band. This is represented in the flow-line by a curve described by a second order polynomial (see Fig. 5.12):-

$$Y = ax^2 + bx + c \qquad (5.1)$$

using the origin of coordinates shown in Fig. 5.12. This may be reduced to:-

$$Y = ax^2 \qquad (5.2)$$

where a can be evaluated from:-

$$\left.\frac{\partial y}{\partial x}\right|_{x = 2x_1} = \tan \beta = 2ax = 2a \cdot 2x_1 = 4ax_1 \qquad (5.3)$$

Therefore:-

$$a = \frac{1}{4x_1} \tan \beta$$

and:-

$$Y = \frac{\tan \beta}{4x_1} x^2 \qquad (5.4)$$

where tan β is the slope of the flow-line after the transition has taken place.

Hence, the direction of flow at the middle of the transition zone is given by the equation:-

$$\left.\frac{\partial y}{\partial x}\right|_{x = x_1} = \tan \beta/2 \qquad (5.5)$$

It may be noticed that this value is independent of the width of the transition zone as long as the zone is symmetric about the point A. As $x_1 \to 0$ the flow-line gets closer to the container and die, and in the limit the direction of flow takes the form:-

$$\frac{\partial y}{\partial x} = \frac{\tan \alpha_D}{2} \qquad (5.6)$$

where α_D is the die semi-angle.

An analogous study can be made of the exit corner which gives similar results.

These boundary conditions were implemented and the problem solved again using the "velocity-pressure" formulation (with bi-linear elements) and the mesh shown in Fig. 5.13. The results, shown in Fig. 5.14 are very much improved as comparison with the slip-line field solution indicates.

Fig. 5.15 shows the effective strain rate distribution for both the traditional and the modified boundary conditions. As expected, both distributions are almost identical except for the decrease in the strain rate concentration found at the die corners.

Case B

Another possible method of overcoming this problem is to take advantage of the discretization character of the finite element technique and eliminate the corner altogether (see Fig. 5.16).

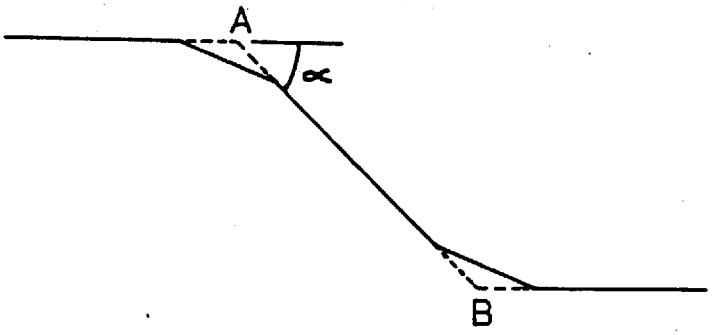

Fig. 5.16

This boundary condition has also been investigated and the results were very similar to those just described. This last technique, however, has the advantage of not having to define "fictitious" boundary conditions at the corners for it is only necessary to modify the mesh slightly.

Both techniques are simple to implement, only requiring specification of data and, therefore, not involving any change in the logic of the computer code. The choice between the two is a subjective one since both render almost identical results and, it may be argued, represent basically the same physical situation.

The same problem was also solved using the "penalty-function" formulation varying the values of the penalty coefficient (α). The extrusion pressure, velocity distribution and hydrostatic stress distribution were compared with those found using the "velocity/pressure" formulation. The results, shown in Fig. 5.17, reveal the same trends as those of the problem discussed in the previous section: the larger the penalty parameter, the closer are the solutions. For a sufficiently large value of α the two solutions are not noticeably different. It is worth mentioning that, if the value of α is <u>too</u> large, the systems of equations resulting from the penalty formulation will be ill-conditioned. Evidence of this phenomenon was not encountered with the values used in this study.

5.5 Rod Extrusion

Axisymmetric extrusion is a process of particular interest since it forms, in effect, the basis for considering the forming of other components. This is a more complicated problem than plane-strain extrusion and it is extensively documented[5.19]. Here, one specific geometry will be considered and the effects of die friction and strain hardening of the material investigated. For the latter

it is necessary to implement a procedure to integrate the strain rates and this will be discussed below before proceeding to look in detail at the problem.

5.5.1 Integration of Strain Rates

The solution obtained by the methods discussed in this work is in terms of velocities and hence, strain rates. For non-steady-state problems, the effective strain rates are added incrementally for each element in order to evaluate the effective strains after a certain amount of deformation. However, extrusion is analysed as a steady-state process, and hence, an alternative technique is necessary for the determination of the effective strains. The technique used in this work is similar to the one suggested by Shah[5.21], however, for the sake of completeness a detailed description is given here.

The strain rates for the elements are assumed to be the values at the centroid of each element (which is the best sampling point for the bi-linear isoparametric element[5.20]). The velocities are known at the nodal points on the corners, with a bi-linear distribution within the element. The coordinates of the centroid of the element, as well as those of the nodal points, are also known. To begin the integration, a point is selected along the entrance boundary so that it can be safely assumed that no straining has occurred before it and, therefore, the effective strain is zero. Given the coordinates of this point, then the radial and axial components of the velocity and the effective strain rate at that point can be determined by interpolation from surrounding nodal point values and centre values respectively. These velocities are then used to find the new position of the point. The effective strain rate is also added incrementally to the effective strain to

determine the effective strain at the new location and the procedure repeated. This procedure, in effect, is the integration of the strain rates along the path of the point from its starting point to its current position, that is:-

$$\bar{\varepsilon} = \int_0^t \dot{\bar{\varepsilon}}\, dt \qquad (5.7)$$

where t stands for time.

This procedure of adding velocity and strain rate incrementally is continued until the point reaches a position beyond the deforming zone such that it can be assumed that no further straining occurs beyond it. Choosing another point on the entrance boundary and following the same procedure allows the determination of another flow-line and the values of effective strain along it. This procedure gives the whole network of grid distortion and effective strain distribution. The value of the effective strain at each elements' centroid can then be determined by interpolating from the network of flow-lines.

5.5.2 Non-Hardening Material

The results obtained for the problems discussed in the preceding sections showed that the results for both "penalty-function" and the "velocity/pressure" formulations were almost identical when the penalty parameter was sufficiently large. In what follows, therefore, only the penalty function will be used, since it is conceptually easier to understand.

As a first step, the problem of the axisymmetric extrusion of a circular rod is considered. The extrusion ratio, defined as the ratio of original to final cross-sectional area, was selected to be

R = 4.0 and the half-cone angle for the die was $\alpha_D = 45^o$.

The problem has been solved for various conditions of friction to assess the influence of friction. Friction is introduced via tangentially applied nodal forces at the nodes in contact with the die.

The mesh used is shown in Fig. 5.18 where it can be seen that modification of the mesh (Case B - previous section) around the die corners is the method used to deal with the singularities. The accuracy desired is set at $||\Delta u||/||u|| \leq 0.005$, and a cut-off value of $\gamma = 10^9$ is chosen to deal with the rigid regions.

5.5.3 - Work-Hardening Material

The next problem considered is that of extrusion of a work-hardening material. For the sake of comparison the same process conditions, namely, R = 4.0, $\alpha_D = 45^o$, are used, although only the frictionless case is considered. Also, the mesh is the same as for the previous case. The calculation is performed using the stress-strain relationship:-

$$\bar{\sigma} = Y_o \, (1 + \bar{\varepsilon}/0.3)^{0.25}$$

where Y_o is the initial yield stress.

In this case, the flow-lines, corresponding to the current velocity field, are constructed after each iteration using the procedure described previously. The effective strains for all elements are also determined and using the stress-strain relationship a corresponding flow stress distribution for the elements is calculated. For the first iteration, the flow stress for all elements is set to be equal to its value at zero strain, i.e. Y_o.

Taking this new flow stress distribution, the next iteration

for the velocity field is carried out and the same procedure repeated until convergence is achieved.

Since the solution depends not only on the velocity distribution but also on the flow stress distribution, when the velocity solution has converged, the flow stress and effective strain distribution also conform to the initially defined relationship. Thus, convergence of the velocity solution gives the correct solution for the work-hardening material.

5.5.4 Results

The finite element analysis of the axisymmetric extrusion gives very extensive data describing the detailed mechanics of the process. However, in order not to confuse the issue with an inordinate amount of graphs and curves, only a few selected results will be presented and discussed in this thesis.

(a) Non-Hardening Material

As stated earlier the axisymmetric extrusion of a rod of non-hardening material was solved using various friction factors, namely, m = 0.0, 0.5 and 1.0; where m is defined by:-

$$\tau = m\, Y_o/\sqrt{3} \qquad \text{(sub-surface layer mode)} \qquad (5.8)$$

The effective strain rate distributions for various frictional conditions are shown in Fig. 5.19. As might be expected, there is some degree of strain rate concentration near the die corners. The strain rate increases gradually from the entrance towards the exit and drops sharply very near the die exit. This suggests the existence of a shear zone close to the exit boundary. It is also

evident that the zone of plastic deformation moves backwards considerably (towards the extrusion plunger) with increasing friction along the die interface, which is consistent with experimental evidence[5.22].

The flow-lines obtained from integration of the velocity field, shown in Fig. 5.20a, reveal the same effect with increasing friction and are qualitatively similar to those obtained by Lambert and Kobayashi[5.23] who used a velocity field without discontinuities.

The distortion of a line which was originally straight is plotted in Fig. 5.20b for two different conditions of friction. Avitzur[5.24] calculated the grid distortion, using a simple pattern of radial velocity, and found 2.1 to be the maximum relative displacement, compared with 1.00, 1.80 and 2.65 found by Lambert and Kobayashi, and values of 1.03, 1.65 and 2.4 for m = 0.0, 0.5 and 1.0 respectively, in the present work. Experimental grid distortion has yielded values of the order of 1.7[5.25]. It can also be seen that the grid distortion considerably increases with friction.

The nodal point forces along the die-workpiece interface are calculated from the stiffness equations. Since these components are in the r and z directions, a transformation has to be carried out to convert them to the direction normal to the die, and from them the normal pressure distribution is obtained. Fig. 5.21 shows the normal die pressure for the various frictional conditions. It can be seen that the pressure is highest at the entrance and it gradually decreases towards the exit, increasing by a small amount just near the exit. This behaviour conforms with the fact that the hydrostatic component of the stresses is expected to be decreasing towards the exit. The trend of the curves for the various frictional conditions is identical and, as expected, reflects the effect of increasing friction as increases in the pressure normal to the die.

The extrusion pressures are also calculated from the stiffness equations. Table 5.5 shows the comparison between the pressures obtained in this work and those obtained from well-known upper-bound analyses. It can be seen that the finite element pressures are an improvement over most of the upper bounds and are in very close agreement with the best upper bound.

Fig. 5.22 shows the distribution of stresses along the axis, for two different frictional conditions. It can be seen that the hydrostatic component becomes less compressive towards the exit. This trend for all the stress components towards tensile behaviour has been argued to be responsible for the occurrence of extrusion defects. It is interesting to notice that the analysis predicts that increase of friction at the die face has the effect of diminishing this trend and hence reducing the possibility of a defect occurring. This last argument is consistent with experimental evidence, as a matter of fact.

(b) Hardening Material

As seen from the calculated vertical grid distortion, shown in Fig. 5.23, the distortion and, therefore, the amount of redundancy of the process is greater for a work-hardening than for a non-work-hardening material. This is because the difference between the velocities at the axis and the periphery at a given section are, as expected, larger when hardening is taken into consideration.

The extrusion pressure is again calculated via the reactions and results in the expression $P/Y_o = 2.36$. The die pressure distribution is shown in Fig. 5.24. It may clearly be noticed that the die is subjected to a greater pressure by the hardening material, but the trend is almost identical to that obtained for the non-hardening material which is shown in the same figure for comparison.

The stress distribution along the axis for both the

TABLE 5.5

Values of $\bar{P}/Y$ for R = 4, $\alpha = 45^{o}$, Axisymmetric Condition

Source	Frictionless m = 0.0	Rough dies m = 1.0	Type of solution
Avitzur[5.5]	2.08	-	Upper bound
Kobayashi[5.27]	1.90	-	Upper bound
Halling and Mitchell[5.26]	2.08	2.87	Upper bound
Pierce[5.28]	2.08	2.88	Upper bound
Lambert and Kobayashi[5.23]	1.69	2.54	Upper bound
Pacheco and Alexander	1.68	2.50	Present F.E.M.
Lambert and Kobayashi[5.23]	1.39	-	Lower bound

hardening and non-hardening materials is shown in Fig. 5.25. The analysis predicts higher stresses, in the compressive sense, for the former and by implication a less likelihood for common extrusion defects to occur.

5.6 Final Remarks

The rigid-plastic finite element method has been applied successfully to the analysis of various extrusion problems. The effect of different treatments for the die corners was assessed leading to what seems a satisfactory way of modelling them. For the plane-strain problems two types of formulations were employed, giving almost identical results for the cases studied. This indicates that one of the formulations, namely, the penalty-function formulation is the best choice because it requires less computer core and less time to get a solution as well as being conceptually simpler to understand.

REFERENCES

5.1 PEARSONS, C. E. and PARKINS, R. N.
"The Extrusion of Metals".
Wiley, New York, (1960).

5.2 SIEBEL, E. and FANGMEIER, E.
"Researches in Power Consumption in the Extrusion and Punching of Metals".
Mitt. K. N. Inst. Einenforschung, Vol. 13, pp. 29-43, (1931).

5.3 HOFFMAN, O. and SACHS, G.
"Introduction to the Theory of Plasticity for Engineers".
McGraw-Hill, New York, (1953).

5.4 JOHNSON, W. and KUDO, H.
"The Mechanics of Metal Extrusion".
Manchester University Press, England, (1962).

5.5 AVITZUR, B.
"Metal Forming : Processes and Analysis".
McGraw-Hill, New York, (1968).

5.6 JOHNSON, W., SOWERBY, R. and HADOW, J. B.
"Plane Strain Slip Line Fields : Theory and Bibliography".
Arnold, London, (1970).

5.7 DEWHURST, P. and COLLINS, I. F.
"A Matrix Technique for Constructing Slip-Line Field Solutions to a Class of Plane Strain Plasticity Problems".
Int. J. Num. Meth. Eng., Vol. 7, pp. 356-378, (1973).

5.8 DAS, N. S., CHITKARA, N. R. and COLLINS, I. F.
"The Computation of Some Slip-Line Field Solutions for Asymmetric Extrusion".
Int. J. Num. Meth. Eng., Vol. 11, pp. 1379-1389, (1977).

5.9 SHABAIK, A. H. and THOMNSEN, E. G.
"Computer Aided Viscioplasticity Solution of some Deformation Problems".
Problems in Plasticity, Vol. 1, Noordhoff Int. Publishing, Gröningen, (1973).

5.10 MEDRANO, R. E. and GILLIS, P. P.
"Viscioplasticity Techniques in Axisymmetric Extrusion".
J. Strain Anal., Vol. 7, p. 170, (1972).

5.11 ZIENKIEWICZ, O. C. and GODBOLE, P. N.
"Flow of Plastic and Visco-Plastic Solids with Special Reference to Extrusion and Forming Processes".
Int. J. Num. Meth. Engng., Vol. 8, pp. 3-16, (1974).

5.12 GOLDBOLE, P. N.
Ph.D. Thesis, University of Wales, (1974).

5.13 ZIENKIEWICZ, O. C.
"The Finite Element Method".
McGraw-Hill, p. 621, (1977).

5.14 ZIENKIEWICZ, O. C. and GODBOLE, P. N.
"Penalty Function Approach to Problems of Plastic Flow of Metals with Large Surface Deformations".
J. Strain Anal., 10, pp. 180-183, (1975).

5.15 NAYAK, G. C. and ZIENKIEWICZ, O. C.
"Elasto-Plastic Stress Analysis : Generalization of Various Constitutive Relations Including Strain Softening".
Int. J. Num. Meths. Eng., 5, pp. 113-135, (1972).

5.16 IWATA, K., OSAKADA, K. and FUJINO, S.
"Analysis of Hydrostatic Extrusion by the Finite Element Method".
Trans. of ASME, J. Engng. for Ind., Vol. 94, p. 697, (1972).

5.17 JOHNSON, W.
"Extrusion Through Wedge Shaped Dies, Part I".
J. Mech. Phys. Sol., Vol. 3, pp. 218-223, (1955).

5.18 SHEN, S. F., MORJAIRA, M. A. and UPADHYA, R. K.
"A Special-Element Technique for Two Dimensional Creeping Viscous Flow in a Domain with Sharp Corners".
Proc. 1st Int. Conf. in Numerical Methods in Laminar and Turbulent Press, Pentech Press, (1978).

5.19 JOHNSON, W. and MELLOR, P. B.
"Engineering Plasticity".
Van Nostrand, (1973).

5.20 BARLOW, J.
"Optimal Stress Locations in Finite Element Models".
Int. J. Num. Meth. Eng., 10, pp. 243-251, (1976).

5.21 SHAH, S.
"Numerical Analysis of Metal-Forming Processes".
Ph.D. Thesis, University of California, Berkeley, (1974).

5.22 GURNEY, F. J. and de PIERRE, V.
"The Influence of the Interface Condition on Plastic Deformation Zone and the Resultant Product Integrity in Extrusion".
J. Eng. Ind., Trans. ASME, Vol. 96, pp. 912-916, (1974).

5.23 LAMBERT, E. R. and KOBAYASHI, S.
"A Theory on the Mechanics of Axisymmetric Extrusion Through Conical Dies".
J. Mech. Eng. Sci., Vol. 10, pp. 367-380, (1968).

5.24 AVITZUR, B.
"Flow Characteristics Through Conical Converging Dies".
Trans. ASME, J. Eng. Ind., Vol. 88, p. 410, (1966).

5.25 PUGH, H. Ll. D., WATKINS, W. T and McKENZIE, T.
"Design Considerations Arising from Cold Extrusion Research".
N.E.L. Report 24, (1962).

5.26 HALLING, J. and MITCHELL, L. A.
"Upper Bound Solution for Axisymmetric Extrusion".
Int. J. Mech. Sci., Vol. 7, p. 277, (1965).

5.27 KOBAYASHI, S.
"Upper-Bound Solutions of Axisymmetric Forming Problems - II".
Trans. ASME, J. Eng. Ind., Vol. 86, p. 326, (1964).

5.28 PIERCE, C. M.
"Forces Involved in the Axisymmetric Extrusions of Metals Through Conical Dies".
Ph.D. Dissertation, Ohio State University, (1966).

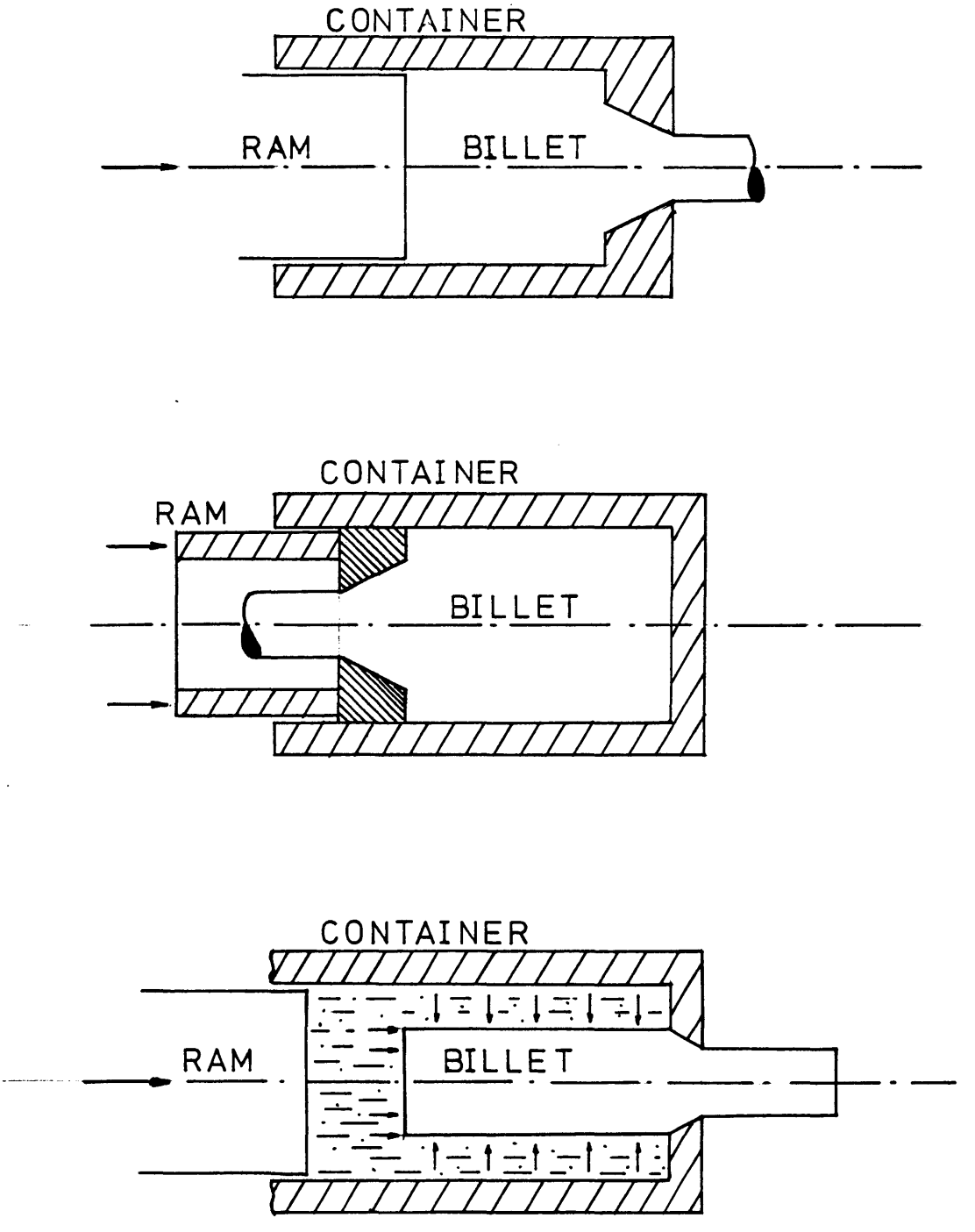

Figure 5.1: Schematic description of the different extrusion processes

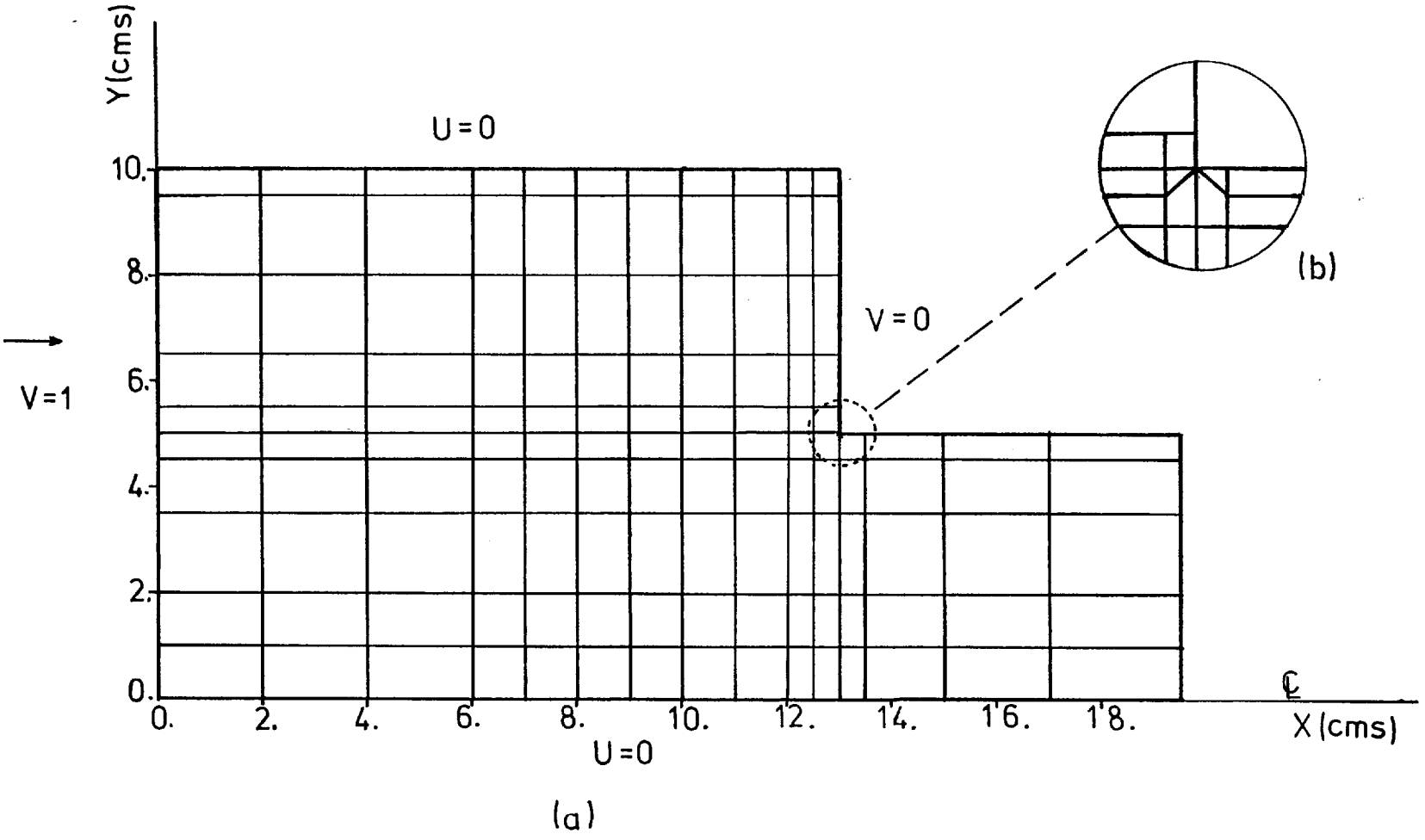

Figure 5.2: Mesh and boundary conditions for plane strain extrusion through frictionless square die

Table 5.2

	PENALTY			u/p
	$\alpha=10^4$	$\alpha=10^6$	$\alpha=10^8$	
U (cm/s)	0.882	1.956	2.054	2.055
P/2K	0.72	1.41	1.40	1.40

(a)

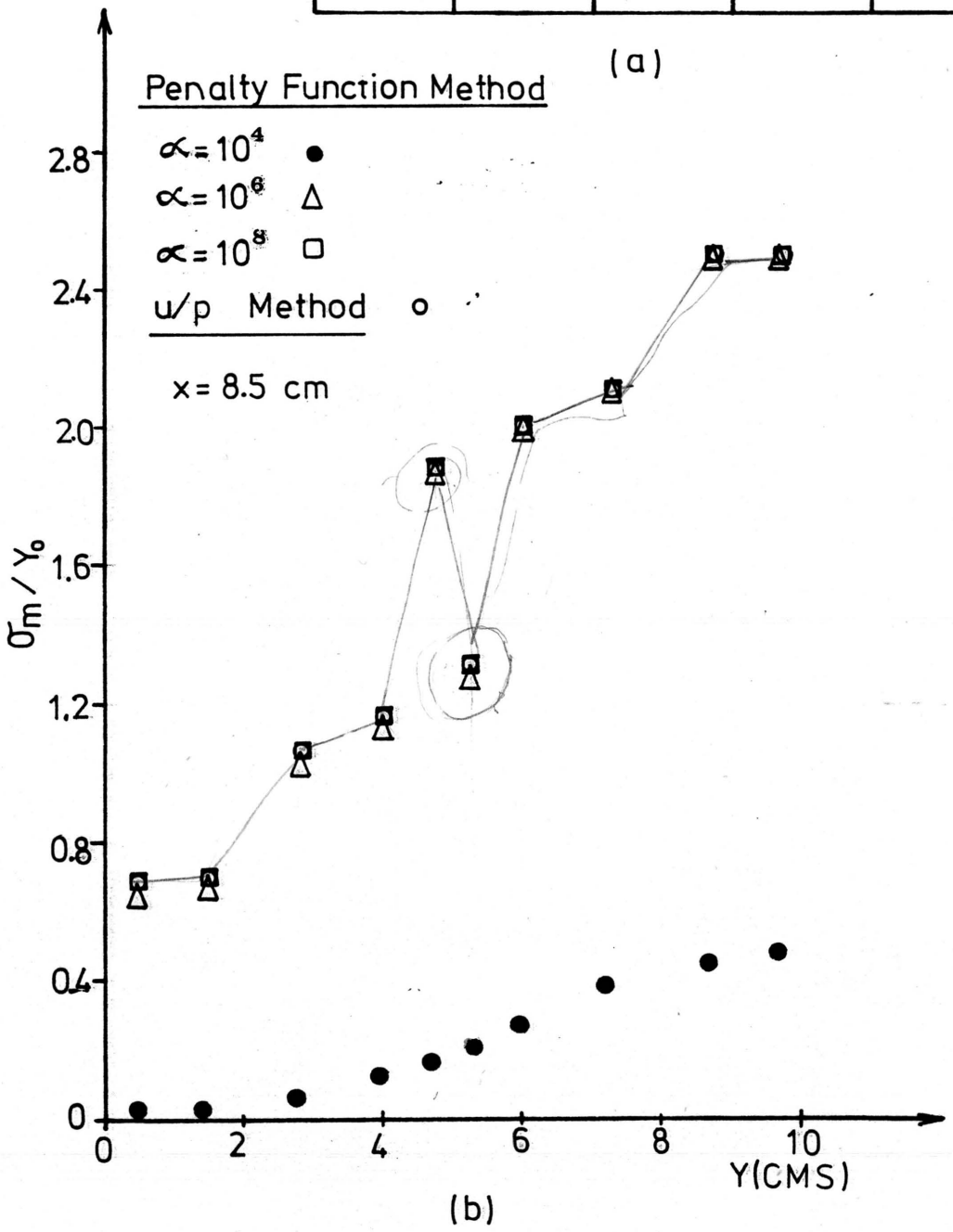

(b)

Figure 5.3: Comparison between 'Velocity/pressure' (u/p) and Penalty Function (Penalty) algorithms.

(a) Exit velocity and extrusion pressure

(b) Hydrostatic (Mean) Stress

Extrusion ratio R=2, Die semi-angle $\alpha_s=90^o$

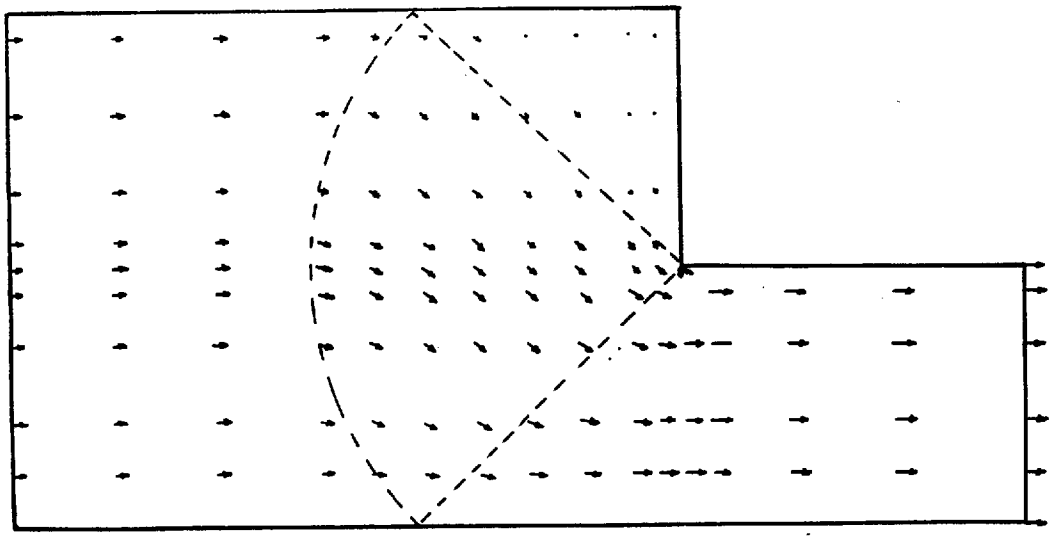

(a)

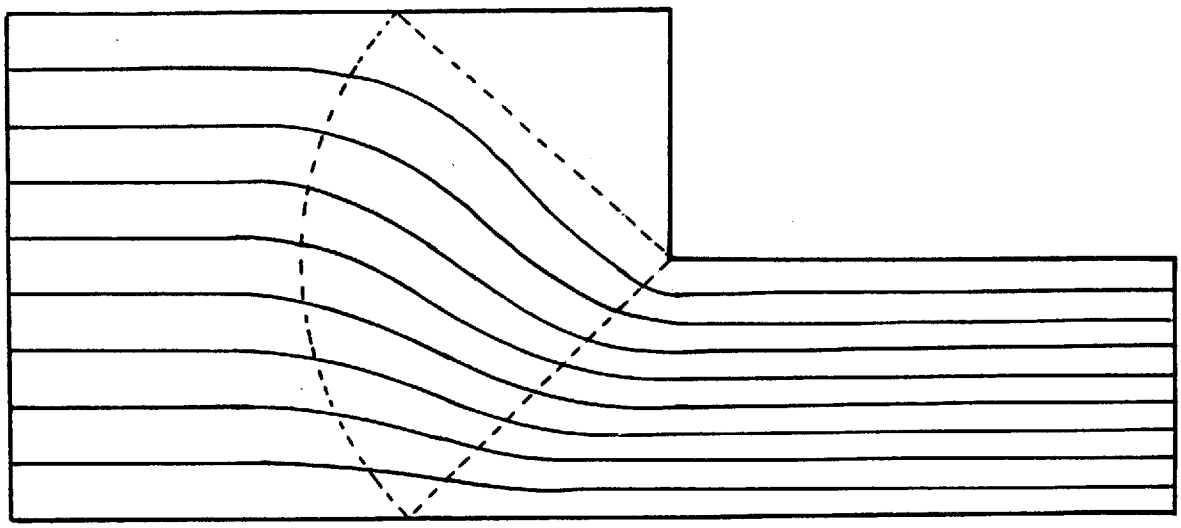

(b)

Figure 5.4: (a) Velocity vectors and (b) Flow lines for the problem of plane strain extrusion. R=2, $\alpha_D = 90^0$

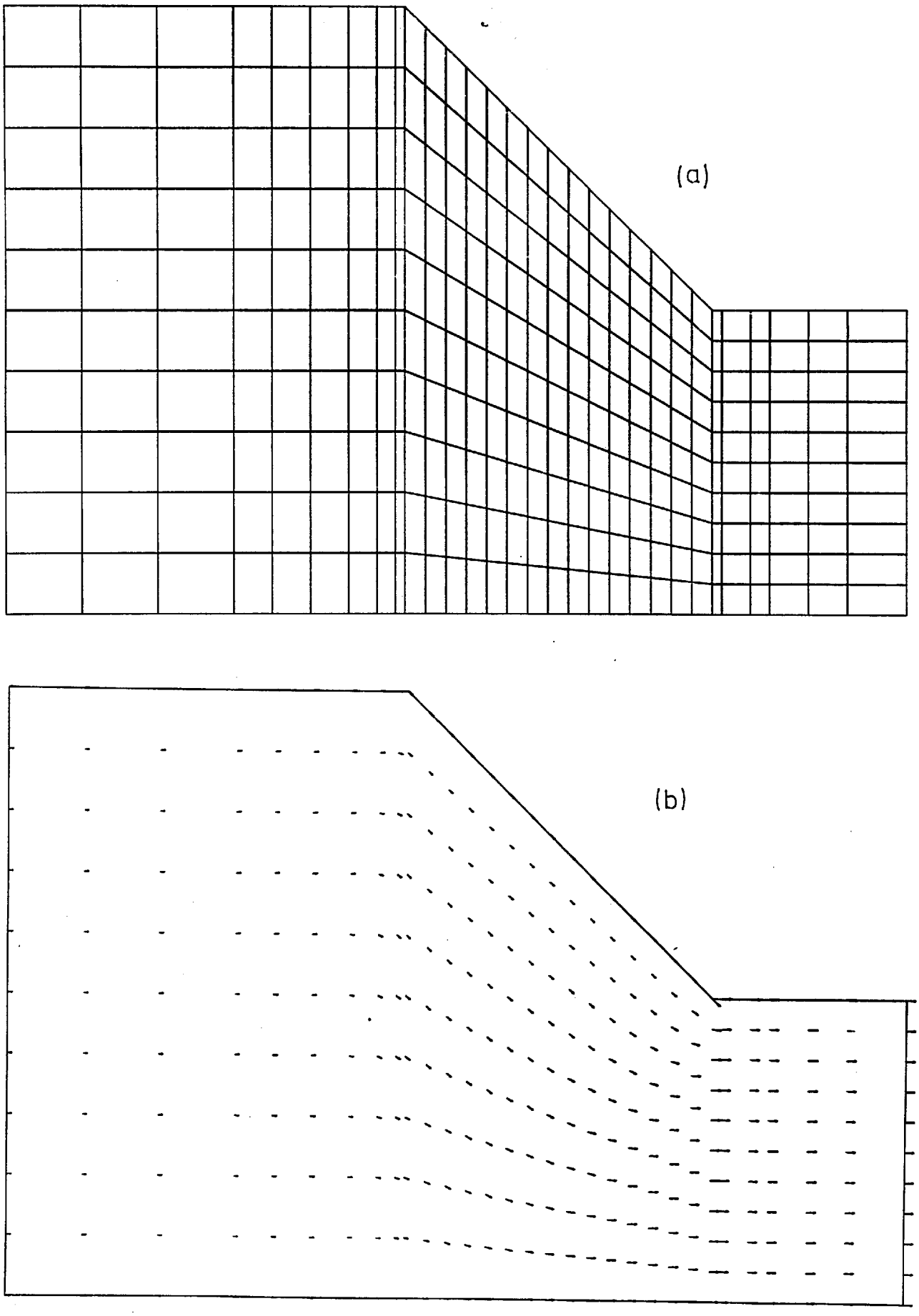

Figure 5.6: (a)Mesh and(b) Velocity vectors

R=2, Die semi-angle= 45^{o}

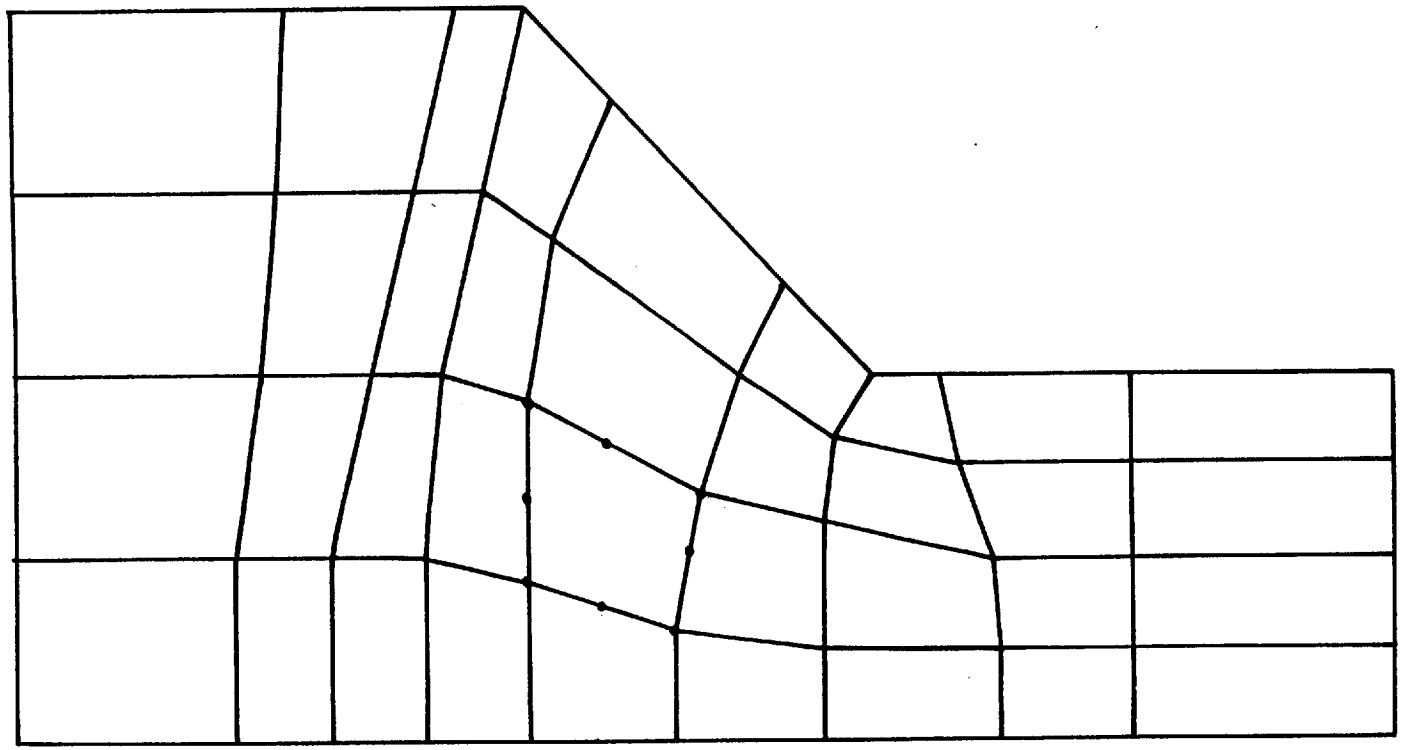

Figure 5.7: Mesh used for analysis of plane strain extrusion (isoparametric quadratic elements)
R=2, Die semi-angle =45^{o}

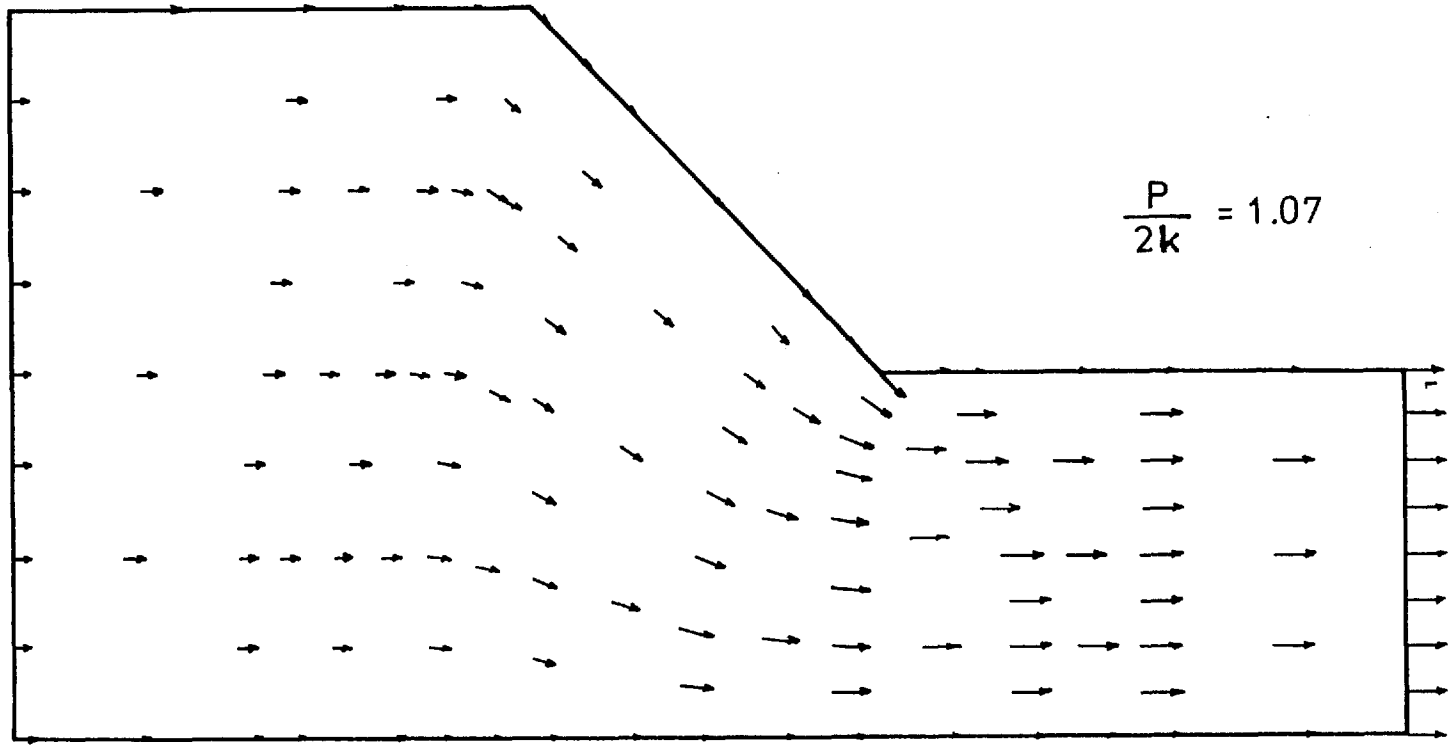

Figure 5.8: Velocity distribution and extrusion pressure obtained using isoparametric quadratic elements. R=2,Die-semi angle=45^{o}

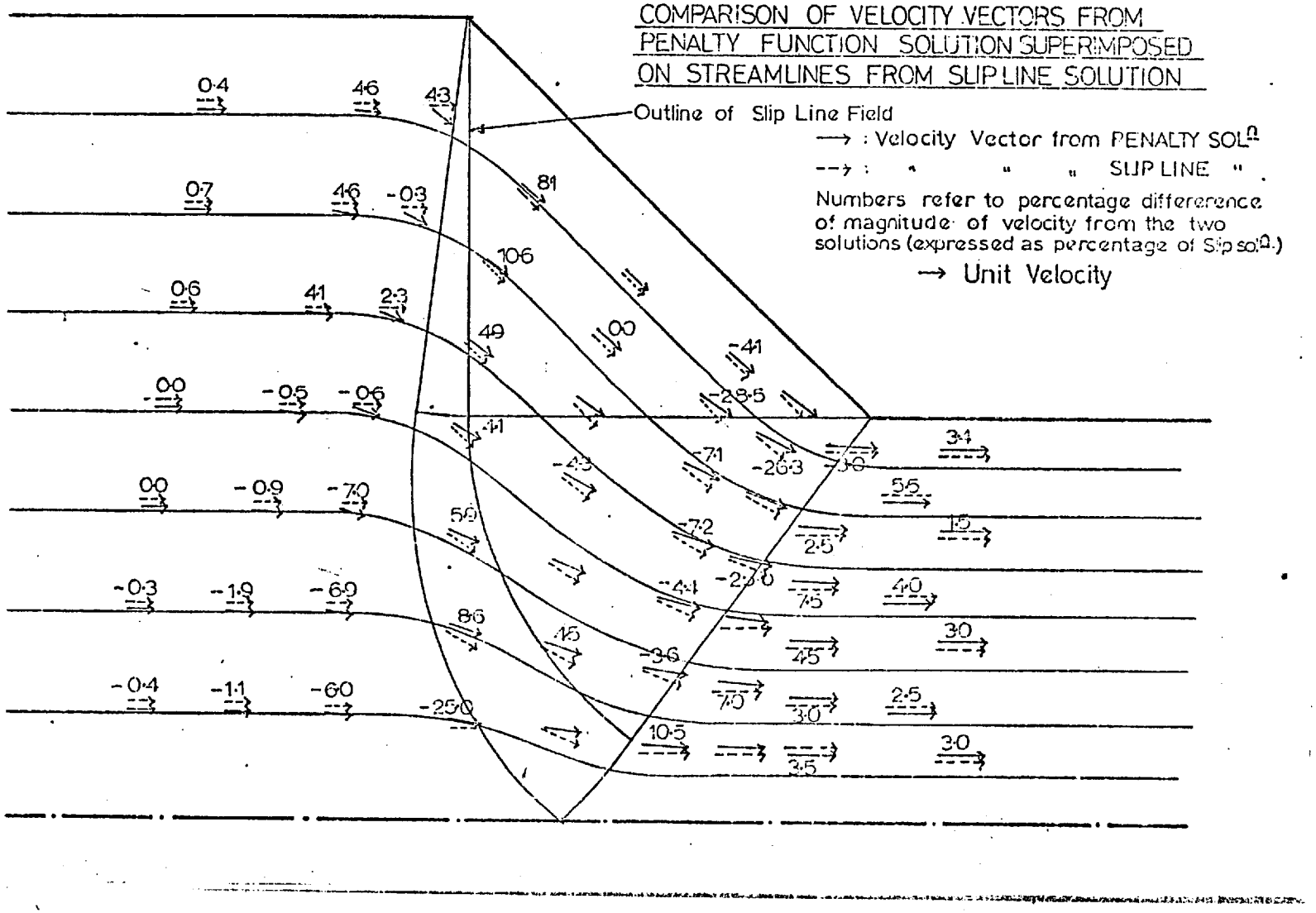

Figure 5·9 After Godbole[5·12]

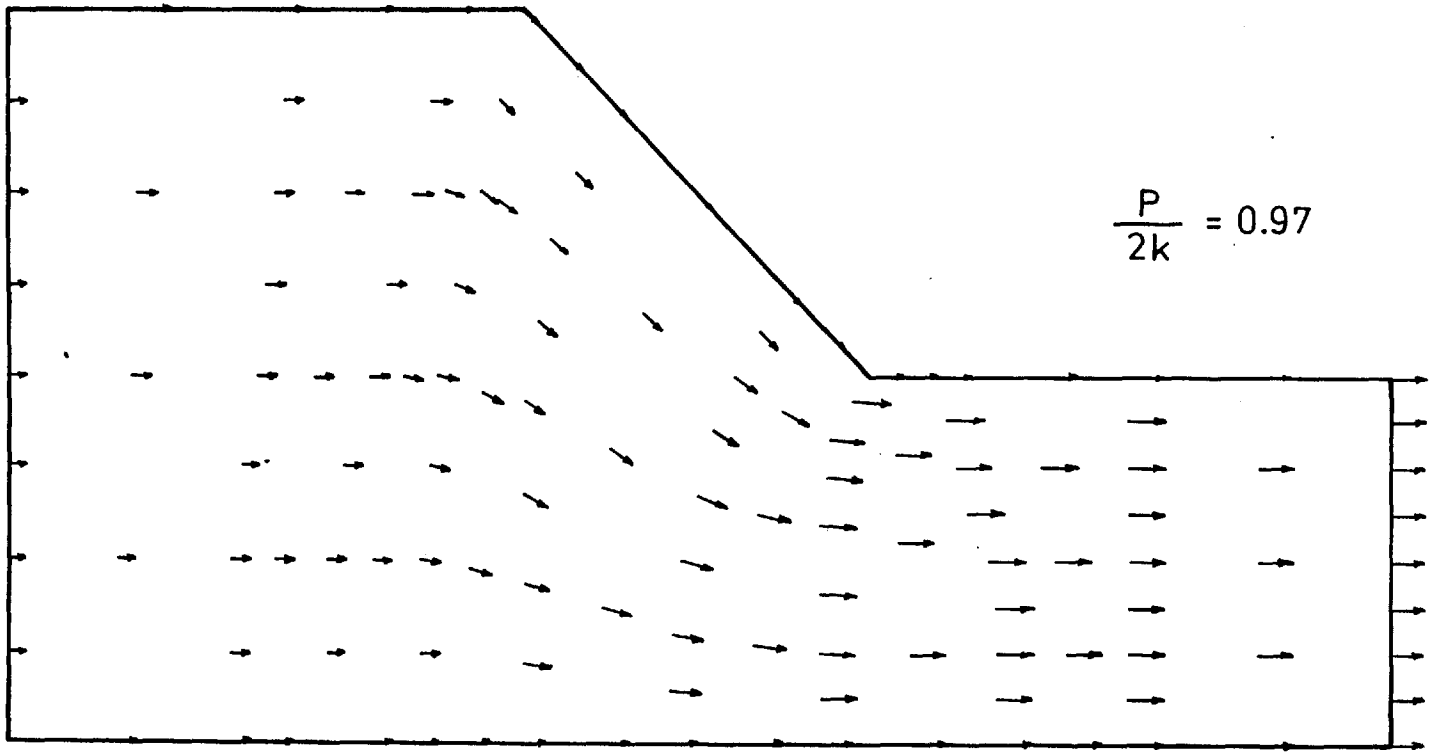

Figure 5.10: Velocity distribution and extrusion pressure (modified exit boundary condition)
R=2,Die semi-angle=45^{o}

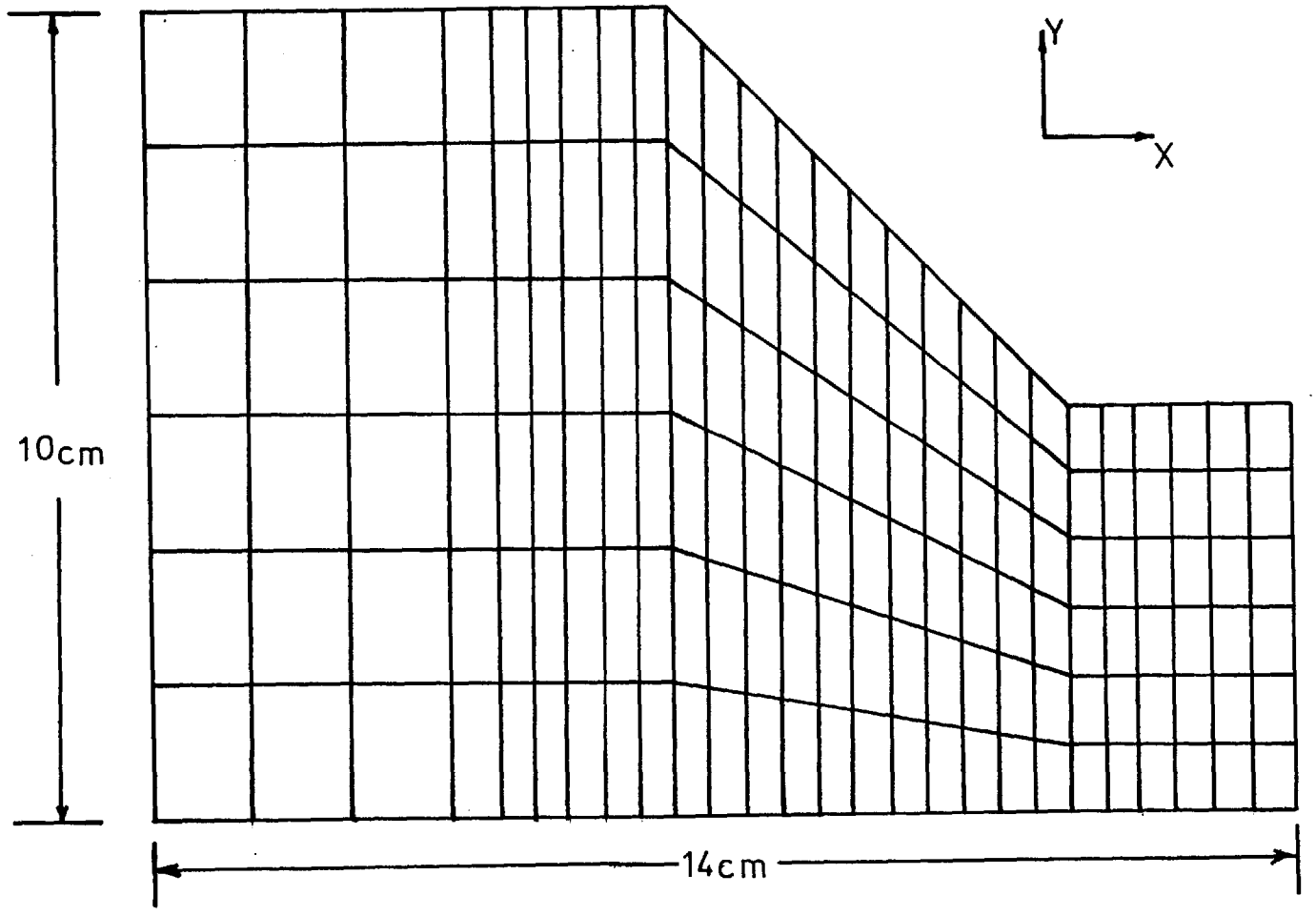

Figure 5.13: Mesh used for recalculation plane extrusion problem with modified boundary conditions. R=2,Die semi-angle=45^{o}

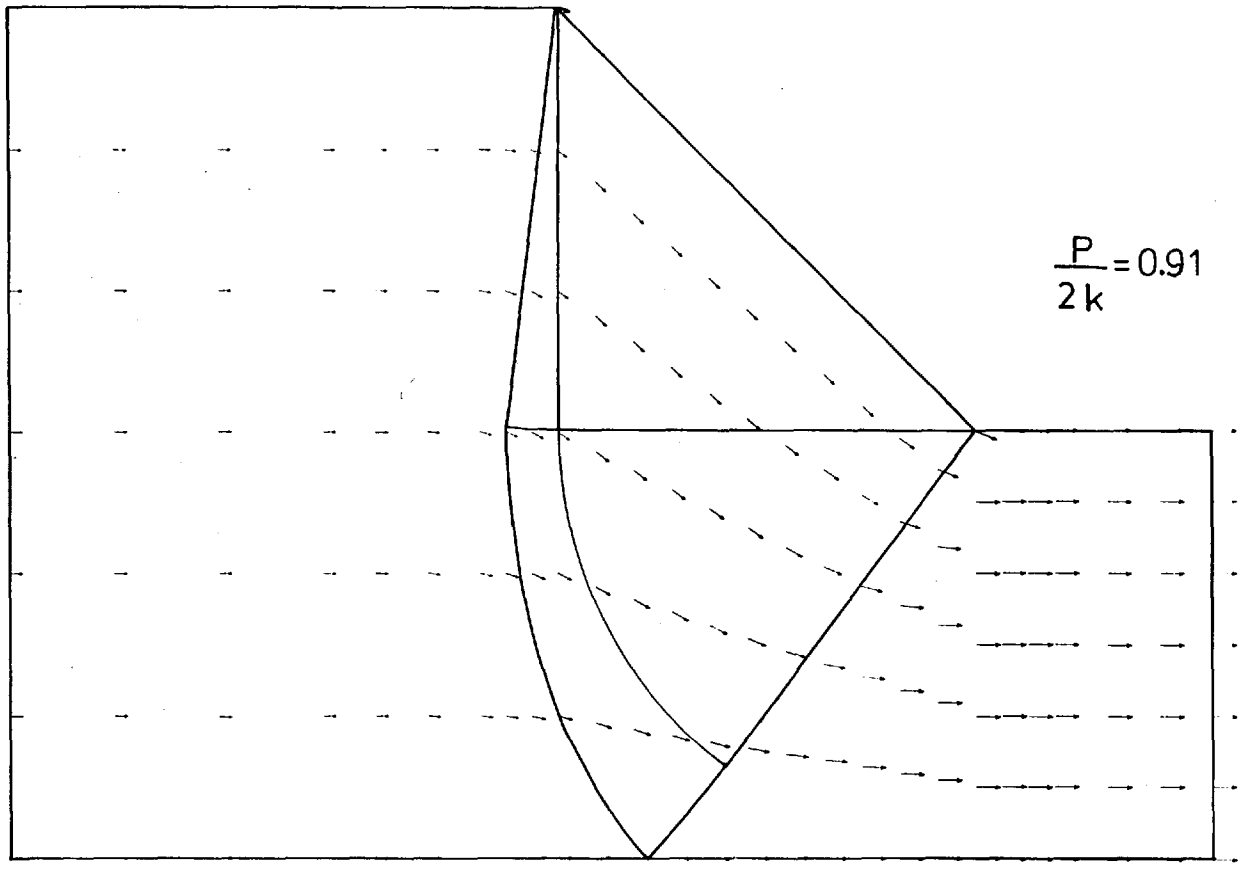

Figure 5.14: Velocity distribution and extrusion pressure. Modified boundary conditions. R=2, Die semi-angle=45^{o}

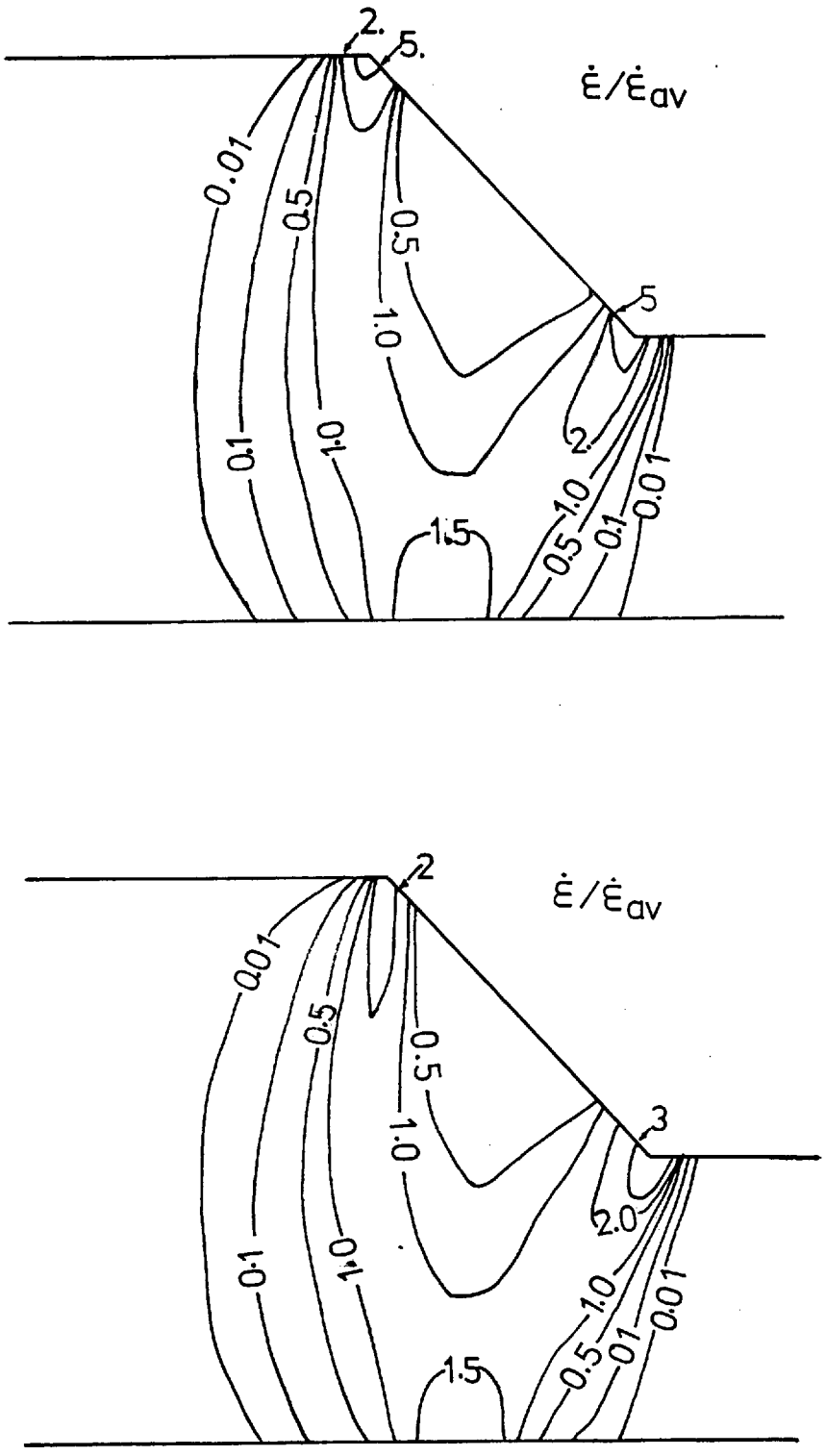

Figure 5.15: Effect of boundary conditions on the effective strain rate . (a) unmodified,(b) Modified.
R=2, Die semi-angle=45^{o}

$$\dot{\varepsilon}_{av} = \frac{V_{exit}.\text{Tan}\,\alpha}{\text{Entry Thickness}}$$

	PENALTY			u/p
	$\alpha=10^4$	$\alpha=10^6$	$\alpha=10^8$	
U(cm/s)	0.95	1.93	1.98	1.98
P/2k	0.71	0.904	0.91	0.91

(a)

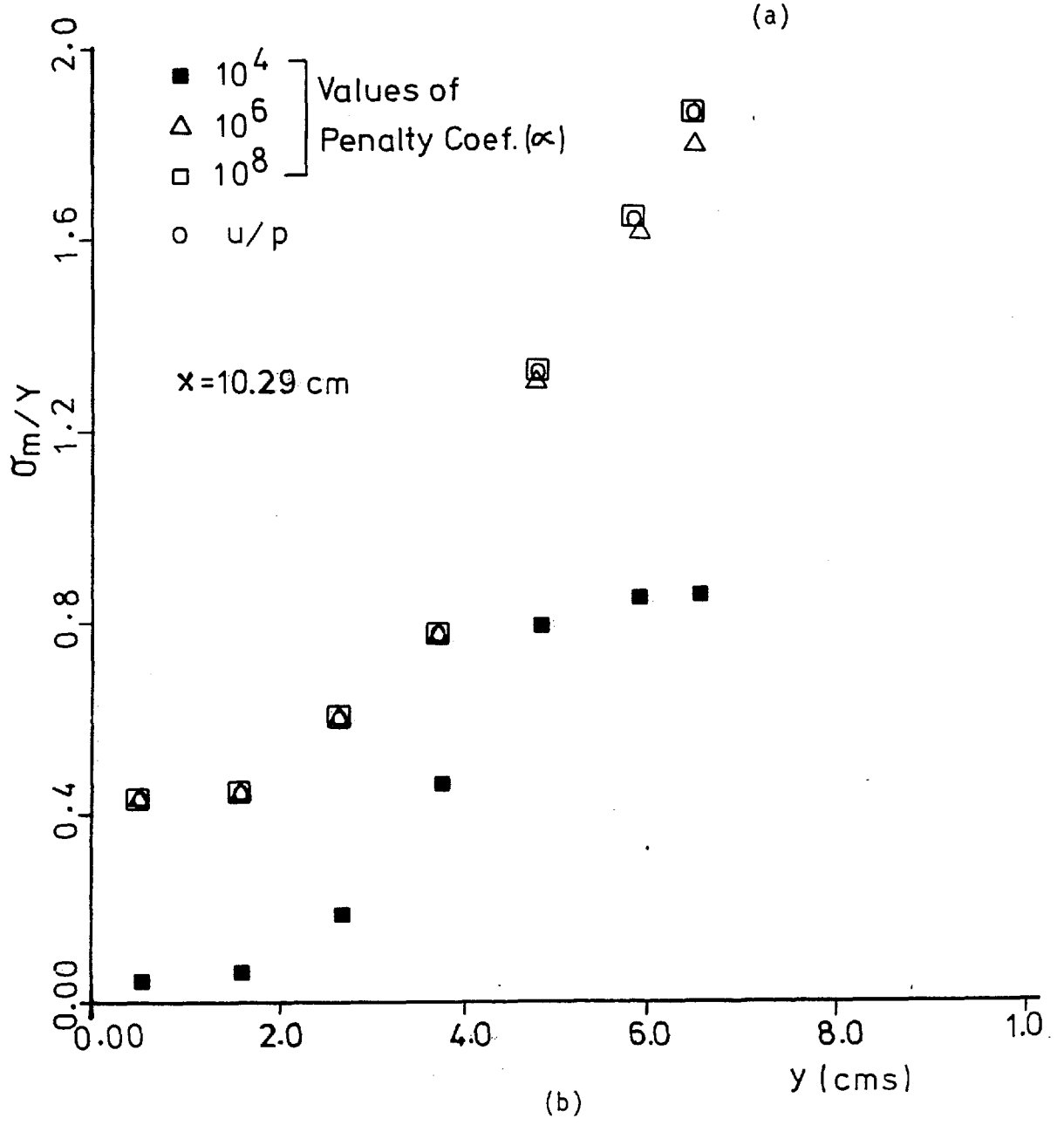

(b)

Figure 5.17: Comparison between (u/p) and Penalty for plane strain extrusion through wedge shaped die.
(a) Exit velocity and extrusion pressure
(b) Hydrostatic (Mean) Stress
R=2, Die semi-angle 45^0

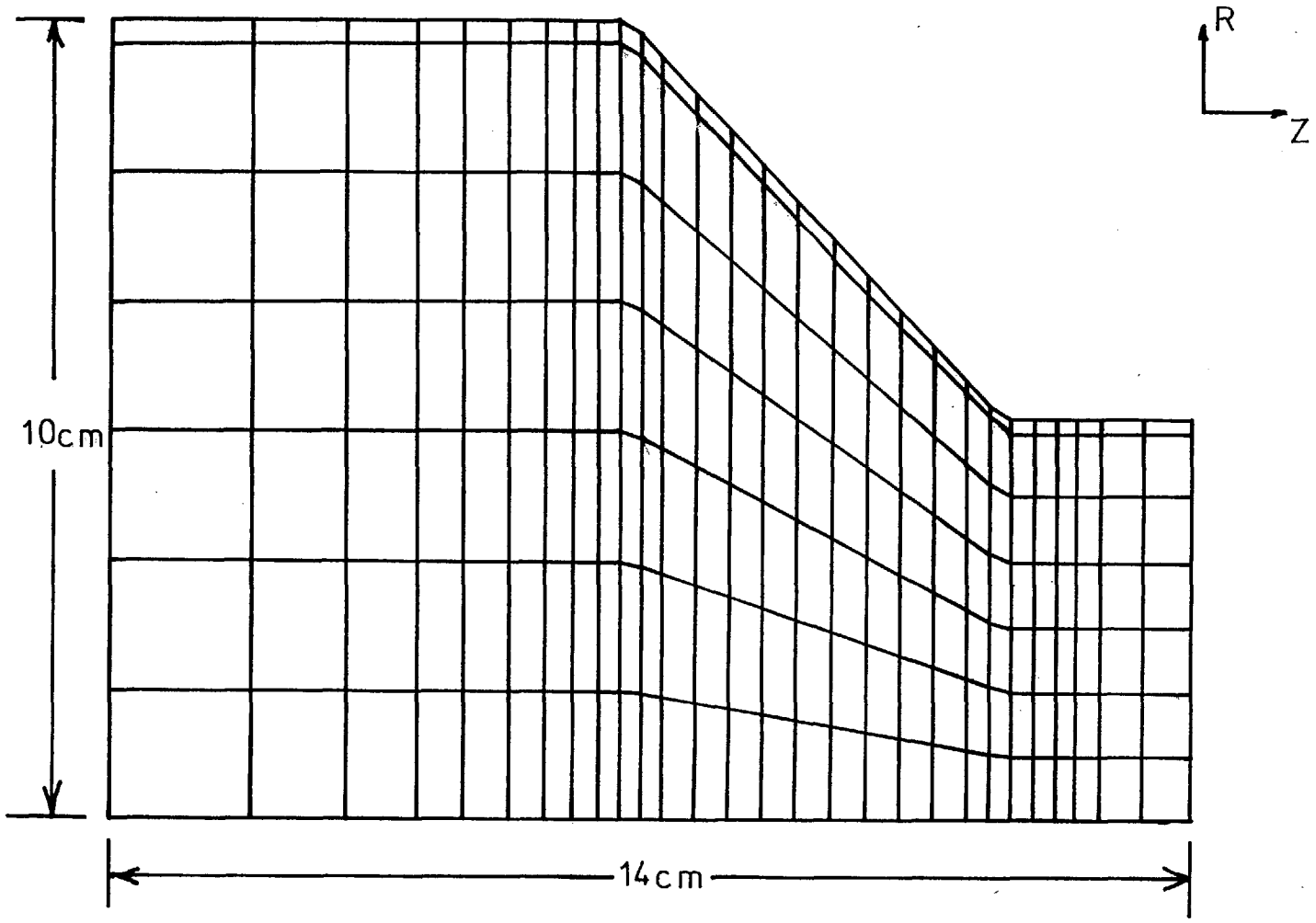

Figure 5.18: Mesh and dimension for the axisymmetric extrusion problem.
R=4,Die semi angle 45^{0}

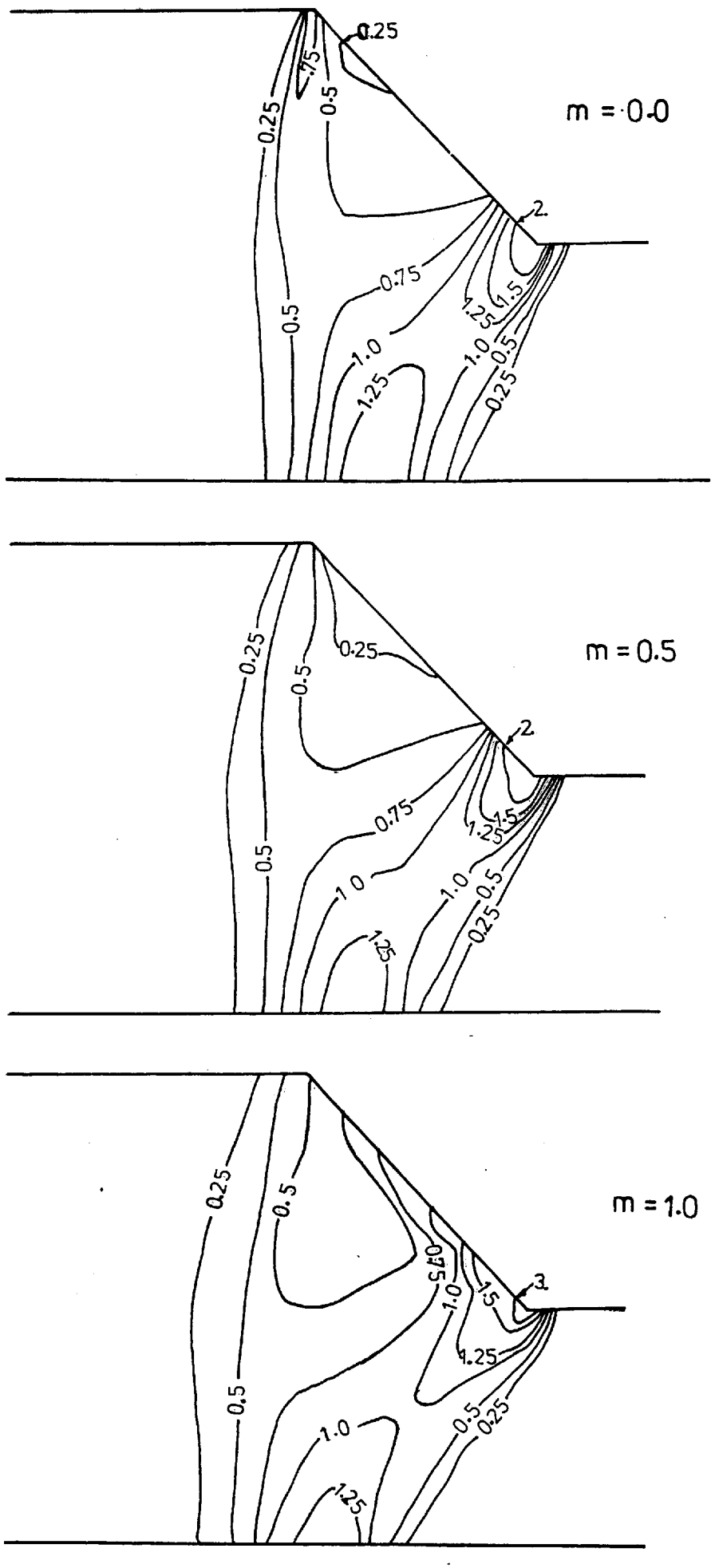

Figure 5.19: Strain rate distribution, $\dot{\varepsilon}/\dot{\varepsilon}_{av}$, for different frictional conditions. R=4, Die Semi-angle=45°

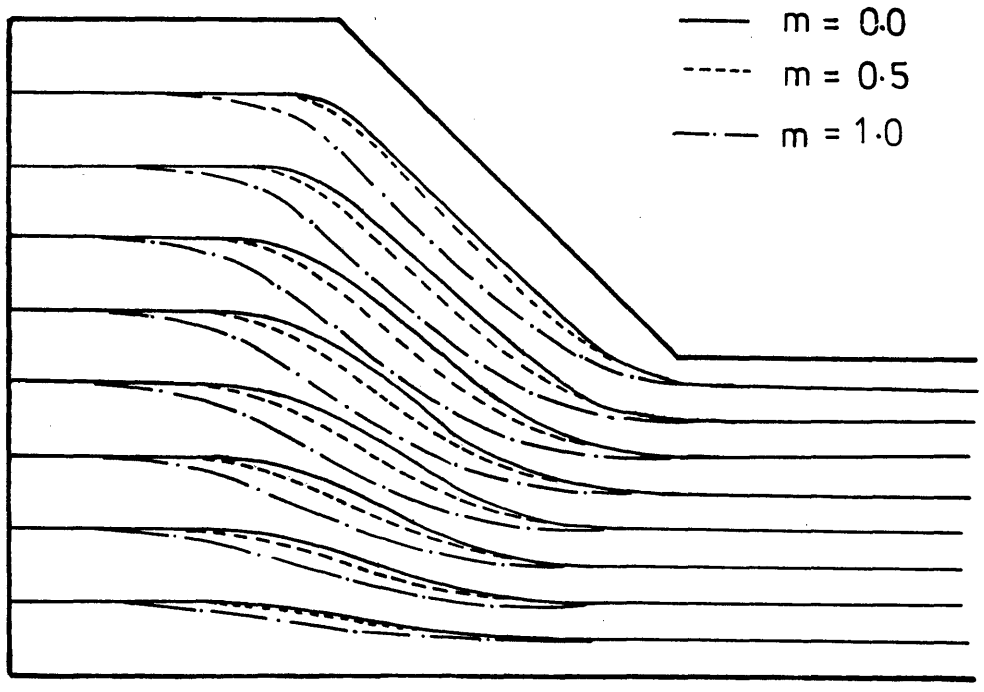

(a)

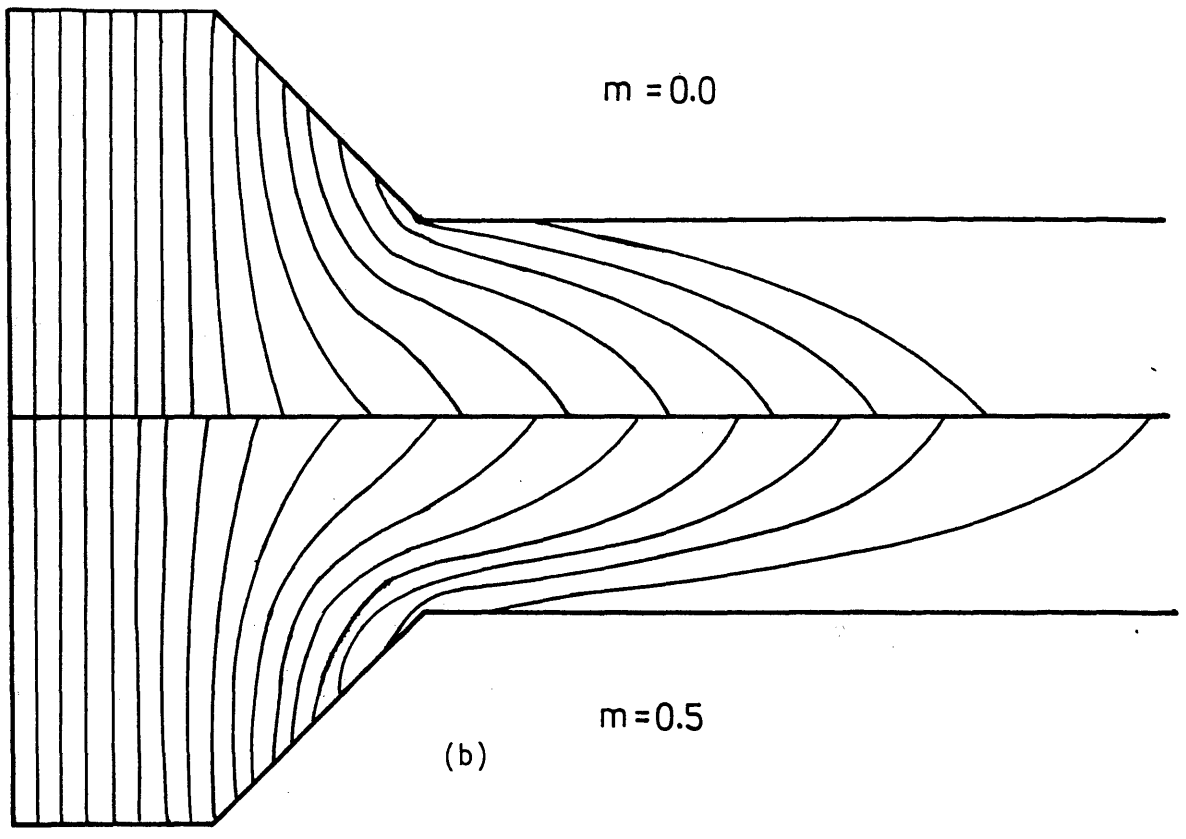

(b)

Figure 5.20: (a) Flow lines; (b) Vertical grid distortion
R=4, Die semi-angle=45^{o}

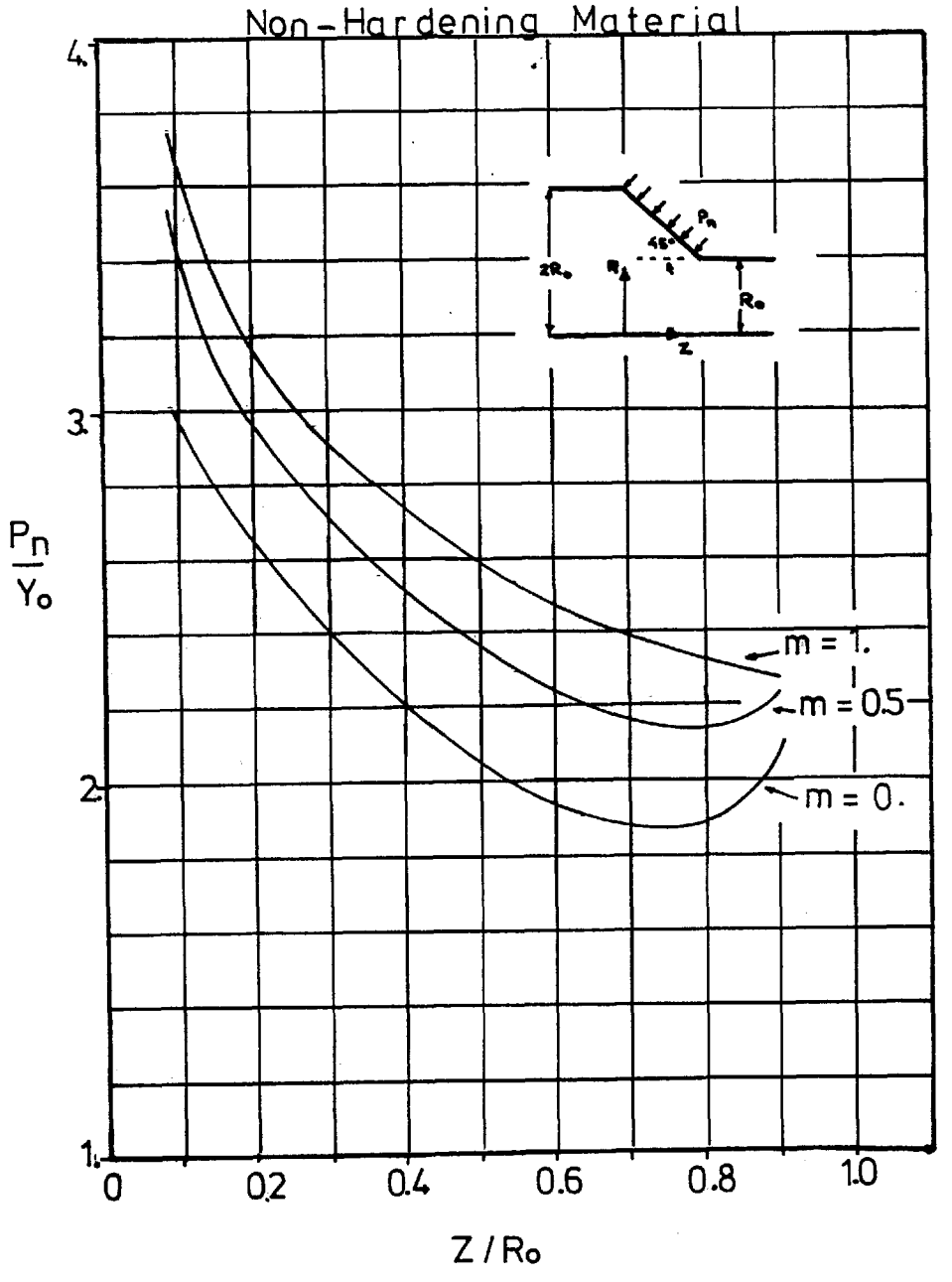

Figure 5.21: Normal die pressure distribution for different frictional conditions. R=4, Die semi-angle=45^{o}

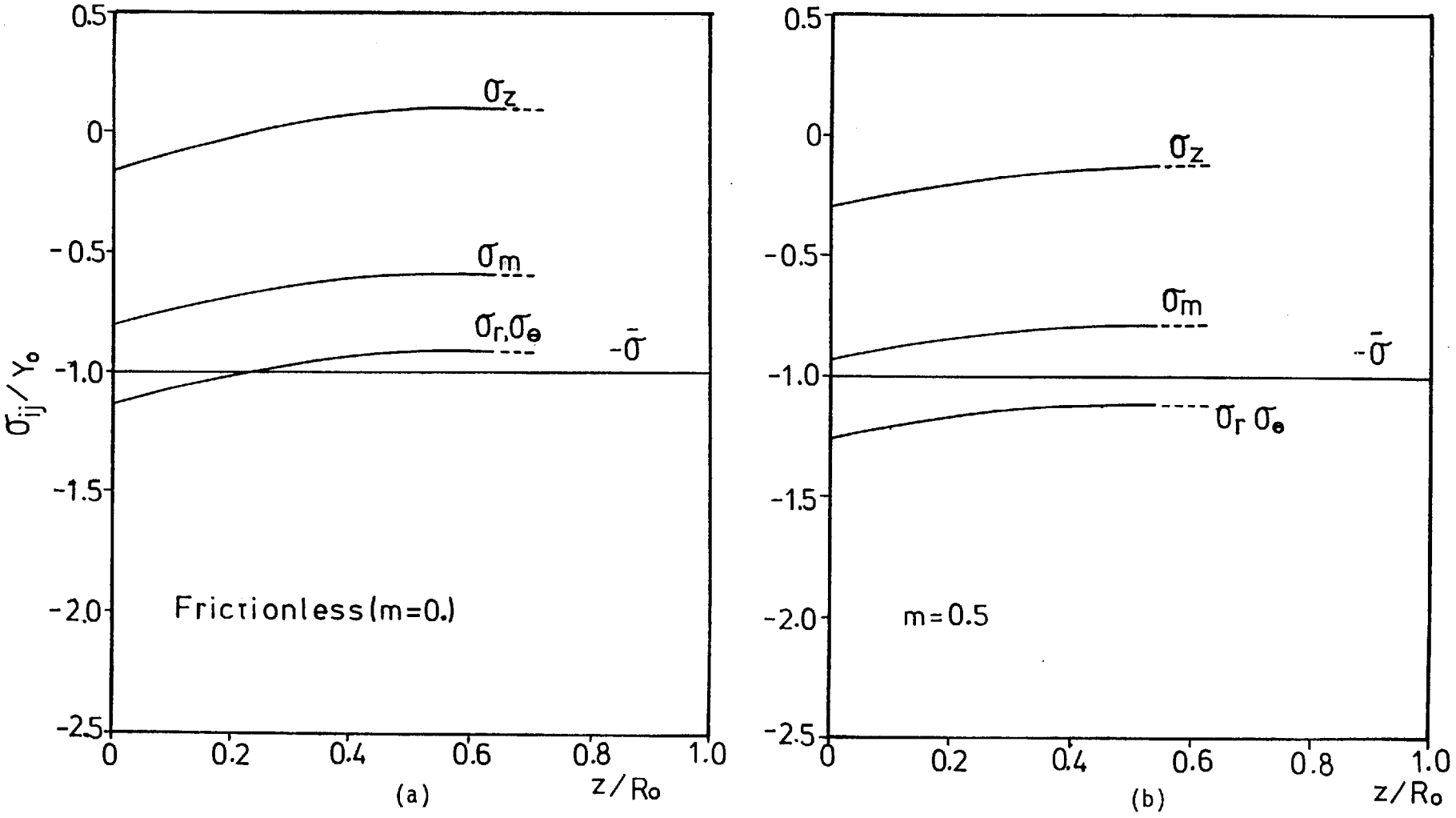

Figure 5.22: Stress history along the axis. Non hardening material. R=4, Die semi-angle=45^o
(a) m=0.0; (b) m=0.5

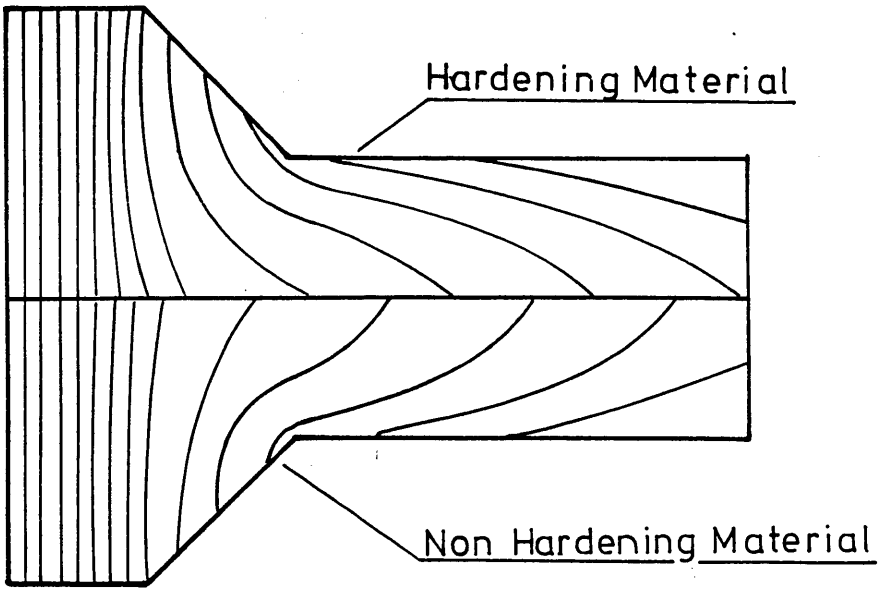

Figure 5.23: Vertical grid distortion.Effect of work-hardening
Frictionless extrusion. R=4,Die semi-angle=45^{o}

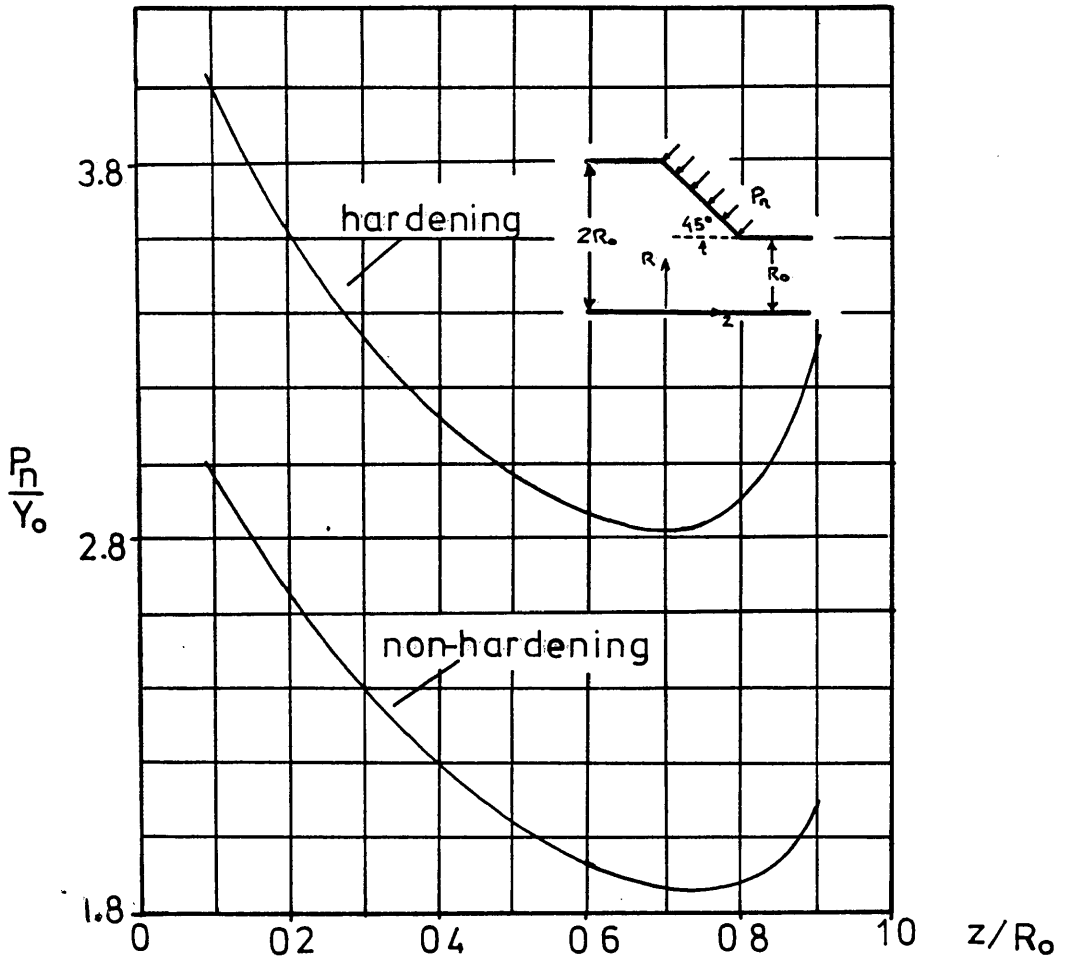

Figure 5.24: Normal die pressure distribution.
R=4, Die semi-angle=45

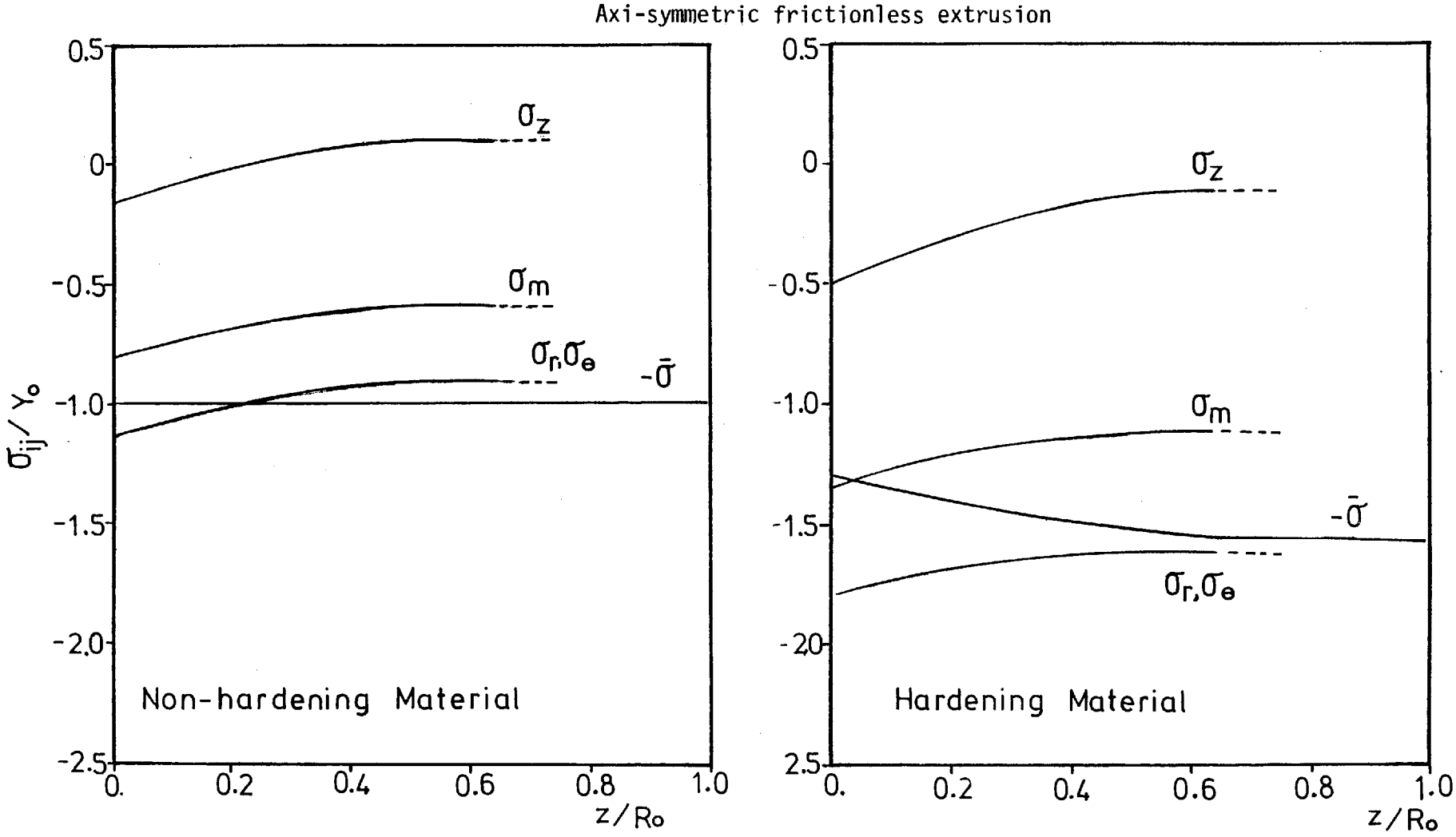

Figure 5.25: Stress history along axis.Effect of work-hardening.R=4,Die semi-angle=45^o

CHAPTER 6

HYDROSTATIC EXTRUSION OF BI-METALLIC RODS

6.1 Introduction

There are a number of requirements in industry which cannot be met satisfactorily by one material and call for the use of combinations of materials either because of structural soundness or because of economic reasons. Bi-metal rods (also called clad metal rods), which are rods or wire of two dis-similar metals, are one of such composite materials. The core, a cylindrical body of one metal, is surrounded by a concentric cylindrical sleeve of another metal. The two metals are usually required to be effectively "interlocked" so as to function effectively together. The usefulness of such materials stems from the possibilities presented by the combination of qualities of dis-similar metals.

A typical example is the case of wire manufacture. Fluctuations in the price of copper and its availability have led manufacturers to search for substitutes. Aluminium was introduced as a substitute material for copper about twenty years ago. Its abundant availability, good conductivity (60% of pure copper), and low price made it very attractive. However, the surface of aluminium oxidizes readily making it difficult to achieve proper contact between aluminium conductors.

To circumvent this difficulty, and still utilize the economy of aluminium, copper-clad aluminium was introduced around 1963. This metal system offers a 50% reduction in weight for equivalent conductivity, as compared to copper, and combines the ability of copper to make good contacts with the light weight and easy avàilability of aluminium. This kind of bi-metallic rods is usually produced by metal forming operations, frequently drawing or extrusion, following cladding.

The object of this chapter is to present an analysis for the mechanics of the hydrostatic extrusion of copper-covered aluminium rods

using the finite element techniques described in the two preceding chapters, comparing the results with experimental data obtained using the procedure described in Chapter 3.

6.2 Previous Work on the Deformation of Composite Sandwich Materials

Arnold and Whitton[6.1] in 1959 are credited with being the first to publish their findings on sandwich rolling of hard materials. The process involved placing a hard metal strip between two layers of softer material.

The rolling process was analysed theoretically on the assumption that plane sections remain plane and that the percentage reduction in both hard and soft materials was the same. Classical theories of rolling were used for the calculation of roll load and torque employing an equivalent yield stress Y_{eq} defined as:-

$$Y_{eq} = \frac{2h_s Y_s + h_h Y_h}{2h_s + h_h} \qquad (6.1)$$

where h = thickness, Y = yield stress and sub-indices s, h indicate soft and hard materials respectively.

This equivalent yield stress was derived by a simplified analysis of the stresses acting on the sandwich strip.

Alexander[6.2] in his discussion to Arnold and Whitton's paper proposed a more formal approach to the problem based on the analysis of plane strain compression of a sandwich and pointing out the inherent difficulties that had to be surmounted if a more detailed analysis of the problem was to be carried out.

Weinstein and Pawelski[6.3], following an approach very similar, in principle, to that proposed by Alexander, developed a theory that could describe the main characteristics of the plane

drawing of sandwich materials.

This theory is simple to understand and it is worth looking into it in some detail, since the basic concepts serve as a basis for almost all the other published work. The specific problem considered was the plane strain drawing of a strip of hard material cladded with a softer material and undergoing uniform deformation.

In considering the plane of entry, if the materials were to be deformed separately (i.e. not in sandwich), the Mohr's circles would appear as in Figs. 6.1a and 6.1b, where the plane strain rigid-perfectly plastic shear yield strength of the matrix, K_m, is assumed greater than that of the surface cladding, K_c. Then, if no sideway stresses are present, ideally, only normal pressures P_m and P_c equal to twice the shear strength exist.

For the sandwich material undergoing uniform deformation, it follows that the lower strength clad material must transmit a compressive stress of magnitude P_m to the matrix material in order to initiate plastic flow. However, it is evident that the cladding material cannot sustain a vertical compressive stress larger than P_c. Thus it becomes necessary to shift the Mohr's circle for the cladding material to the left, as in Fig. 6.1c, so that the transverse compressive stress through both materials can be P_m. Whilst this shift of the Mohr's circle of the weaker material ensures compatibility of the transverse stresses, it also indicates that a longitudinal compressive stress must act on the weaker material in order to satisfy equilibrium conditions. This compressive stress must be generated across the interface of the two materials since no sideways tension or compression exists. This means that the stronger material must be subject to a tensile stress to regain overall force equilibrium, that is, both Mohr circles must now shift to the right as shown in Fig. 6.1d. A shear stress τ_m must, therefore, exist at the sandwich inter-

face as the mechanism for generating the different stress components.

This theory was elaborated in detail for the plane drawing problem and its predictions compared favourably with experimental evidence.

Atkins and Weinstein[6.4] further extended this work and proposed models to describe the plastic behaviour of sandwich composites in tension, compression, rolling, drawing and extrusion, including work-hardening effects.

It is worth pointing out that although these analyses were somewhat more formal than that of Arnold and Whitton, they arrive at the same concept of using an equivalent yield stress which is a function of the volumetric fractions of each material, i.e. Equation (6.1). Also, the analysis suggests that the individual rates of hardening are of little or no consequence.

Afonja and Sansome[6.5] studied the problem of sandwich rolling, arriving at similar results to those of Atkins and Weinstein. In fact, these last authors have said that both analyses are identical[6.6].

Chia and Sansome[6.7], following the same basic assumptions, dealt with the problem of the axisymmetric drawing of bi-metallic rod.

Helman[6.30] has also used the same approach to tackle the augmented hydrostatic extrusion of bi-metallic rod.

A preliminary experimental investigation of the extrusion of rod, tube and can from combinations of dissimilar materials has been made by E. Whitfield[6.8] at N.E.L. The results showed that flow of metals during the co-extrusion process is dependent on their relative mechanical properties and dimensions, and on the geometrical disposition of the dissimilar metals in the original billet as well as the die geometry.

Whitfield also carried out experiments in order to assess the minimum value of the initial cladding thickness for successful

extrusion of copper-covered billets of mild steel into rods, tubes and cans[6.9]. He found this value to be dependent on the extrusion ratio of the particular experiment and that the ratio of initial cladding thickness/extrusion ratio was approximately constant.

B. Avitzur[6.10] made a very comprehensive analysis of the mechanical conditions of the bi-metallic extrusion (drawing) process, using the upper bound method and his well-tried spherical velocity fields. He aimed at producing a criterion for the analysis of failure modes. The main variables defining the process were:-

(i) Percentage reduction in area.

(ii) Semi-cone angle of the die.

(iii) Die land length.

(iv) Friction.

(v) Relative size of the core related to the cladding tube.

(vi) Ratio of the flow stress of the core to the flow stress of the tube.

(vii) Prescribed body tractions (front tension in extrusion and back tension in drawing).

He reasoned that when the process departed from homogeneous deformation some sort of fracture was to be expected even though each material separately is a highly ductile material. The two metals chosen for the study were aluminium and copper using them both as tube

and core materials. The results were presented in graphs and agreed favourably with some selected experimental evidence.

The paper presented some general trends to apply as failure criteria, even if these tendencies may be violated occasionally:-

(i) The harder the cladding, for $Y_c/Y_t < 1$, the more likely it is that fracture will occur.

(ii) The harder the core, for $Y_c/Y_t > 1$, the more likely it is that core fracture will occur.

(iii) The greater the departure of the strength ratio from unity, the more likely it is that fracture will occur and the narrower becomes the range of process variables within which sound flow is likely to occur.

(iv) The higher the mean pressure (higher back pressure, lower front tension), the wider the range of variables for which sound flow is expected. Thus in extrusion, the range of sound flow is wider than that in drawing.

(v) In general, the higher the friction, the narrower the range for sound flow, except that core fracture in extrusion is deferred by higher friction.

This analysis was restricted, in the sense that only one mode of deformation was studied (uniform deformation) and no means of predicting alternative modes were presented.

Zoerner et al[6.11] studied experimentally the hydrostatic extrusion of hard core clad rods with special consideration to the

influence on the mechanics of the process of the bond between core and sleeve. The results showed that fracture in hard core clad rod is not controlled by an inherent brittleness of the materials but by process variables.

Osakada et al[6.12] developed a theoretical analysis to predict the mode of deformation of bi-metallic rods with a hard core during hydrostatic extrusion using the upper bound method. The effects of the end of the billet, yield stress ratio, fraction of the harder core, extrusion ratio, die angle and frictional shear factors at the interface and die surface were considered in the analysis.

They proposed a velocity field different to that of Avitzur's in the sense that it could describe more than one mode of deformation. This general velocity field was used to calculate the extrusion pressure and the field giving the lowest extrusion pressure was taken as the mode of deformation most likely to occur for the given conditions.

The theoretical analysis predicted that uniform deformation will be attained when the die angle is low and the frictional stress at the interface is high. The cladding type of deformation will occur when the inner material is hard and the interface friction is relatively low and the die angle is large.

Osakada and Niimi[6.13] derived a general expression for the radial flow field which includes all possible boundary shapes and applied it to the extrusion of composite materials.

Hartley[6.14] also proposed a velocity field for the extrusion of piecewise tubes, but unlike that of Osakada et al[6.12], he assumed that the flow of the materials converged to the same point.

Lugosi et al[6.15] have recently combined features of the velocity fields proposed by Osakada et al and Osakada and Niimi to permit the core and tube to converge to different points while

incorporating general expressions for the boundaries of the deforming regions.

They assumed that the core and tube emerge from the die with the same velocity and allowed for relative slip between the constituents during deformation. This model was used for a preliminary analysis of the effect of interfacial friction on the deformation process characteristics.

Story et al[6.16] have carried out an experimental analysis in order to assess the influence that the combination of variables leading to failure has on the hydrostatic extrusion of a niobium-titanium superconducting alloy, in a pure aluminium matrix, into a back (receiver) pressure. Results showed that increasing the receiver pressure increased the range of acceptable process variables to produce sound flow.

Alexander and Hartley[6.17] carried out a comparative study of experimental results obtained from the hydrostatic extrusion of copper covered aluminium rods with the prediction of theories of increasing complexity, including one based on a finite element analysis. The experimental results were shown to be characterised by an equation of the well-known form:-

$$P = W + K \ell n\, R \qquad (6.2)$$

where P = extrusion pressure, W and K are constants, and R is the extrusion ratio. The constants W and K were found to be a linear function of the volume fraction of the core. The extrusion pressures calculated using these "equivalent" constants were in satisfactory agreement with the experimental values. The finite element analysis of the problem was carried out using the penalty function approach. They were able to predict the shape of the interface which was in

remarkable agreement with the experiments.

Holloway et al[6.18] analyzed primarily the conical deformation modes that were found within their tests of conventional extrusion of bi-metallic rods. Their main contribution was a semi-empirical approach to find an upper bound for the extrusion pressure. This approach was based on the graphical evaluation of the velocity discontinuities after considering plane strain slip-line solutions, or the observed flow pattern. These velocities were then simply squared and assumed to be the velocity discontinuity pattern of the axisymmetric situation. Substitution of these velocity dis-continuities in the appropriate expressions (Equation 3, Ref.[6.18]) and use of an equivalent yield stress resulted in upper bound extrusion pressures which were found to be in good agreement with experimental values. However, this approach neglects the rate of internal energy dissipation in diametrical compression of the deformable material between each of the pairs of assumed tangential velocity discontinuity surfaces.

Matsuura and Takase[6.19] carried out experiments to study the hydrostatic extrusion of aluminium-covered copper rods. They presented some general conclusions:-

(i) The relation between the extrusion pressures and the die semi-angle is different from that existing for the extrusion of a single metal.

(ii) Within the limits of the experiments ($Y_c/Y_t \leq 4$), the empirical relation $P = A + B \ln R$ can be used to estimate the hydrostatic extrusion pressure.

(iii) The greater the reduction imposed on the rod the larger the

volumetric fraction of copper in the product.

(iv) The application of a back pressure prevented failure of the core.

(v) Experimental values of the compressive yield stress agree very well with results calculated by the "Law of Mixture", namely, $Y_{eq} = Y_{c.f} + (1 - f) \cdot Y_t$, which is none other than the equivalent yield stress used by earlier authors (see Equation (6.1)).

The same authors[6.20] have recently analysed the problem using the finite element technique. They adopted an elastic-plastic approach based on Yamada's theory[6.21] and restricted their analysis to the initial stages of the process, presenting in graphical form the development of the plastic deformation zones and the relation between the extruding pressure and the displacement of the billet end. This was to be expected due to the fact that the limitations of the formulation employed (see Chapter 4) do not permit the steady state mode of deformation to be analysed.

Chitkara and Crawford[6.22] carried out an experimental investigation into the forward extrusion of short length billets of composite materials through square dies under both plane strain and axisymmetric flow conditions. Aluminium and copper were the materials chosen, using them in turn as either core or cladding. They present some modes of deformation which had not been reported before. Most of these modes are due to the very particular configuration of the sandwich employed and are not likely to be encountered in practical situations.

They also modified the work of Adie and Alexander[6.23] and

Halling and Mitchell[6.24] on the extrusion of single materials to find a graphical upper bound for the extrusion of sandwich materials.

N. Ahmed[6.25] carried out investigations in the hydrostatic extrusion of copper clad aluminium wire trying to assess the influence of die design, extrusion ratio, extrusion pressure, product velocity, percentage of core and the ratio of flow stress of copper to aluminium, presenting definite results for the limited number of cases studied.

Holloway et al[6.26] extended earlier work by Sheppard and Raybould[6.27] and calculated the rate of heat transfer and the average temperature rise during the extrusion of composite materials. They assumed that the heat generated was also a function of the core volumetric fraction. Theoretical predictions of the temperature rise experienced at the die throat agreed very well with experiments.

Hawkins and Wright[6.28] present experimental evidence in an effort to justify the use in theoretical analysis of an equivalent flow stress related to the individual yield stresses and volume fractions of the sandwich components. They also put forward an explanation for the reported existence of an optimum cladding to core thickness ratio in sandwich rolling (see Refs.[6.1],[6.4],[6.5]).

Blazynski and Townley[6.29] have modified approximate upper bound, force equilibrium (slab method) and Shield-type[6.31] axisymmetrical analyses to account for the effects of friction and strain hardening in plane-strain, plug drawing of coaxially, integrally welded bi-metallic tubing without back-pull. They found that the upper bound approach was more accurate in the lower range of strains, whereas, the lower bound theorems were a better approximation in the higher range. They concluded that a Shield-type analysis is to be preferred because of its ability to indicate the distribution and magnitude of shear stresses.

Helman[6.30] tackled the problem of drawing assisted

hydrostatic extrusion of copper-covered stainless steel rod. He adapted the method of weighted residuals to integrate the Prandtl-Reuss equations and obtained an approximate polynomial solution for the stress distribution associated with Avitzur's well-known spherical velocity field. These stresses together with the strains were used to calculate, using the same numerical technique, the temperature distribution inside the deforming region. The loads calculated were shown to agree satisfactorily with experimental results. The stress distribution and, by implication, the temperature distribution are incorrect, in the writer's opinion. The reason for this is that he assumed incorrect boundary conditions, namely, that the shear, radial and circumferential stresses were zero at the axis of symmetry. Although the first of these conditions is true because of the axi-symmetric condition, the other two are undoubtedly incorrect.

6.3 Finite Element Analysis

As is evident from the literature just reviewed, a fair amount of effort has been put into the study of the deformation processing of composite rods, especially to problems similar to the ones considered here. Indeed, calculation of the pressures required to extrude (or draw) bi-metallic rods can be accomplished by a number of methods, from simple semi-empirical approaches to complex upper bounds requiring the use of the computer. However, there is still a need to understand the detailed mechanics of the process especially those concerning the stress and strain fields developed inside the deformation zone.

The finite element techniques developed in the last two chapters provide a way to carry out a detailed analysis of the problem with a minimum number of assumptions.

6.3.1 Statement of the Problem

The billets considered for this analysis are composite materials in which the inside material (aluminium) is softer than the outside material (copper). A typical configuration of the process is shown in Fig. 6.2. In cross section, the inner core is a circular solid rod and the surrounding harder material is an annular tube of internal and external radii R_{c_1} and R_{t_1}, respectively. The fraction of the cross-sectional area of the inner material, f, is, therefore, defined as:-

$$f = R_{c_1}^2 / R_{t_1}^2 \tag{6.3}$$

The total extrusion ratio is given by:-

$$R = R_{t_1}^2 / R_{t_2}^2 \tag{6.4}$$

where R_{t_2} is the radius of the tube after extrusion (the die semi-angle is denoted by α_D).

Both materials are assumed to be rigid-plastic whose experimentally determined stress-strain relations (Chapter 3) are fitted for the purposes of the finite element analysis by polynomials of the form:-

$$\bar{\sigma} = A + B\bar{\varepsilon} + C\bar{\varepsilon}^2 + D\bar{\varepsilon}^3 + E\bar{\varepsilon}^4 + F\bar{\varepsilon}^5 + G\bar{\varepsilon}^6 \tag{6.5}$$

where $\bar{\sigma}$ is the yield stress, $\bar{\varepsilon}$ is effective strain and the polynomial coefficients take the following values, if $\bar{\sigma}$ is in MN/m^2:-

Copper (MN/m^2)	Aluminium (MN/m^2)
A = 94.880	A = 53.207
B = 944.890	B = 169.210
C = - 1408.200	C = - 200.930
D = 1143.900	D = 166.960
E = - 504.760	E = - 77.530
F = 114.670	F = 18.119
G = - 10.492	G = - 1.673

It is assumed that no relative movement between the two metals occurs at the interface and, hence, the interface is considered as the superposition of the limit surfaces of both metals. Furthermore, both materials are assumed to be subjected to the same pressure at the billet end (the open end) and moving at the same entry velocity.

The latter assumption is justified by the experimental arrangement used in this work (see Chapter 3).

6.3.2 Interface Shape

One of the unknowns of the problem is the position and shape of the interface. Of course, this shape could be assumed a priori or an experimentally determined one could be used. However, neither of these alternatives takes full advantage of the method and in fact reduce its predictive character. Besides, if the interface can be predicted, an additional comparison with experimental results is available for the purposes of validation of the theoretical model.

As has been stated before, the results of the finite element analysis are given in terms of a set of axial and radial velocities at each nodal point. Since the direction of material flow is defined by these velocities, this data can be used to find the position of the metal interface.

Price[6.32], when analyzing the dieless drawing problem, considered various schemes to modify the position of nodal points using the velocities. He found that the best scheme was the one proposed by Alexander and Turner[6.33]. This scheme was chosen for this work and it will be described below for the sake of completeness.

In Fig. 6.3 the arrowed lines represent the directions of material flow which may be expressed as a slope, S given by:-

$$S = \frac{V_r}{V_z} \tag{6.6}$$

The intermediate nodal point, I, has a slope, S_I, represented by the dotted line IA. IB is the slope, S_J, of the adjacent nodal point. The new radial coordinate of nodal point J is in position midway between points A and B defined by:-

$$r_J = r_I + \frac{(S_J + S_I)}{2} \cdot Z_n \tag{6.7}$$

where Z_n is the axial distance between the points and remains unaltered. The solution procedure starts with a "guessed" shape and position, namely, a conical interface and uniform reduction (see Fig. 6.2). After each iteration the velocities are used to modify the radial position of the internal nodal points. Since the solution depends on the distribution of the metals within the deforming region, when convergence is achieved for the velocities the position of the interface conforms with them. Thus, it can be argued that convergence of the velocity solution also gives the correct position of the interface.

6.3.3 Computational Conditions

Following the experimental work, various configurations were

analyzed using the finite element method. Table 6.1 shows the conditions used.

TABLE 6.1

Die semi-angle (α_D)	Reduction (R)	Core percentage (f)
20^o	2, 3.05 and 7.865	0.735 and 0.327
45^o	2, 3.05 and 4.08	0.735 and 0.327

It was shown in the previous chapter that, provided the incompressibility condition was properly satisfied, both the penalty and velocity-pressure formulation give almost identical solutions. Hence, only the penalty function formulation is used in this chapter together with the techniques developed to include strain hardening effects. Bi-linear isoparametric elements with appropriate selective integration schemes are used.

Figs. 6.4 and 6.5 show some of the meshes employed. It is important to notice that the singularities at the corners of the die are dealt with using the "Case B" method introduced in the previous chapter, namely, by "eliminating" the corner from the continuum to be modelled.

The process was analyzed assuming zero friction at the die-tube interface; this is warranted by experimental evidence concerning friction in hydrostatic extrusion[6.34].

A cut-off value, $\gamma = \frac{2}{3}\bar{\sigma}/\dot{\bar{\varepsilon}}$, of 10^9 was specified in order

to deal with the "rigid regions". Convergence value was set at $||\Delta\bar{u}||/||\bar{u}|| \leq 0.0005$. A penalty coefficient (α) of 10^9 was chosen.

6.4 Finite Element and Experimental Results

6.4.1 Extrusion Pressure

The theoretical extrusion pressures are calculated from the reactions derived from the stiffness equations. These are plotted against the natural logarithm of the extrusion ratio in Figs. 6.6 and 6.7.

It is clear that irrespective of the values of the core fraction f and the die semi-angle α_D and in common with conventional monometallic hydrostatic extrusion, the level of energy involved in the process increases with reduction. It can also be seen that the effect of the core fraction is correctly predicted.

Correlation between experiment and theory is excellent for the 40^o die, but not so good for the 90^o die. This is perhaps due to the fact that, for the latter case, the elements used in the analysis are more distorted, which, in general, lowers the accuracy of the element. Because of this, and in order to save space, the rest of the results will only be presented for the 40^o die.

6.4.2 Interface Shape

The main attraction of the finite element method is its ability to predict the fine detail of the behaviour. Plate 6.1 shows billets that have been split on a meridional plane to show the detailed shape of the interface between the aluminium core and the copper tube. In Figs. 6.8 and 6.9 the measured shape of the interfaces for different core fractions and reduction is shown in detail and compared with the shape predicted by the finite element analysis

using the technique described in Section 6.3.2. The agreement is quite good, even though this could be improved if a more accurate convergence were set. Simple analyses of the upper bound type give no information at all in this respect. Moreover, the simple conical interface often assumed can be seen not to conform with the actual behaviour.

Another feature worth mentioning is that the finite element method predicts, for the given conditions, the same reduction for both materials, which is indeed what the experimental evidence shows.

6.4.3 Kinematics of the Process

Figs. 6.10 and 6.11 depict the effective strain rate ($\dot{\bar{\varepsilon}}$) distribution for different reductions and core fractions. As might be expected, there is some degree of strain-rate concentration near the die corners. As in monometallic extrusion the strain rate increases gradually from the entrance towards the die exit and drops sharply near the exit, suggesting the existence of shear zones. It can also be seen that the boundaries between the rigid and deforming regions differ from the often assumed spherical shape, especially at the die entry. This agrees with experimental evidence[6.15]. The effective strain rate distributions also suggest that, for a given reduction, the effect of different core fractions is more marked towards the die exit and close to the die wall.

Integration of the velocity field and the strain rate distribution yields the grid distortion and the effective strain distribution respectively.

Figs. 6.12 - 6.15 show the grid distortions and corresponding effective strain distribution for the cases considered. The grid distortions suggest that the outer material (the tube) is "pulled forward" by the core. This is revealed by the convex shape of the

grid distortions in the tube. Analagously, the flow in the core seems to be restricted by the outer material, and this is also reflected in the shape of the grid distortions near to the metal interface, especially at greater reductions (see Figs. 6.14, 6.15, 6.24 and 6.25, for example). The amount of strain hardening in the outer material is greater near the die than near the interface. This trend seems to be slightly reversed towards the exit when the initial core fraction is small (see Figs. 6.13b and 6.15b). Equally, the amount of strain in the core is greater near the interface than near the axis of the workpiece at the beginning of deformation and the trend seems to reverse towards the exit. However, for all the conditions considered, and in common with monometallic extrusion, in the product the strain is lowest near the axis and gradually increases towards the periphery.

6.4.4 Stress Distribution

The stress distributions are readily derived from the finite element analysis and are shown in Figs. 6.16 to 6.19.

These distributions are more difficult to discuss due to the impossibility of measuring stress experimentally. However, some trends are identifiable and these can be discussed.

As expected, all the normal stresses show a tendency to become less compressive towards the die exit. This is in sharp contrast to the results reported in Helman's thesis[6.30] where, as previously discussed, incorrect boundary conditions led to illogical stress distributions.

The radial stress distribution for all conditions exhibit different characteristics. In the middle of the deforming region the radial stresses are fairly constant across a given section and a slight concentration appears, as expected, at the exit corner. Near

the entry region the stress concentration at the die corner seems to extend well inside the specimen. A possible explanation for this is that at the beginning of plastic flow the change of slope of the metal interface acts as a die corner creating additional radial stress concentrations. These characteristics in the radial stress distributions are more evident at large reductions, see Figs. 6.18a and 6.19a. The axial stress distribution is very important since this stress is considered to have a great influence on the occurrence of fracture. It is very difficult to identify a general trend across a given section because of the effect of the interface and because of the nature of the technique used for averaging the stresses used in the drawing of the contours, namely, averaging the stresses at the nodes. However, some specific features can be identified. The stresses close to the interface tend to be less compressive in the tube which agrees with the elementary theory explanation of the softer (core) material "pulling" the harder (tube) material. It can also be noticed that for the greater core fraction the axial stresses in the tube become less compressive earlier, which suggests a great likelihood of fracture occurring (see Figs. 6.16b and 6.18b). In the core the stresses become more compressive as we move away from the axis, but this trend is reversed close to the interface.

The shear stress distributions show that the stresses are greater near the die surface and steadily decrease towards the axis of the specimen. An exception to this trend is the case shown in Fig. 6.19d, where the maximum shear stress occurs on the interface near the die exit. The contours also give an insight as to where the material starts shearing.

Figs. 6.20 and 6.21 show the normal stress distribution at the interface for different conditions. The normal stress is always compressive and, except for a small increase at the beginning of

deformation, it decreases (in the compressive sense) towards the exit. This suggests that the metal interface behaves as a die surface with respect to the core material.

6.5 The Use of the Finite Element Analysis as an Experimental Tool

The relatively good agreement between the experimental and theoretical results warrants the use of the theoretical analysis as a tool in the study of the hydrostatic extrusion of composite materials.

The one feature of the process chosen for closer study here is the effect of interfacial friction in the process.

In order to carry out such a study an hypothetical case has been analysed. For convenience, one of the configurations already analysed is chosen, namely, copper-covered aluminium rod, $f = 0.327$, $\alpha_D = 20^o$ and $R = 3.05$.

6.5.1 Introduction of Interface Friction

Introduction of friction at the interface presents a problem due to the Eulerian character of the finite element formulation. At low friction it is impossible to guess a priori the relative position of nodal points at the interface (the contact surface of both metals); furthermore, it can no longer be assumed (as in the previous cases) that contact points belonging to both the sheath and the core have the same velocity.

The simplest way to overcome this difficulty is to take advantage of the main considerations of the friction model most often used in metal-working analysis. This model considers that the work-piece in contact with the tools can be represented as a material of constant shear strength τ_c. However, instead of letting $\tau_i = k$, as for sticking friction, we consider that the interface shear strength may be some constant fraction m of the yield strength in shear where m

is called the interface friction factor:-

$$m = \frac{\tau_i}{k} = \frac{\text{interface shear strength}}{\text{yield stress in shear}} \tag{6.8}$$

Values of m vary from 0 (perfect sliding) to 1 (sticking).

It is then simple to extrapolate this model to finite element analysis by considering a thin layer of elements with elemental properties in accordance with relation (6.8). These kinds of elements were originally proposed by Zienkiewicz et al[6.35] and have been used successfully by Hartley et al[6.36] for the study of ring compression.

It seems, however, that the problem under consideration does not fall within the limits of the model just mentioned, since, at the interface, it is not at all clear what should be regarded as workpiece and what as tool surface. However, it appears logical to think of the softer material as the workpiece. Therefore, a thin layer of elements is interposed at the interface with elemental properties according to:-

$$m = \frac{\tau_i}{k_s} \tag{6.9}$$

where k_s is the current yield shear stress of the softer material. This will apply independently of the sandwich configuration.

This technique eliminates the problems outlined before and in fact reduces the problem to the extrusion of a composite rod with an additional component fixed to the original two. The interface friction factor is varied between 0.1 and 1.0 and the other computational conditions are kept the same.

Two different end conditions are considered. First, both sheath and core are assumed to have the same entry velocity, and

second, the products are assumed to have the same exit velocity; this last assumption is equivalent to solving the drawing problem.

6.5.2 Results

It has been shown experimentally[6.15] that interfacial friction plays a major role in this process, especially on the occurrence of fracture. Fig. 6.22 shows the axial stress distribution across the tube thickness and the exit. This section was chosen because the results from previous work suggest that this is where the higher tensile stresses are likely to occur. It can be seen that for all frictional conditions the stresses are more compressive near the die surface than near the interface, becoming more tensile at the interface at low friction. This suggests that fracture of the tube material is more likely to occur when the interfacial shear yield strength is low. This is in agreement with existing experimental evidence[6.15]. In fact the only fracture encountered in the experimental part of this work, see Plate 6.2, was found to be in a specimen where oil had seeped through to the interface.

Fig. 6.23 shows the variation of extrusion pressure with interfacial friction: a small variation of about 6% is observed across the range considered and, conforming to elemental theory, it takes more energy to extrude a composite with low interfacial shear yield strength. Although the results presented hitherto are for the first end condition (see previous section), the trend is the same for both end conditions.

Figs. 6.24 and 6.25 show the grid distortion and position of the interface for different interface friction and for the extrusion and drawing end conditions respectively. For the extrusion end condition, the finite element analysis predicts that at low interfacial friction the softer material (core) moves faster than the

harder material (tube) within the deforming region since it is less restricted. However, both materials leave the die at the same velocity and suffer the same reduction, the shape of the interface not being noticeably affected, which seems to suggest a stick-slip situation at the interface.

For the drawing end condition, the grid distortion suggests a completely different mode of flow at low interfacial friction. The softer material (core) moves slower than the harder material (tube) within the deforming region. In fact, the entry velocities of both material are different which implies that a low friction non-uniform deformation is present. Further evidence of this is shown in Fig. 6.26, where it can be seen that the core suffers more deformation than the tube.

It is also worth noticing that for high interfacial friction the grid distortions for both end conditions are almost identical.

6.6 Final Remarks

The finite element analysis of the extrusion of composite rod-tube combinations gives information which cannot be provided by any other theoretical method. The extrusion pressures predicted (which are usually taken as a measurement of the accuracy of theoretical models) are in good agreement with experiments. However, this is only a minimal part of the data that the method can produce. The kinematical characteristics of the process together with the stress distributions are all described for the first time, to the author's knowledge, and should be helpful for establishing the conditions necessary to give effective metallurgical bonding at the interface.

The finite element technique can be used as a theoretical tool to study the effect of varying the different parameters of the

process, rendering information that otherwise is not possible to predict theoretically.

Various general conclusions can be drawn from the results presented here:-

(a) For all the conditions studied uniform deformation of both components occurs.

(b) The interfacial shape is not conical, as is often assumed.

(c) There seems to be evidence to suggest that fracture of the sheath material is more likely when the core fraction is large and/or when the interfacial shear yield strength is low.

(d) The assumption that both materials have the same entry or exit velocity seems to affect the finite element results, and should be very carefully considered before trying to extrapolate results to accommodate specific actual conditions.

REFERENCES

6.1 ARNOLD, R. R. and WHITTON, P. W.
"Stress and Deformation Studies for Sandwich Rolling Hard Metals".
Proc. Inst. Mech. Engrs., Vol. 173, p. 241, (1959).

6.2 ALEXANDER, J. M.
Discussion to Reference 1, Ibid.

6.3 WEINSTEIN, A. S. and PAWELSKI, O.
"Plane Strain Drawing of Sandwiched Metals".
Proc. 8th Int. M.T.D.R. Conf., p. 961, (1967).

6.4 ATKINS, A. G. and WEINSTEIN, A. S.
"The Deformation of Sandwiched Materials".
Int. J. Mech. Sci., Vol. 12, pp. 641-657, (1970).

6.5 AFONJA, A. A. and SANSOME, D. H.
"A Theoretical Analysis of the Sandwich Rolling Process".
Int. J. Mech. Sci., Vol. 15, pp. 1-14, (1973).

6.6 ATKINS, A. G. and WEINSTEIN, A. S.
Comment on Reference 5, Int. J. Mech. Sci., Vol. 15, p. 943, (1973).

6.7 CHIA, H. T. and SANSOME, D. H.
"Theoretical Study of the Drawing of Bi-Metal Rod and Tube".
Proc. 15th Int. M.T.D.R. Conf., (1974).

6.8 WHITFIELD, E.
"A Preliminary Study of the Co-Extrusion of Dissimilar Metals".
N.E.L. Report No. 265, (1967).

6.9 WHITFIELD, E.
"Effect of Plating Thickness on Cold Extrusion of Plated EN 2E Steel".
N.E.L. Report No. 268, (1967).

6.10 AVITZUR, B.
"The Production of Bi-Metal Wire".
The Wire Journal, 3, pp. 42-49, (1970).

6.11 ZOERNER, W., AUSTEN, W. and AVITZUR, B.
"Hydrostatic Extrusion of Hard Core Clad Rod".
Trans. of ASME, J. Basic Engng., Series D, 94, pp. 78-80, (1972).

6.12 OSAKADA, K., LIMB, M. and MELLOR, P. B.
"Hydrostatic Extrusion of Composite Rods with Hard Cores".
Int. J. Mech. Sci., Vol. 15, pp. 291-307, (1973).

6.13 OSAKADA, K. and NIIMI, Y.
"A Study on Radial Flow Field for Extrusion Through Conical Dies".
Int. J. Mech. Sci., Vol. 17, pp. 241-254, (1975).

6.14 HARTLEY, C. S.
"Upper Bound Analysis of Extrusion of Axisymmetric, Piece-Wise Homogeneous Tubes".
Int. J. of Mech. Sci., Vol. 15, pp. 651-663, (1973).

6.15 LUGOSI, R., HARTLEY, C. S. and MALE, A. T.
"The Influence of Interface Shear Yield Strength on the Deformation Mechanics of an Axisymmetric Two Component System".
Proc. V. NAMRC, pp. 105-113, (1977).

6.16 STORY, J. M., AVITZUR, B. and HAHN, W. C.
"The Effect of Receiver Pressure on the Observed Flow Pattern in the Hydrostatic Extrusion of Bi-Metal Rods".
Trans. of ASME, J. of Engng. for Ind., Vol. 98, pp. 909-913, (1976).

6.17 ALEXANDER, J. M. and HARTLEY, C. S.
"On the Hydrostatic Extrusion of Copper-Covered Aluminium Rods".
Int. Conf. on Hydrostatic Extrusion, University of Stirling, Scotland, (1973).

6.18 HOLLOWAY, C., BASSET, M. B. and SHEPPARD, T.
"On Load Pressure Requirements During the Cold Extrusion of Composite Materials".
Proc. 17th Int. M.T.D.R. Conf., pp. 388-399, (1976).

6.19 MATSUURA, Y. and TAKASE, K.
"Characteristics on Hydrostatic Extrusion of Composite Materials".
Report of the Castings Research Laboratory, Waseda University, No. 22, pp. 41-55, (1971).

6.20 MATSUURA, Y. and TAKASE, K.
"Study on Plastic Deformation in Hydrostatic Extrusion".
Report of the Castings Research Laboratory, Waseda University, No. 27, pp. 41-50, (1976).

6.21 YAMADA, Y.
Int. J. Mech. Sci., Vol. 10, p. 343, (1968).

6.22 CHITKARA, N. R. and CRAWFORD, J.
"Characteristics Features in the Incremental Extrusion of Short Slugs of Composite Materials Through Square Dies".
Proc. 20th Int. MTDR, (1979).

6.23 ADIE, J. F. and ALEXANDER, J. M.
"A Graphical Method of Obtaining Hodographs for Upper Bound Solution to Axisymmetric Problems".
Int. J. Mech. Sci., Vol. 9, p. 349, (1967).

6.24 HALLING, J. and MITCHELL, L. A.
"An Upper Bound Solution for Axisymmetric Extrusion".
Int. J. Mech. Sci., Vol. 7, p. 277, (1965).

6.25 AHMED, N.
"Extrusion of Copper Clad Aluminium Wire".
J. of Mech. Work. Tech., 2, pp. 19-32, (1978).

6.26 HOLLOWAY, C., BASSET, M. B. and SHEPPARD, T.
"On Temperature Rise During the Extrusion of Composite Materials".
J. of Mech. Work. Tech., 1, pp. 343-359, (1978).

6.27 SHEPPARD, T. and RAYBOULD, D.
J. Inst. Met., Vol. 101, pp. 33-44, (1973).

6.28 HAWKINS, Q. and WRIGHT, J. C.
"Observation of the Deformation Properties of Sandwich Materials".
Int. J. Mech. Sci., Vol. 14, pp. 875-883, (1972).

6.29 BLAZYNSKI, T. Z. and TOWNLEY, S.
"The Methods of Analysis of the Process of Plug Drawing of Bimetallic Tubing Applies to Implosively Welded Composites".
Int. J. Mech. Sci., Vol. 20, pp. 785-797, (1978).

6.30 HELMAN, H.
"Hydrostatic Extrusion of Bimetallic Composites".
Ph.D. Thesis, Imperial College, University of London, (1976).

6.31 BLAZINSKY, T. Z.
"Metal Forming, Tool Profiles and Flow".
MacMillan, (1976)

6.32 PRICE, J. W. H.
Ph.D. Thesis, University of London, (1977).

6.33 ALEXANDER, J. M. and TURNER, T. W.
"A Preliminary Investigation of the Dieless Drawing of Titanium and Some Steels".
Proc. 15th Int. MTDR, (1975).

6.34 DUNN, P. and LENGYEL, B.
"Lubrication and Friction in Hydrostatic Extrusion/Drawing".
J. Inst. Met., 100, p. 317, (1972).

6.35 ZIENKIEWICZ, O. C., JAIN, P. C. and OÑATE, E.
"Flow of Solids During Forming and Extrusion. Some Aspects of Numerical Solutions".
Univ. College of Swansea, Civil Engineering Dept., Rep. C/R/283/76, (1976).

6.36 HARTLEY, P., STURGESS, C. E. N. and ROWE, G. W.
"Friction in Finite-Element Analyses of Metal Forming Processes".
Int. J. Mech. Sci., Vol. 21, p. 301, (1979).

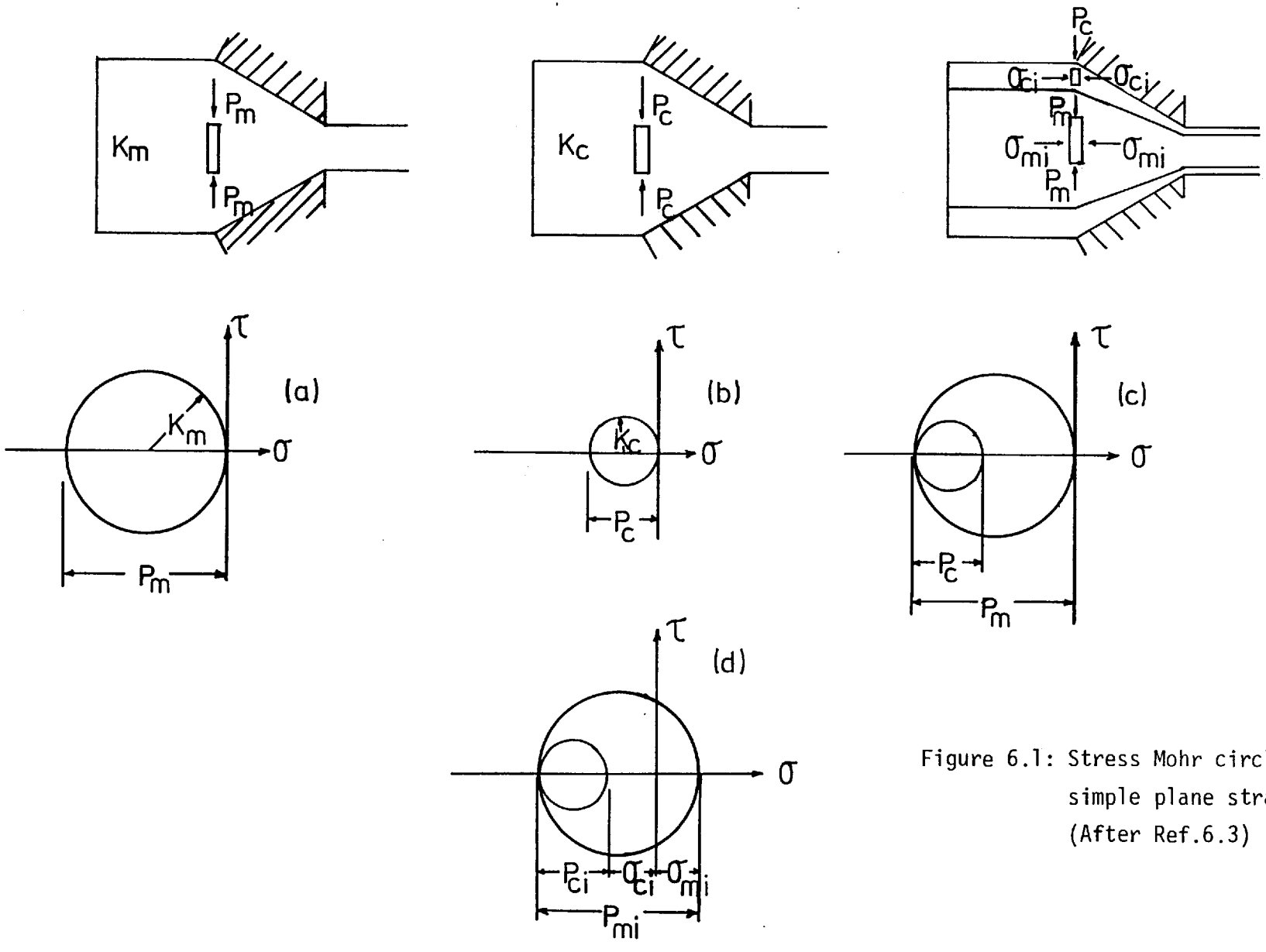

Figure 6.1: Stress Mohr circles for simple plane strain drawing. (After Ref.6.3)

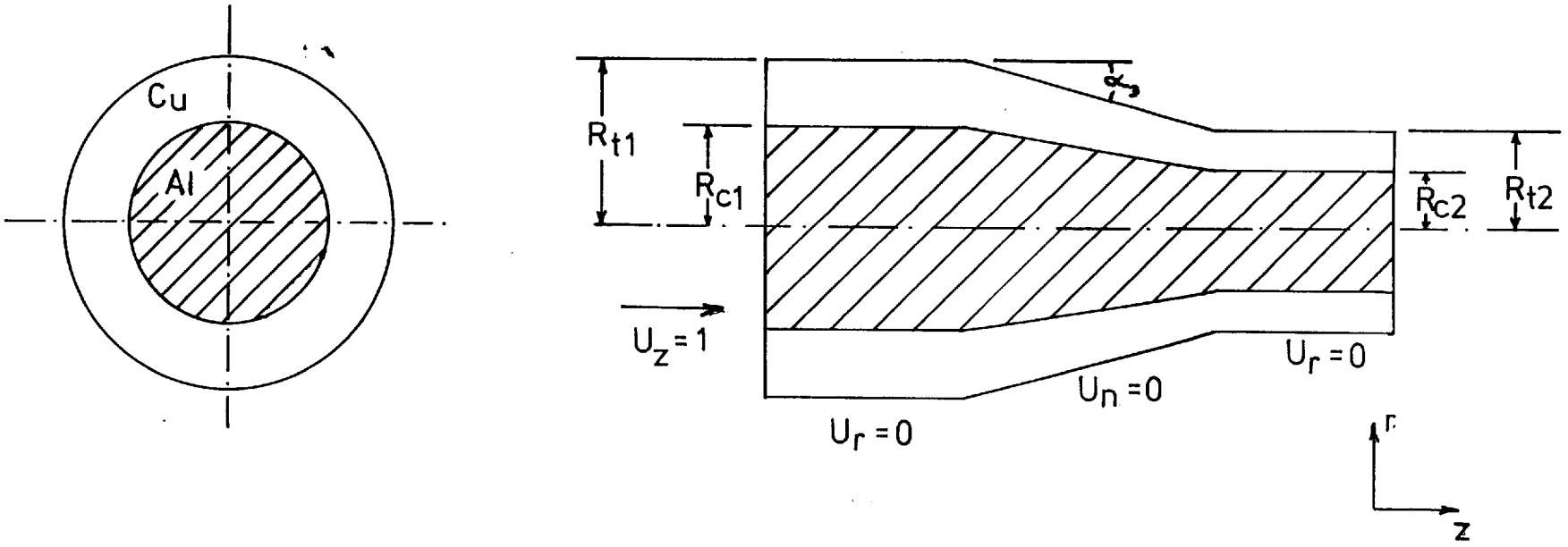

Figure 6.2: Geometry of a composite specimen.

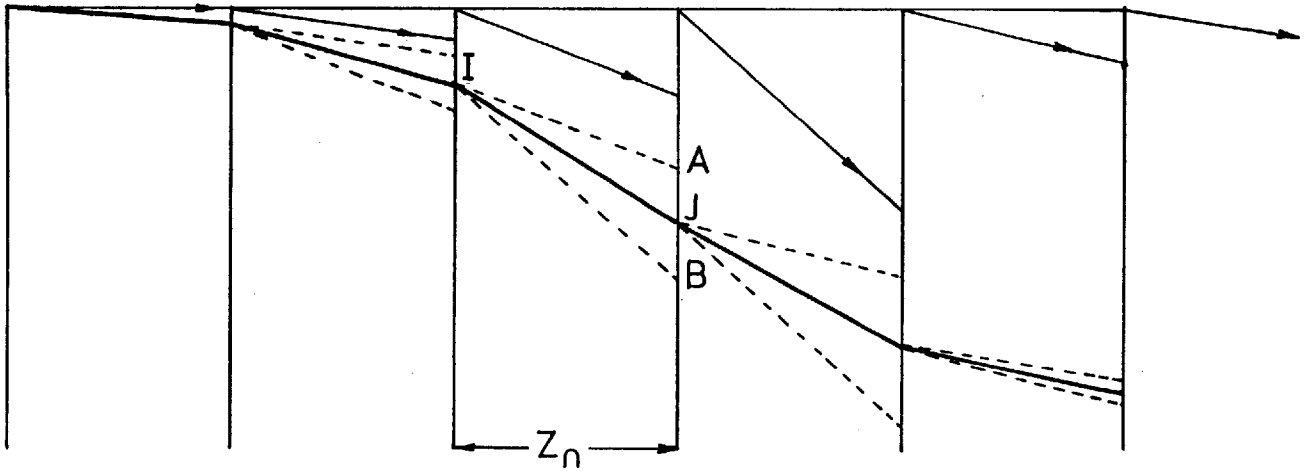

Figure 6.3: Modification of nodal coordinates according to velocity slopes (After Ref.6.33)

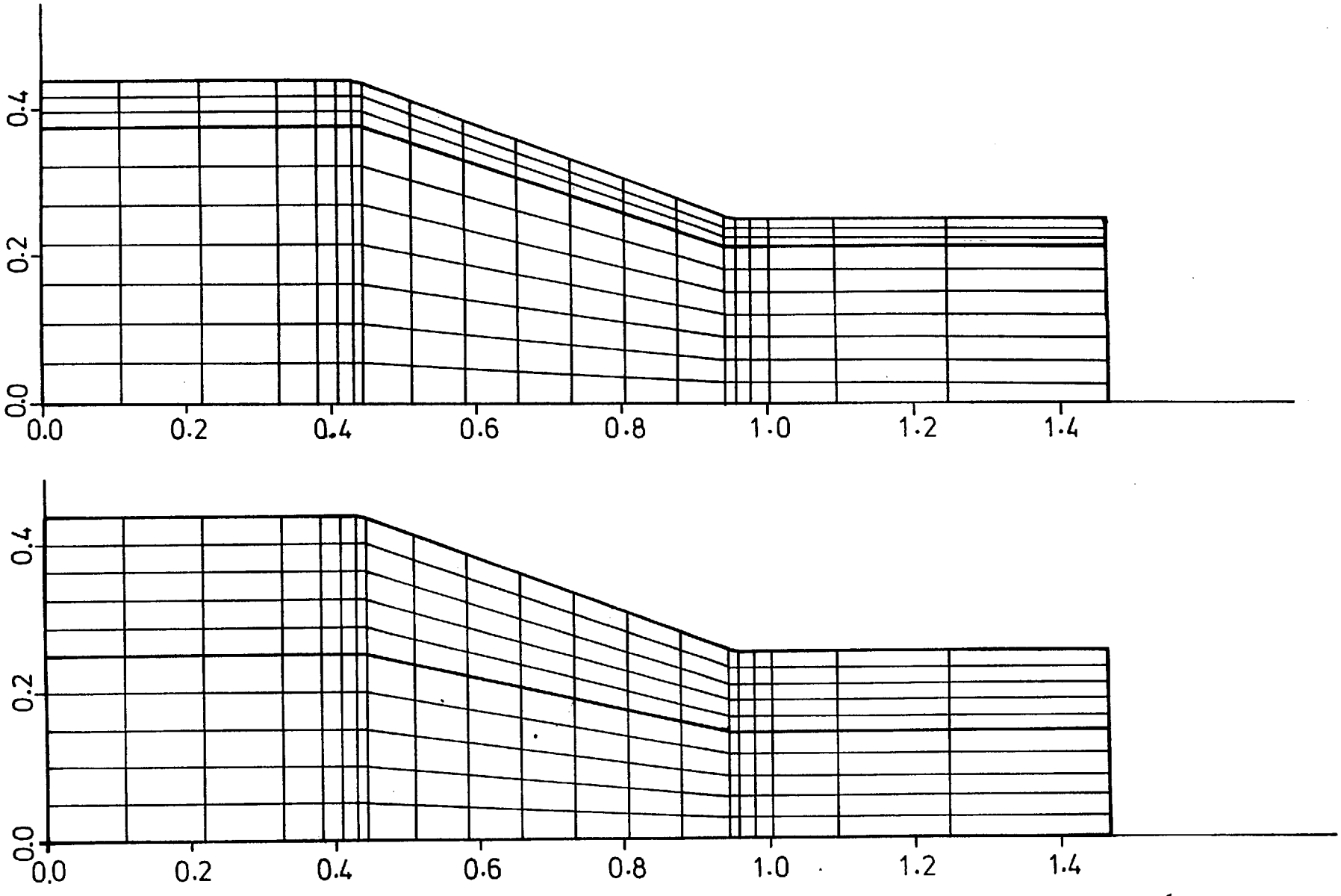

Figure 6.4: Mesh used for finite element analysis. R=3.05,Die semi-angle =20^{o}

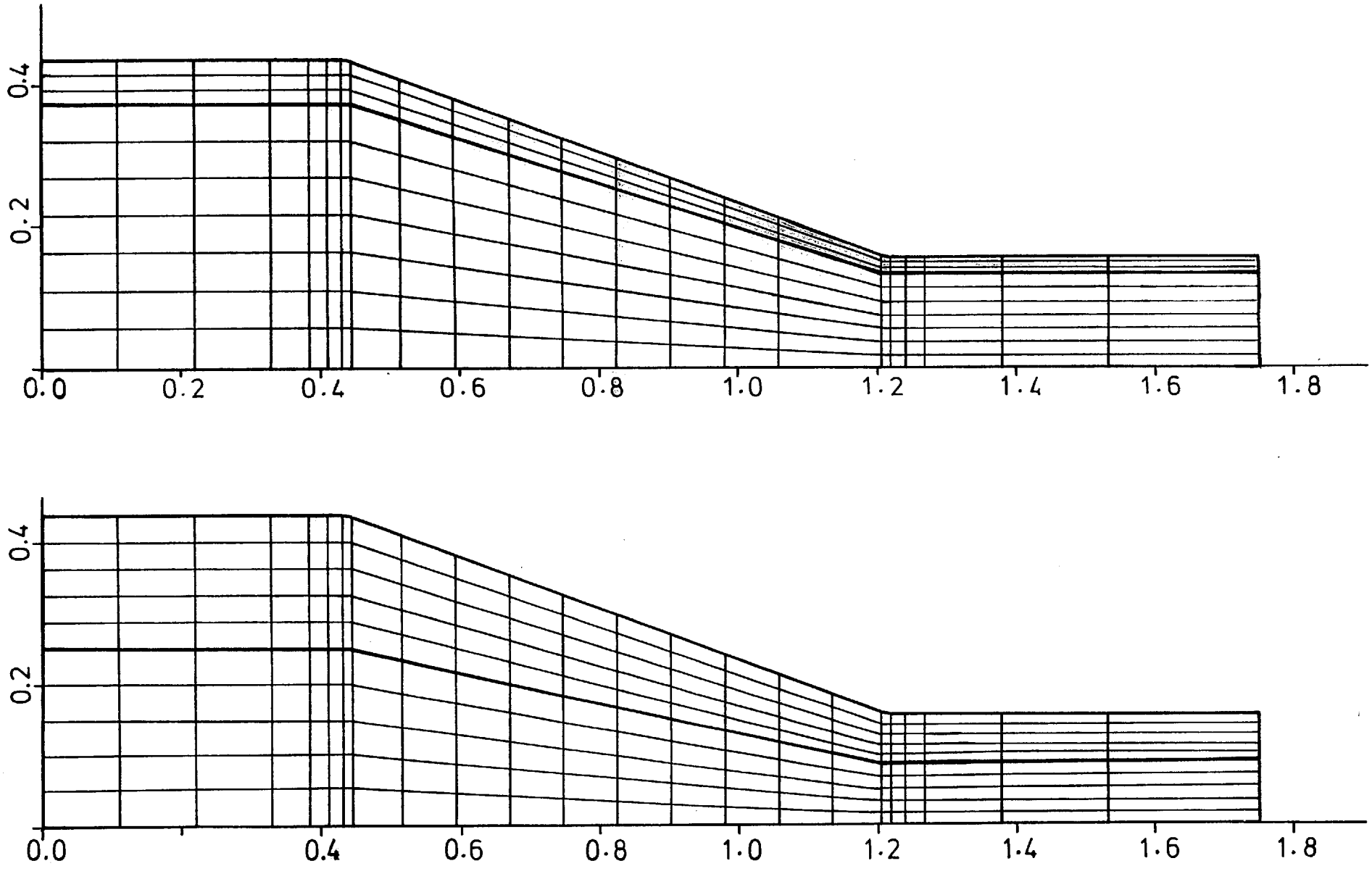

Figure 6.5: Mesh used for finite element analysis. R=7.865,Die semi-angle=20^{o}

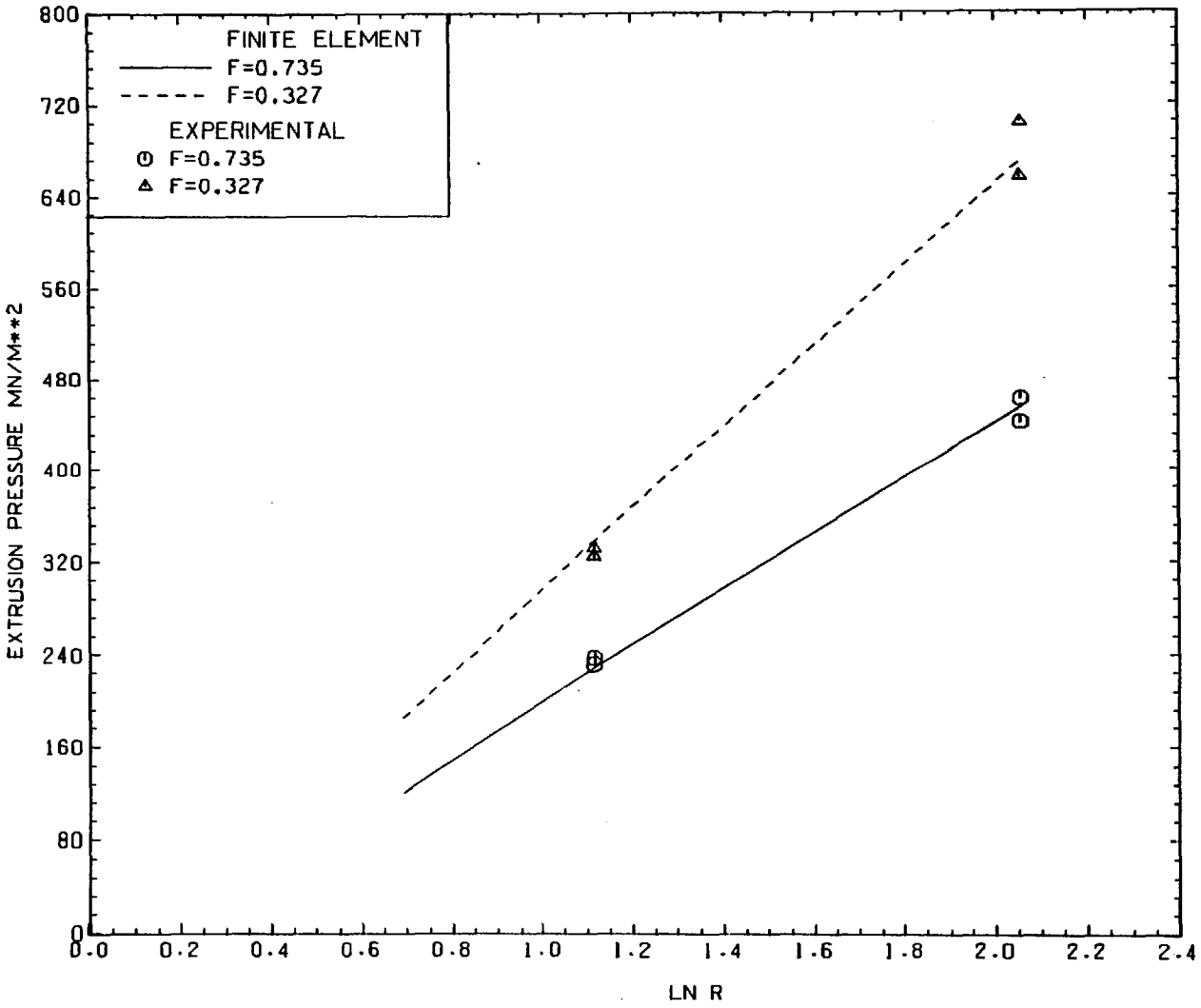

Figure 6.6: Extrusion pressure versus natural logarithm of reduction.
Die semi-angle=20^{o}

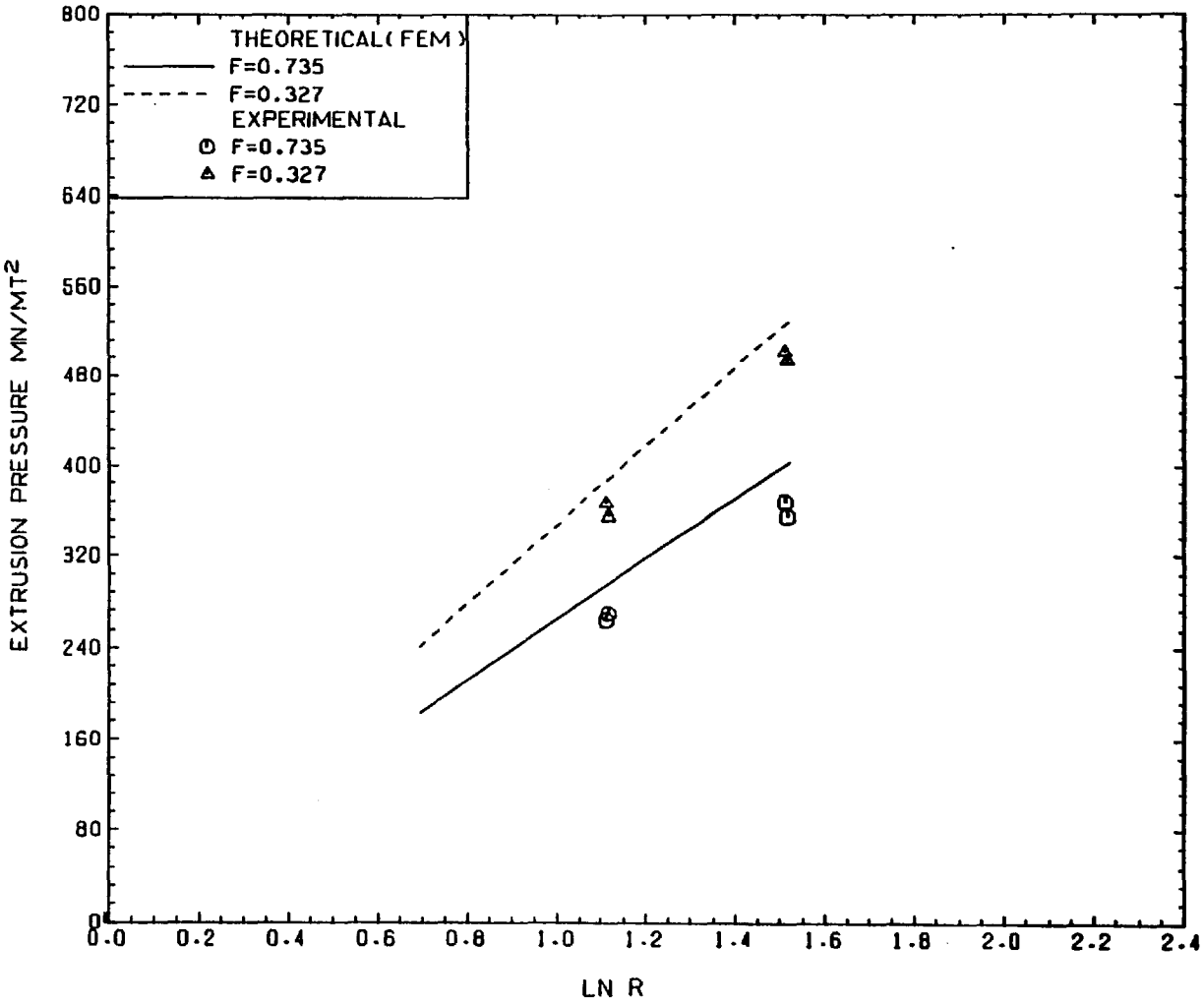

Figure 6.7: Extrusion pressure versus natural logarithm of reduction.
Die semi-angle=45^{o}

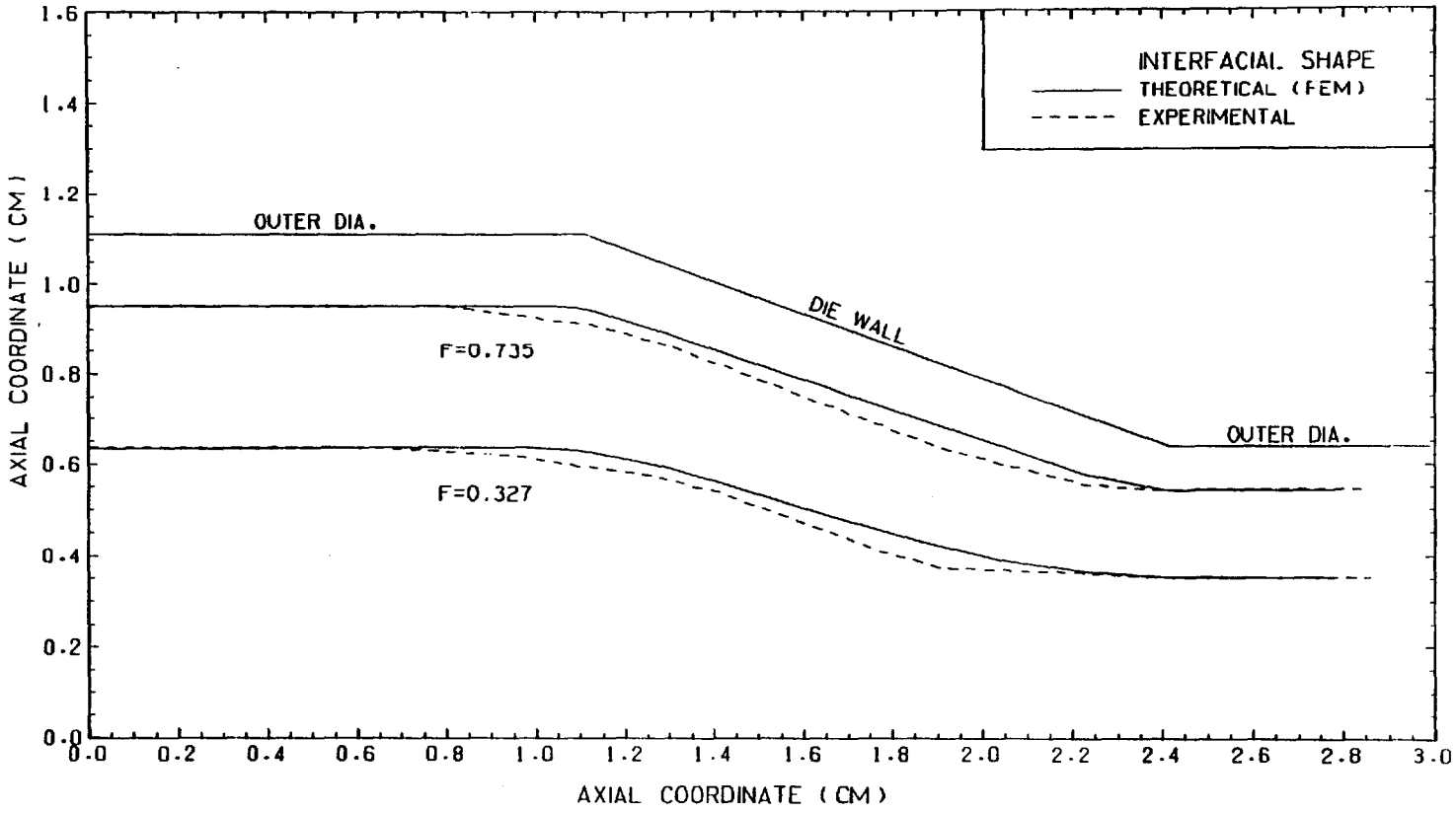

FIG 6.8 COMPARISON OF MEASURED AND PREDICTED INTERFACIAL SHAPE.
DIE ANGLE=40. REDUCTION=3.05

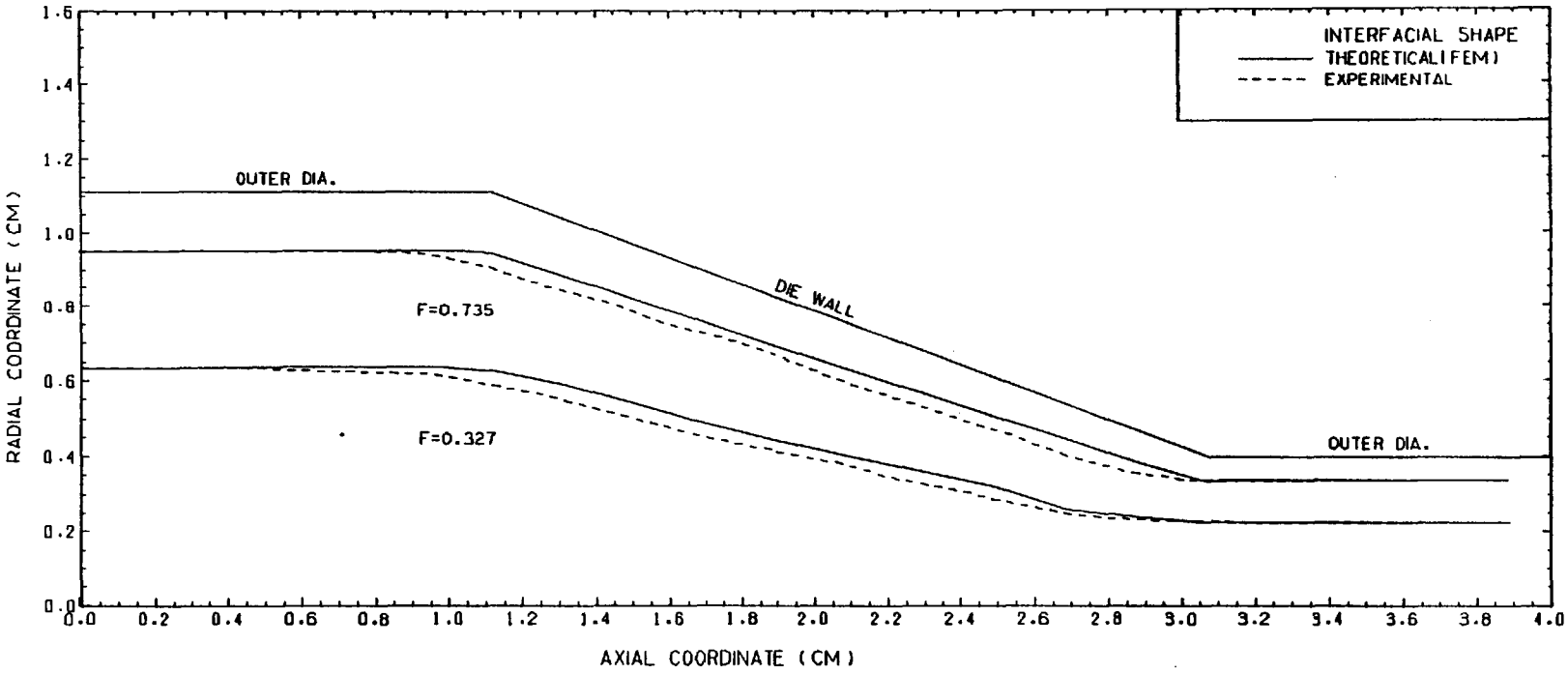

FIG6.9 COMPARISON OF MEASURED AND PREDICTED INTERFACIAL SHAPE.
DIE ANGLE=40. REDUCTION=7.865 .

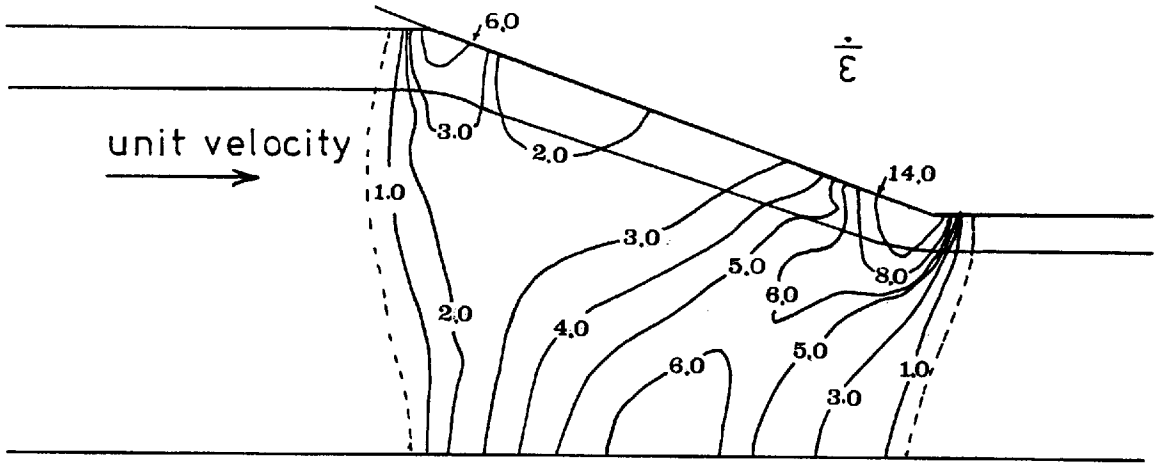

(a)

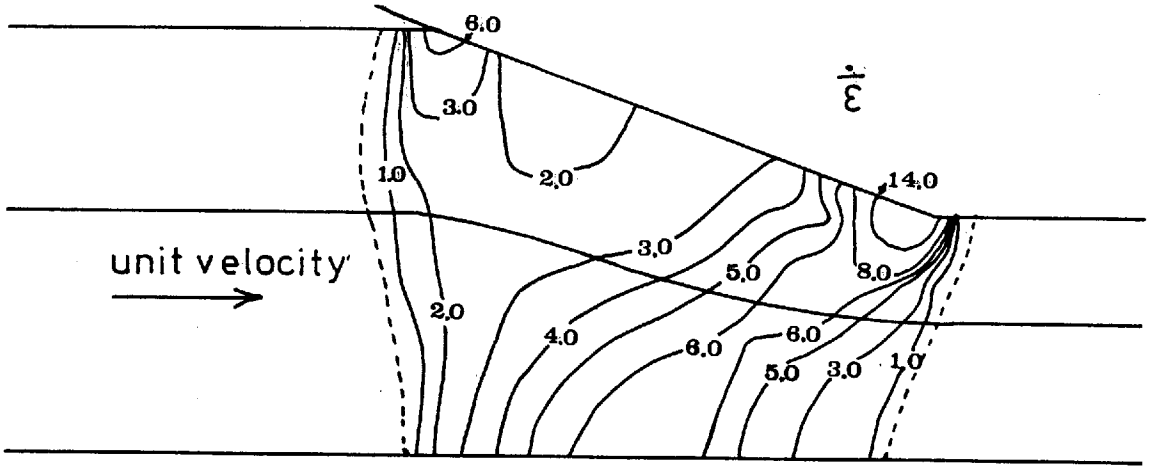

(b)

Figure 6.10: Effective strain rate distribution.
R=3.05,Die semi-angle=20^{0}.
(a) f=0.735 (b) f=0.327

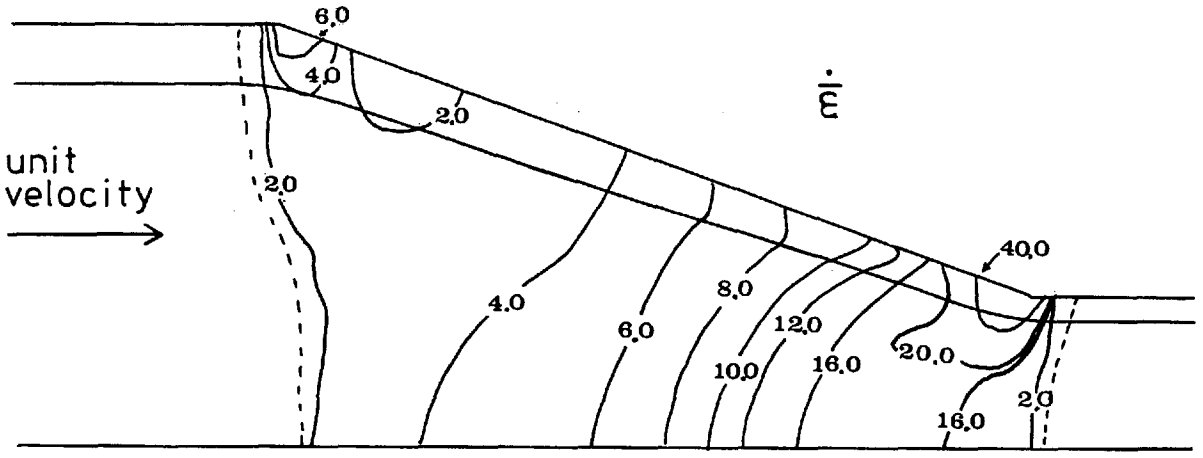

(a)

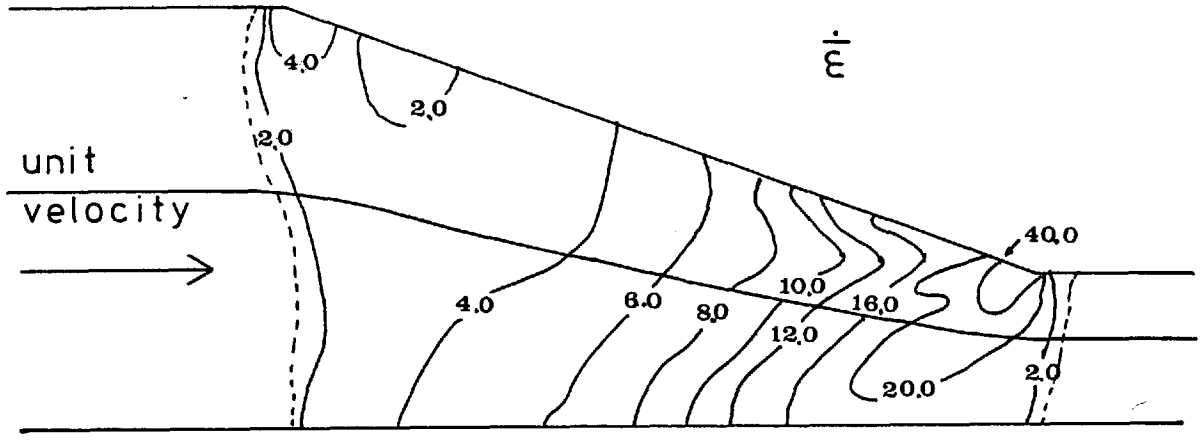

(b)

Figure 6.11: Effective strain rate distribution.
R=7.865,Die semi-angle=20^{o}
(a) f=0.735 (b) f=0.327

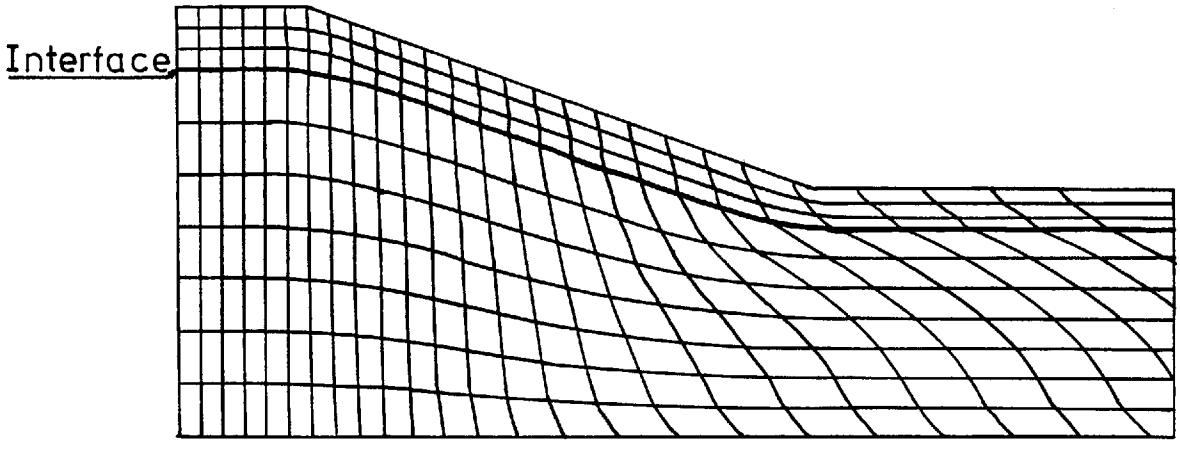

(a)

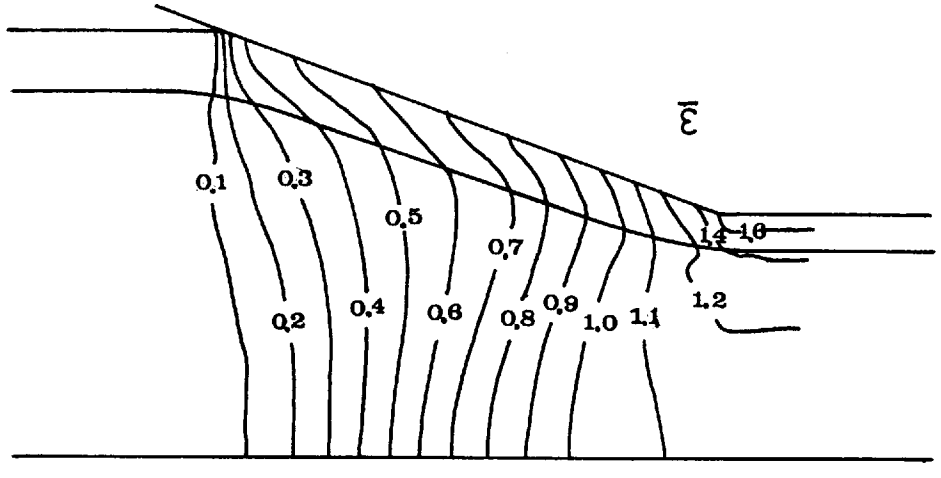

(b)

Figure 6.12: (a) Grid distortion; (b) Effective strain distribution
R=3.05, f=0.735, Die semi-angle=20^{o}

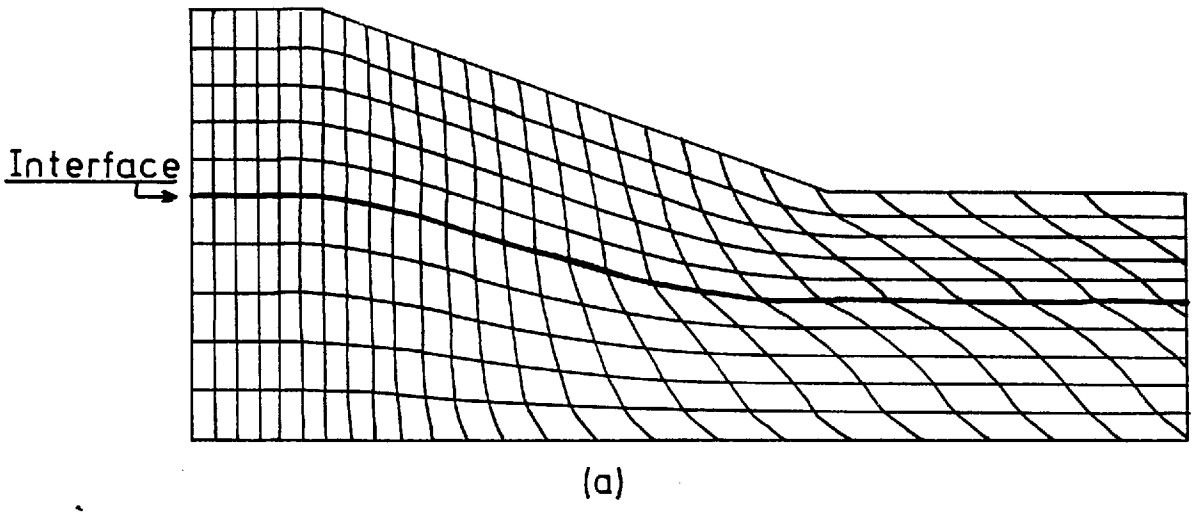

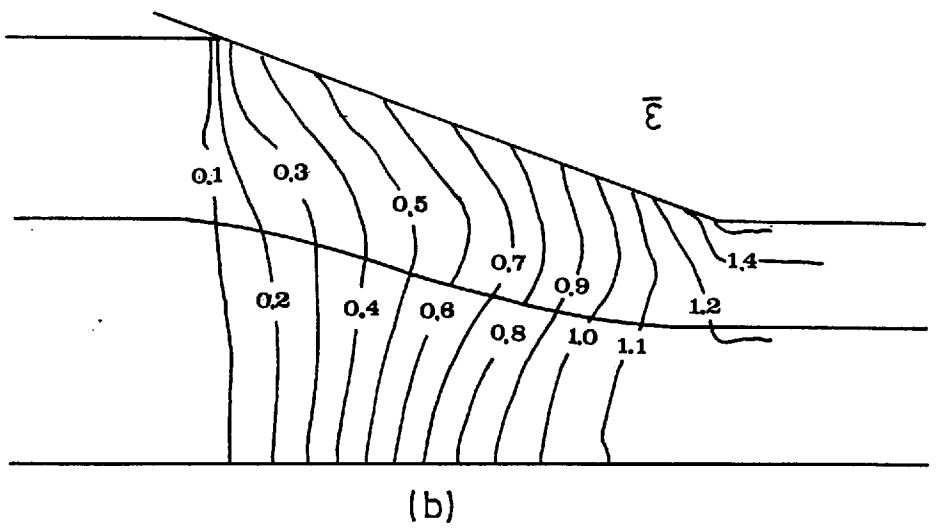

Figure 6.13: (a) Grid distortion; (b) Effective strain distribution.
R=3.05, f=0.327, Die semi-angle=20^{o}

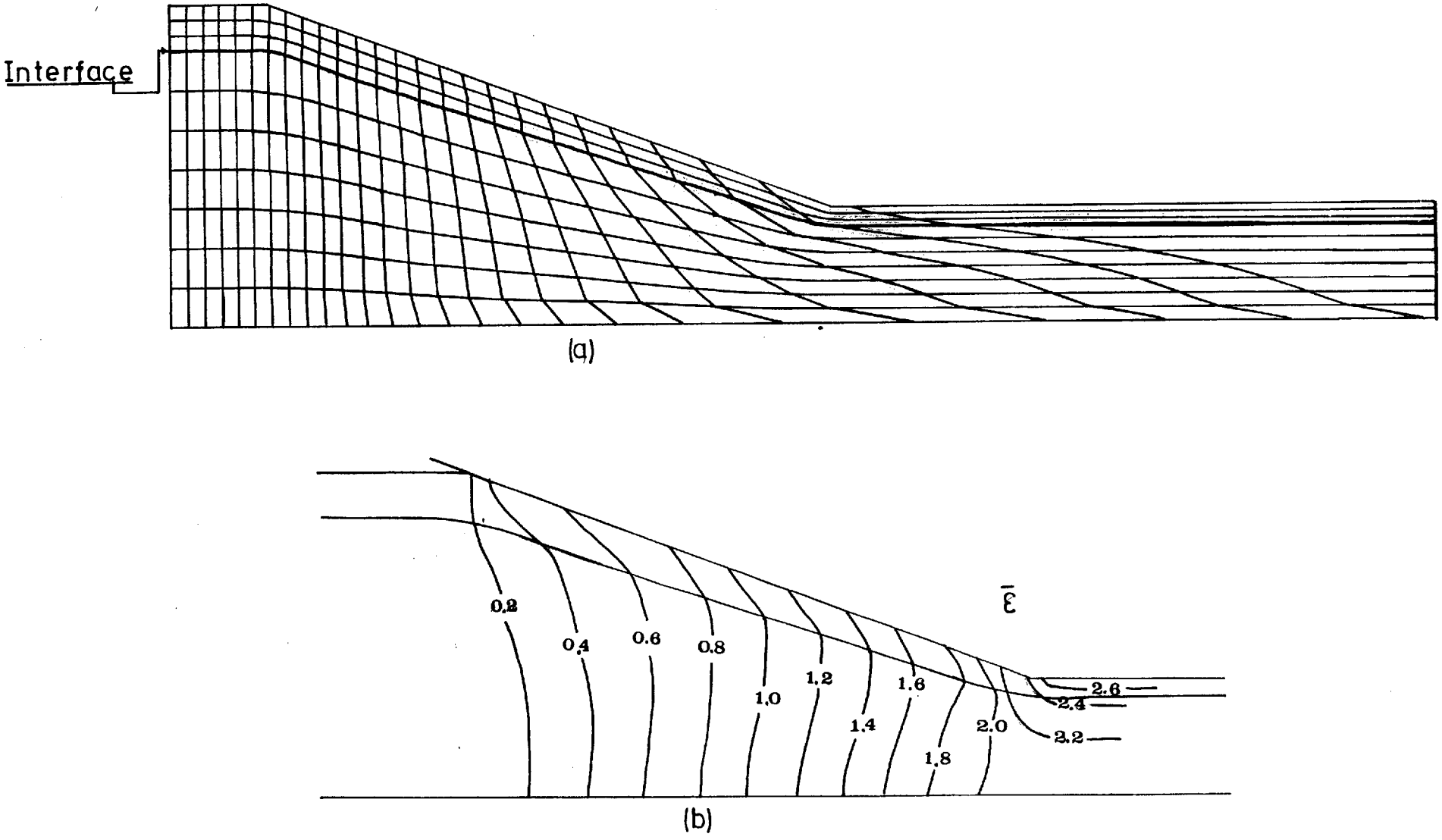

Figure 6.14: (a) Grid distortion; (b) Effective strain distribution
R=7.865,f=0.735,Die semi-angle=20^{0}

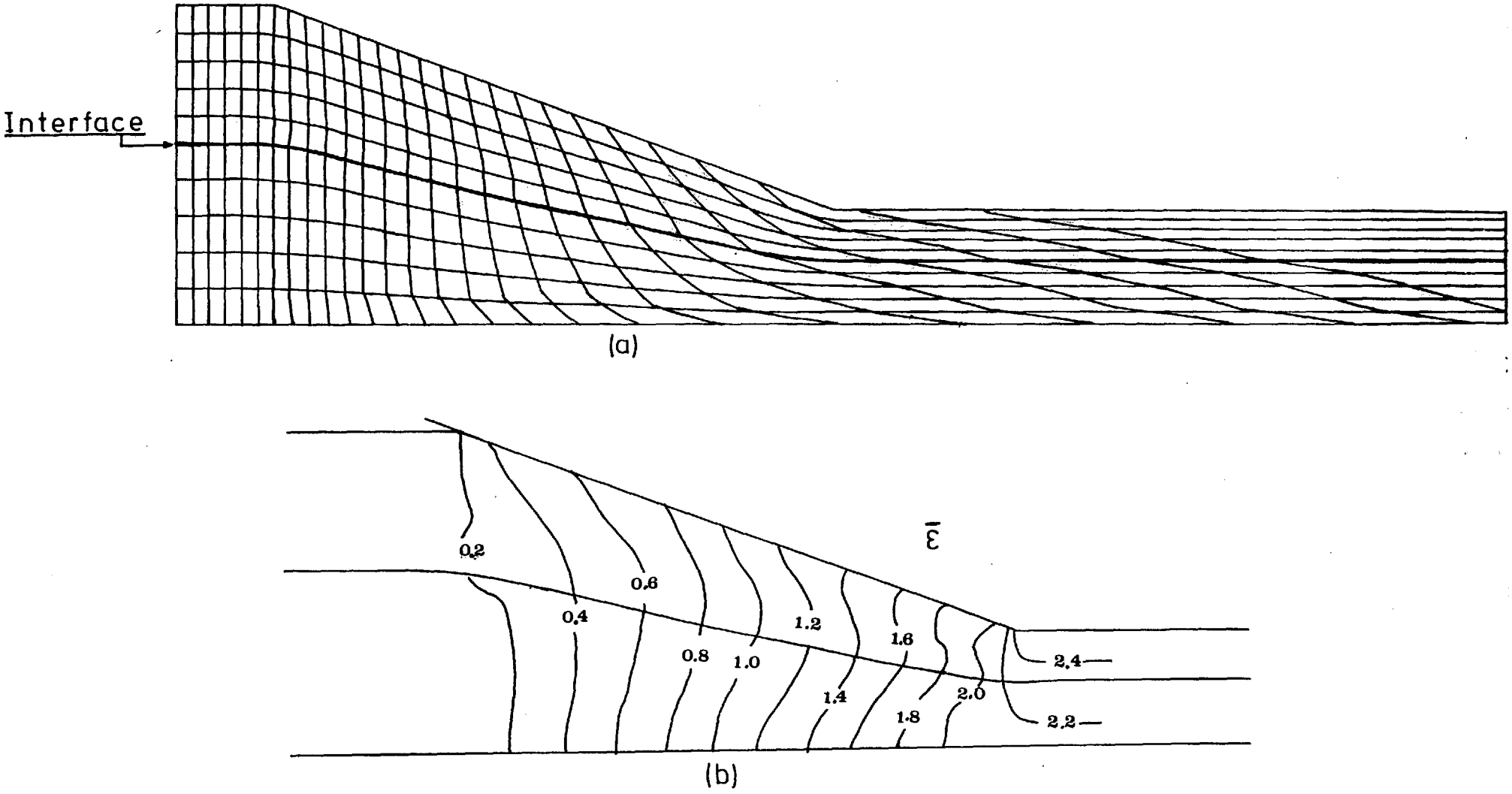

Figure 6.15: (a) Grid distortion; (b) Effective strain distribution.
R= 7.865, f=0.327, Die semi-angle=20^{0}

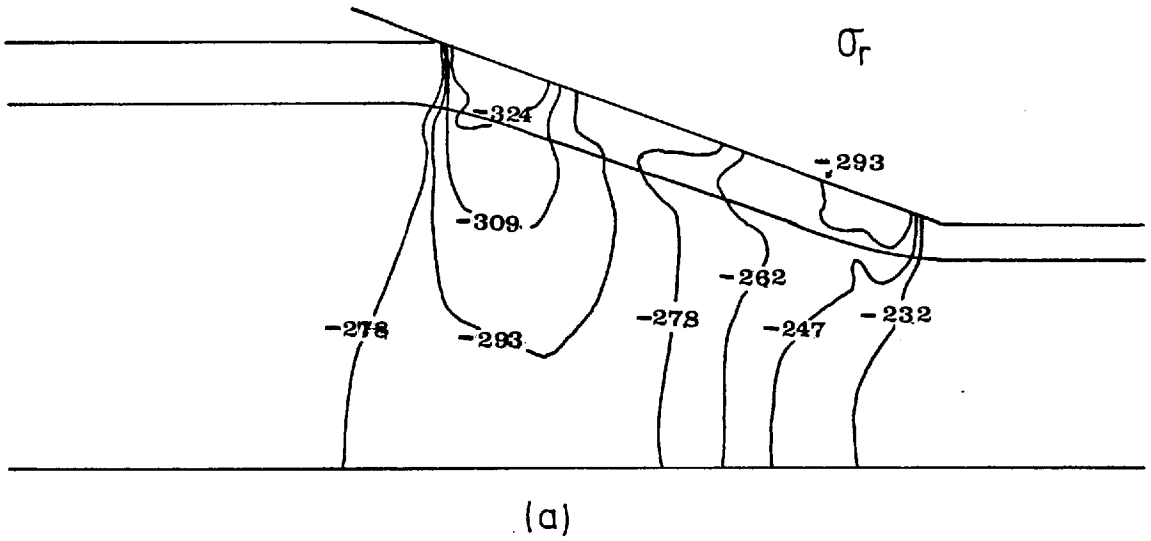

(a)

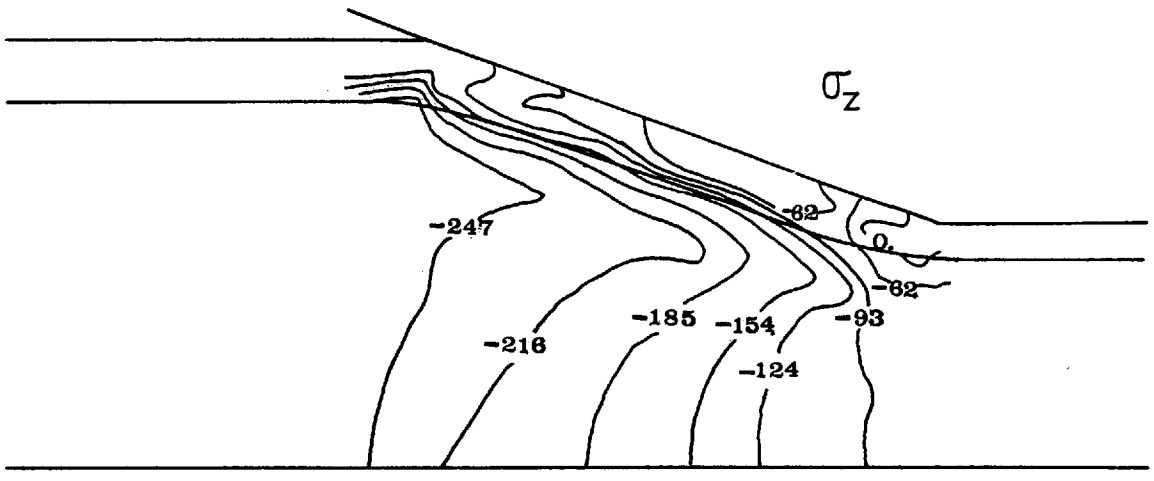

(b)

Figure 6.16: Iso-stress contours (MN/m^2).
R=3.05,f=0.735,Die semi-angle=20^o

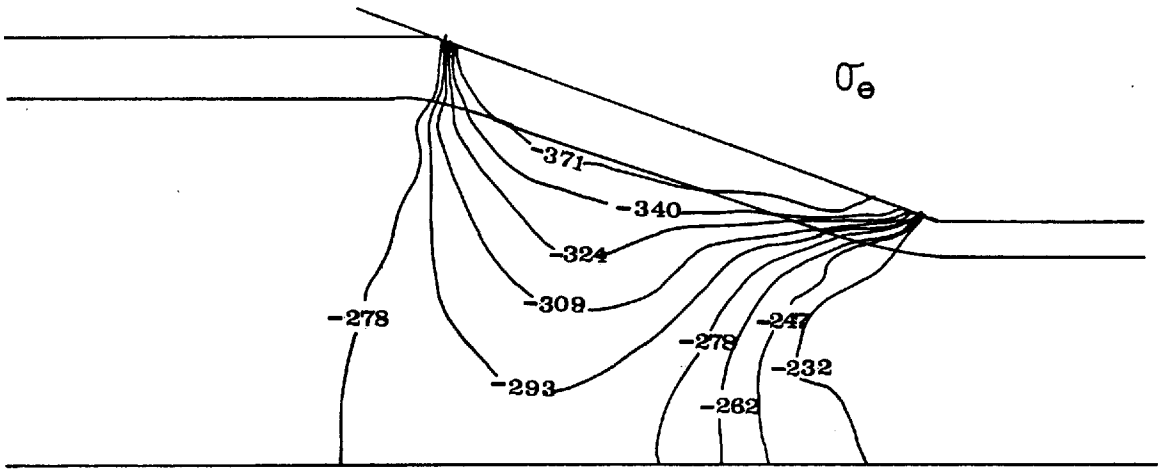

(c)

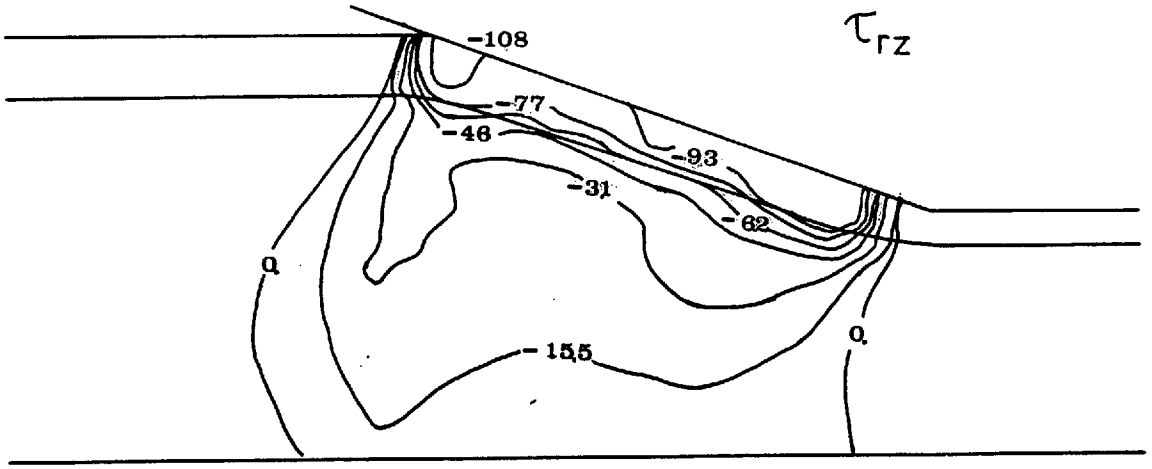

(d)

Figure 6.16 (Cont.)

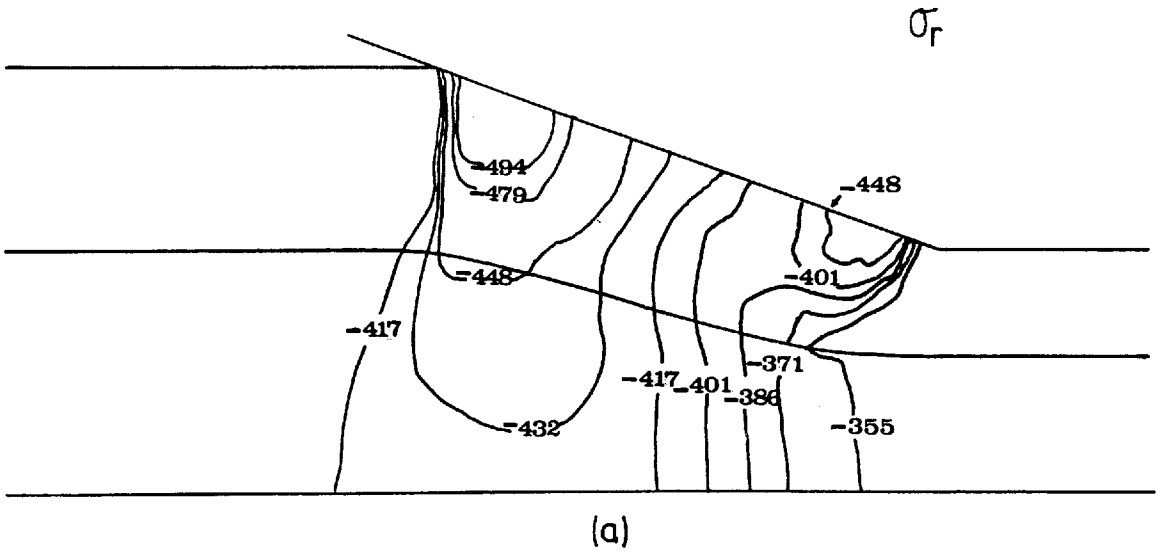

(a)

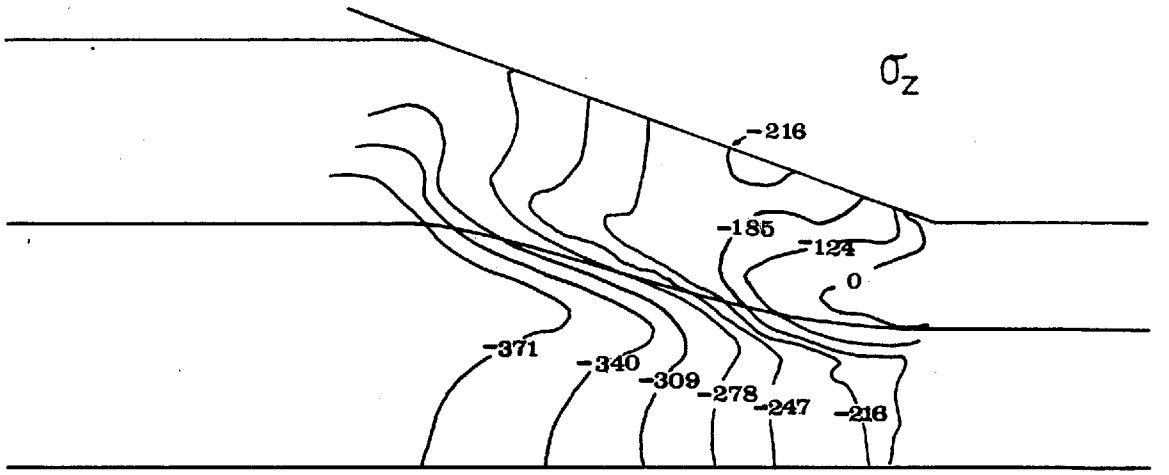

(b)

Figure 6.17: Iso-stress contours.(MN/m^2)
R=3.05,f=0.327,Die semi-angle=20^o

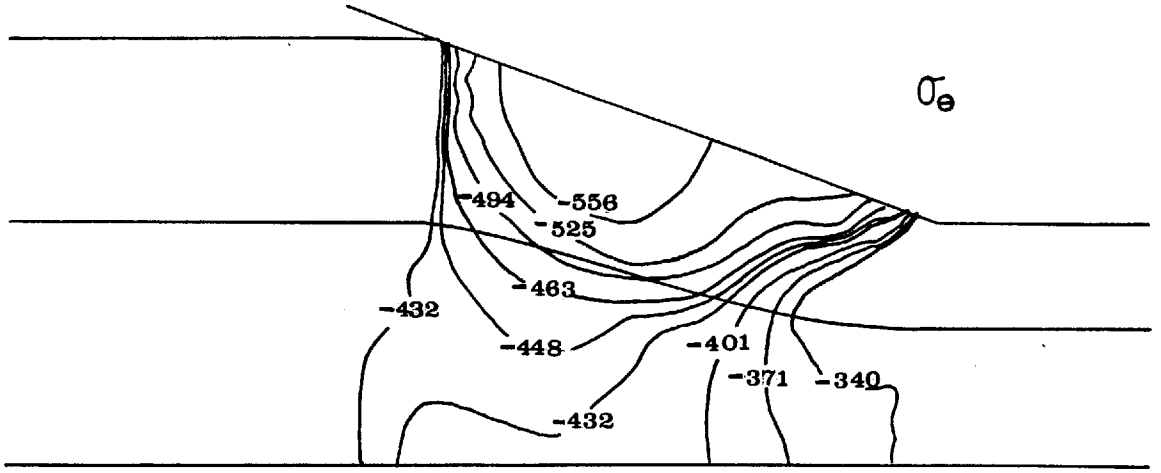

(c)

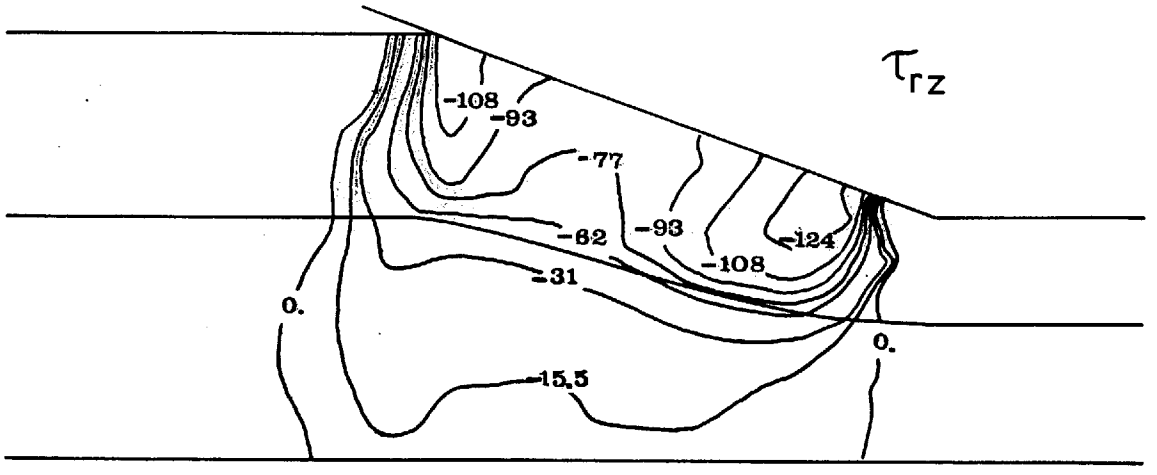

(d)

Figure 6.17 (Cont.)

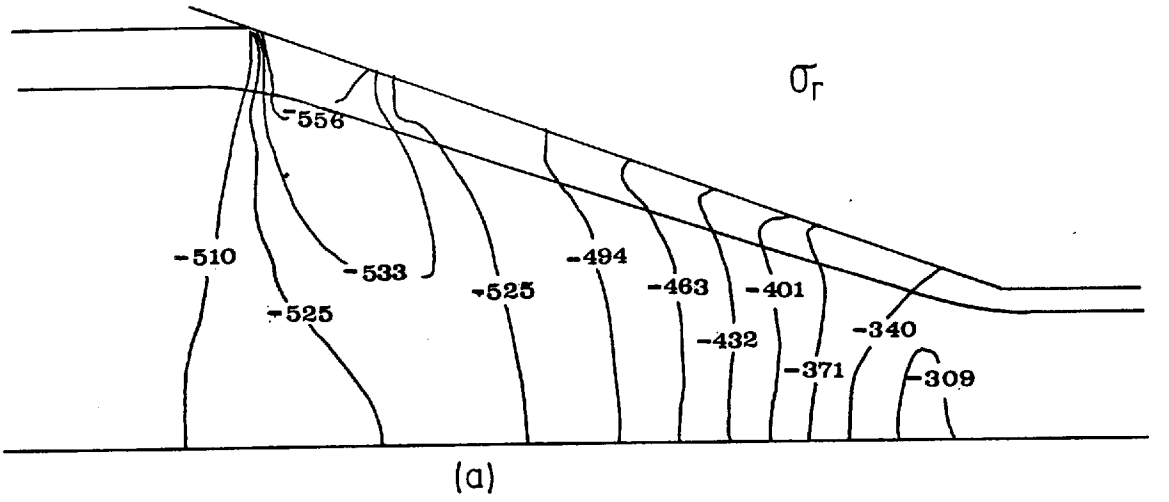

(a)

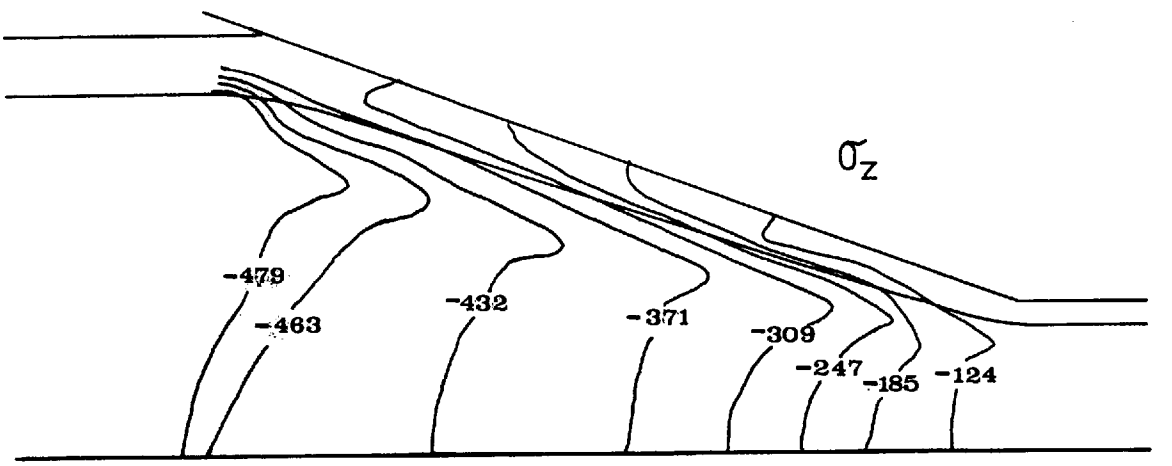

(b)

Figure 6.18: Iso-stress contours (MN/m^2)
R=7.865,f=0.735,Die semi-angle=20^o

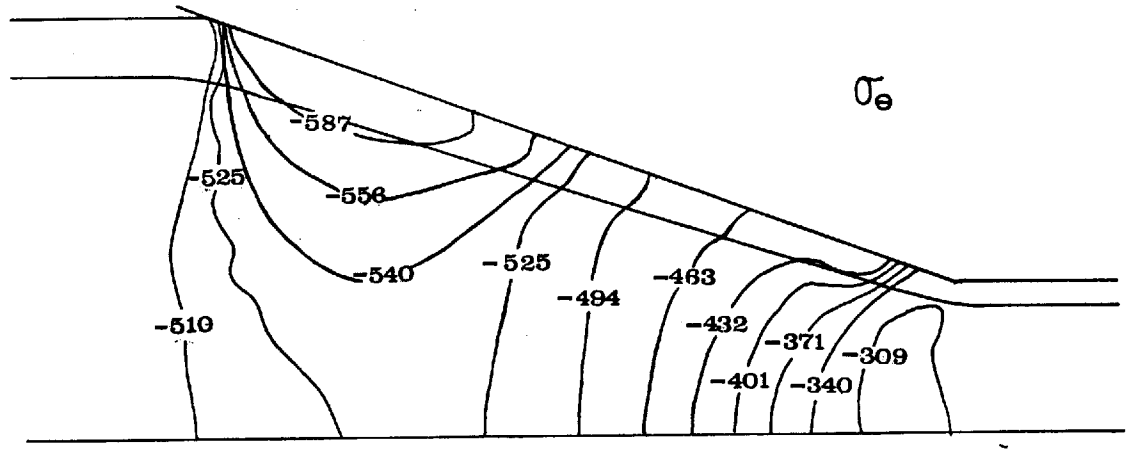

(c)

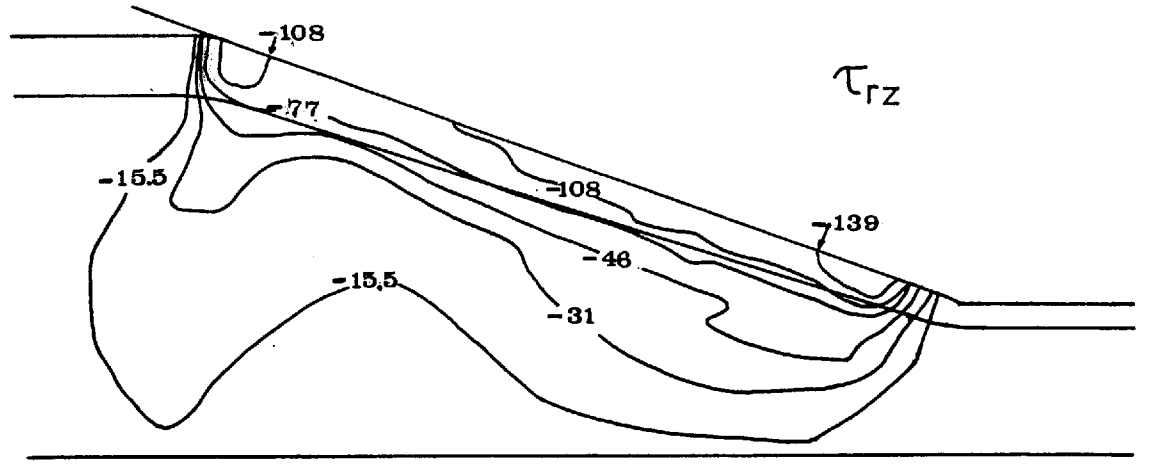

(d)

Figure 6.18 (Cont.)

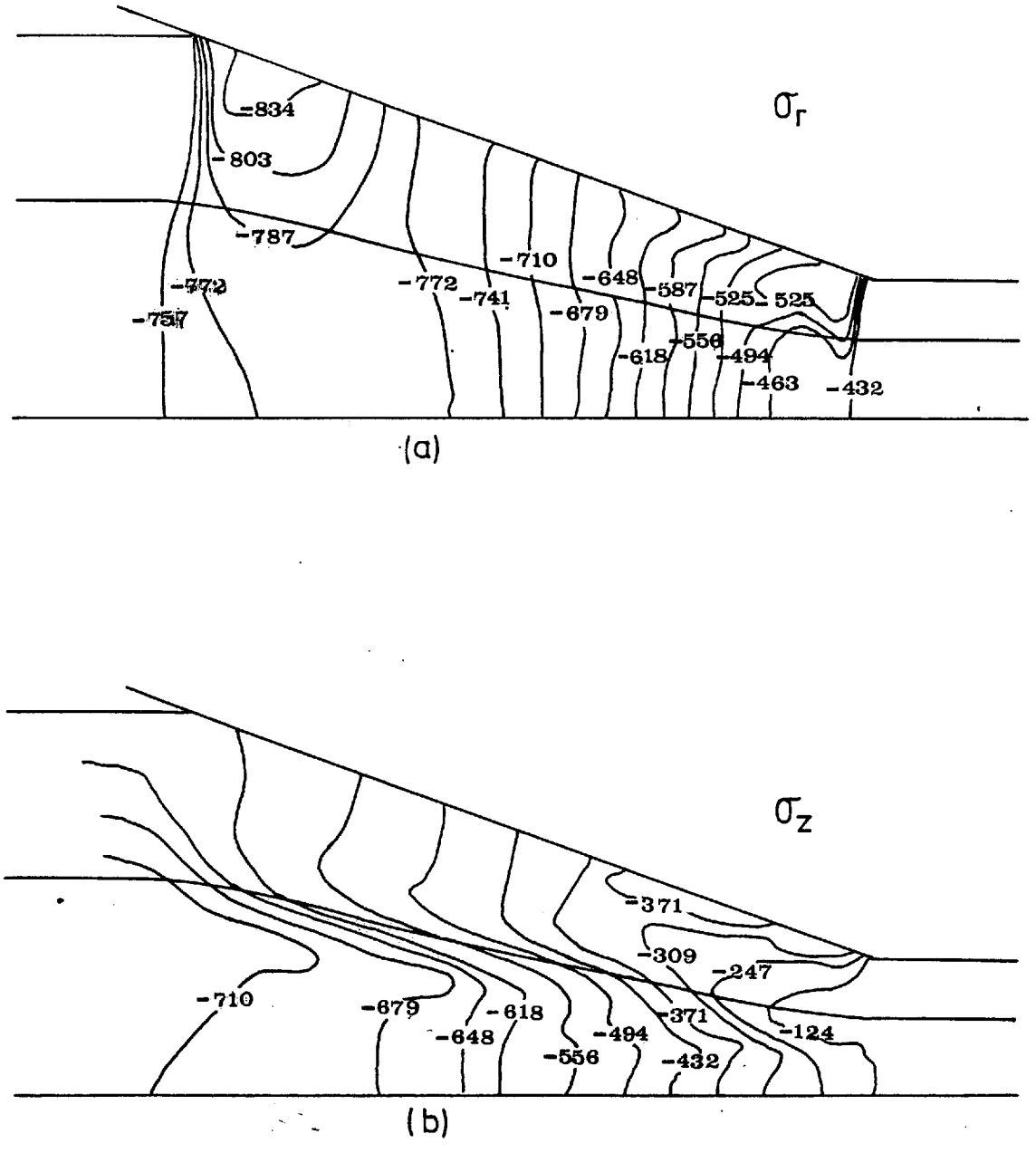

Figure 6.19: Iso-stress contours (MN/m^2)
R=7.865,f=0.327,Die semi-angle=20^o

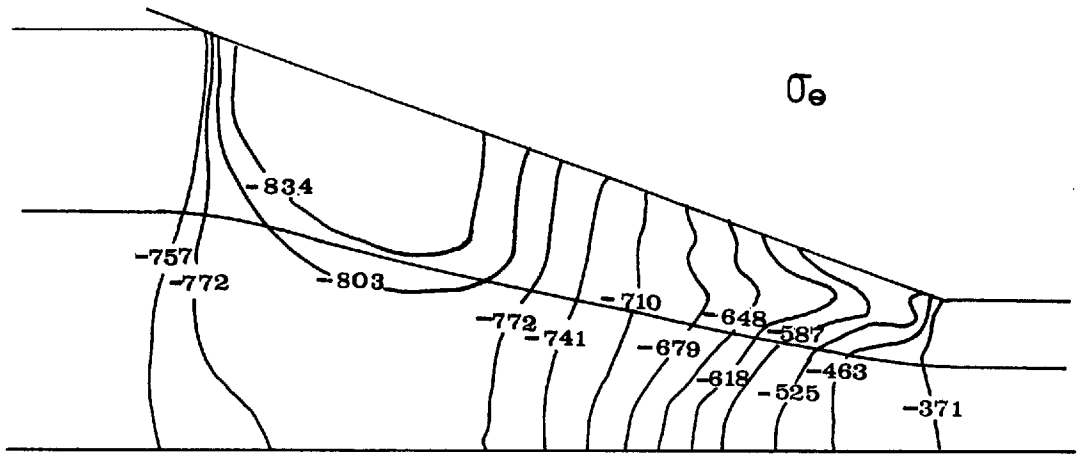

(c)

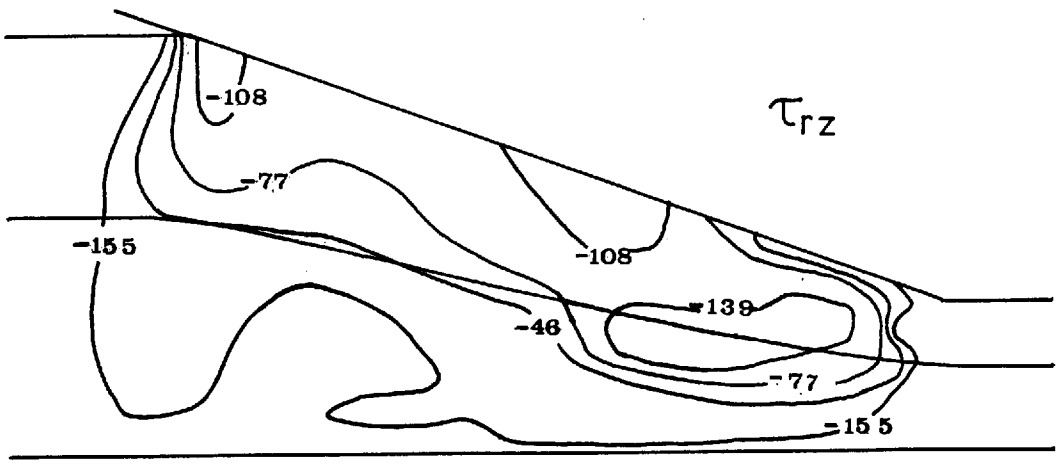

(d)

Figure 6.19 (Cont.)

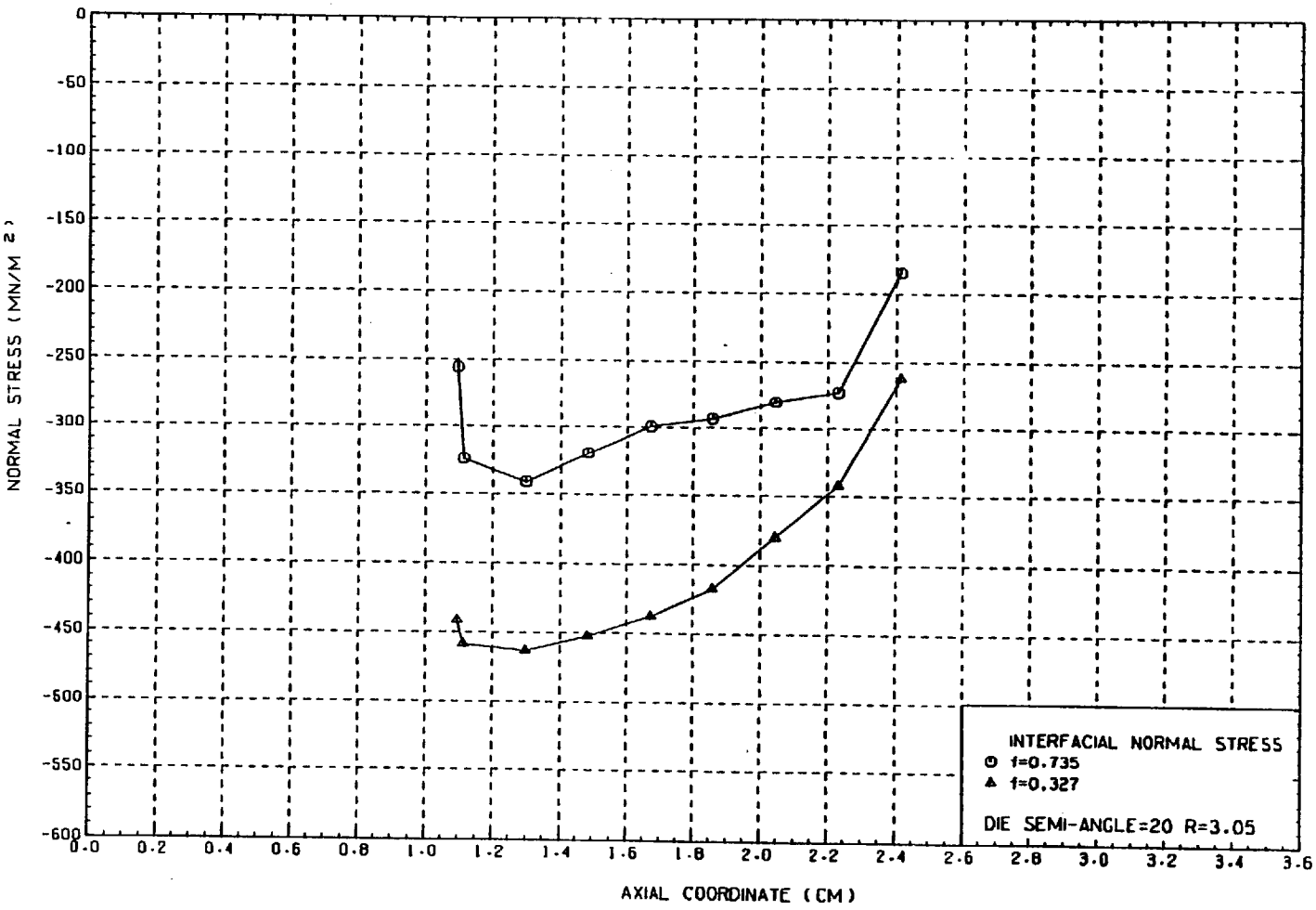

Figure 6.20: Normal pressure distribution at the interface
R=3.05,Die semi-angle=20^{0}

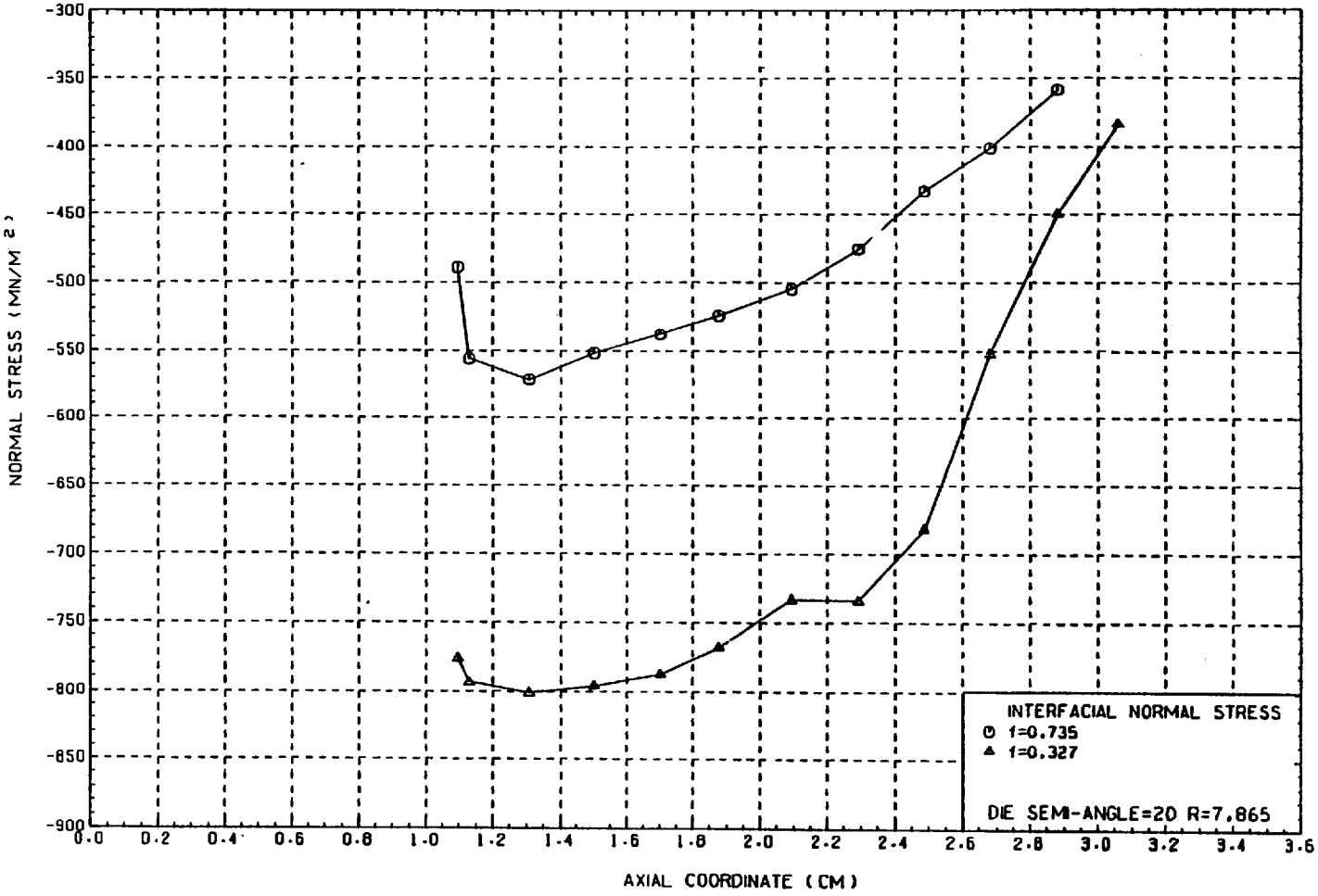

Figure 6.21: Normal pressure distribution at the interface.
R=7.865,Die semi-angle=20^{0}

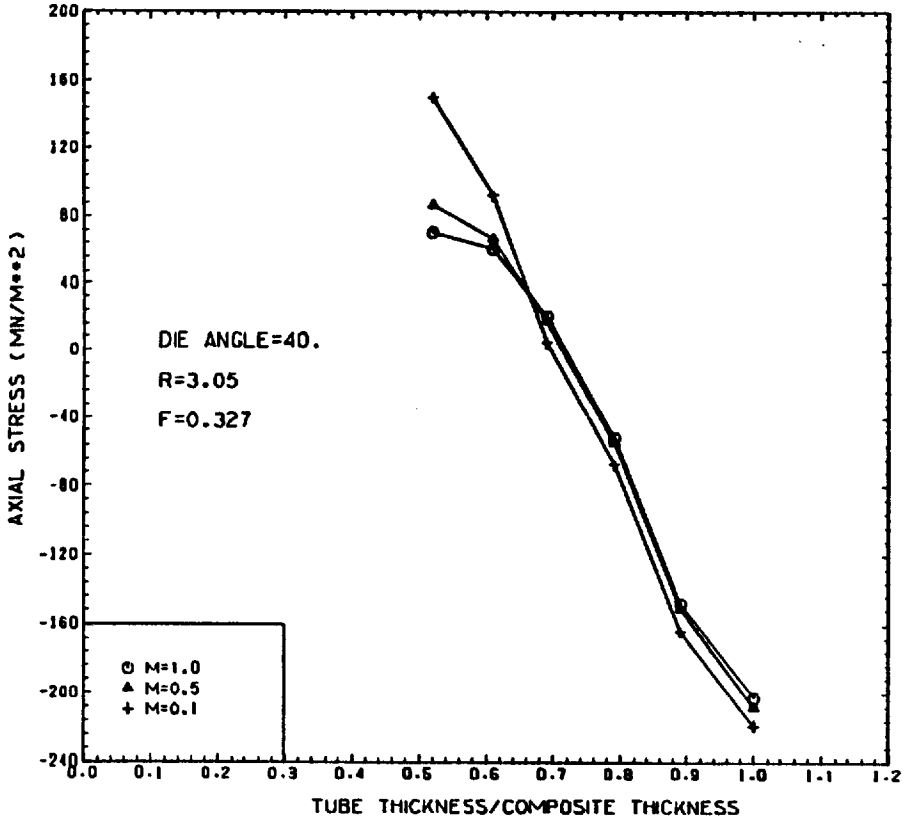

Fig 6.22: EFFECT OF INTERFACE FRICTION ON STRESS DISTRIBUTION ACROSS THE TUBE THICKNESS JUST BEFORE THE DIE EXIT

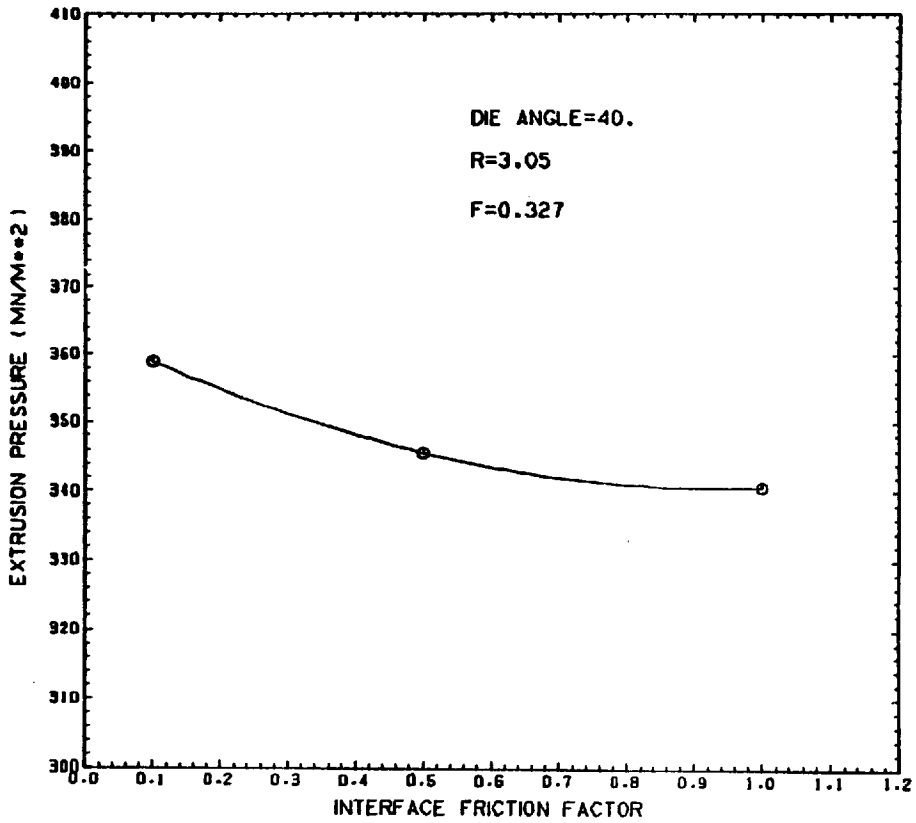

Fig 6.23: EXTRUSION PRESSURE VS. INTERFACE FRICTION

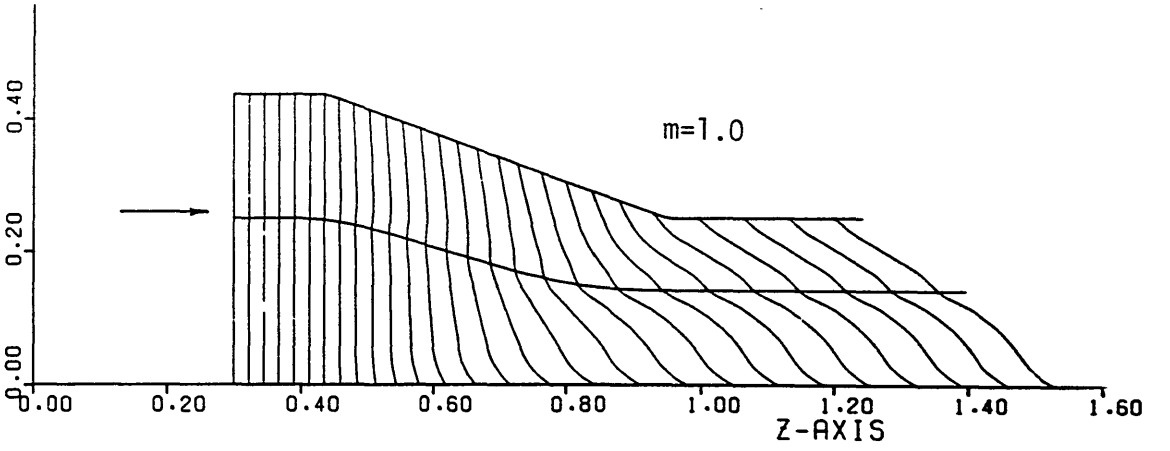

(a)

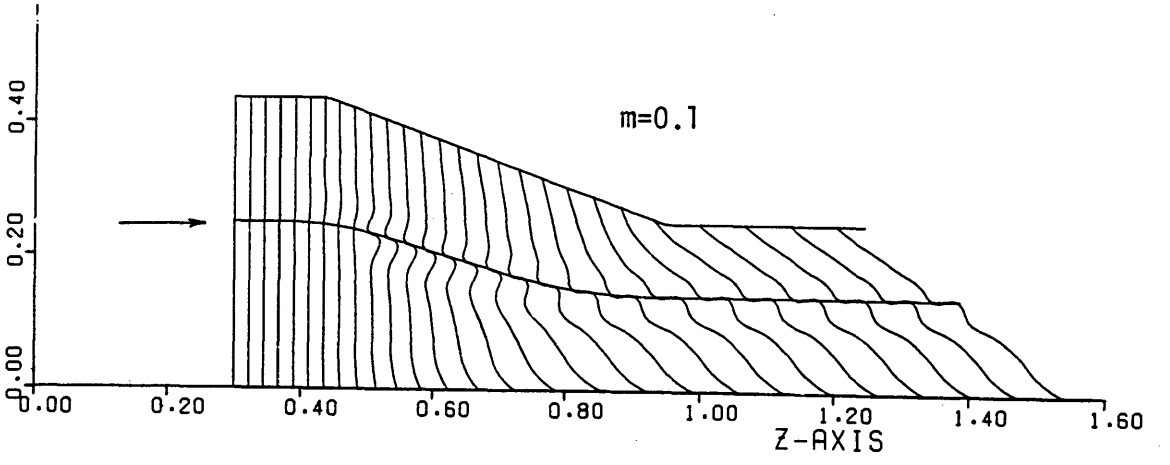

(b)

Figure 6.24: Effect of Interfacial friction on grid distortion
(Extrusion end condition)
R=3.05,f=0.327,Die semi-angle $=20^{o}$

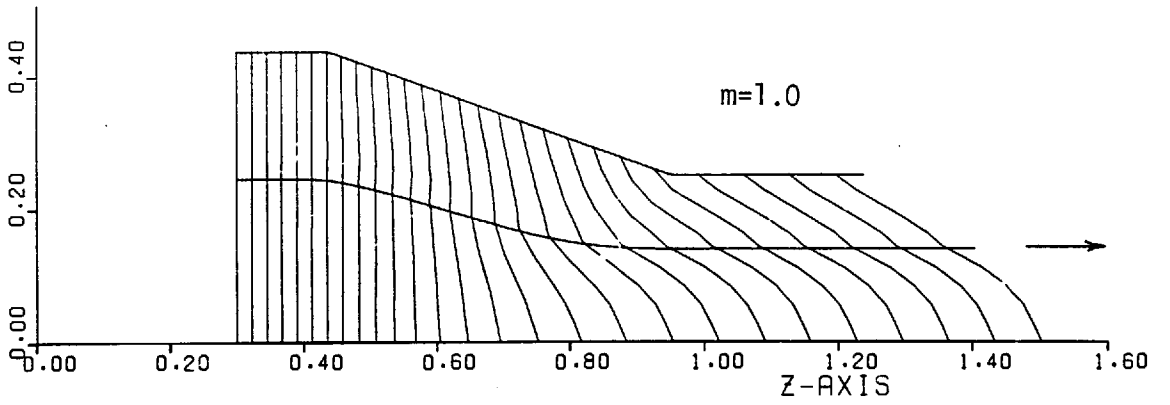

(a)

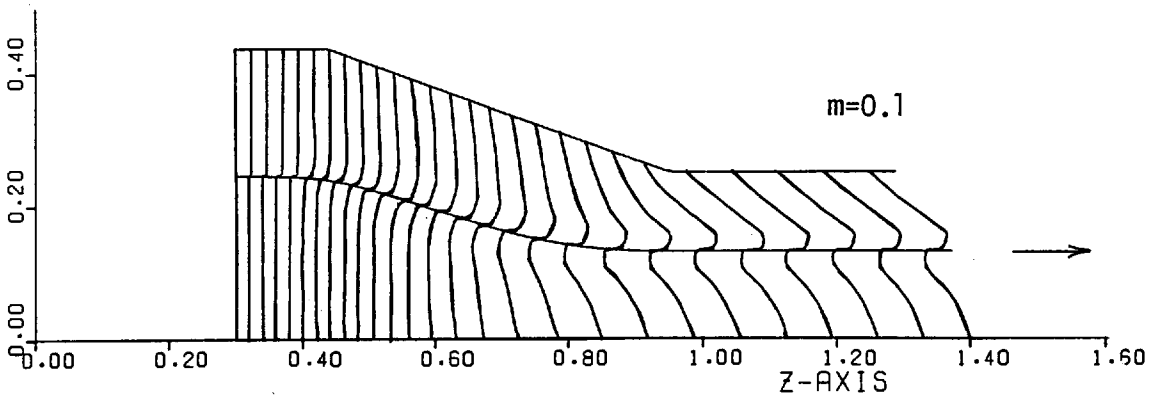

(b)

Figure 6.25: Effect of interfacial friction on grid distortion
(Drawing end condition)
R=3.05,f=0.327,Die semi-angle=20^{o}

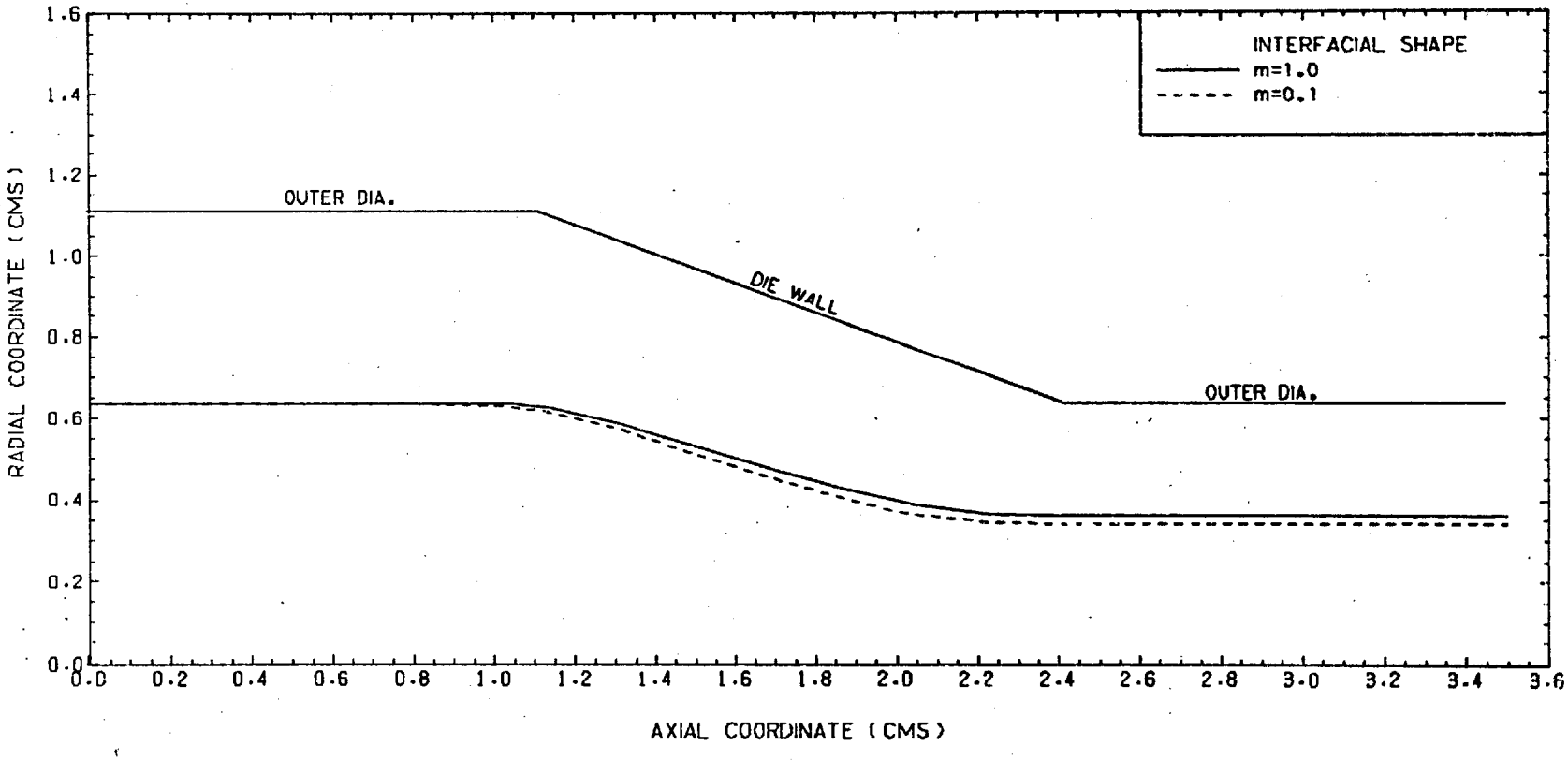

Fig. 6·26: EFFECT OF INTERFACE FRICTION ON THE INTERFACIAL SHAPE

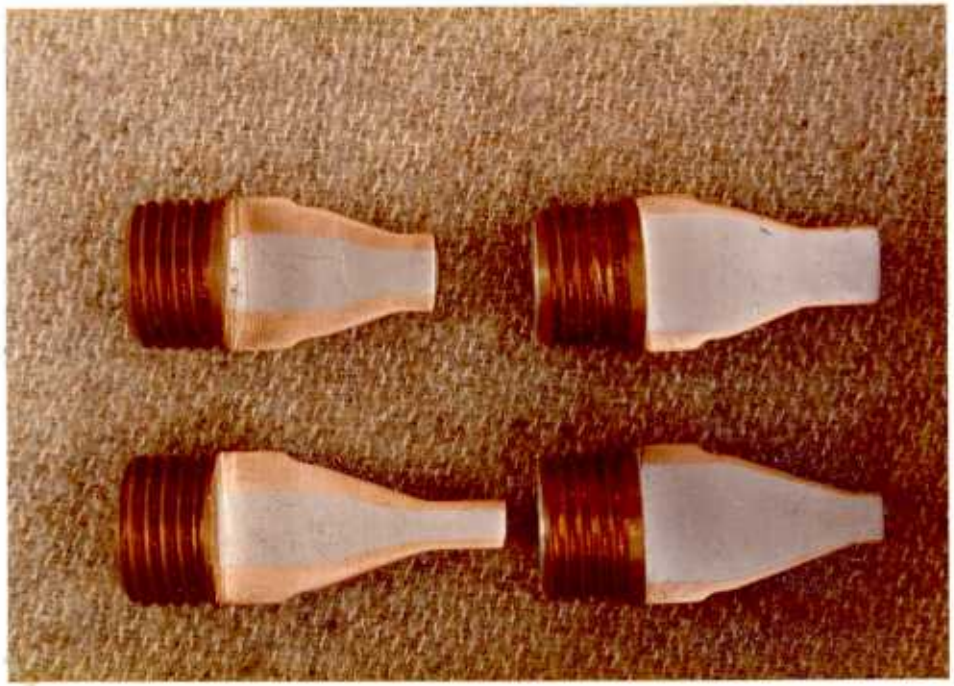

Plate 6.1: Specimens sectioned along the meridional plane.

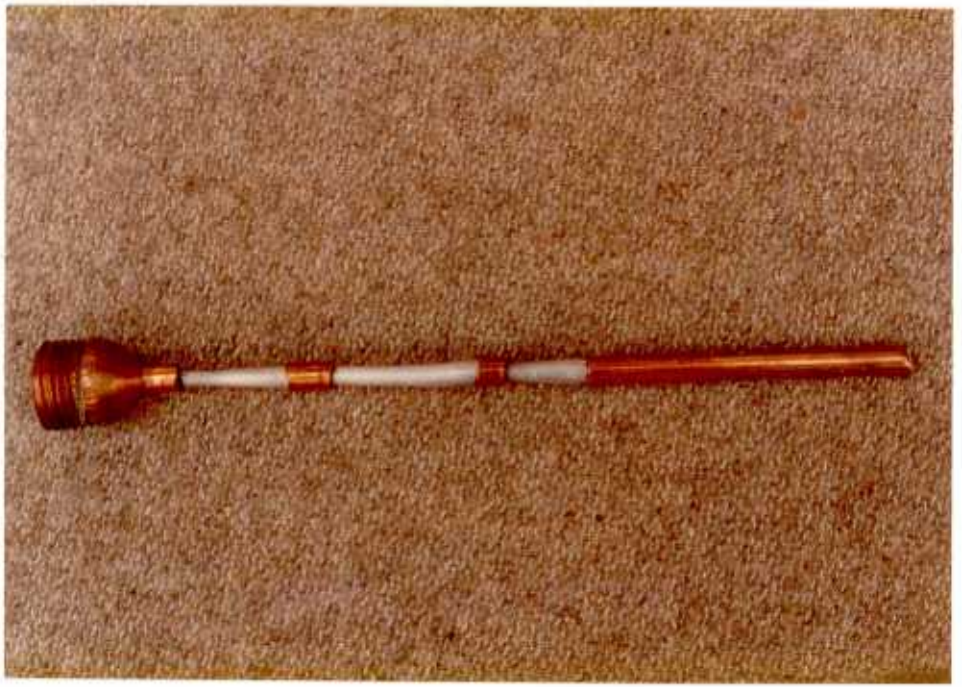

Plate 6·2

CHAPTER 7

NON-STEADY STATE PROBLEMS

7.1 General

All the processes considered so far in this work have been of the steady-state type, i.e. problems where the mode of deformation remains constant throughout most of the duration of the process.

If steady-state conditions do not exist, the problem has to be analyzed as a transient one. Furthermore, if body forces are not introduced by inertia (acceleration) effects, so that dynamic terms can be neglected, the problem can be treated as quasistatic. The present chapter is concerned with using finite element techniques for this type of process.

For such problems the velocity of flow is first established for the initial configuration and then these velocities, determined at the nodal points, allow the new position of the mesh to be determined at a subsequent time increment Δt, by a suitable updating procedure. With the new boundary and altered mesh, new flow conditions are established.

As each new flow solution starts in an "Eulerian" manner from the present configuration, very large deformations can be readily followed by a simple process of repetition of the solution in updated coordinates.

Clearly, for accuracy, small time intervals need to be considered, but as all calculations are restarted at each new configuration the question of incrementing Eulerian type stresses, which often presents difficulty in elasto-plastic analyses, does not arise.

The field of application for this kind of analysis is obviously vast, ranging from the simple upsetting of a cylinder, to forging problems presenting complicated flow patterns. Some of these problems are analyzed in what follows.

7.2 Plane Strain Compression of a Block

Although this problem is not analyzed as a transient one, it is included in this chapter because it provides a good starting point towards assessing the accuracy of finite element solutions for this class of problem, since exact slip-line field solutions exist for a plastic-rigid material.

The problem of compressing a rectangular block of metal between rough parallel dies was first investigated by Prandtl[7.1] who deduced that the slip-lines were cycloids. Later Prager[7.2] showed that this type of field can be obtained by using a simple geometric property of the Mohr's circle. Alexander[7.3] considered the effect of Coulomb friction at the faces of parallel rigid dies on the compression load, providing an "intermediate" solution between the perfectly rough and frictionless dies.

The specific problem considered here is the plane strain compression of a rectangular block of rigid-perfectly material between rough dies which approach each other with a relative speed of two units, see Fig. 7.1a.

The problem is analyzed using the penalty-function formulation developed previously. Because of symmetry, only one quadrant needs to be modelled and this was done using bi-linear quadrilateral elements. The mesh used, together with the assumed boundary conditions, is shown in Fig. 7.1b. Two configurations were analyzed, namely, $w/h = 1.6$ and $w/h = 3.6$; a constant yield stress of 120 MN/m^2, a cut-off factor (γ) equal to 10^9 and a penalty coefficient $\alpha = 10^8$ were selected.

The results are presented as velocity distributions and upsetting loads and compared with existing slip-line solutions[7.4], see Fig. 7.2. It can be seen that the velocity distribution conforms well with the slip-lines, even though the finite element method does

not allow for the discontinuities that the slip-line theory considers. The upsetting pressures also compare well with the slip-line values.

7.3 Upsetting of Cylindrical Billet

7.3.1 Introduction

The frictionless compression of a circular, solid cylinder between parallel flat dies as shown in Fig. 7.3a is a relatively simple operation. This simplicity makes it useful as a test for measuring the stress-strain properties of materials when this data is required for high strains. Unlike the tension test no instability due to necking is present. Furthermore, the test can be carried out to strains in excess of 2.0 if the material is ductile. Upsetting, as compression is often called, is also one of the major manufacturing processes in metal forming.

The apparent simplicity turns into relative complex deformation when, as is usual, friction is present at the die-workpiece interface. The deformation is homogeneous when there is no friction, but with friction the distribution of the compressive stress is non-uniform, and the average compression stress differs from the flow stress. Moreover, the frictional resistance restricts the flow at the contact surface, whilst the metal at the specimen mid-height can flow outward undisturbed. This leads to a "barrelled" specimen profile, and internally a region of undeformed metal is created near the platen surfaces.

The complexity of non-uniform deformation is also manifest by the fact that a part of the initially free surface comes into contact with the die during compression: this is known as "folding".

7.3.2 Previous Work

Due to the importance of compression as a test for

determining properties, most of the early work was mainly concerned with the average pressure required by compression. In recent investigations, however, attention has been directed toward finding the detailed deformation characteristics in relation to the occurrence of surface cracks[7.5-7.7], with a view to imposing knowledge of fracture mechanics in large strain deformation processes.

Some of the analyses worth mentioning are the analysis by Siebel[7.8], the slab method analysis by Schroder and Webster[7.9] and the upper-bound solutions by Johnson[7.10], Kudo[7.11], Kobayashi[7.12] and Avitzur[7.13].

A number of experimental investigations have also been undertaken for the determination of pressure distribution, deformation, etc. For specimens of height to diameter ratio larger than 1.6, a double bulge was observed by Nagamatsu et al[7.14]. The pressure pin technique was employed by Van Rooyen and Backofen[7.15] to obtain the pressure distribution on the dies. This distribution was also determined experimentally by Takahashi[7.16]. Both these studies show that when the height to diameter ratio is greater than 0.6, the pressure distribution has the form of a reversed friction-hill; the pressure distribution is of the normal form for ratios smaller than 0.6. The finite element method has also been extensively used (in its various forms) to analyze this problem. A survey of that work was presented in Chapter 4 and it will not be repeated here except when required.

7.3.3 Computational Conditions

In 1976 Kudo and Matsubara[7.17] proposed a joint programme under the auspices of C.I.R.P* to analyze the different

---

* The "Collège Internationale Recherche et Production".

numerical methods available for the analysis of metal forming processes. In that connection they proposed a test problem which is the one chosen here to demonstrate and assess the capabilities of the penalty-function formulation used in this work.

The problem is that of upsetting of a cylindrical billet having a diameter of 20 mm and a height of 30 mm between perfectly rough parallel platens (see Fig. 7.3a).

Both non-hardening and hardening material are considered (see Fig. 7.3b), the yield stress being defined as:-

$Y_o = 0.7$ (KN/mm^2) (non-hardening) (RPN)

$Y = Y_o + 0.3\,\bar{\varepsilon}$ (KN/mm^2) (hardening) (RPH)

Because of symmetry only one quadrant needs to be modelled. The continuum is divided into 150 bi-linear quadrilateral elements as recommended in Ref.(7.17). This idealization is shown in Fig. 7.3b together with the boundary conditions used. The problem is first solved for the frictionless condition, thereby providing a further check of the formulation since the exact solution is known in this case.

A penalty coefficient (α) equal to 10^8 and a cut-off factor ($\gamma = \frac{2}{3}\,\bar{\sigma}/\dot{\bar{\varepsilon}}$) of 10^9 were chosen; a one-percent reduction in height was selected as the size of an increment. The solution with the convergence norm $||\Delta\underset{\sim}{u}||/||\underset{\sim}{u}||$ less than 0.005 was considered acceptable for each step. The calculations were continued up to 60% reduction in height in both cases. The average number of iterations for each step was two and four to five for the frictionless and the sticking friction cases respectively.

7.3.4 Results and Discussion

(a) Frictionless Compression

The results given by the finite element method for the frictionless case show that homogeneous deformation is modelled very well, the mesh deforming uniformly and remaining completely cylindrical throughout the deformation process. Fig. 7.4 shows the deformed mesh at two different stages, namely, 30% and 60% reduction in height. The results also show that there is no detectable departure from constant volume, proving that the "penalty" is behaving in the correct way.

The upsetting loads, calculated via the reactions obtained from the stiffness equations, are shown in Fig. 7.5. Agreement with the analytical solution is excellent. In Fig. 7.5 et seq, RPN means rigid-plastic-non-hardening material and RPH means rigid-plastic-hardening material. The stresses at the equatorial outside surface are shown in Fig. 7.6. Again, agreement with the "exact" solution is excellent.

(b) Sticking Friction

A more complicated pattern of deformation is found when the material is assumed to stick to the platens. The grid distortions for various reductions in height are shown in Fig. 7.7. It can be seen that a rigid region of almost spherical shape is formed below the platen face, the size of this zone reducing with increase of reduction.

A phenomenon in simple compression, known as "folding", is that of a part of the original free surface coming into contact with the die during compression. This tendency can be seen to start at about 20% and material folds between 30% and 40% reduction. If a finer mesh were to be used near the surfaces, it would be found that the folding will occur earlier in the process.

The amount of folding can be more clearly seen in Fig. 7.8 where some typical profiles of the side surface of the upset specimen are reproduced. No appreciable difference in the side profiles for the hardening and non-hardening materials is observed. Careful examination of the bulge factor (see Fig. 7.9) reveals, however, that bulging is slightly more marked for the non-hardening material (Bulge factor is defined as maximum diameter/initial diameter).

The variation of stresses in the element at the equatorial surface is shown in Fig. 7.10 for both materials. The tensile circumferential stress develops and the compressive axial stress decreases its magnitude as the reduction in height increases. At large reductions the axial stress becomes tensile. These results are in agreement with experimental evidence[7.18].

The upsetting loads calculated via the reactions are shown in Fig. 7.11 for both materials. The analysis again predicts the expected trend for the two materials. However, the curves lay above those for the friction-free condition only after folding has occurred. The curves of load versus reduction in height found in this thesis coincide with those found by other formulations (see Ref.[7.18]).

7.4 Extrusion-Forging

Many hot and cold forging and extrusion processes involve flow in more than one major direction. Knowledge of these modes of flow is of importance in the design of the optimum size and shape of the billet. However, until recently, this type of problem was regarded as too complex for accurate analysis leaving the analyst at the mercy of "rule of thumb" methods. One simulative test often used involves the formation of a central boss on a disc by compression between a platen and a die having a central orifice (see Fig. 7.12). The length of boss formed under given conditions gives a guide to flow behaviour.

In this section the finite element method is applied to this relatively simple problem of compound flow under various conditions.

7.4.1 Previous Work

Although the open extrusion-forging problem is a relatively simple problem very few analyses of it are available. Kudo[7.11] considered the analagous plane-strain operation using the concept of unit rectangular regions with an assumed kinematically admissible velocity field which satisfied the boundary conditions. The rate of energy dissipation was computed through optimization of a pseudo-independent parameter. Burgdorf[7.19] carried out experimental and analytical work. His analysis was based on an approximate stress state and was only concerned with billets having a low height-diameter ratio such that the deformation was almost entirely confined to one mode.

A similar problem in which holes in the upper and lower die permitted simultaneous extrusion from both ends of the workpiece was considered by Pomp et al[7.20]. The experimental results were reported in terms of the actual amount of extrusion and hence the presence of different modes of flow was not identified. Saida et al[7.21] applied an upper-bound approach to the problem and analyzed the problem for various frictional conditions. Jain et al[7.22] modified the work of Saida et al and analyzed the problem of simple extrusion-forging, identifying three different modes of flow which depended on frictional and geometrical characteristics. Newham and Rowe[7.23] used the slip-line field theory to analyze the problem and were able to predict the transition between the different modes of flow.

Recently, Osman and Bramley used the UBET (Upper Bound Elemental Technique) to solve the problem incrementally finding good agreement with Jain's work. Price and Alexander[7.24] have analyzed a similar problem using the finite element (penalty-function formulation)

presenting the results in terms of the deformed geometry.

7.4.2 Computational Conditions

The calculations were carried out for a cylinder with a height-diameter ratio of 0.75 (H_o = 0.75 in (19.05 mm), D_o = 1 in (25.4 mm)). Three different hole sizes were considered, namely, d = 0.75 in (19.05 mm), d = 0.5 in (12.7 mm) and d = 0.25 in (6.35 mm). Conditions of "sticking friction" were assumed at both die and platen. However, one of the geometries was also considered with the frictionless condition at the platen. A penalty coefficient (α) equal to 10^8 and a cut-off factor (γ) of 10^9 were chosen. 1% reduction in height was selected as the size of the increment and the calculations were continued up to 80% reduction in height in most cases. A solution with the convergence norm $||\Delta\underset{\sim}{u}||/||\underset{\sim}{u}|| \leq 0.01$ was considered acceptable for each step; an average of two to six iterations for each step was enough to obtain that convergence.

The material was assumed to be rigid-perfectly plastic with a yield stress of Y_o = 0.7 KN/mm^2.

7.4.3 Mesh Updating

Initially, the problem was solved using the most logical and simple updating scheme, namely, the new position of the nodal points was determined using the velocity at each nodal point. This scheme worked satisfactorily for small reductions in height. However, at relatively large reductions the elements tended to be badly shaped, reaching a point where they crossed over each other causing the calculations to be stopped. Fig. 7.13 illustrates the sequence just described; note that because of symmetry, only half the specimen needs to be modelled.

Price and Alexander[7.24] encountered the same difficulty

when solving a similar problem. They circumvented the difficulty by updating only the boundary nodes and then redefining the interior elements arbitrarily. A scheme on the same lines was implemented in this study and the problem re-analyzed. The scheme was successful in the sense that the crossing of elements was eliminated. However, some badly shaped elements were still encountered during the calculation, resulting in illogical modes of flow. This was mainly due to the fact that the element nearest to the die corner (element C in Fig. 7.13f), because of the boundary condition imposed (full friction), will always remain badly shaped no matter what internal rearrangements are made.

A new scheme was then developed to modify the mesh and enable the analysis to be carried out up to large reductions eliminating the crossing of elements and avoiding, as much as possible, highly distorted elements. The basis of the scheme is similar to the one just described, namely, updating of the boundary nodes with a subsequent arbitrary redefinition of the internal elements. The procedure was mainly directed towards modelling the complex flow pattern occurring at the die corner. This was carried out by including a new layer of elements to the metal surface that is going to form the extrudate and using a very small element at the die corner to justify the assumption that the model represents the shearing that is likely to occur. The procedure is better understood by studying the schematic description depicted in Fig. 7.14. The scheme was successful and the results are discussed below.

Price and Alexander argued that the shape of the deformed elements was the only "memory" they had of their previous deformation hence, modifications of the mesh should be as few as possible. This would be correct if a pure "Lagrangian" frame of reference was used. In the "penalty-function" formulation used by them and in this work the current configuration is chosen as the reference state and thus,

the "memory" of previous deformation is "stored" in the material properties (if they are history-dependent). Therefore, if some way could be found of interpolating the material properties from the "unmodified" mesh to the "modified" mesh, problems involving material whose flow stress is history-dependent could be easily tackled. This is not necessary for the problems treated in this thesis since only rigid-perfectly plastic materials are used.

7.4.4 Results and Discussion

The problem of open extrusion forging is a compound flow process where the material may flow radially through the gap between the die and the platen or extrude into the cavities. The main characteristics of the flow are better represented by plotting the percentage total height as a function of percentage reduction of the flange (see Fig. 7.15).

It can be seen that, in general, there is an initial stage during which the total height decreases. As deformation proceeds, this is followed by a stage in which the total height remains constant, until finally a rapid increase in height is observed. It is seen in Fig. 7.15 that the range for the first stage becomes narrower with increasing hole size, and at a ¾ in (19.05 mm) hole diameter this upsetting stage vanishes. The transition from the second to the third stage is delayed with increasing hole size, thus giving a wider range of the second stage for the larger hole diameter. These characteristics deduced from the finite element analysis are in good agreement with experimental results and upper bound analyzes of similar geometries[7.22] (see Fig. 7.16).

However, this is not the only information that the finite element solution gives; the velocity distribution and shape of the deformed billet are readily derived from the analysis and these are

shown in Fig. 7.17 for a specified geometry at various reductions in height.

The three different stages already described are easily identified together with their associated velocity fields. During the first stage (Figs. 7.17a - 7.17c) the velocity field suggests that metal will feed out of the zones beneath the hole and that the total height will decrease as deformation proceeds. Two rigid zones can be identified: one directly beneath the die hole and one near the platen which is, in fact, a zone of very small velocity (dead zone). This dead zone extends in both the vertical and horizontal (into the flange) directions until it occupies all the material beneath the hole, including the extrudate and the lower part of the flange, signalling the transition to the second stage (see Fig. 7.17d). Further reduction in height results only in deformation of the flange in an upsetting mode with the central core remaining rigid. The velocity fields suggests that deformation takes place by metal shearing against a rigid core (see Figs. 7.17d - 7.17g), which accounts for the crossing of elements encountered when no rearrangement of the mesh is used.

Further reduction in height brings about the third stage, where the predicted velocity field shows upsetting on the outside and extrusion in the central core, with a neutral zone in the flange that tends to move outwards. The net result is a rapid increase in total height (see Figs. 7.17h - 7.17i).

Another interesting comparison readily available is between the profile of the outside surfaces predicted for the three different hole sizes considered (see Fig. 7.18). The most striking characteristic is the mode of deformation for the larger hole size which, as shown in Fig. 7.15, only deforms in the second stage mode. This results in a rather unsymmetric bulging when compared with the other two. Also, it can be seen that folding is more pronounced in the early stages (Figs.

7.18a and 7.18b) and is localized on the die, the rest of the billet being practically undeformed until the flange reduction is relatively large. The bulged surfaces for the two other geometries are relatively similar at low reductions (see Figs. 7.18a and 7.18b) with folding occurring at both the die and the platen. The similarity disappears at large reductions, the bulging and folding being more pronounced for the smaller hole size (see Figs. 7.18c and 7.18d).

It can also be seen that at low reductions the larger the hole the larger the total height; the trend being reversed at large reductions.

In order to study the effect of friction in the process, one of the geometries, namely, H_o/D_o = 0.75 and d = 0.5 in (12.7 mm), was analyzed for a frictionless platen. The effect of this on the total height is shown in Fig. 7.19 together with the variation for the full friction case for comparison. It can be seen that the transition from the first stage to the second stage takes place at a larger reduction than with sticking friction. The extent of the second stage is shortened and the transition to the third stage occurs at a higher flange reduction. Furthermore, the total height is always less than for the sticking friction condition.

The deformed billet and the corresponding velocity fields for various reductions are shown in Fig. 7.20. The velocity fields suggest that the main effect of reduced friction is to facilitate radial flow in the upsetting mode of deformation (see Figs. 7.20a - 7.20d) which delays both transitions. It can also be seen that, unlike the case of full friction at the platen, no dead zones are easily identifiable during the early stages of deformation. Also, when the second stage sets in, the dead zone does not extend as much into the flange (see Fig. 7.20e).

It is worth mentioning that the velocity fields for this

problem are also a solution for the problem in which a hole in the upper and lower die permits extrusion from both ends, in which case the geometry shown in Fig. 7.20 is, for reasons of symmetry, one quadrant.

7.5 Concluding Remarks

This chapter has shown the successful application of the penalty-function to non-steady state problems. The implementation of computational schemes for continuum modelling extended the method to problems of compound flow. Indeed, such schemes are necessary if processes where internal shearing is present are to be modelled.

REFERENCES

7.1 PRANDTL, L.
"On the Penetration Hardness of Plastic Materials and the Hardness of Indentors".
Z. angew. Math. Mech., 1, p. 15, (1921).

7.2 PRAGER, W.
"A Geometrical Discussion of the Slip-Line Field in Plane Plastic Flow".
Trans. R. Inst. Technol., Stockholm, p. 65, (1953).

7.3 ALEXANDER, J. M.
"The Effect of Coulomb Friction in Plane-Strain Compression of a Plastic-Rigid Material".
J. Mech. Phys. Solids, 3, p. 233, (1955).

7.4 ROWE, G.
"An Introduction to the Principles of Metal Working".
E. Arnold, London, (1965).

7.5 KOBAYASHI, S.
"Deformation Characteristics and Ductile Fracture of 1040 Steel in Simple Upsetting of Solid Cylinders and Rings".
Trans. of ASME, J. of Engng. for Ind., Vol. 92, pp. 391-399, (1970).

7.6 LEE, P. W. and KUHN, H. A.
"Fracture in Metalworking Processes".
Technical Report to American Iron and Steel Institute, April, (1972).

7.7 COCKROFT, M. G. and LATHAM, D. J.
"A Simple Criterion of Fracture for Ductile Metals".
National Engng. Lab. Rep. No. 240, July, (1966).

7.8 SIEBEL, E.
"The Plastic Forming of Metals".
Translated by J. H. Hitchcock, Reprinted from Steel, pp. 55-61, (1934).

7.9 SCHROEDER, W. and WEBSTER, D. A.
"Press-Forging Thin Sections : Effect of Friction, Area, and Thickness on Pressure Required".
Trans. ASME, J. Appl. Mech., Vol. 16, pp. 289-294, (1949).

7.10 JOHNSON, W.
"Over-Estimates of Load for some Two-Dimensional Forging Operations".
Proc. 3rd U.S. Natl. Congress Appl. Mech., ASME (NY), (1958).

7.11 KUDO, H.
"An Upper-Bound Approach to Plane Strain Forging and Extrusion, Parts I, II and III".
Int. J. Mech. Sci., Vol. 1, pp. 57-83, 229-252, 366-368, (1960).

7.12 KOBAYASHI, S.
"Upper Bound Solutions of Axi-symmetric Forming Problems".
Trans. ASME, J. Engng. Ind., Vol. 86, pp. 122-126, (1964).

7.13 AVITZUR, B.
"Metal Forming : Processes and Analyses".
McGraw-Hill, New York, (1968).

7.14 NAGAMATSU, A., MUROTA, T. and JIMMA, T.
"On the Non-Uniform Deformation of Material in Axially Symmetric Compression Caused by Friction".
Bull. of J.S.M.E., Vol. 14, pp. 331-338, (1971).

7.15 VAN ROOYEN, G. T. and BACKOFEN, W. A.
"A Study of Interface Friction in Plastic Compression".
Int. J. Mech. Sci., Vol. 1, pp. 1-27, (1960).

7.16 TAKAHASHI, S.
"The Distribution of Contact Pressures in Compressing Cylindrical Specimens".
(Japanese), J. Japan Soc. Tech. Plasticity, Vol. 6, pp. 271-279, (1965).

7.17 KUDO, H. and MATSUBARA, S.
"Revised Proposal for a Joint Examination Programme of the Validity of Various Numerical Methods for the Analysis of Metal Forming Processes".
Submitted to the Meeting of the Scientific Technical Committee "F", 26th CIRP General Assembly, Paris, (1976).

7.18 KUDO, H. and MATSUBARA, S.
"The Joint Examination Programme of the Validity of Various Numerical Methods for the Analysis of Metal Forming Processes".
Interim Report, August, (1977).

7.19 BURGDORF, M.
Ind. Anzeiger 89(64), p. 19, (1967).

7.20 POMP, A., MUENKER, T. and LUEG, W.
Mitt. K. Wil. Inst. Eisen, 2o, p. 265, (1938).

7.21 SAIDA, Y., LEE, C. H. and KOBAYASHI, S.
"Some Aspects of Friction in Forging Problems".
Presented at the II Inter-American Conference on Materials Technology, Mexico City, (1970).

7.22 JAIN, S. C., BRAMLEY, A. N., LEE, C. H. and KOBAYASHI, S.
"Theory and Experiment in Extrusion Forging".
Proc. of the 11th MTDR Conference, (1970).

7.23 NEWNHAM, J. A. and ROWE, G. W.
"An Analysis of Compound Flow of Metal in a Simple Extrusion/Forging Process".
J. Inst. Metals, Vol. 101, (1973).

7.24 PRICE, J. W. H. and ALEXANDER, J. M.
"Specimen Geometries Predicted by Computer Model of High Deformation Forging".
Int. J. Mech. Sci., 21, pp. 417-430, (1979).

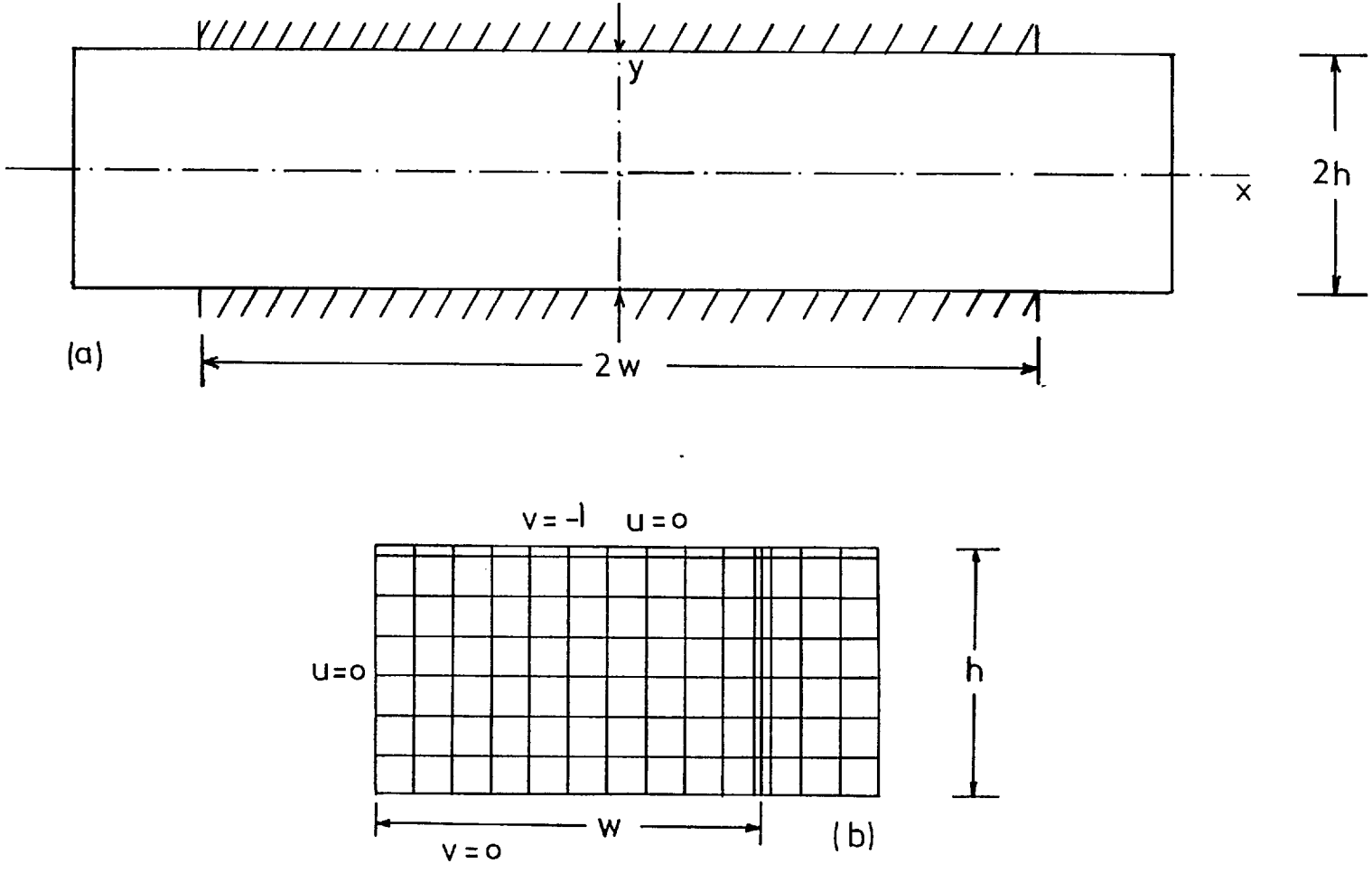

Figure 7.1: Plane strain compression of a block.(a) Schematic description of the problem
(b) Mesh and boundary conditions

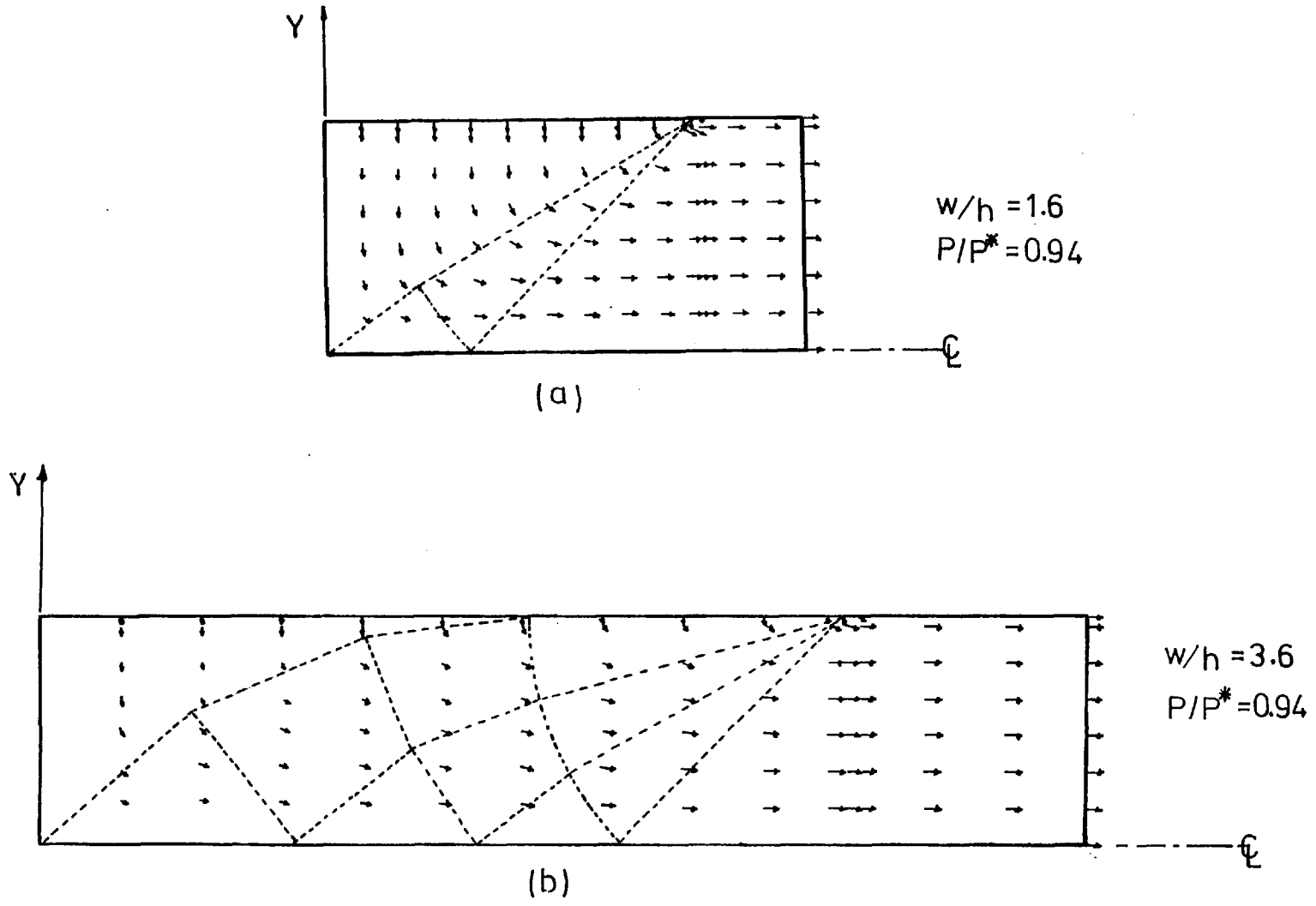

Fig 7.2: Velocity Fields for Plane Compression of a Block.

[→ , P] F.E.M. ; [----, P*] S.L.F.

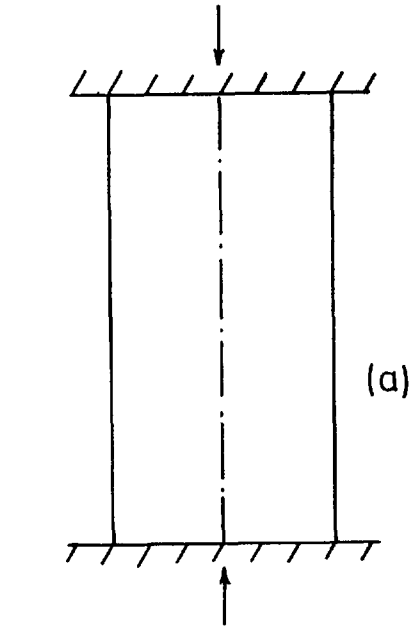

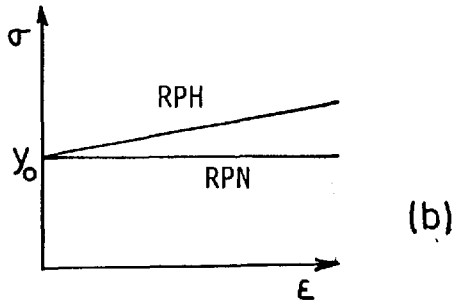

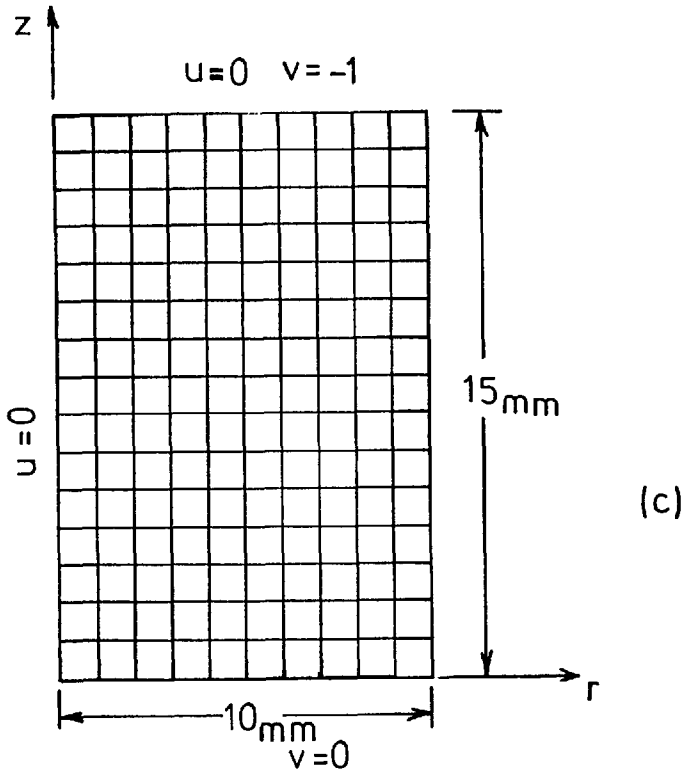

Figure 7.3: Upsetting of a cylinder. (a) Schematic description of the problem
(b) Stress-Strain curves; (c) Mesh and boundary conditions

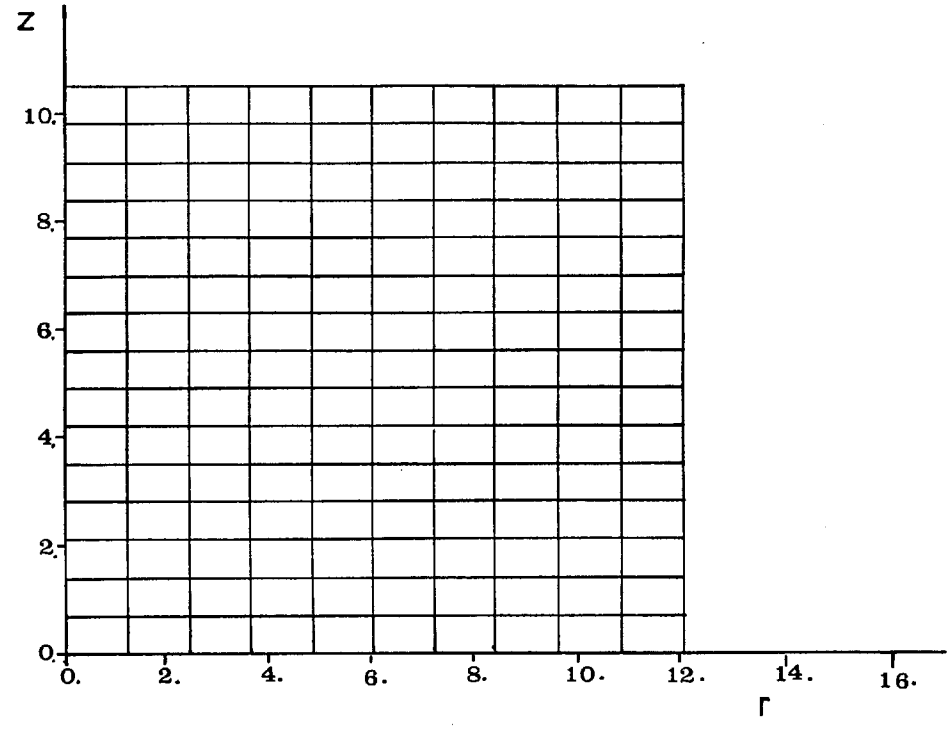

(a)

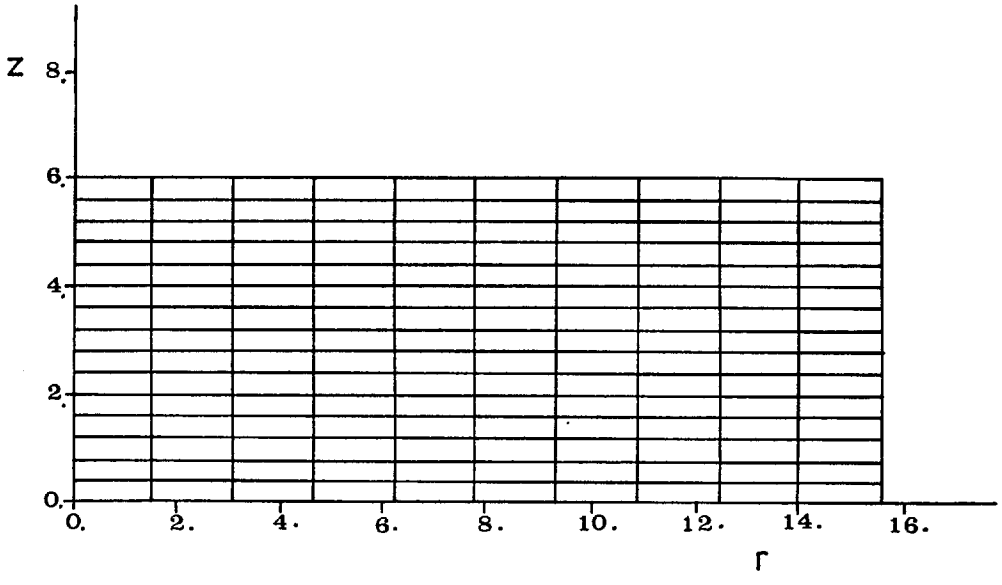

(b)

Figure 7.4: Deformed grid for frictionless upsetting
(a) 30% ; (b) 60%

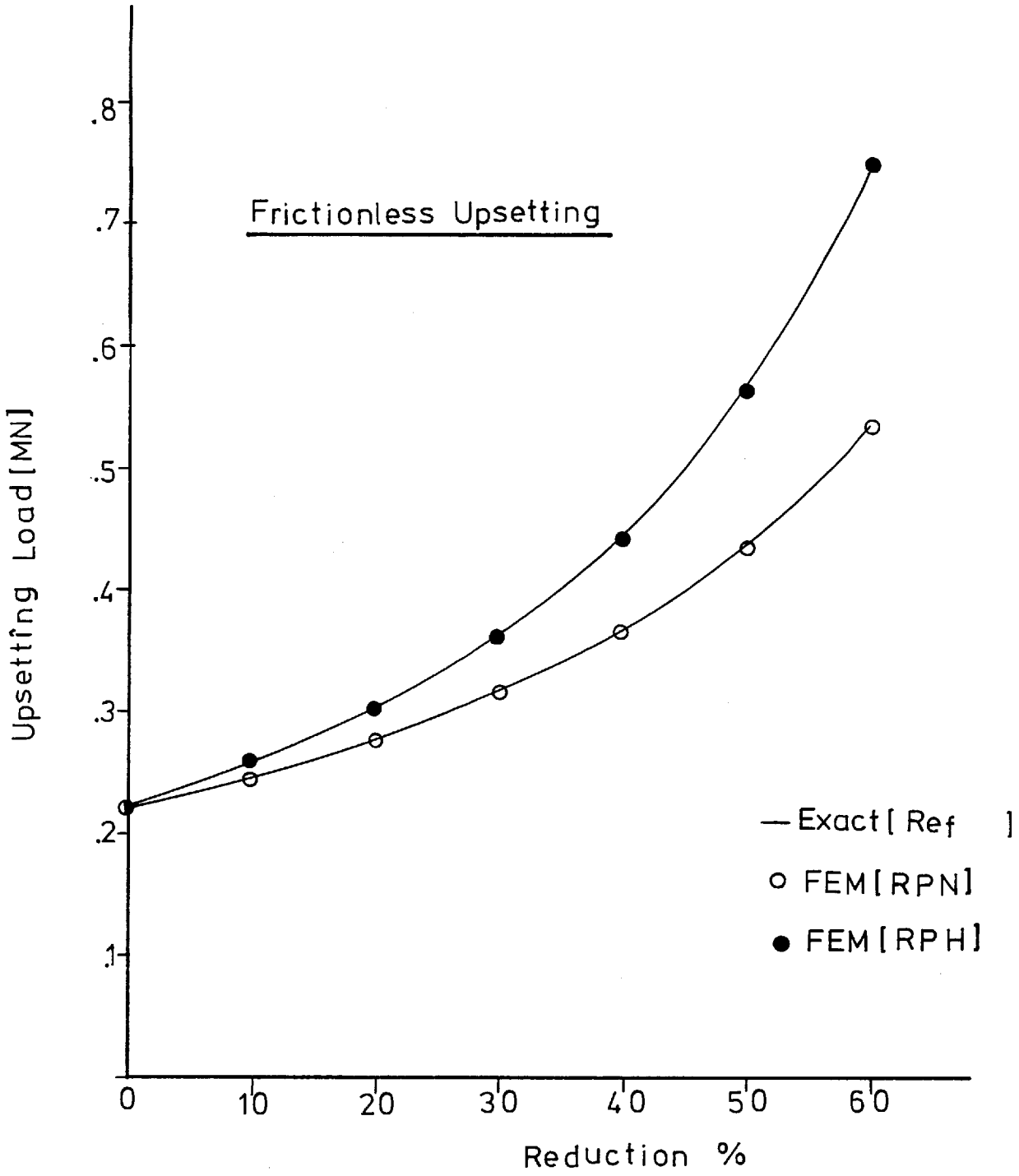

Figure 7.5: Load Vs Reduction (Frictionless upsetting)

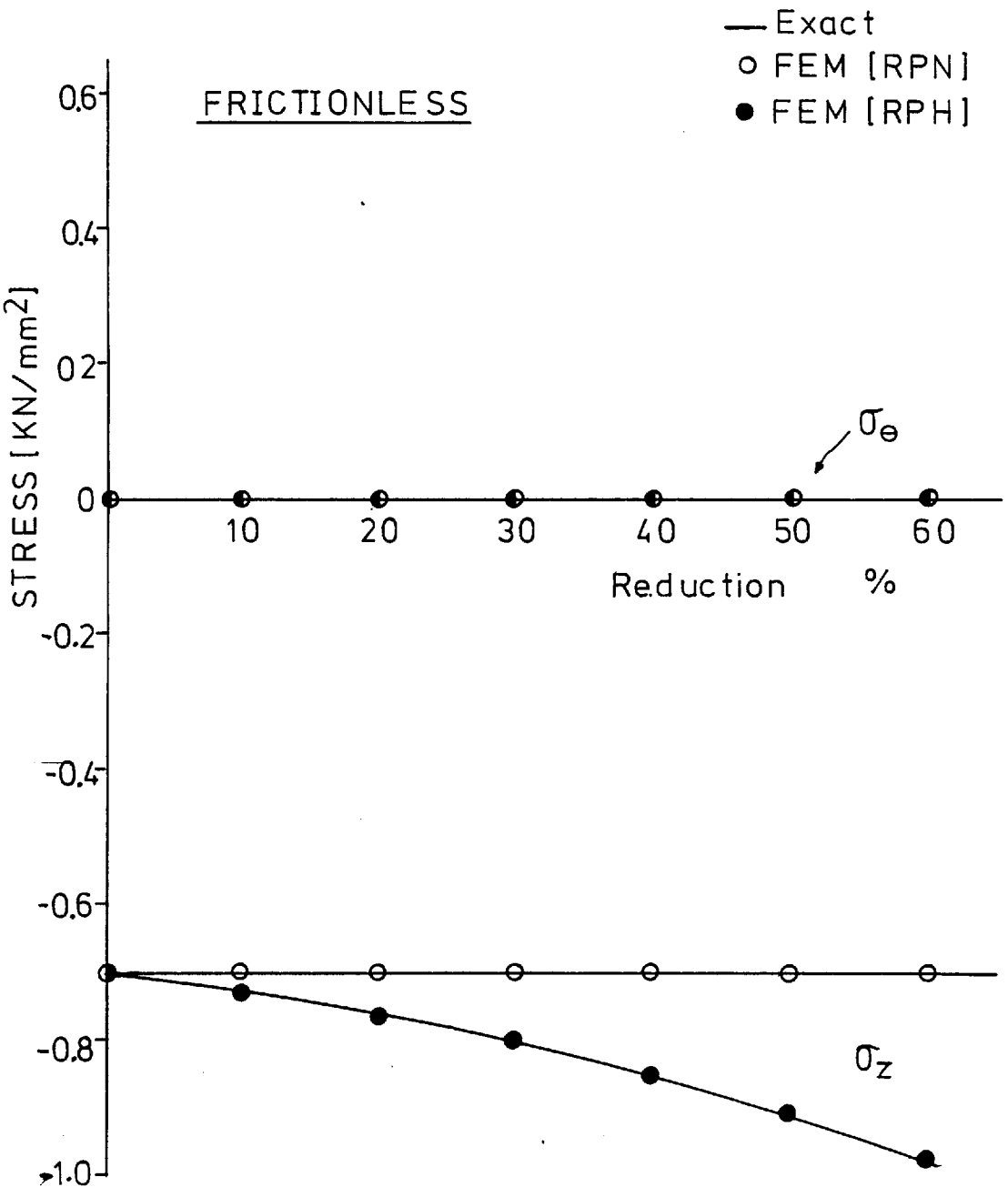

Figure 7.6: Stresses at the equatorial element
(frictionless upsetting)

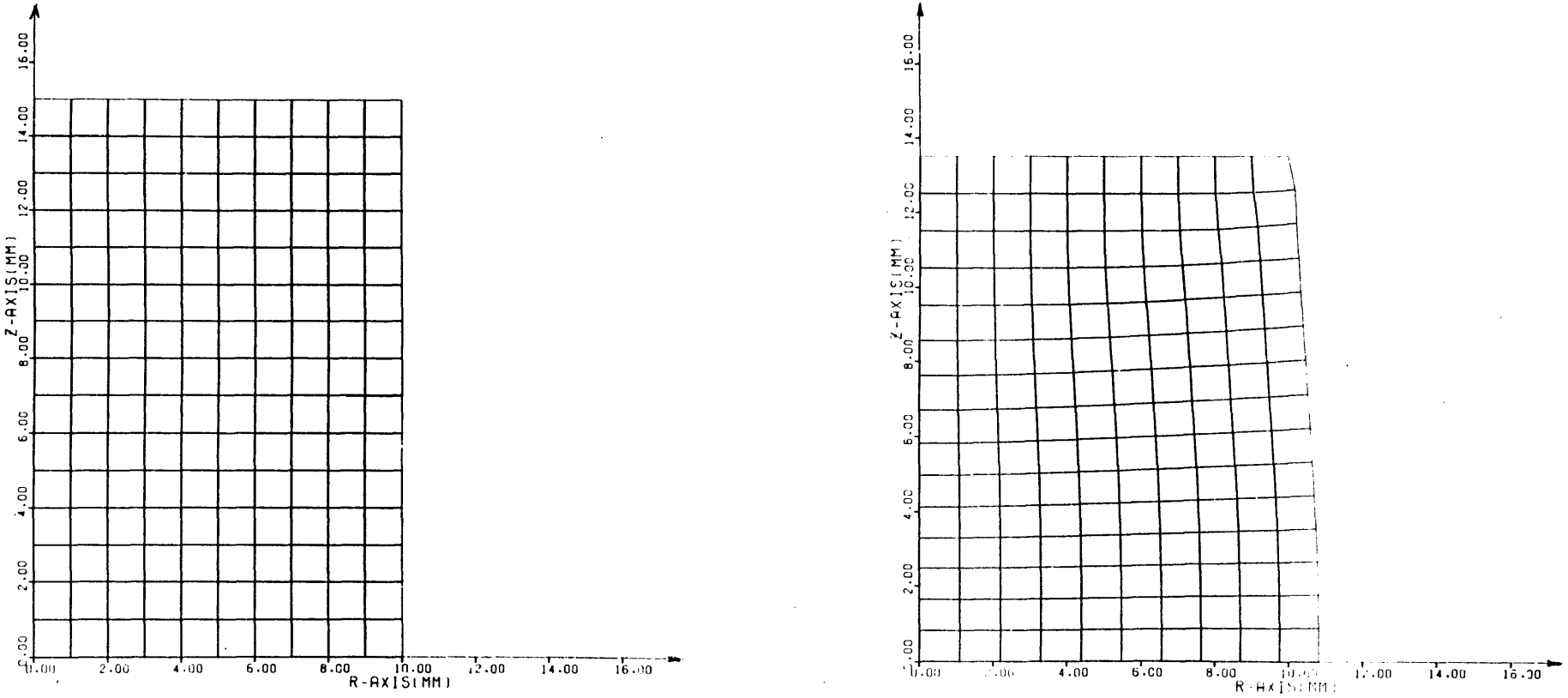

(a) 0 %

(b) 10 %

Figure 7.7: Upsetting of a cylinder between rough platens.
Grid distortion at various reductions.

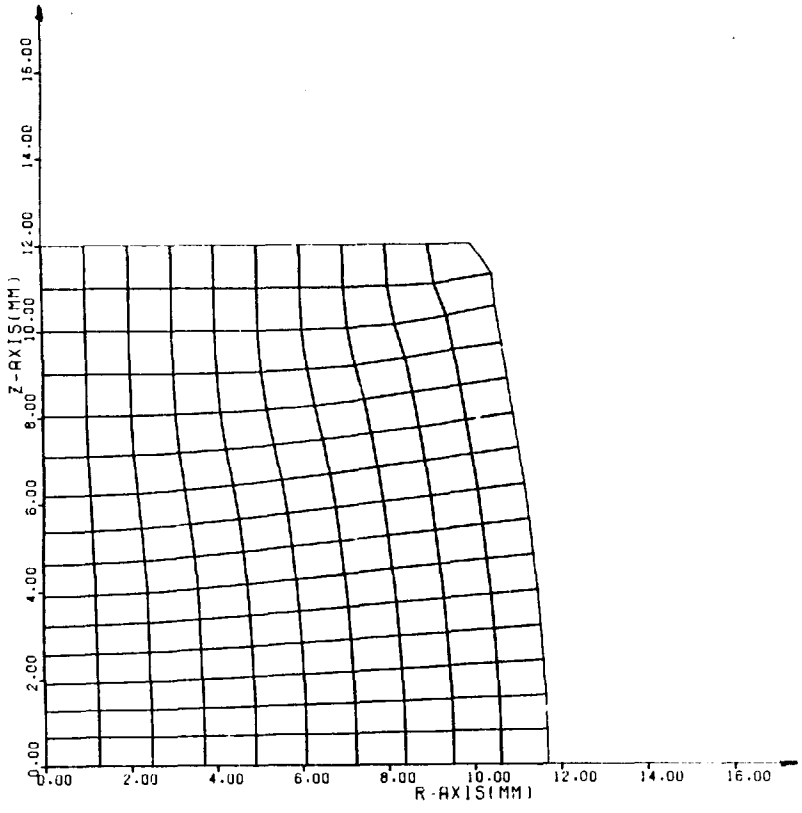

(c) 20 %

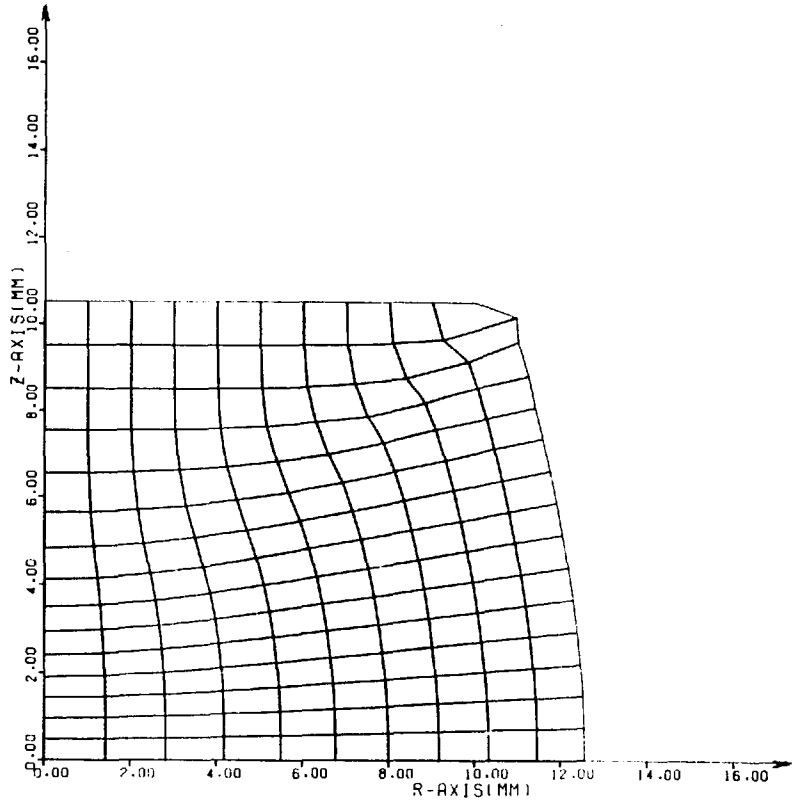

(d) 30 %

Figure 7.7 (Cont.)

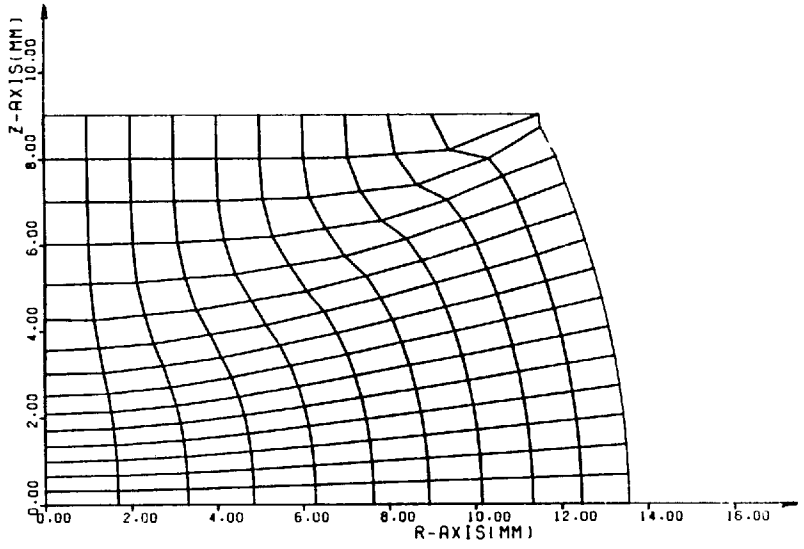

(e) 40 %

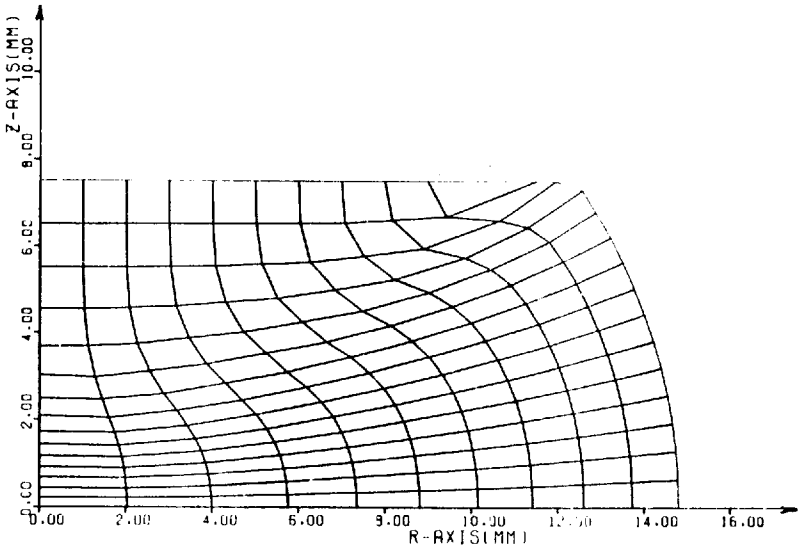

(f) 50 %

Fig 7.7 (Cont.)

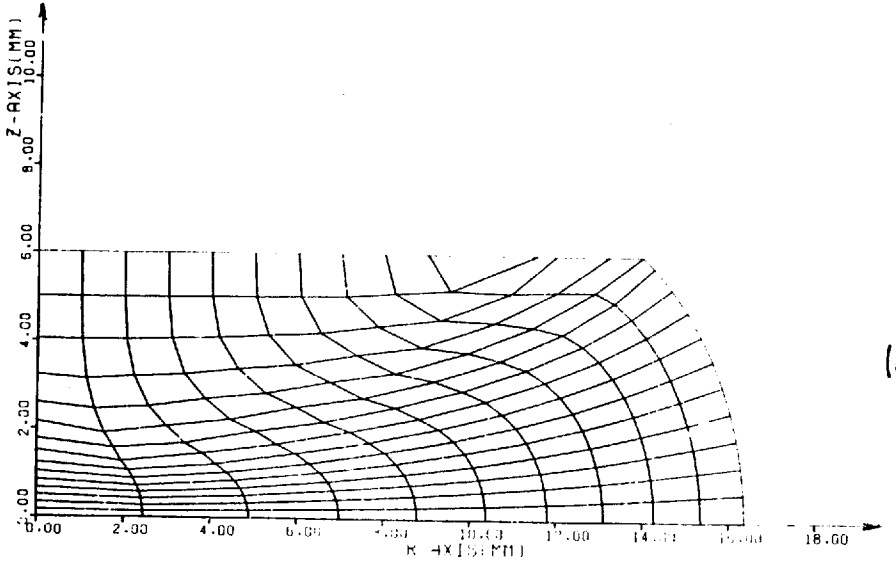

(g) 60 %

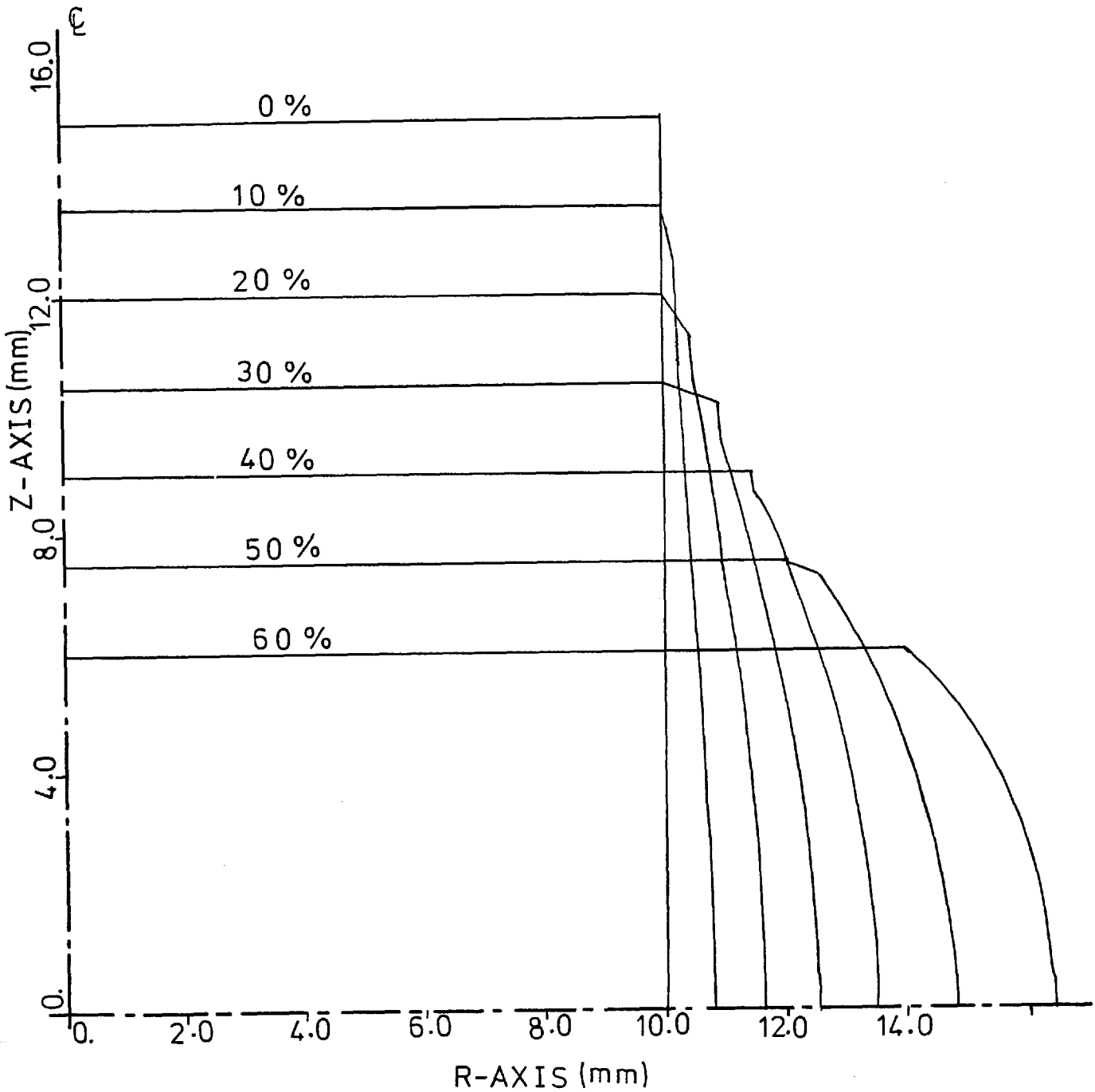

Fig 7.8: Profile of Side Surface at various Reductions (RPH)

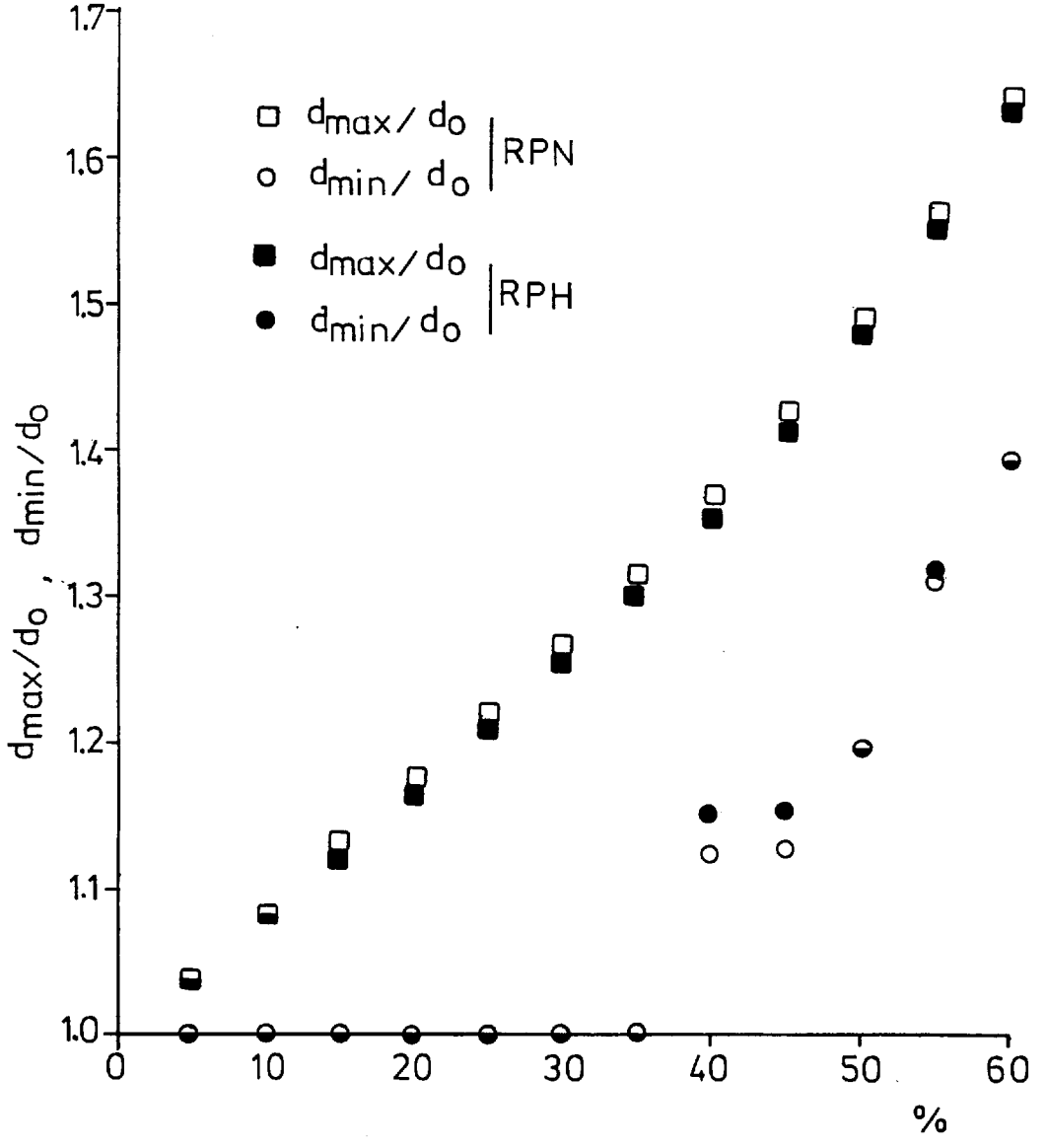

Figure 7.9: Bulge factor Vs reduction in height.

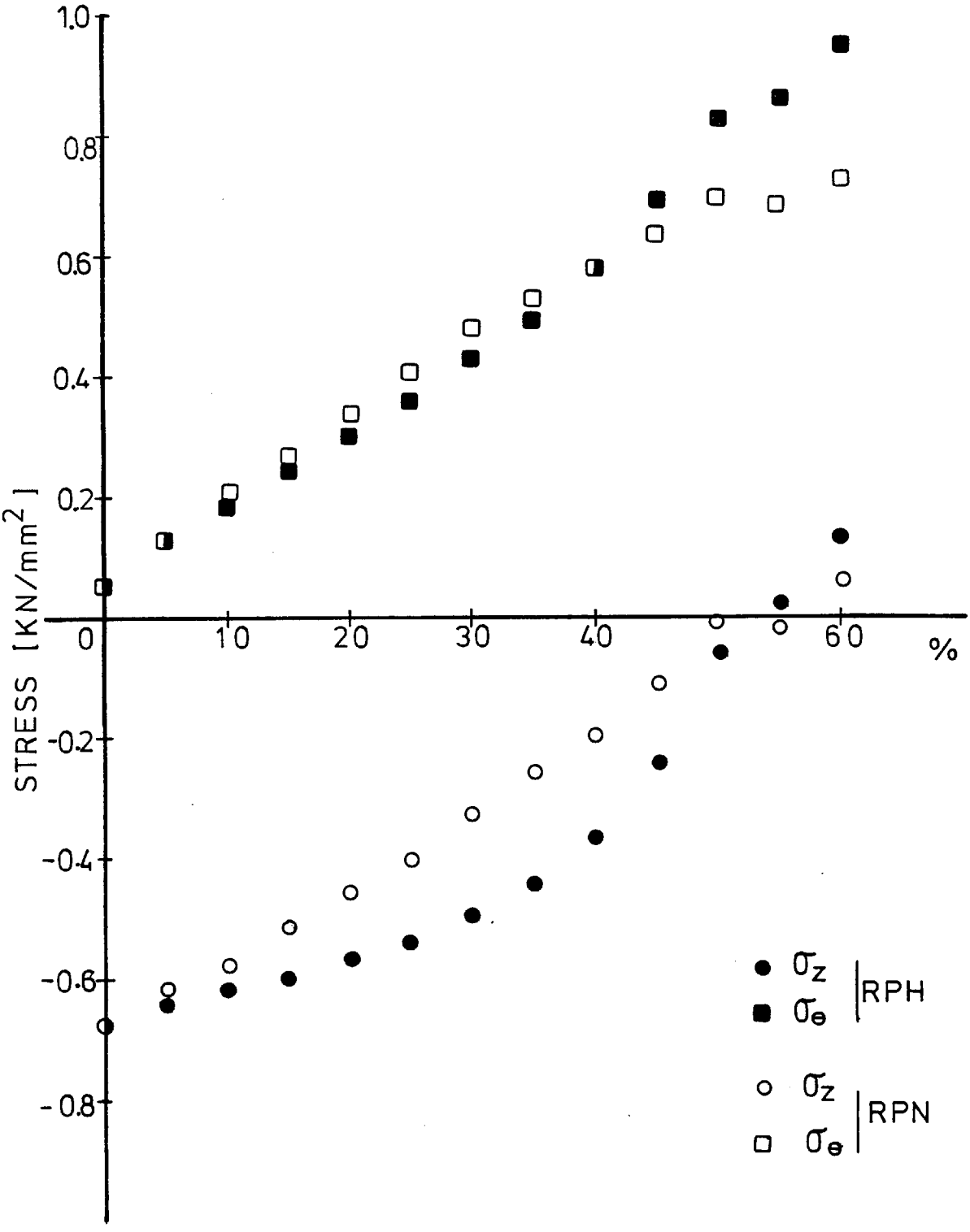

Figure 7.10: Stresses at equatorial element.

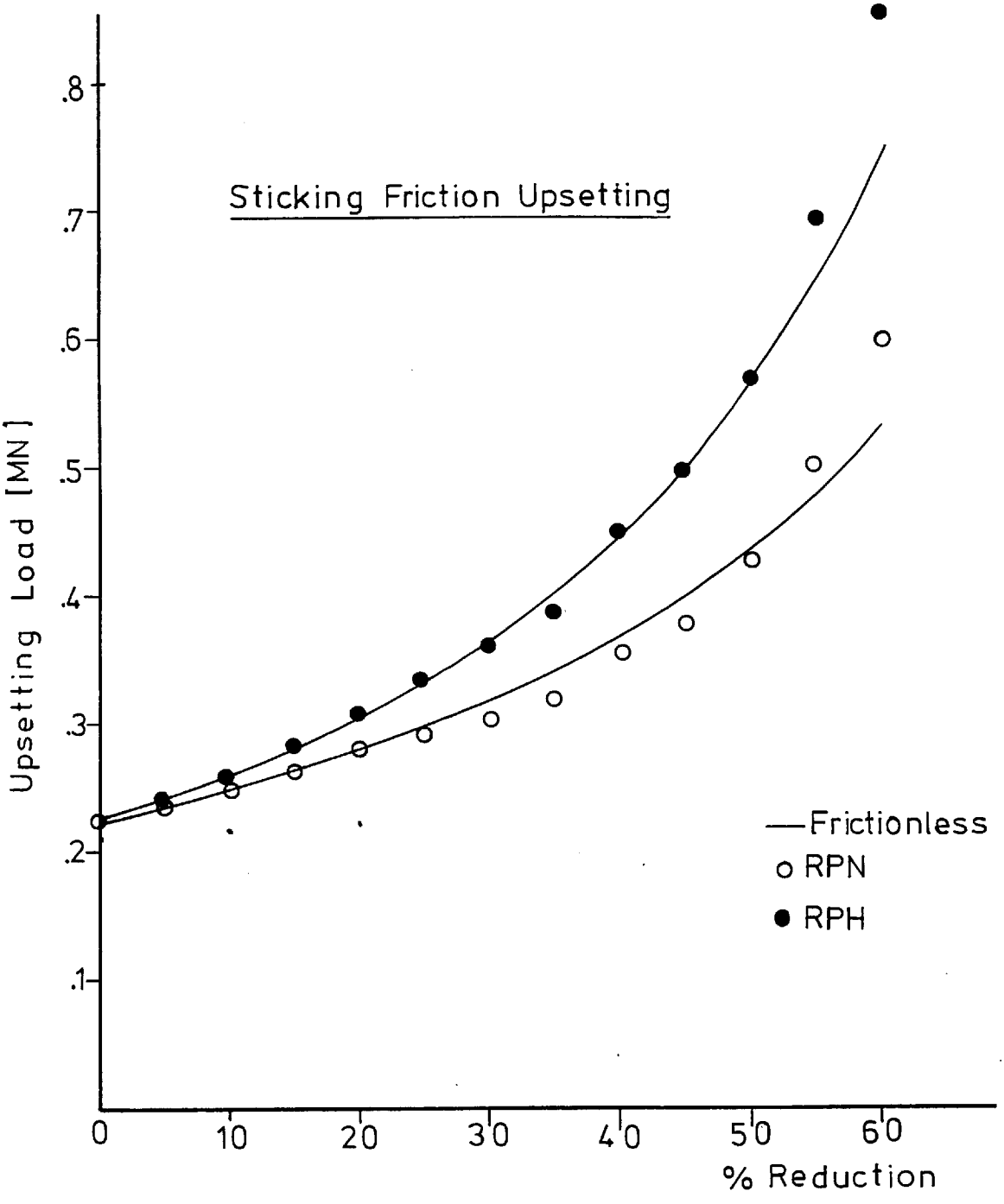

Fig 7.11: Upsetting Load vs Reduction

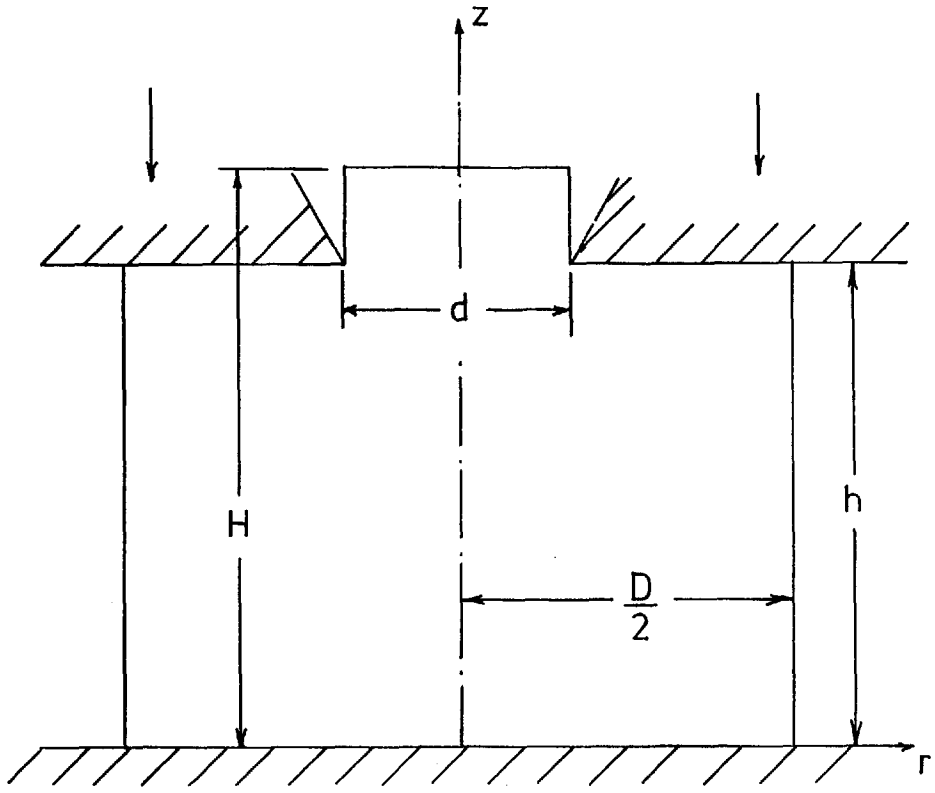

Figure 7.12: Schematic description of the open extrusion-forging process.

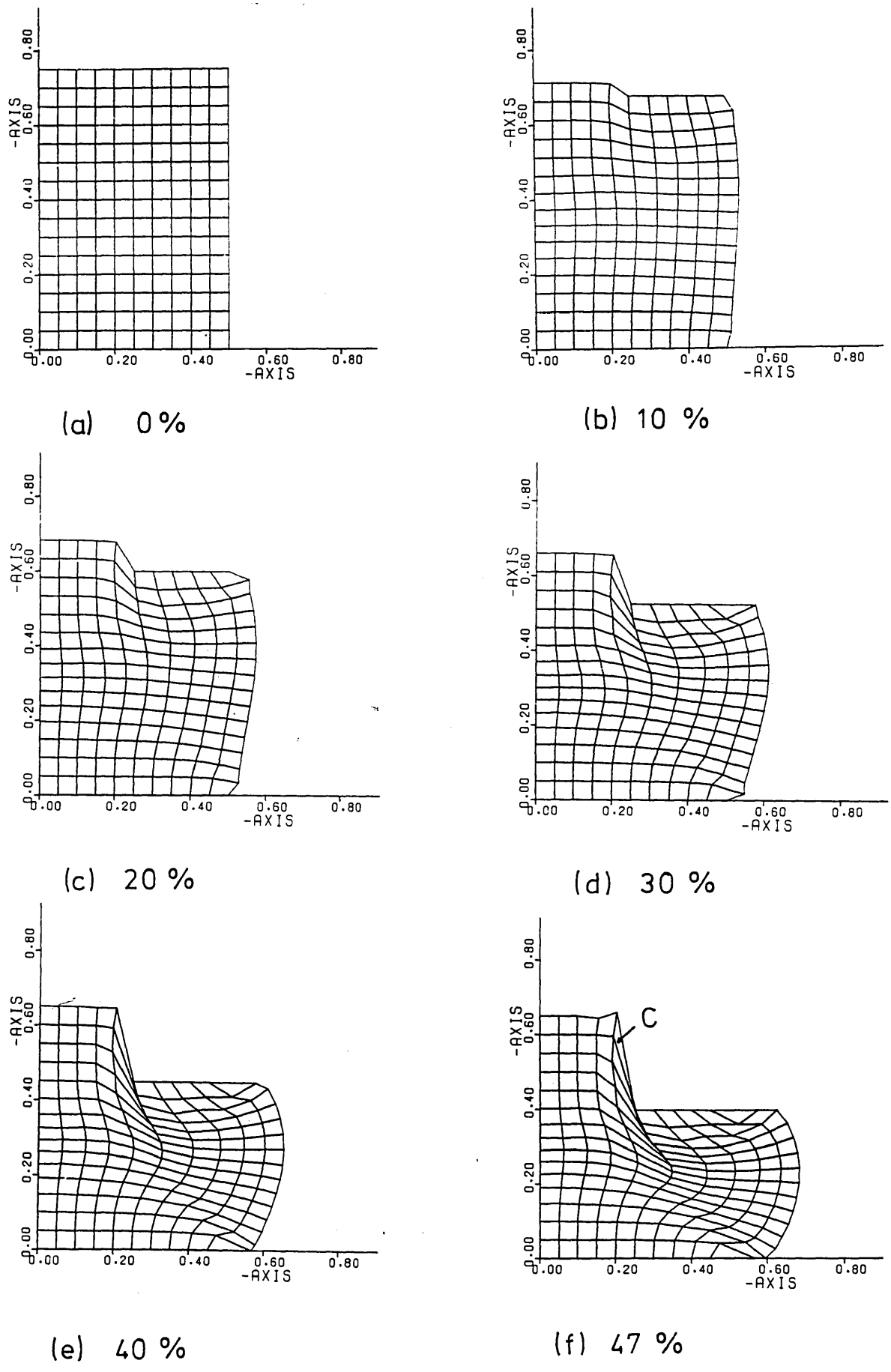

Figure 7.13: Extrusion-forging. Deformed grid at various stages.
(Mesh is not modified at any stage)

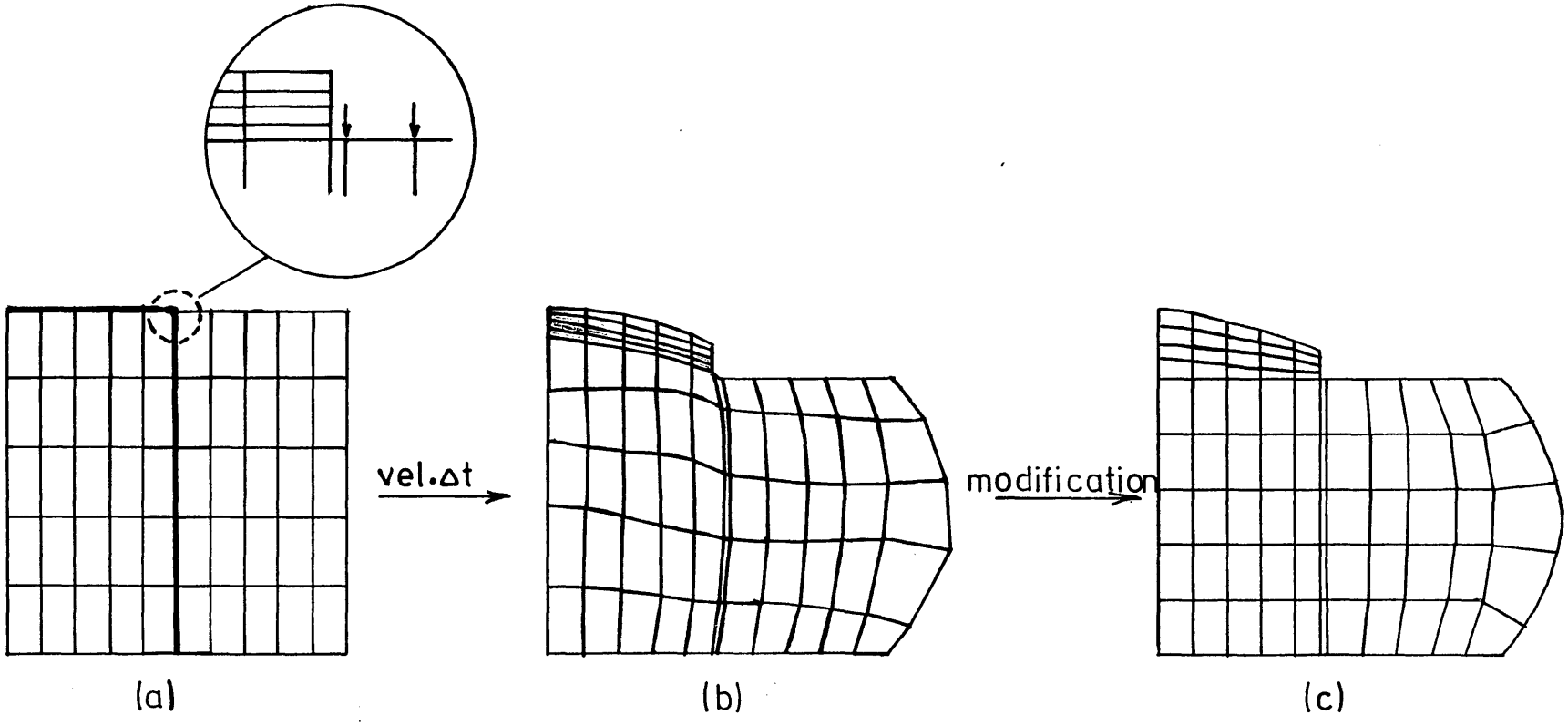

Figure 7.14: Schematic description of the mesh modification procedure.

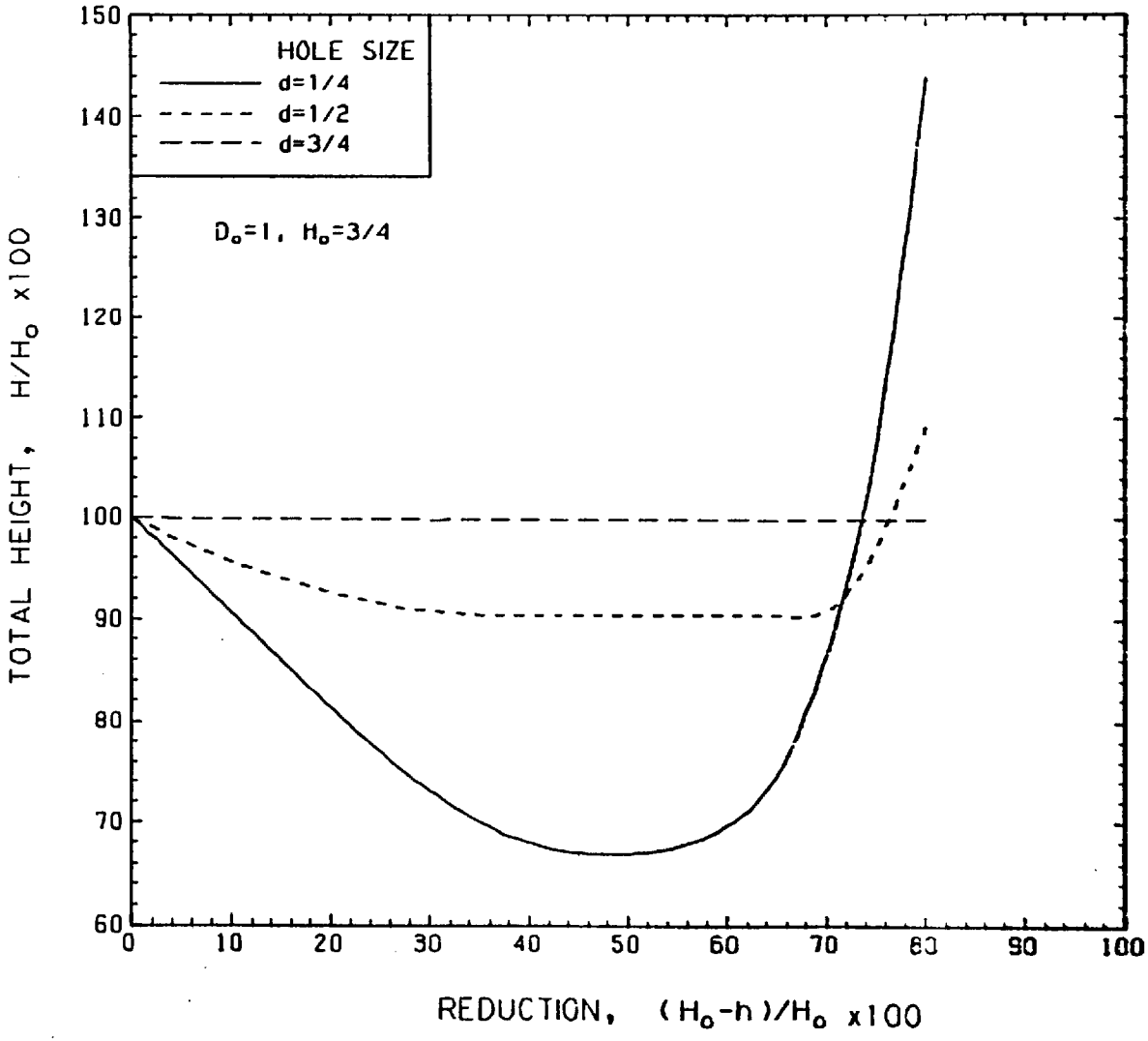

Figure 7.15: Effect of hole size on total height of extrusion (Finite Element Analyisis)

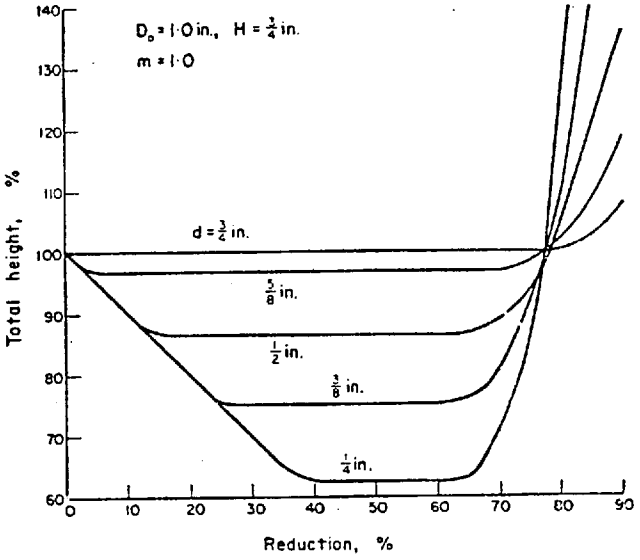

Effect of hole size on total height of extrusion (theoretical).

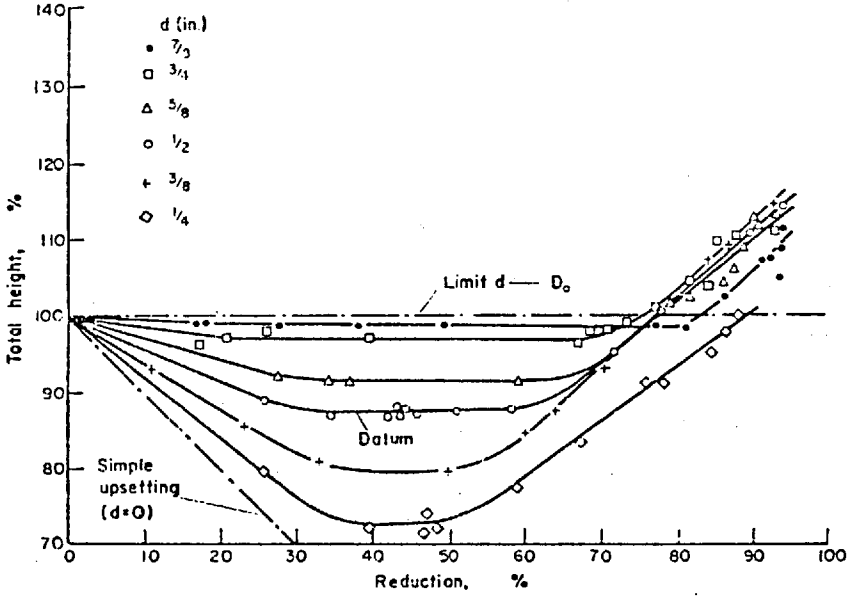

Experimental metal flow characteristics—Influence of die hole diameter

Figure 7.16: Theoretical and experimental results reported in Ref.7.22

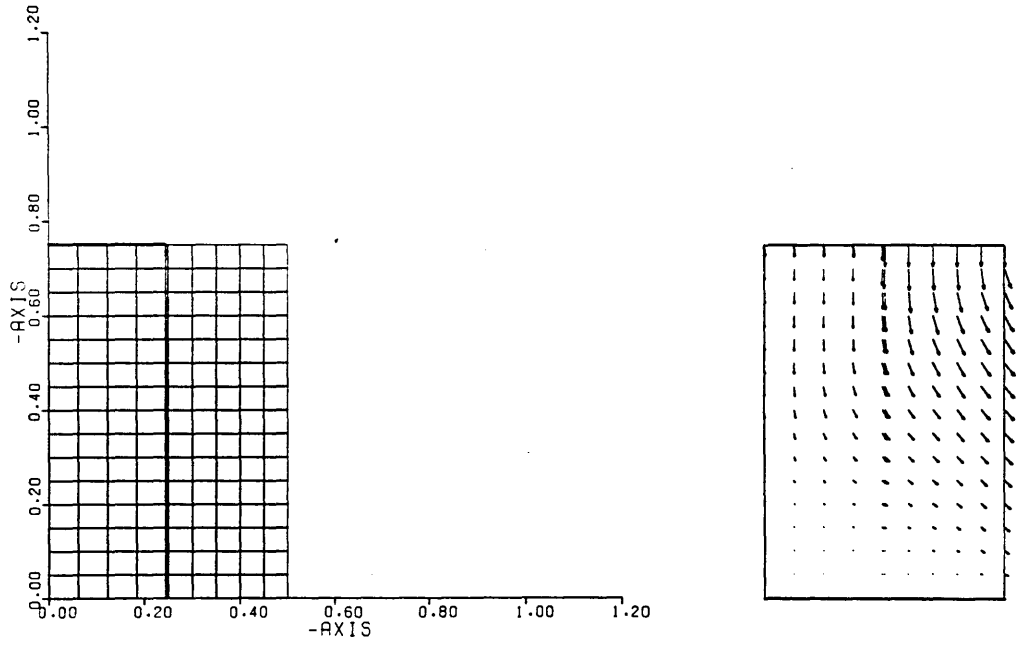

(a) 0 %

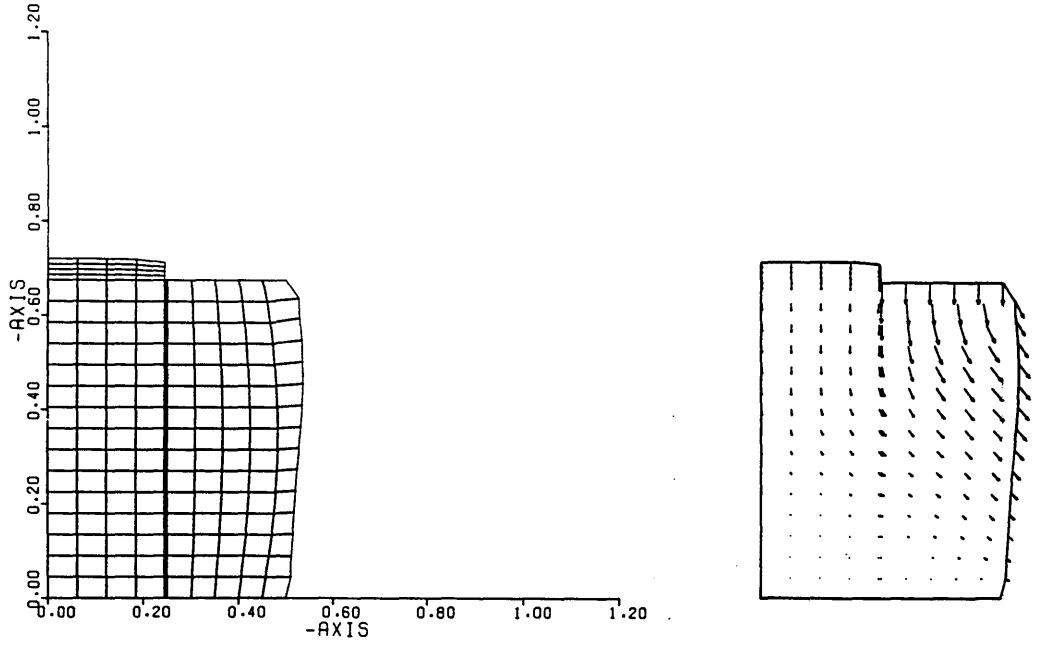

(b) 10 %

Figure 7.17: Extrusion-Forging between rough platen and rough die.
Deformed geometry and velocity fields at various reductions.

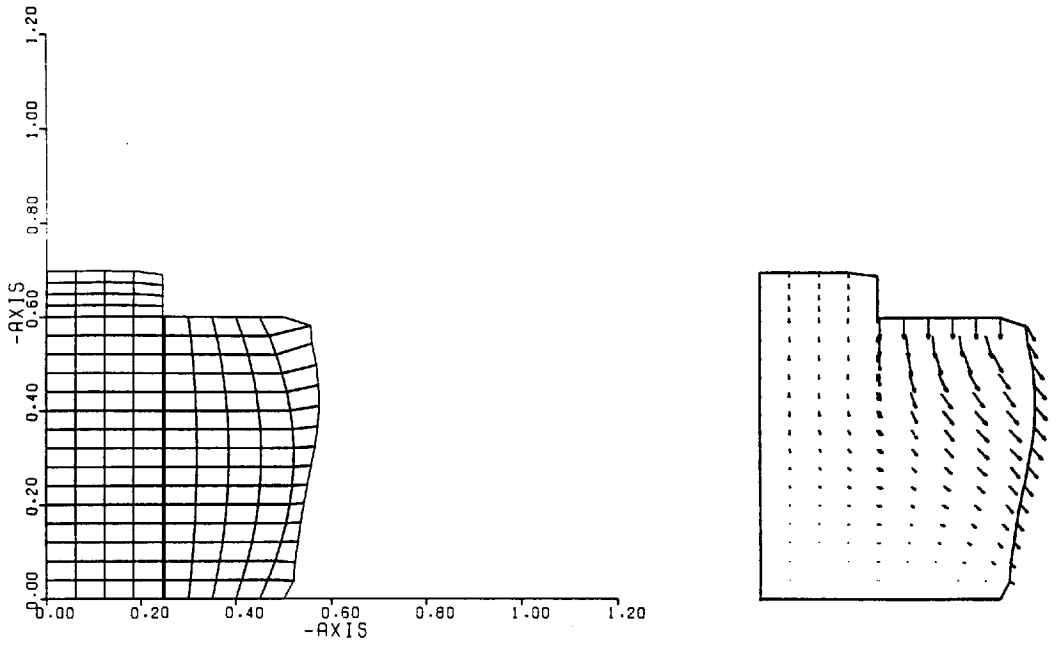

(c) 20 %

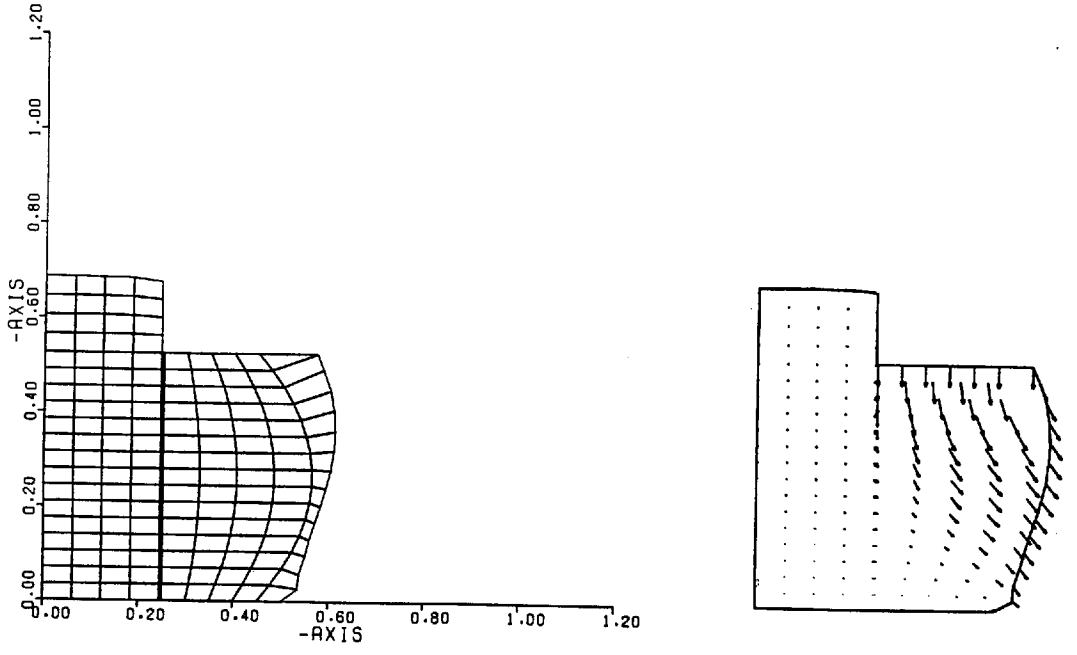

(d) 30 %

Figure 7.17 (Cont.)

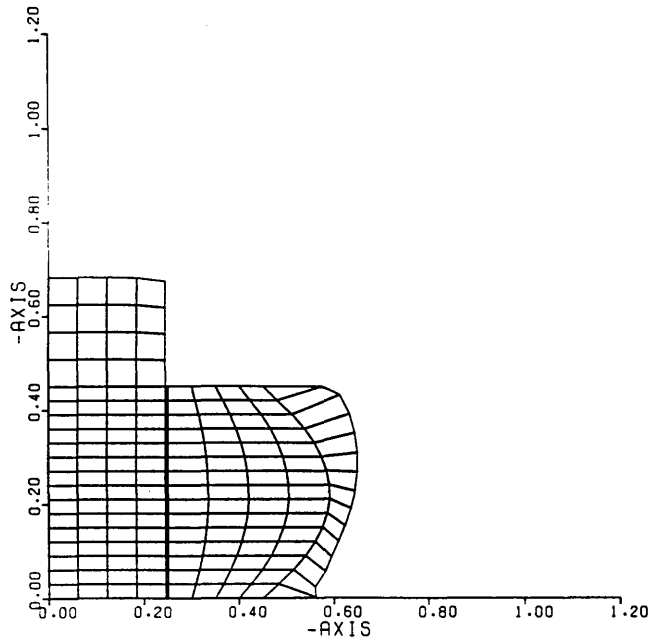

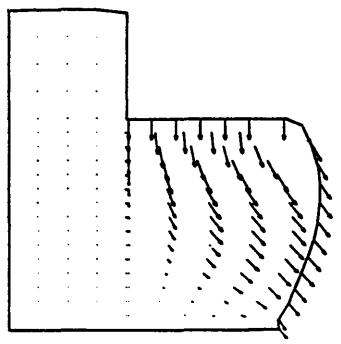

(e) 40 %

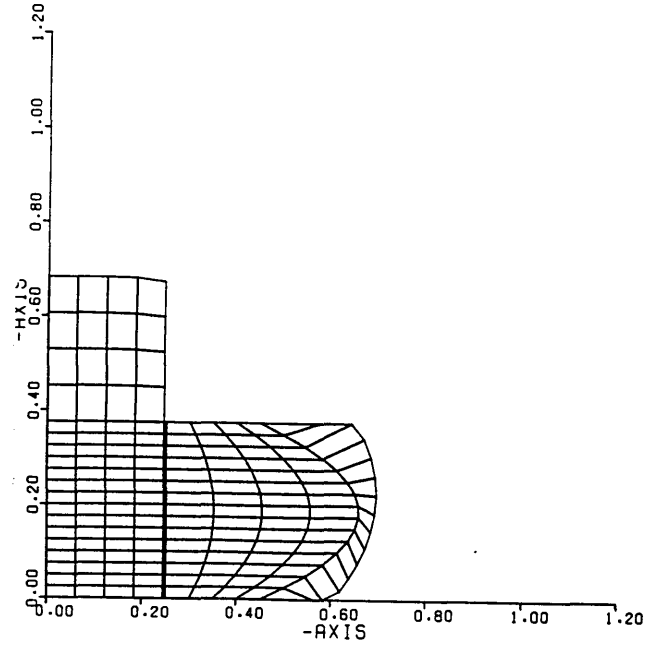

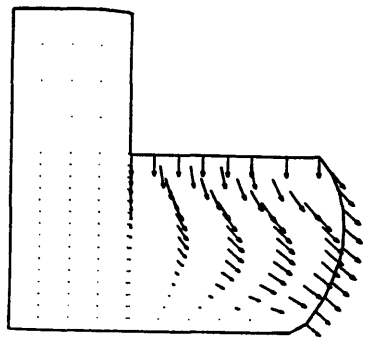

(f) 50 %

Figure 7.17 (Cont.)

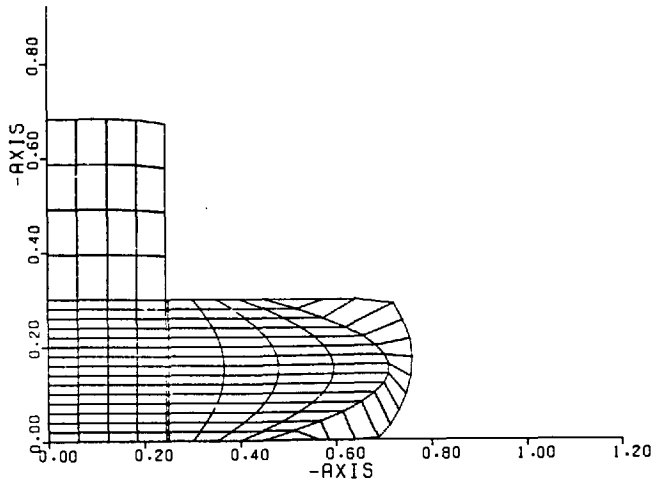

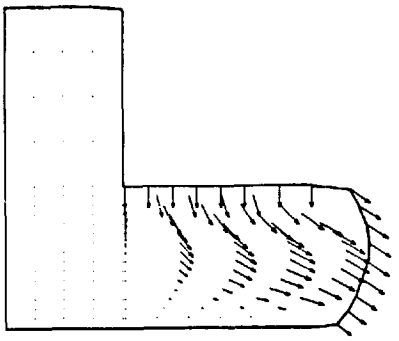

(g) 60 %

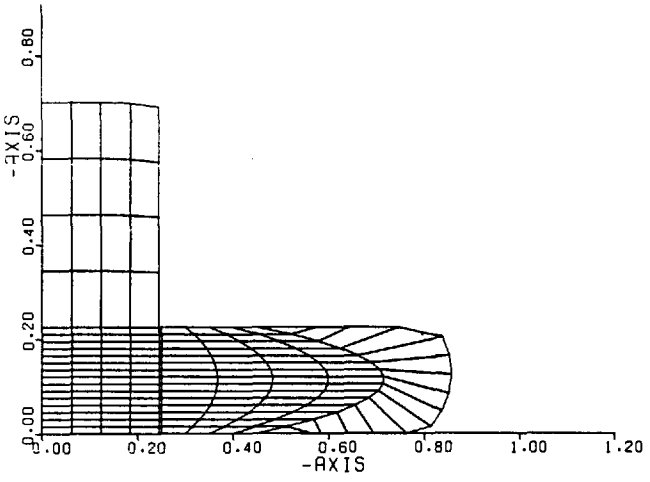

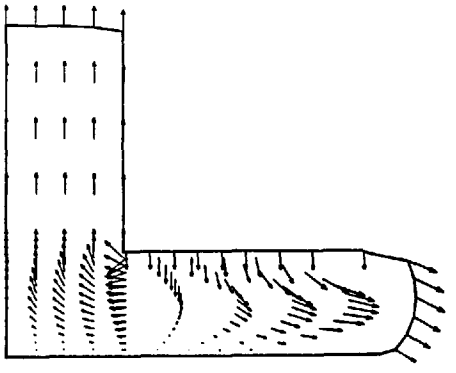

(h) 70 %

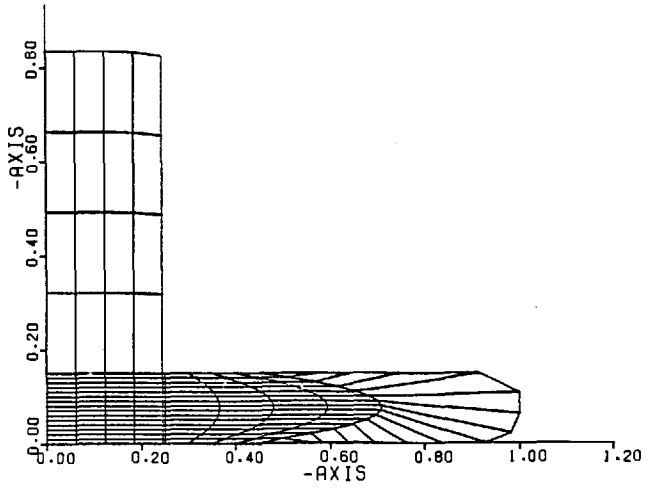

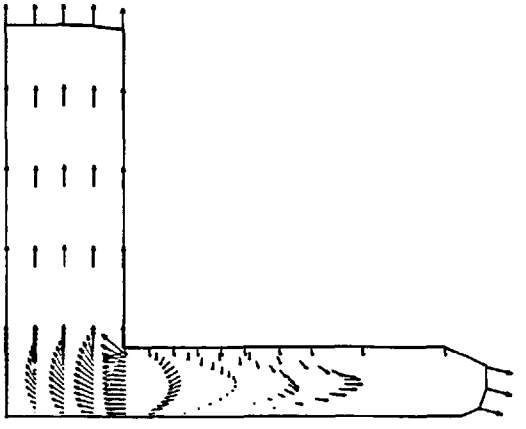

(i) 80 %

Figure 7.17 (Cont.)

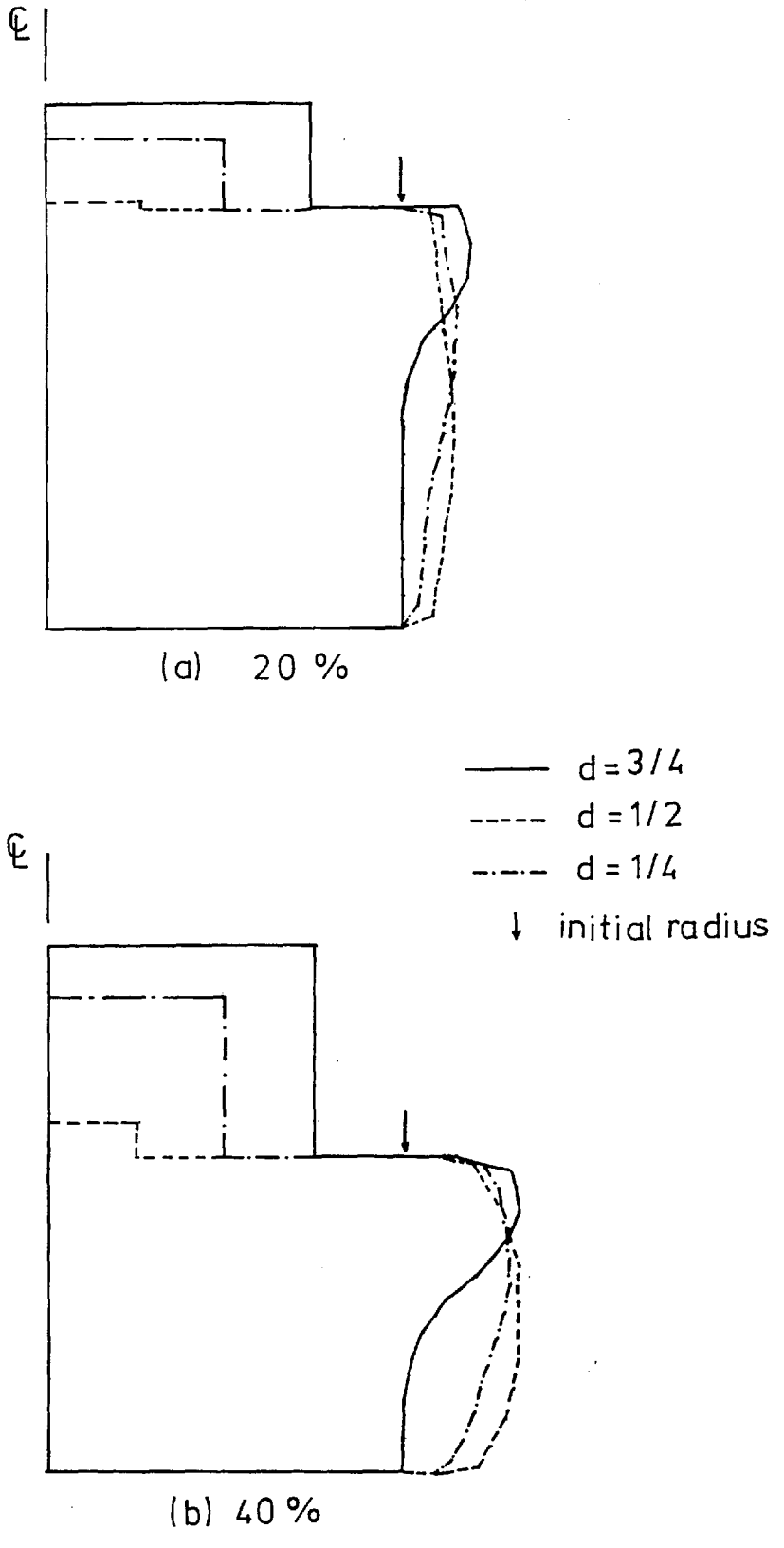

Figure 7.18: Outside surfaces at various reductions.

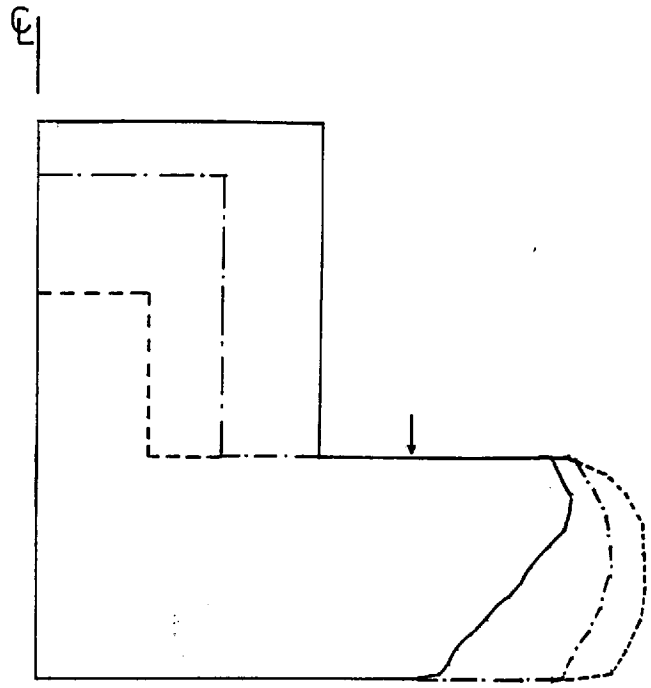

(c) 60 %

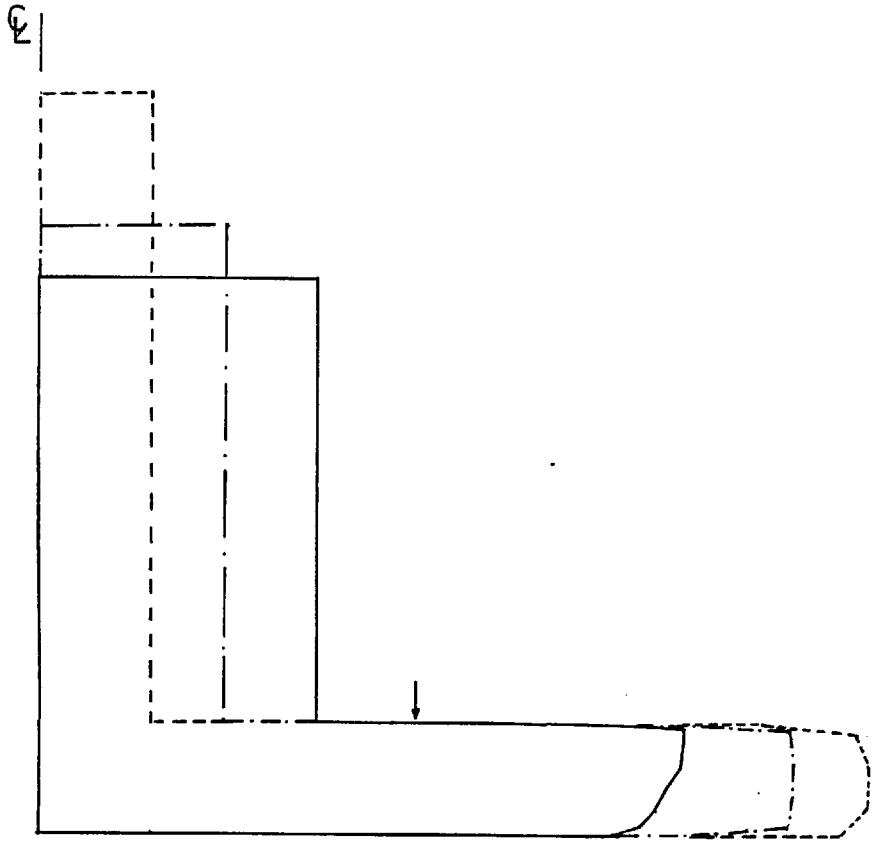

(d) 80 %

Figure 7.18 (Cont)

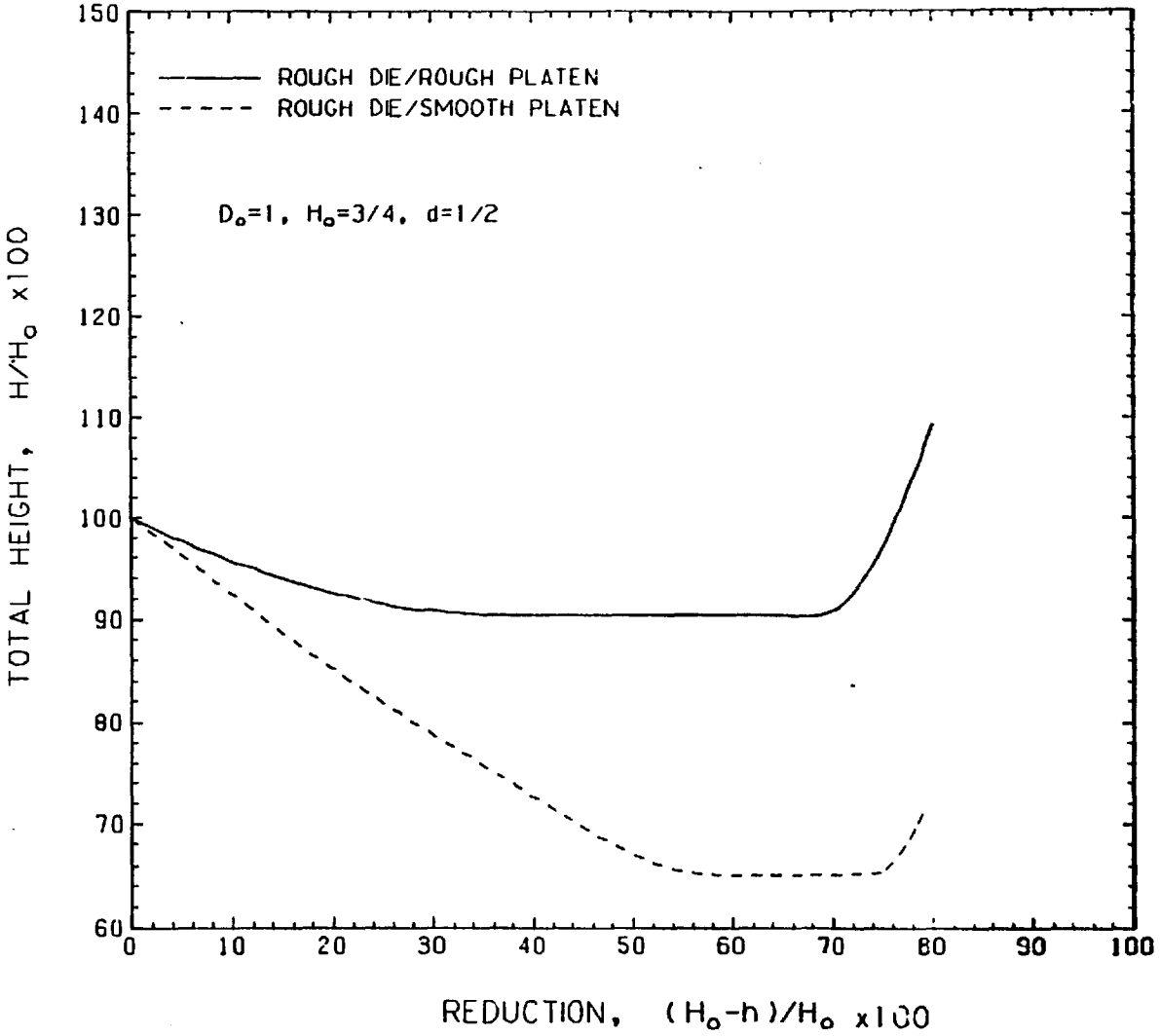

Figure 7.19: Effect of friction on total height of extrusion (Finite Element Analysis)

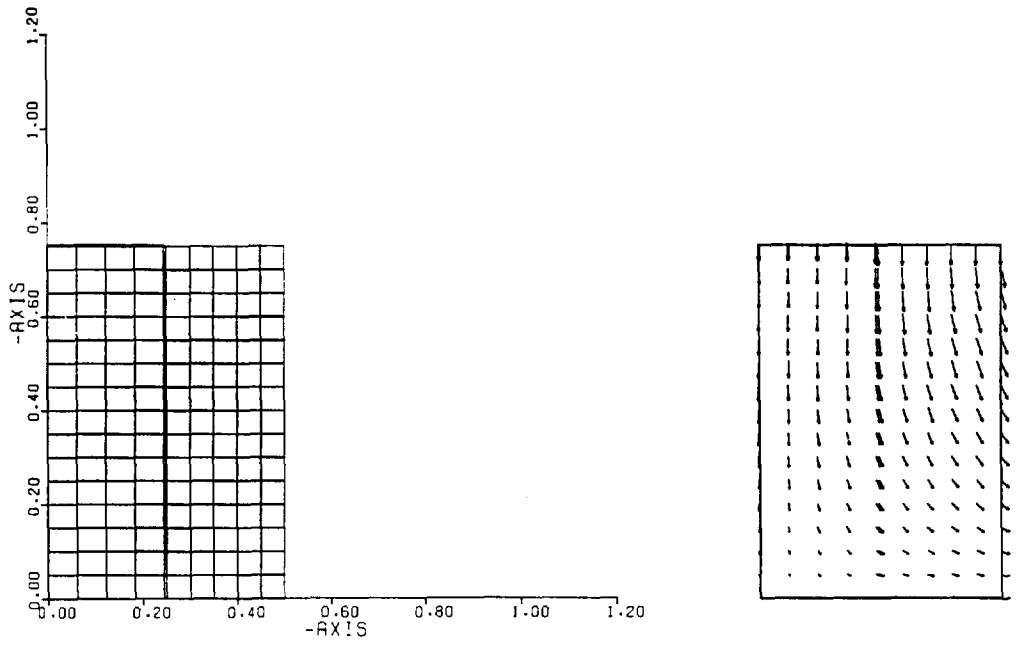

(a) 0 %

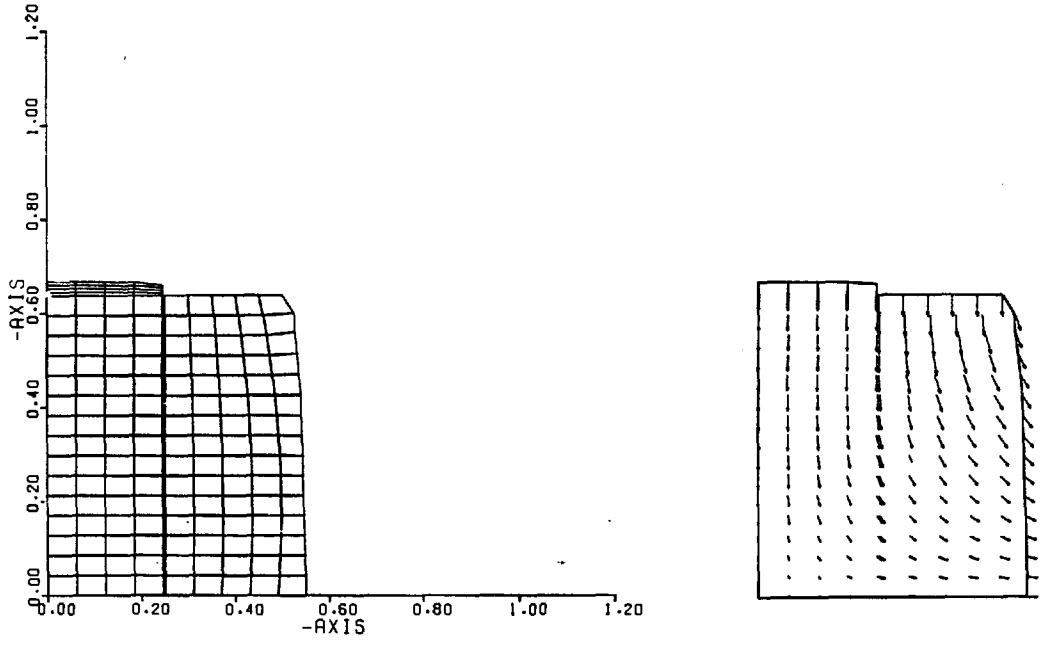

(b) 15 %

Figure 7.20: Extrusion-Forging between rough die and smooth platen.
Deformed geometry and velocity field at various reductions.

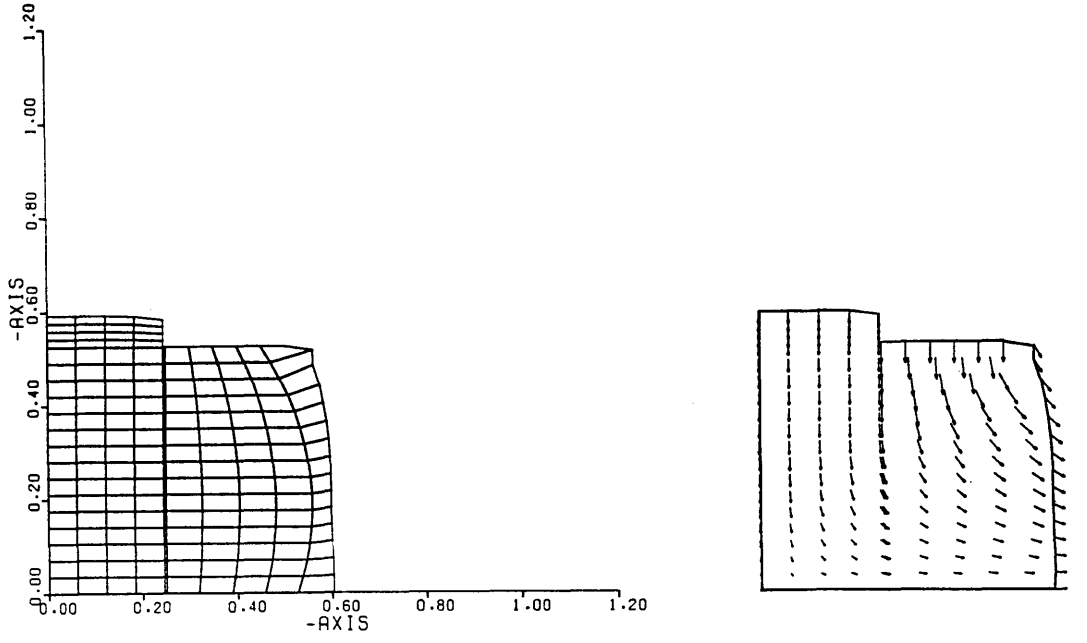

(c) 30 %

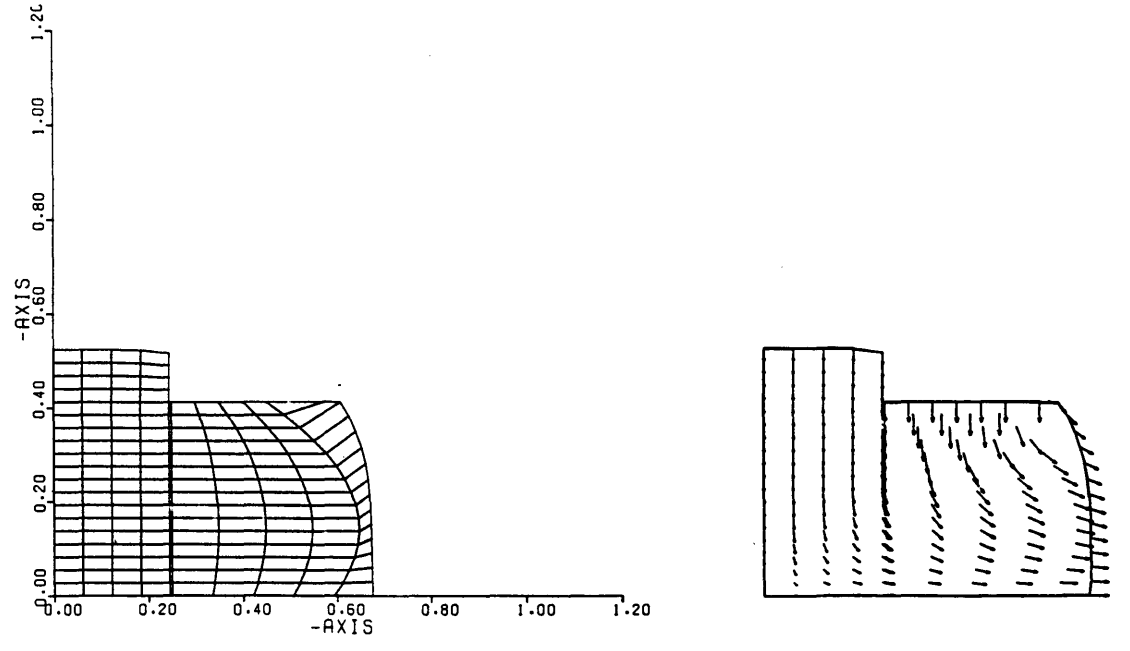

(d) 45 %

Figure 7.20 (Cont.)

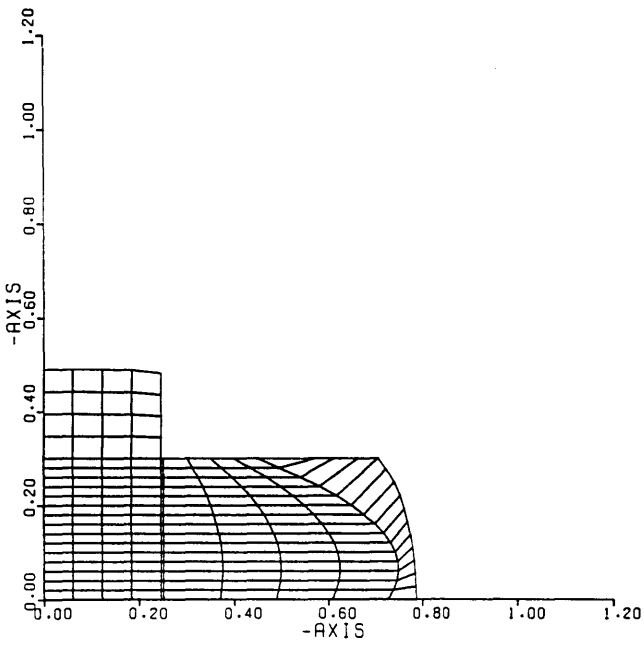

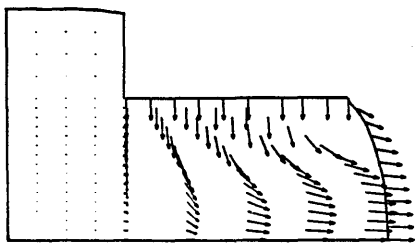

(e) 60 %

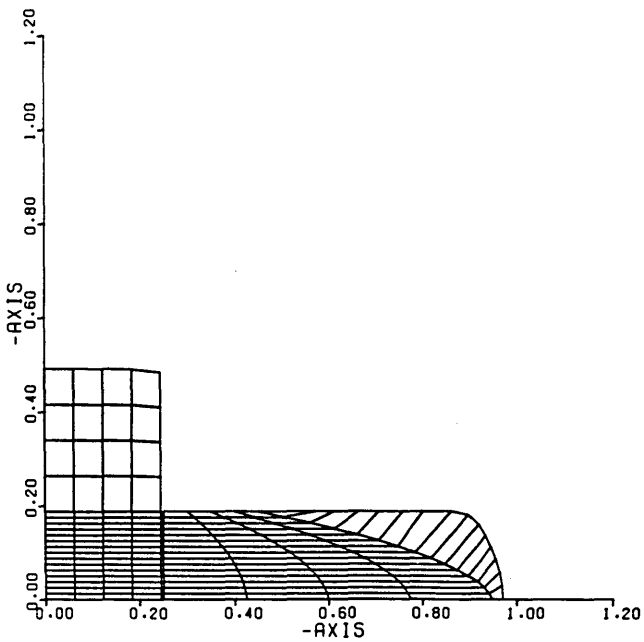

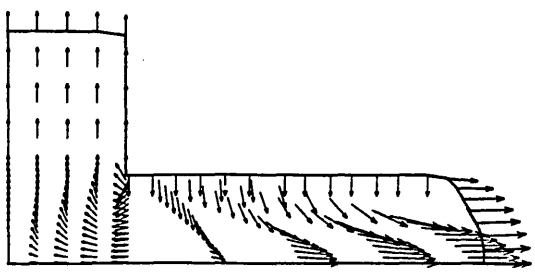

(f) 75 %

Figure 7.20 (Cont.)

CHAPTER 8

CONCLUSIONS AND SUGGESTIONS FOR FURTHER WORK

8.1 General Conclusions

At the beginning of the work, the first objective was to analyze the stress and strain fields developed during the extrusion of bi-metallic rods. It was decided that the most suitable tool for the analysis was the finite element method, in specific, rigid-plastic formulations that have been recently developed.

The formulations were presented in detail and various computer programs were written and implemented using the FORTRAN language. The formulations chosen as the most adequate, namely, the penalty-function and the velocity-pressure approach, were assessed as to their suitability by solving a number of simple extrusion problems in both plane-strain and axisymmetric conditions. The analysis provided information about the detailed mechanics of the process giving velocity, strain and stress fields. The extrusion pressures, which are in general the only information obtained from relatively complex analyses, are only a small part of the information given by the finite element analysis and compare favourably with existing solutions.

The results also indicated that, for the elements used in this work (bi-linear Lagrangian quadrilaterals), there was no appreciable difference between the solutions given by the two formulations. Therefore, it was decided to use the penalty-function formulation for the rest of the work, since it requires less computer resources and is conceptually easier to visualize and implement.

Whilst dealing with simple extrusion problems, techniques to handle the die corners and include work-hardening effects were developed and implemented. The treatment of the die corners, although not strictly formal, was found to be an improvement over previous techniques.

The finite element method was then used to analyze the complex deformation process developed during extrusion of bi-metallic

rods. Various configurations were analyzed and the resulting predictions were compared with experimental evidence obtained using an existing experimental set-up. The experiments were by no means exhaustive, but fulfilled the main objective of providing data to assess the theoretical solutions.

The predicted extrusion pressures were in good agreement with the experimental ones, especially for dies with a relatively small included angle. Comparisons of the interfacial shape also showed good agreement between experimental results and finite element predictions. It can be argued that since the extrusion pressure (energy requirement) and the interfacial shape (kinematical characteristic) are correctly predicted, the stress and strain fields given by the solution represent a fair description of the process.

The formulations were then extended to deal with non-steady processes. They were used to analyze the simple upsetting problem and the incremental extrusion forging process. The main characteristics of the complex deformation patterns were predicted and found to be in good agreement with available experimental data and theoretical analyses.

It would seem, therefore, that the rigid-plastic finite element formulations, especially using the penalty-function approach, can be used with success in the analysis of metal forming problems. However, the solutions presented in this thesis are by no means "exact" and should be judged in the light of the mathematical and physical approximations intrinsic in the model. Indeed, one must be aware of the limitations of the model and avoid falling a prey to the "Computer equals Oracle" syndrome. For example, if it were desired to predict residual stress distributions in products subjected to large deformations (to predict fatigue strength, for example), then it would be necessary to use an elastic-plastic formulation of the finite

element method.

8.2 Suggestions for Further Work

The programs developed in this thesis are readily applicable to the analysis of any steady-state process, e.g. asymmetric extrusion, rolling, tube extrusion, rolling of sandwich plates, etc. (Some preliminary results for the rolling problem are presented in Appendix 1).

A logical extension of the model is the prediction of temperature distributions developed during the deformation processes.

In order to do that, the temperature development dependent on the energy dissipation in the process must be considered and hence the thermal equilibrium equation must be solved. For plane flow, this equation takes the form:-

$$\rho C \left[u \frac{\partial T}{\partial x} + v \frac{\partial T}{\partial y} \right] - K \left[\frac{\partial^2 T}{\partial x^2} + \frac{\partial^2 T}{\partial y^2} \right] - \dot{Q} = 0 \qquad (8.1)$$

where ρ is the density, C is the specific heat, K is the thermal conductivity, T is the temperature, $\dot{Q} = \sigma'_{ij} \dot{\varepsilon}_{ij}$ is the rate of heat generation and u and v are velocity components in the x and y directions respectively.

The numerical solution of this equation is discussed in standard finite element texts[8.1]. The problem can be solved either as an uncoupled flow[8.2] or as a coupled flow[8.3].

Once the temperature distribution is found, it is a simple matter to introduce the dependence of the flow stress of the material on temperature (and strain and strain rate). In order to do this, various relations have been proposed. Inouye[8.4] has used the expression:-

$$\bar{\sigma} = \sigma_0 \, \bar{\varepsilon}^n \, \dot{\bar{\varepsilon}}^m \exp (A/Tk) \tag{8.2}$$

where σ_0, n, m, A and k are constants. Samantha[8.5] has succeeded in establishing an empirical law of the form:-

$$\bar{\sigma} = A + B \ln \bar{\varepsilon} + T (C + D \ln \bar{\varepsilon} + E \ln \dot{\bar{\varepsilon}} + F \ln \bar{\varepsilon} \ln \dot{\bar{\varepsilon}}) \tag{8.3}$$

where A, B, C, D, E and F are constants. Recently, Tay et al[8.6] have assumed the well-known empirical equation:-

$$\bar{\sigma} = \sigma_0 \, \bar{\varepsilon}^n \tag{8.4}$$

and introduced the effects of strain rate and temperature by making σ_0 and n in Equation (8.4) functions of a velocity modified temperature defined as[8.7]:-

$$T_{MOD} = T (1 - m \ln \dot{\bar{\varepsilon}}/\dot{\bar{\varepsilon}}_0) \tag{8.5}$$

Other formulae are discussed in the book by Thomsen et al[8.7].

It should also be possible to include the dependence of the thermal properties on the temperature.

REFERENCES

8.1 ZIENKIEWICZ, O. C.
"The Finite Element Method".
McGraw-Hill, (1977).

8.2 ZIENKIEWICZ, O. C., JAIN, P. C. and OÑATE, E.
"Flow of Solids During Forming and Extrusion : Some Aspects of Numerical Solutions".
Int. J. Solids Struct., 14, pp. 15-38, (1978).

8.3 ZIENKIEWICZ, O. C., OÑATE, E. and HEINRICH, J. C.
"Plastic Flow in Metal Forming, I - Coupled Thermal Behaviour in Extrusion, II - Thin Sheet Forming".
Applications of Numerical Methods to Forming Processes, AMD-Vol. 28, ASME, New York, (1978).

8.4 INOUYE, K.
"Studies on the Hot-Working Strength of Steels".
(In Japanese), Tetsu to Hagano, 41, p. 593, (1955).

8.5 SAMANTA, S. S.
"Effect of Strain-Rate on Compressive Strength of Steel at Elevated Temperatures".
Proc. Conf. on Deformation Under Hot Working Conditions, Univ. Sheffield, pp. 122-130, (1966).

8.6 TAY, A. O., FARMER, L. E. and OXLEY, P. L. B.
"A Numerical Method for Calculating Temperature Distributions in Metal Working Processes".
Int. J. Mech. Sci., Vol. 22, pp. 41-57, (1980).

8.7 McGREGOR, C. W. and FISHER, J. C.
Trans. ASME, J. Appl. Mech., 13, A11, (1946).

8.8 THOMSEN, E. G., YANG, C. T. and KOBAYASHI, S.
"Plastic Deformation in Metal Processing".
Macmillan, New York, (1965).

APPENDIX 1

ANALYSIS OF FLAT ROLLING : PRELIMINARY RESULTS

A1.1 Introduction

The rolling process is of fundamental importance in metal forming and has been the subject of a great deal of attention throughout the years. A number of theories have been proposed for both hot and cold rolling, varying in complexity and accuracy. The problem, in general, is not one of steady-state flow, but if the sheet to be rolled is long enough, it can be approximated as such and, therefore, it can be analyzed using the methods presented in this thesis.

A1.2 Finite Element Analysis of a Hot Rolling Problem

The present investigation was prompted by discrepancies existing in the literature. Zienkiewicz et al have, in a recent publication*, attempted to solve the hot rolling problem. They chose the same configuration used by Alexander** in his definitive account of the various rolling theories and applied the velocity/pressure finite element formulation with the aim of obtaining the torque and roll force encountered during the process. Their results compared poorly with the "exact" solution of Alexander and led them to the conclusion that more research was necessary before the rolling problem could be tackled.

Although further research is clearly needed before any problem, in any field of endeavour, is fully solved, their failure to attain a solution was apparently not due to the unsuitability of the method, but to their unfortunate misinterpretation of the geometric characteristics of the problems as proposed by Alexander.

---

* ZIENKIEWICZ, O. C., JAIN, P. C. and ONATE, E.
"Flow of Solids During Forming and Extrusion : Some Aspects of Numerical Solutions".
University College of Swansea, Civil Engineering Department, Rep. C/R/283/76, (1976).

** ALEXANDER, J. M.
"On the Theory of Rolling".
Proc. Roy. Soc. Ln. A. 326, pp. 535-563, (1972).

Because of symmetry, only half the continuum has to be modelled. This they did, but failed to realize that the values of initial and final thickness given by Alexander were for the whole slab and used them as the dimensions for the half-continuum they modelled. Obviously this is another problem altogether and, inevitably, led to their reported bad agreement with the analytical solution presented by Alexander. Moreover, they failed to realize that the values given by Alexander for the roll force were for unit width (inches) and, consequently, the equivalence between Imperial units and S.I. units they carried out was mistaken (see Fig. A1.1).

Thus, in order to show that the rigid-plastic finite element formulations are adequate for the analysis of rolling, the problem has been re-analyzed and the results are discussed below.

A1.3 Computational Conditions

The problem was analyzed using the penalty function formulation with bi-linear quadrilateral elements. A penalty coefficient (α) of 10^8 and a cut-off factor for the rigid regions ($\gamma = \frac{2}{3}\bar{\sigma}/\dot{\bar{\varepsilon}}$) of 10^9 were selected. The material is assumed to be rigid-perfectly plastic with a yield stress, $Y_o = 8546$ N/cm^2. No slip is assumed to occur between the roll and the metal (sticking friction). The mesh and boundary conditions used are shown in Fig. A1.2.

A1.4 Results and Discussion

The torque and roll force are readily obtained from the finite element analysis and are shown in Table A1.1. It can be seen that they compare well with the analytical and numerical solution presented by Alexander (op. cit.).

Obviously, it is not possible to produce results that are in complete agreement, since the two solutions are vastly different in

their assumptions.

TABLE A1.1

	Alexander (op. cit.)	FEM
Torque	24311 N.cm/cm	24291 N.cm/cm
Roll Force	43078 N/cm	38989 N/cm

The roll pressure is readily calculated from the numerical analysis, see Fig. A1.3. It is seen that the well-known friction-hill is obtained and it suggests that the neutral surface is somewhere just after the middle of the contact arc.

The velocity distribution and the grid distortion obtained from the finite element analysis are presented in Fig. A1.4. It can be seen that the surface expands practically to its final dimension within a relatively small region around the plane of entry. In this region the inside parts of the slab are still undeformed. The grid distortion also suggests that as the slab moves along the arc of contact the surface suffers little deformation while the plastic region seems to extend more and more deeply into the slab. This is in qualitative agreement with experimental evidence* and to the writer's knowledge, it has never been predicted theoretically.

---

* OROWAN, E.
"The Calculation of Roll Pressure in Hot and Cold Flat Rolling".
Proc. Instn. Mech. Engrs., 150, p. 152, (1943).

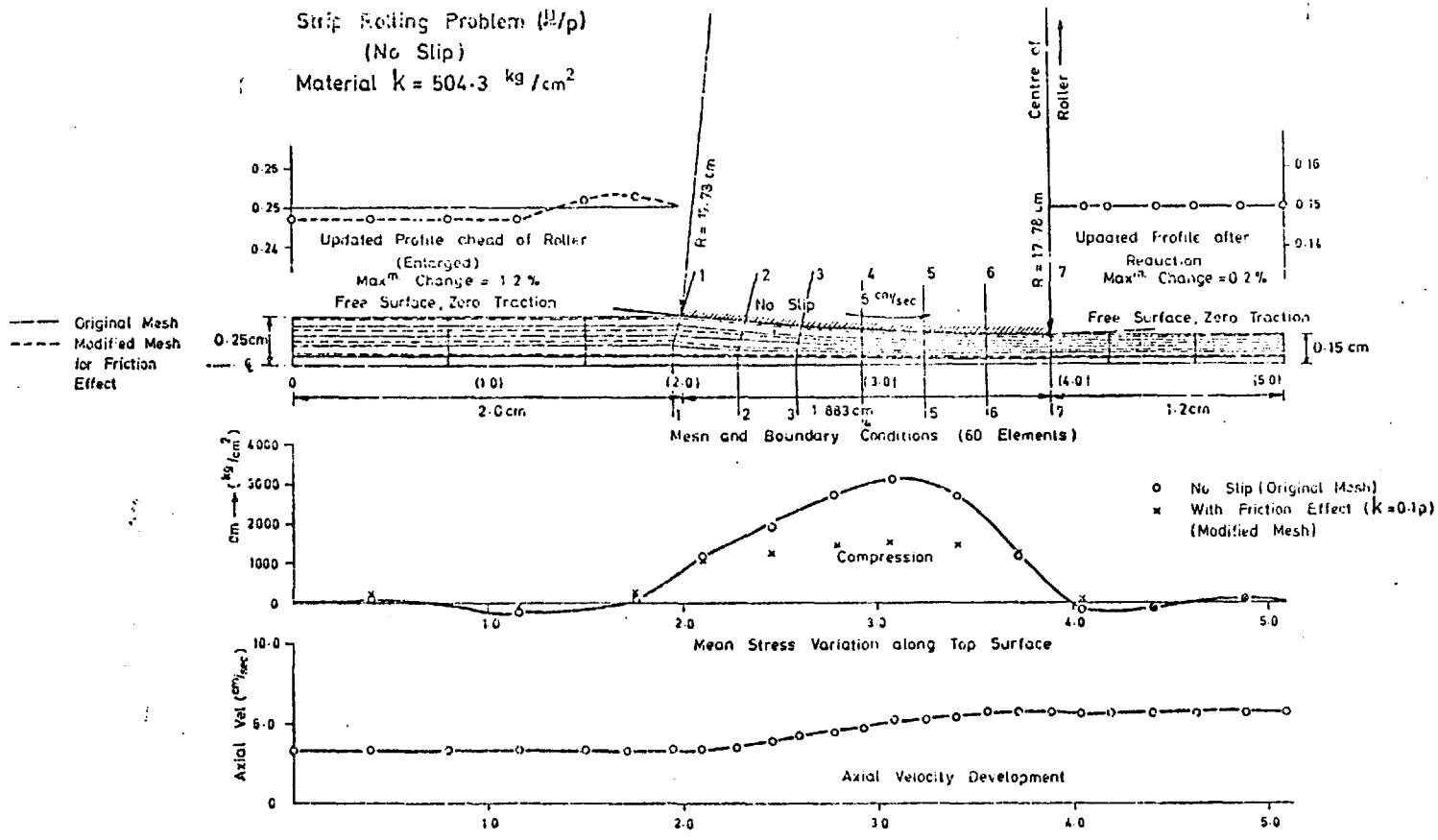

	No Slip, Constant k (μ/p) 21 El.	60 El.	With Friction Effect	(Constant k) Values given by Alexander	(Constant Mean k) Values given by Ford & Alexander
Rolling Force	4841·3 kg	4286·6 kg	2809·3 kg	11159·4 kg	3213·0 Kg
Torque	4644·2 kg cm/cm	4013·9 kg cm/cm	2520·2 kg cm/cm	6309 kg cm/cm	4095·0 Kg cm/cm

Figure A1·1 After Zienkiewicz Op.cit.

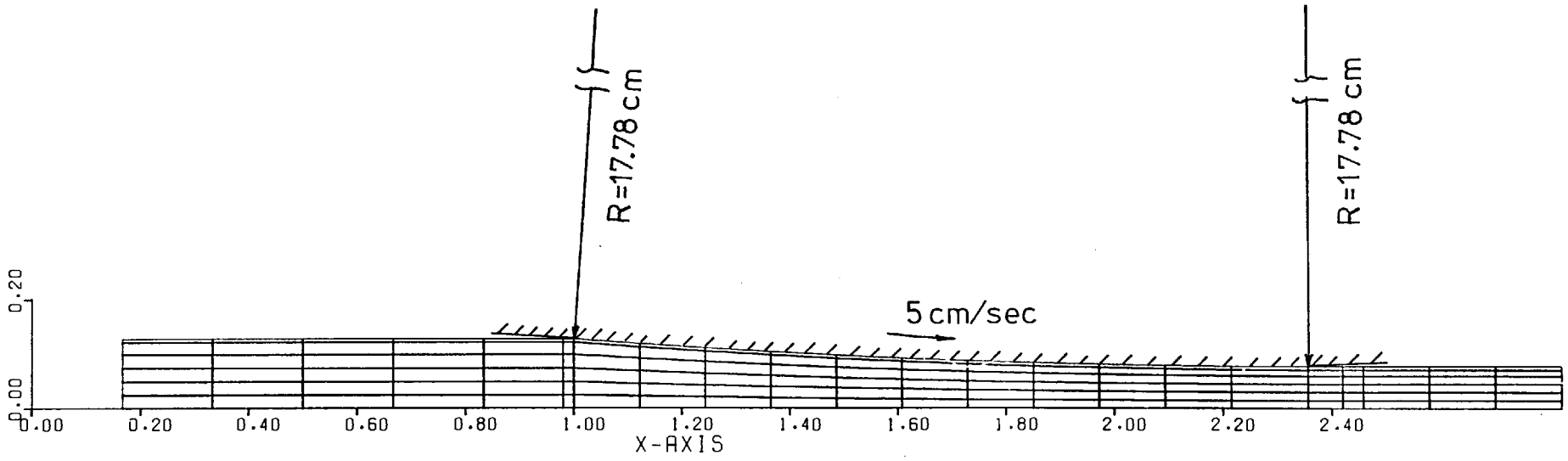

SYMMETRIC FLAT HOT ROLLING (ALEXANDER1972)
FINITE ELEMENT IDEALIZATION. 161 NODES AND 132 ELEMENTS.

Figure A1.2

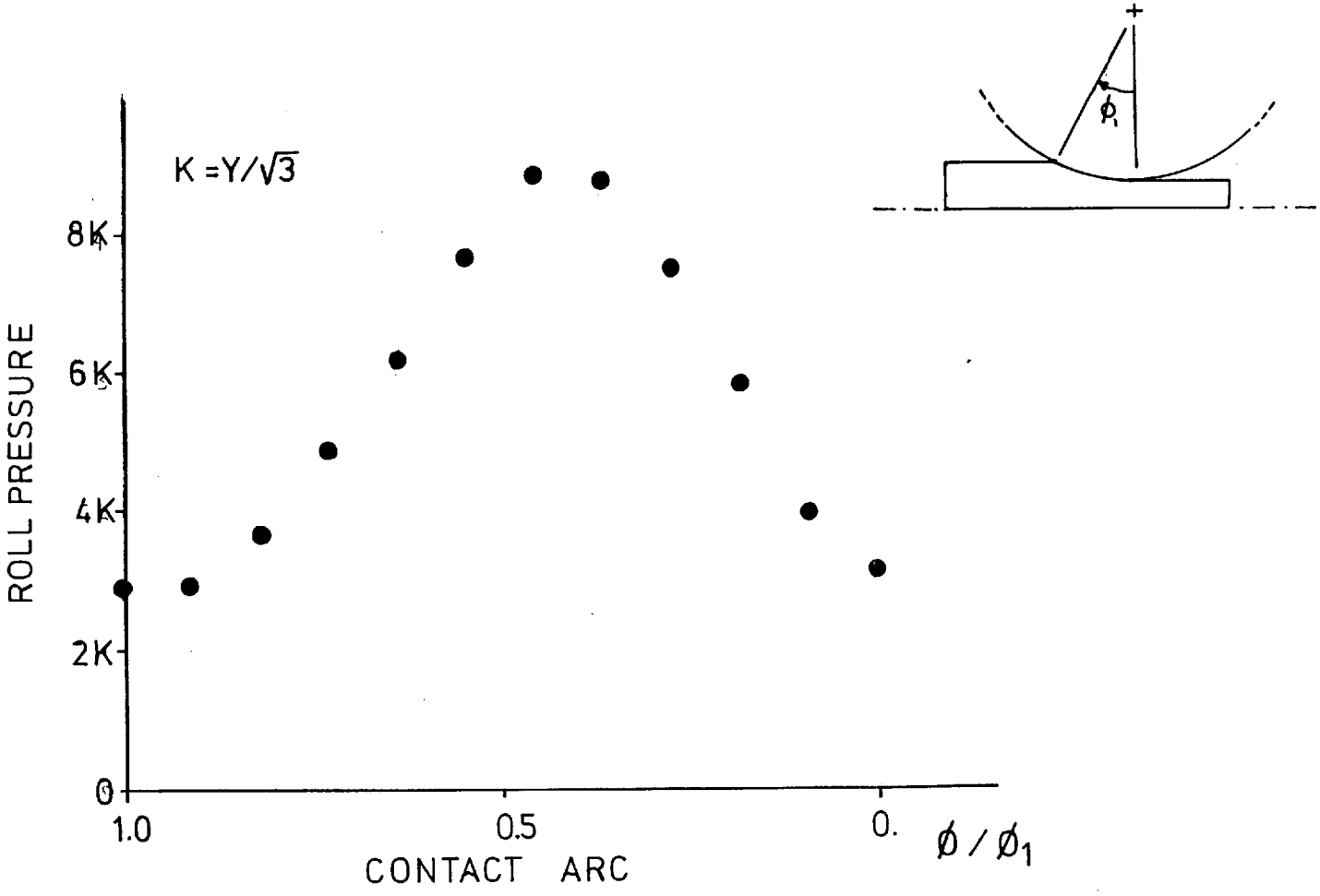

Figure A1.3 Roll pressure distribution.

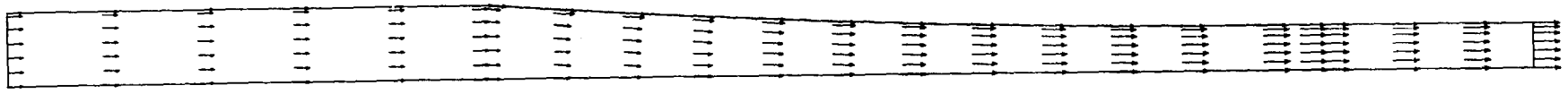

(a)

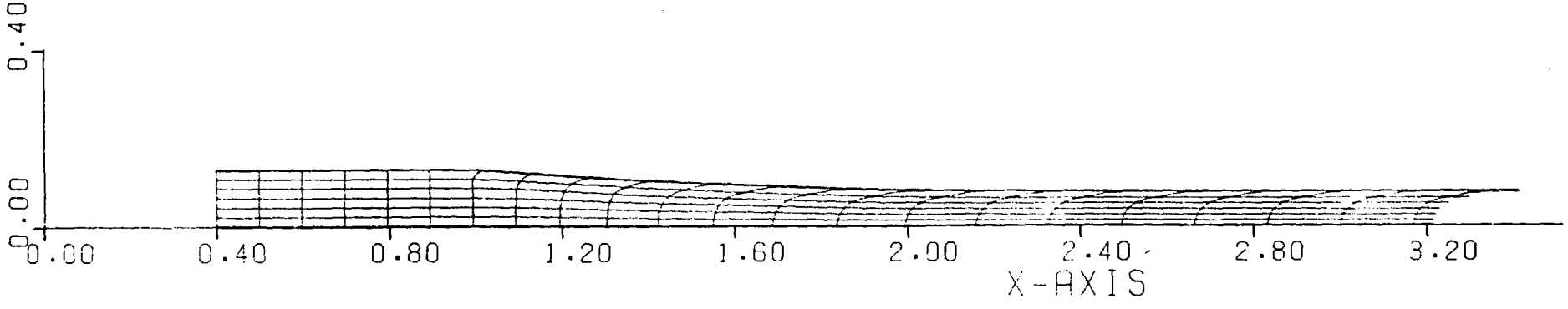

(b)

Figure A1.4 (a) Velocity distribution and (b) Grid distortion for the flat rolling problem.

APPENDIX 2

COMPUTER PROGRAMS

A2.1 Introduction

The finite element formulations presented in this thesis are readily programmed for digital computers and in fact they would be of little use if computers were not available to solve the large number of equations that result from the discretization process and to handle the large output that the procedure generates.

A number of programs have been written during the course of this work for both steady and non-steady state problems. The final version of these programs are presented and briefly described here.

Programs are written in standard FORTRAN IV and, with the exception of the plotting routines, are machine independent. Single precision was used throughout; this was found to give enough accuracy when using the CDC 6500 computer at the Imperial College Computer Centre (ICCC).

The layout and the various parts of these programs are described in what follows.

A2.2 General Description of the Programs

The programs are divided into a number of subroutines and a master program which controls the flow of operation (see Figs. A2.1 and A2.2). The programs use bi-linear quadrilateral elements with numerical integration, however, other kinds of elements could be easily implemented.

The programs are built around a band solver which, although not the most sophisticated, is the most simple to implement. The writer believes that the argument for simplicity is very strong and it should be the over-riding aim when no economical pressures are present.

Thus, the programs are by no means the most efficient that

could have been written and they could be greatly improved. However, this is beyond the scope of this work and will be left to potential users.

The listing of the programs presented at the end of this appendix are compiled copies and, therefore, free of programming errors. Comment cards have been used generously and it is hoped that they make the programs self-explanatory to anyone fluent in the Fortran language.

(a) Program 1

This program is designed to solve steady-state problems using the penalty function formulation. Both plane strain and axisymmetric problems can be treated as well as hardening and non-hardening materials. The program has facilities for plotting the flow lines and the grid distortion.

(b) Program 2

This program is also aimed at solving steady-state problems and is based on the velocity/pressure formulation. Since this program was only used in the initial stages of the work it was not developed to the extent Program 1 was and it can only deal with non-hardening materials. However, it can easily be extended to deal with hardening materials by the inclusion of the appropriate subroutines.

(c) Program 3

This program is designed to solve non-steady state problems in a quasistatic manner using the penalty function formulation. Both plane strain and axisymmetric problems can be treated as well as hardening and non-hardening materials.

As discussed in Chapter 7, some modification has to be made

to the mesh at intermediate stages, but since these modification procedures are problem dependent, only the simplest one is presented here.

The program has facilities for plotting the deformed geometry and the velocity fields at different stages of the calculation.

All programs have facilities for punched output which is used for contouring and plotting with existing computer packages.

A2.3 Program Terminology

Here we present the meaning of the variables most common to all the programs:-

ALPHA	Penalty coefficient
IPLAX	00 Plane Strain
	01 Axisymmetric
NP	Number of nodal points
NE	Number of elements
NB	Number of restrained boundary nodes
NPC	Number of loaded nodes
NMAT	Number of element material types
NEQ	Number of equations
NBAND	Bandwidth
NBF	Number of nodes where reactions are calculated
NITER	Iteration counter
TITLE(8)	8 word title array
CORD(NP,2)	Nodal point coordinate array
NOP(NE,4)	Element correction array
IMAT(NE)	Element material type array
NBC(NB)	Array of restrained nodes

NREST(NB)	Boundary condition type 01 Restricted in the x (r) direction 02 Restricted in the y (z) direction 11 Restricted on both directions 03 Skewed boundary
XPRE(NB)	x (r) velocity imposed at nodal point
YPRE(NB)	y (z) velocity imposed at nodal point; angle of the skew when NREST = 03
NQ(NPC)	Array of loaded nodes
R(NPC,2)	Array of nodal loads
NF(NBF)	Array of nodes where reactions are calculated
SK(NEQ,NBAND)	Master stiffness matrix
R1(NEQ)	Load vector. After elimination the space is used for the solution vector.
EST(2*NBF,2*NBAND)	Array containing the stiffness equations for reaction calculation
EPS(NE,6)	Strain rate array
STR(NE,5)	Stress array
TEPS(NE)	Effective strain vector
VEL(2,NP)	Velocity array

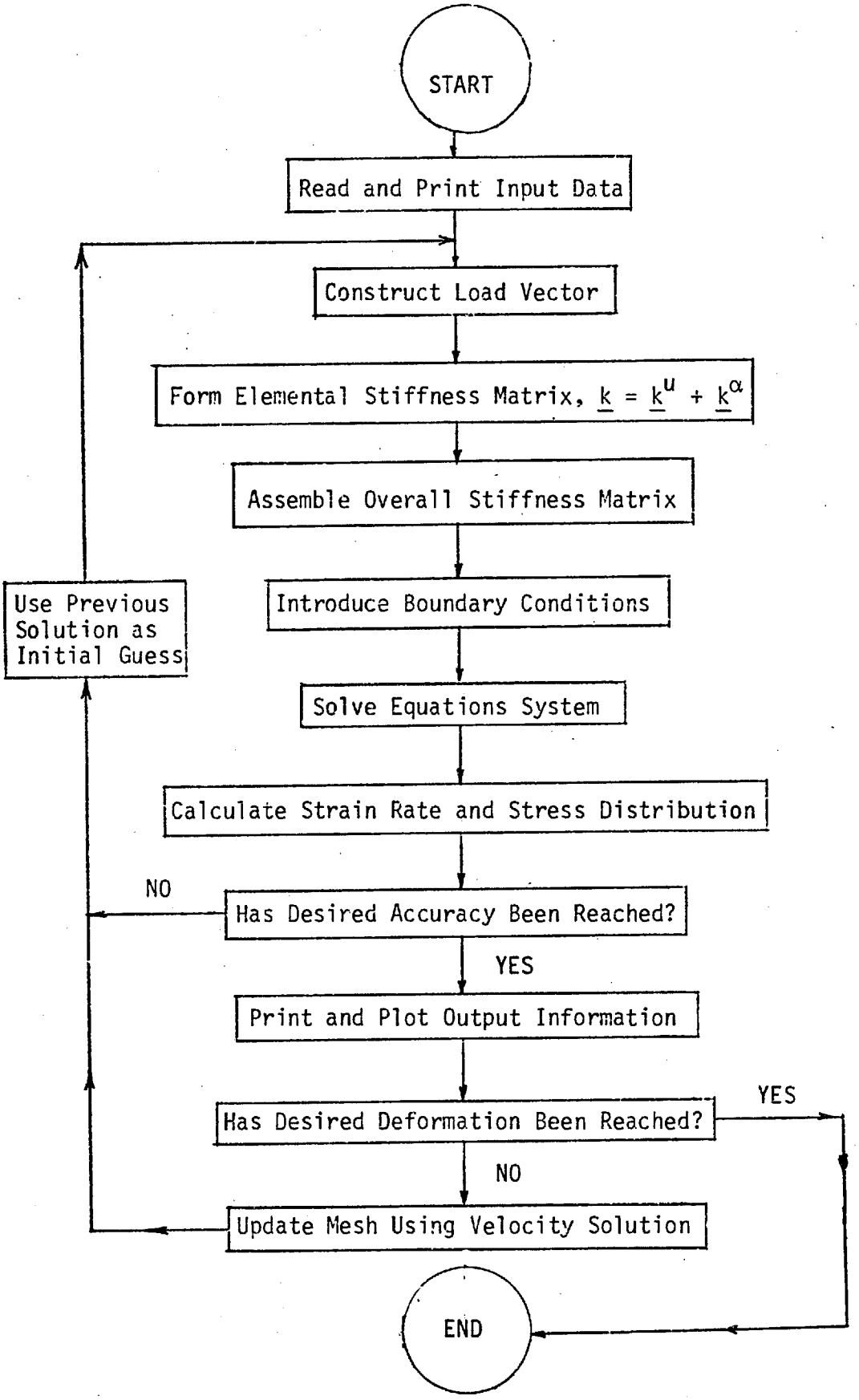

Fig. A2.2 Flow chart for the finite element solution of non-steady state problems (penalty function)

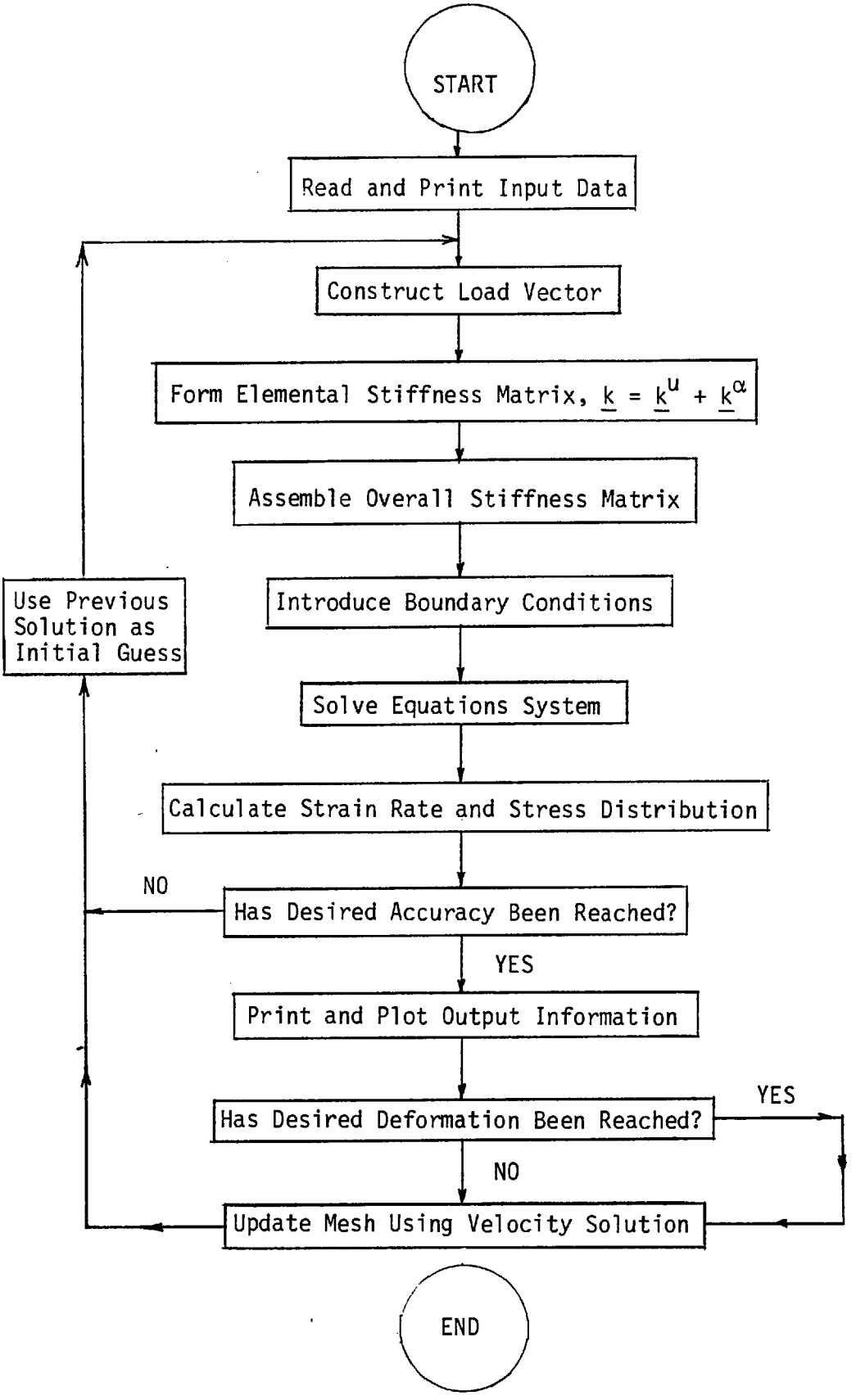

Fig. A2.2 Flow chart for the finite element solution of non-steady state problems (penalty function)

PROGRAM 1

SOLUTION OF STEADY-STATE PROBLEMS (PENALTY FUNCTION)

```
      PROGRAM MAIN (INPUT,OUTPUT,TAPE6=OUTPUT,TAPE5,TAPE4,TAPE1,TAPE62)

C ***************************************************************************
C * THIS PROGRAM HAS BEEN DESIGNED TO SOLVE STEADY-STATE PROBLEMS IN        *
C * METAL WORKING USING THE FINITE ELEMENT METHOD.                          *
C * THE MATERIAL IS ASSUMED TO BE RIGID-PLASTIC AND INCOMPRESSIBLE,THIS     *
C * LATTER CONSTRAINT BEING INTRODUCED BY MEANS OF A PENALTY FUNCTION.      *
C * THE PROGRAM USES BILINEAR ISOPARAMETRIC ELEMENTS WITH REDUCED/SE-       *
C * LECTIVE INTEGRATION.                                                    *
C ***************************************************************************
C       * WRITTEN BY LUIS A. PACHECO, ING. MEC., M.SC.(MANC)  *
C             *IMPERIAL COLLEGE UNIVERSITY OF LONDON*
C                 *FINAL VERSION SPRING 1979*
C       *********************************************************
C
C
      COMMON /BLK1/ NP,NE,NB,NPC,NMAT,NEQ,NBAND,NITER,TITLE(8),NBF,NEDGE
      COMMON /BLK2/ CORD(297,2),NOP(260,4),IMAT(260),ELOAD(260,8)
      COMMON /A/ VRIG,IPLAX,ALPHA,IHARD
      COMMON /B/ NTIMES,NDI,NDJ,NMAX,YSTART,YDIE,YEXIT,YMAX,RENTER,REXIT
     1,RCORE,STEP,NLIN,VSCAL
C
C.....READ NECESSARY INPUT INFORMATION
C
      ALPHA = 10.E+07
      CALL PRELIM
C
C.....DETERMINE BANDWIDTH AND NUMBER OF EQUATIONS
C
      NEQ = NP*2
      J = 0
      DO 20 N = 1,NE
      DO 20 I = 1,4
      DO 10 L = 1,4
      KK = IABS(NOP(N,I)-NOP(N,L))
      IF (KK-J.LE.0) GO TO 10
      J = KK
   10 CONTINUE
   20 CONTINUE
      NBAND = 2*(J+1)
      VRIG = 1.E+09
C
C.....READ THE EXTERNAL LOADS IF ANY.FORM VECTOR LOAD
C
      NITER = 0
   30 CALL LOAD
C.....FORM AND SOLVE THE EQUATION SYSTEM
C
      CALL FORMK
      CALL SOLVE
C
C.....CHECK THE CONVERGENCE.
C
      CALL CONVER (NCONV)
      CALL STRAIN
      IF (NLIN.EQ.1) NCONV = 1
      IF (NITER.EQ.20) NCONV = 1
C.....FIND THE EFFECTIVE STRAIN DISTRIBUTION IF REQUIRED.
C.....FIND THE FLOW LINES AND GRID DISTORTION
      IF (IHARD.EQ.1.AND.NCONV.EQ.0) CALL FLOW (0)
      IF (NCONV.EQ.1) CALL FLOW (1)

C.....CALCULATE BOUNDARY FORCES IF REQUIRED.
      CALL CFORC

C.....MODIFY MESH ACCORDING TO VELOCITY SLOPES.
      IF (NCONV.EQ.0) CALL MODMES
      IF (NCONV.EQ.1) GO TO 40
      NITER = NITER+1
      GO TO 30
C
C.....WRITE RESULTS
C
   40 CALL STRAIN
      CALL DOUT
      STOP
      END

      SUBROUTINE PRELIM
C
C.....THIS SUBROUTINE READ AND PRINT THE NECESSARY
C.....INPUT INFORMATION
C
      COMMON /BLK1/ NP,NE,NB,NPC,NMAT,NEQ,NBAND,NITER,TITLE(8),NBF,NEDGE
      COMMON /BLK2/ CORD(297,2),NOP(260,4),IMAT(260),ELOAD(260,8)
      COMMON /BLK3/ YIELD(4),NBC(65),NREST(65),NQ(40),R(40,2),XPRE(65),Y
     1PRE(65),NF(25)
      COMMON /BLK4/ STR(260,5),EPS(260,6),VEL(2,297),TEPS(260)
      COMMON /A/ VRIG,IPLAX,ALPHA,IHARD
      COMMON /B/ NTIMES,NDI,NDJ,NMAX,YSTART,YDIE,YEXIT,YMAX,RENTER,REXIT
     1,RCORE,STEP,NLIN,VSCAL
C
C.....READ TITLE AND CONTROL VARIABLES
C
      READ (5,1090) TITLE
      WRITE (6,1170) TITLE
      READ (5,1040) NP,NE,NB,NPC,NEDGE,NBF,NMAT,I1,IPLAX
      IF (IPLAX.EQ.0) WRITE (6,1110)
      IF (IPLAX.EQ.1) WRITE (6,1130)
      WRITE (6,1120) NP,NE,NB,NPC,NEDGE,NBF,NMAT,I1
      READ (5,1000) NLIN,IHARD,NTIMES,NDI,NDJ,NMAX
      WRITE (6,1010) NLIN,IHARD,NTIMES,NDI,NDJ,NMAX
      READ (5,1020) YSTART,YDIE,YEXIT,YMAX,RENTER,REXIT,RCORE,STEP,VSCAL
      WRITE (6,1030) YSTART,YDIE,YEXIT,YMAX,RENTER,REXIT,RCORE,STEP,VSCA
     1L
      WRITE (6,1150) ALPHA
C
C.....READ MATERIAL INFORMATION
C
      READ (5,1140) (N,YIELD(N),L=1,NMAT)
      WRITE (6,1240)
      WRITE (6,1160)
      WRITE (6,1100) (N,YIELD(N),N=1,NMAT)
C
C.....READ NODAL INFORMATION.
C
      READ (5,1050) (N,(CORD(N,M),M=1,2),L=1,NP)
C
C.....READ ELEMENTS INFORMATION.
C
      READ (5,1060) (N,(NOP(N,M),M=1,4),IMAT(N),L=1,NE)
C
C.....READ BOUNDARY CONDITIONS
C
      READ (5,1070) (NBC(I),NREST(I),XPRE(I),YPRE(I),I=1,NB)
      IF (NBF.EQ.0) GO TO 10
      READ (5,1080) (NF(I),I=1,NBF)
C
C.....PRINT INPUT INFORMATION IF REQUIRED.
```

```
C
   10 IF (I1.EQ.0) GO TO 20
      IF (IPLAX.EQ.0) WRITE (6,1190)
      IF (IPLAX.EQ.1) WRITE (6,1230)
      WRITE (6,1050) (N,(CORD(N,M),M=1,2),N=1,NP)
      WRITE (6,1200)
      WRITE (6,1060) (N,(NOP(N,M),M=1,4),IMAT(N),N=1,NE)
   20 IF (NBF.EQ.0) GO TO 30
      WRITE (6,1220)
      WRITE (6,1180) (NF(I),I=1,NBF)
   30 WRITE (6,1210)
      WRITE (6,1070) (NBC(I),NREST(I),XPRE(I),YPRE(I),I=1,NB)
      RETURN
C
C
 1000 FORMAT (6I5)
 1010 FORMAT (1HO,"NLIN=",I1,/,1H ,"IHARD=",I1,/,1H ,"NTIMES=",I2,/,1H ,
     1"NDI=",I2,/,1H ,"NDJ=",I2,/,1H ,"NMAX=",I3)
 1020 FORMAT (9F8.3)
 1030 FORMAT (1HO,"YSTART=",E12.5,/,1H ,"YDIE=",E12.5,/,1H ,"YEXIT=",E12
     1.5,/,1H ,"YMAX=",E12.5,/,1H ,"RENTER=",E12.5,/,1H ,"REXIT=",E12.5,
     2/,1H ,"RCORE=",E12.5,/,1H ,"STEP=",E12.5,/,1H ,"VSCAL=",E12.5)
 1040 FORMAT (9I5)
 1050 FORMAT (I10,2F10.4)
 1060 FORMAT (6I5)
 1070 FORMAT (2I10,2F10.3)
 1080 FORMAT (16I5)
 1090 FORMAT (8A10)
 1100 FORMAT (1H ,I5,F15.4)
 1110 FORMAT (1HO,"PLANE STRAIN PROBLEM",/,1H ,20(1H*))
 1120 FORMAT (1HO,"NUMBER OF NODES=",I3,/,1H ,"NUMBER OF ELEMENTS=",I3,/
     1,1H ,"NUMBER OF NODES WITH BOUNDARY CONDITIONS=",I3,/,1H ,"NUMBER
     2OF LOADED NODES=",I3,/,1H ,"NUMBER OF LOADED EDGES=",I3,"NUMBER OF
     3 NODES WHERE REACTIONS ARE CALCULATED=",I3,/,1H ,"NUMBER OF MATERI
     4ALS=",I3,/,1H ,"PRINT CONTROL VARIABLE(I1)=",I2)
 1130 FORMAT (1HO,"AXISYMMETRIC PROBLEM",/,1H ,20(1H*))
 1140 FORMAT (I5,F15.4)
 1150 FORMAT (1HO,"PENALTY COEFFICIENT=",E12.5)
 1160 FORMAT (1H ,2X,"MAT",3X,"YIELD POINT")
 1170 FORMAT (1H1,8A10)
 1180 FORMAT (1H ,20I5)
 1190 FORMAT (1HO,6X,"NODES",3X,"COORD X",3X,"COORD Y")
 1200 FORMAT (1HO,"ELEMENT",4X,"NODES",9X,"IMAT")
 1210 FORMAT (1HO,"BOUNDARY CONDITIONS",/,1H ,5X,"NODES",4X,"CONDITION",
     13X,"XPRE",5X,"YPRE")
 1220 FORMAT (1HO,"THE NODAL POINTS AT WHICH FORCE CALCULATIONS ARE DESI
     1RED")
 1230 FORMAT (1HO,6X,"NODES",3X,"COORD-R",3X,"COORD-Z")
 1240 FORMAT (1HO,"MATERIAL PROPERTIES")
      END

      SUBROUTINE LOAD
C
C.....THIS SUBROUTINE FORMS THE VECTOR LOAD R1.
C
      COMMON /BLK1/ NP,NE,NB,NPC,NMAT,NEQ,NBAND,NITER,TITLE(8),NBF,NEDGE
      COMMON /BLK2/ CORD(297,2),NOP(260,4),IMAT(260),ELOAD(260,8)
      COMMON /BLK3/ YIELD(4),NBC(65),NREST(65),NQ(40),R(40,2),XPRE(65),Y
     1PRE(65),NF(25)
      COMMON SK(594,30),R1(594),EST(50,60),FR(25),FZ(25),FPUR(50)
      COMMON /A/ VRIG,IPLAX,ALPHA,IHARD
C
C.....ZERO LOAD ARRAY.
C
      DO 10 J = 1,NEQ

   10 R1(J) = 0.0
      IF (NPC.EQ.0.AND.NITER.GT.0.AND.NEDGE.EQ.0) RETURN
      IF (NITER.GT.0) GO TO 50
      IF (NPC.EQ.0.AND.NEDGE.EQ.0) GO TO 110
      IF (NPC.EQ.0) GO TO 30
      IF (IPLAX.EQ.0) WRITE (6,1020)
      IF (IPLAX.EQ.1) WRITE (6,1010)
      DO 20 N = 1,NPC
      READ (5,1030) NQ(N),(R(N,K),K=1,2)
   20 CONTINUE
      WRITE (6,1030) (NQ(N),(R(N,K),K=1,2),N=1,NPC)
   30 IF (NEDGE.EQ.0) GO TO 50
C.....DISTRIBUTED LOADING.
      DO 40 N = 1,NE
      DO 40 J = 1,8
   40 ELOAD(N,J) = 0.0
      CALL SURF
      WRITE (6,1000) (N,(ELOAD(N,J),J=1,8),N=1,NE)
   50 IF (NPC.EQ.0) GO TO 70
      DO 60 N = 1,NPC
      DO 60 K = 1,2
      IC = (NQ(N)-1)*2+K
   60 R1(IC) = R(N,K)+R1(IC)
   70 IF (NEDGE.EQ.0) GO TO 120
      NNE = 4
      DO 100 N = 1,NE
      DO 90 J = 1,NNE
      NLOCAL = NOP(N,J)
      DO 80 MM = 1,2
      IC = (NLOCAL-1)*2+MM
      JC = (J-1)*2+MM
   80 R1(IC) = R1(IC)+ELOAD(N,JC)
   90 CONTINUE
  100 CONTINUE
      GO TO 120
  110 WRITE (6,1040)
  120 RETURN
C
C
 1000 FORMAT (1H ,I5,2X,8E12.5)
 1010 FORMAT (1HO,"PRESCRIBED EXTERNAL LOADS",///,"NODES",3X,"FORCE-R",3
     1X,"FORCE-Z")
 1020 FORMAT (1HO,"PRESCRIBED EXTERNAL LOADS",///,"NODES",3X,"FORCE-X",3
     1X,"FORCE-Y")
 1030 FORMAT (I10,2F10.3)
 1040 FORMAT (1HO,"NO EXTERNAL LOADS PRESCRIBED")
      END

      SUBROUTINE SURF
C.....THIS SUBROUTINE CALCULATES THE NODAL LOADS DUE TO
C.....SURFACE LOADING.
      COMMON /BLK1/ NP,NE,NB,NPC,NMAT,NEQ,NBAND,NITER,TITLE(8),NBF,NEDGE
      COMMON /BLK2/ CORD(297,2),NOP(260,4),IMAT(260),ELOAD(260,8)
      COMMON /A/ VRIG,IPLAX,ALPHA,IHARD
      DIMENSION NOPRS(3), PRESS(3,2), ELCOD(2,3), SHP(3,9), PGASH(2), DG
     1ASH(2), XL(1), YL(1), SG(9), TG(9), WG(9)
      NODEG = 2
      NODFN = 2
      XL(1) = 1.
      YL(1) = 1.
      WRITE (6,1000)
C.....LOOP OVER EACH LOADED EDGE.
```

```
      DO 80 IEDGE = 1,NEDGE
C.....READ DATA LOCATING THE EDGE AND APPLIED LOAD.
      READ (5,1010) NEASS,(NOPRS(IODEG),IODEG=1,NODEG)
      WRITE (6,1020) NEASS,(NOPRS(IODEG),IODEG=1,NODEG)
      READ (5,1030) ((PRESS(IODEG,IDOFN),IODEG=1,NODEG),IDOFN=1,2)
      WRITE (6,1030) ((PRESS(IODEG,IDOFN),IODEG=1,NODEG),IDOFN=1,2)
C.....COORDINATES OF THE NODES OF THE ELEMENT EDGE.
      DO 10 IODEG = 1,NODEG
      LNODE = NOPRS(IODEG)
      DO 10 IDIME = 1,2
   10 ELCOD(IDIME,IODEG) = CORD(LNODE,IDIME)
C.....ENTER LOOP FOR NUMERICAL INTEGRATION.
      NGAUSS = 2
      CALL PGAUSS (NGAUSS,LINT,SG,TG,WG)
      DO 70 IGAUSS = 1,NGAUSS
C.....EVALUATE SHAPE FUNCTION AT SAMPLING POINTS.
      CALL SHAPE (SG(IGAUSS),-1.,XL,YL,SHP,DETJAC,2)
      RBAR = 0.0
      DO 20 KI = 1,NODEG
   20 RBAR = RBAR+SHP(3,KI)*ELCOD(1,KI)
      IF (IPLAX.EQ.0) RBAR = 1.0
C.....CALCULATE COMPONENTS OF THE EQUIVALENT NODAL LOADS
      DO 30 IDOFN = 1,2
      PGASH(IDOFN) = 0.0
      DGASH(IDOFN) = 0.0
      DO 30 IODEG = 1,NODEG
      PGASH(IDOFN) = PGASH(IDOFN)+PRESS(IODEG,IDOFN)*SHP(3,IODEG)
   30 DGASH(IDOFN) = DGASH(1DOFN)+SHP(1,IODEG)*ELCOD(IDOFN,IODEG)
      DVOLU = WG(IGAUSS)*RBAR
      PXCOM = DGASH(1)*PGASH(2)-DGASH(2)*PGASH(1)
      PYCOM = DGASH(1)*PGASH(1)+DGASH(2)*PGASH(2)
C.....ASSOCIATE THE EQUIVALENT NODAL EDGE LOADS
C.....WITH AN ELEMENT.
      NNE = 4
      DO 40 INODE = 1,NNE
      NLOCA = NOP(NEASS,INODE)
      IF (NLOCA.EQ.NOPRS(1)) GO TO 50
   40 CONTINUE
   50 JNODE = INODE+NODEG-1
      KOUNT = 0
      DO 60 KNODE = INODE,JNODE
      KOUNT = KOUNT+1
      NGASH = (KNODE-1)*NODFN+1
      MGASH = (KNODE-1)*NODFN+2
      IF (KNODE.GT.NNE) NGASH = 1
      IF (KNODE.GT.NNE) MGASH = 2
      ELOAD(NEASS,NGASH) = ELOAD(NEASS,NGASH)+SHP(3,KOUNT)*PXCOM*DVOLU
   60 ELOAD(NEASS,MGASH) = ELOAD(NEASS,MGASH)+SHP(3,KOUNT)*PYCOM*DVOLU
   70 CONTINUE
   80 CONTINUE
      RETURN
C
C
 1000 FORMAT (1HO,5X,38HLIST OF LOADED EDGES AND APPLIED LOADS)
 1010 FORMAT (3I5)
 1020 FORMAT (1H ,I10,5X,2I5)
 1030 FORMAT (4F10.3)
      END

      SUBROUTINE FORMK
C.....THIS SUBROUTINE FORMS THE OVERALL STIFFNESS MATRIX
C.....AND STORES IT IN RECTANGULAR FORM.
      COMMON /BLK1/ NP,NE,NB,NPC,NMAT,NEQ,NBAND,NITER,TITLE(8),NBF,NEDGE
      COMMON /BLK2/ CORD(297,2),NOP(260,4),IMAT(260),ELOAD(260,8)
      COMMON /BLK3/ YIELD(4),NBC(65),NREST(65),NQ(40),R(40,2),XPRE(65),Y
     1PRE(65),NF(25)
      COMMON SK(594,30),R1(594),EST(50,60),FR(25),FZ(25),FPUR(50)
      DIMENSION SE(8,8)
C.....INITIALIZE THE ARRAYS
      DO 10 N = 1,NEQ
      DO 10 M = 1,NBAND
   10 SK(N,M) = 0.0
C
C.....SCAN ELEMENTS
C
      DO 80 II = 1,NE
      CALL QUAD2 (SE,II)
C
C.....FORM THE STIFFNESS MATRIX SK
C
C.....FIRST ROWS
C
      DO 70 JJ = 1,4
      NROWB = (NOP(II,JJ)-1)*2
      IF (NROWB) 70,20,20
   20 DO 60 J = 1,2
      NROWB = NROWB+1
      I = (JJ-1)*2+J
C
C.....THEN COLUMNS
C
      DO 50 KK = 1,4
      NCOLB = (NOP(II,KK)-1)*2
      DO 40 K = 1,2
      L = (KK-1)*2+K
      NCOL = NCOLB+K+1-NROWB
C
C.....SKIP STORING IF BELOW BAND
C
      IF (NCOL) 40,40,30
   30 SK(NROWB,NCOL) = SK(NROWB,NCOL)+SE(I,L)
   40 CONTINUE
   50 CONTINUE
   60 CONTINUE
   70 CONTINUE
   80 CONTINUE
C
C.....PREPARATION FOR FORCE CALCULATION
C.....STORE THE ROWS OF SK WHICH ARE NECESSARY.
C
      IF (NBF.EQ.0) GO TO 140
      NBAND2 = 2*NBAND-1
      DO 90 I = 1,NBF
      IZ = 2*I
      IR = IZ-1
      DO 90 J = 1,NBAND2
      EST(IZ,J) = 0.0
   90 EST(IR,J) = 0.0
      DO 130 I = 1,NBF
      II = NF(I)
      IZ = 2*II
      IR = IZ-1
      IIZ = 2*I
      IIR = IIZ-1
      DO 100 J = NBAND,NBAND2
      JJ = J-NBAND+1
      EST(IIR,J) = SK(IR,JJ)
  100 EST(IIZ,J) = SK(IZ,JJ)
```

```
      DO 120 J = 1,NBAND
      NR = IR-J+1
      NZ = IZ-J+1
      JJ = NBAND-J+1
      IF (NR.LE.0) GO TO 110
      EST(IIR,JJ) = SK(NR,J)
  110 IF (NZ.LE.0) GO TO 120
      EST(IIZ,JJ) = SK(NZ,J)
  120 CONTINUE
      FPUR(IIR) = R1(IR)
  130 FPUR(IIZ) = R1(IZ)
C
C.....INSERT DISPLACEMENT BOUNDARY CONDITIONS
C
  140 DO 150 N = 1,NB
      I = NBC(N)
      IR = 2*I-1
      IZ = IR+1
      NC = NREST(N)
C
C.....CHECK IF THE X VELOCITY IS PRESCRIBED
C
      IF (NC.EQ.1.OR.NC.EQ.11) CALL CONDE (IR,XPRE(N))
C
C.....CHECK IF THE Y VELOCITY IS PRESCRIBED
C
      IF (NC.EQ.2.OR.NC.EQ.11) CALL CONDE (IZ,YPRE(N))
C
C.....CHECK IF THE POINT IS ALONG AN INCLINED BOUNDARY
C
      IF (NC.EQ.3) THETA = XPRE(N)*3.1415927/180.
      IF (NC.EQ.3) CALL BCMIX (I,THETA)
  150 CONTINUE
      RETURN
      END

      SUBROUTINE QUAD2 (SE,INE)
C
C.....THIS SUBROUTINE FORMS THE ELEMENTAL STIFFNESS MATRIX.
C
      COMMON /BLK1/ NP,NE,NB,NPC,NMAT,NEQ,NBAND,NITER,TITLE(8),NBF,NEDGE
      COMMON /BLK2/ CORD(297,2),NOP(260,4),IMAT(260),ELOAD(260,8)
      COMMON /BLK3/ YIELD(4),NBC(65),NREST(65),NQ(40),R(40,2),XPRE(65),Y
     1PRE(65),NF(25)
      COMMON /BLK4/ STR(260,5),EPS(260,6),VEL(2,297),TEPS(260)
      DIMENSION D(4,4), SE(8,8), A(4,8), XL(4), YL(4)
      COMMON /A/ VRIG,IPLAX,ALPHA,IHARD
      DIMENSION B(4,8), SHP(3,9), SG(9), WG(9), TG(9)
      N = INE
C.....INITIALIZE THE ARRAYS
      NNE = 4
      IF (NOP(N,4).EQ.0) NNE = 3
      NNE2 = NNE*2
      DO 10 I = 1,4
      DO 10 J = 1,4
   10 D(I,J) = 0.0
      DO 20 I = 1,NNE2
      DO 20 J = 1,NNE2
   20 SE(I,J) = 0.0
      DO 30 MM = 1,NNE
      XL(MM) = CORD(NOP(N,MM),1)
   30 YL(MM) = CORD(NOP(N,MM),2)
      NINT = 2
      IPEN = 0
C.....COMPUTE GAUSS POINTS AND WEIGHT FACTORS
   40 CALL PGAUSS (NINT,LINT,SG,TG,WG)
C.....FORM STRAIN DISPLACEMENT MATRIX B.
      DO 200 L = 1,LINT
      XBAR = 0.0
      DO 50 NN = 1,3
      DO 50 LL = 1,NNE
   50 SHP(NN,LL) = 0.0
      CALL SHAPE (SG(L),TG(L),XL,YL,SHP,DETJAC,NNE)
      IF (DETJAC) 60,60,70
   60 WRITE (6,1000) N
      WRITE (6,1010)
      WRITE (6,1020) (KF,(CORD(KF,LF),LF=1,2),KF=1,NP)
      STOP
   70 DO 80 LI = 1,NNE
      J = 2*LI
      I = J-1
      B(1,I) = SHP(1,LI)
      B(1,J) = 0.0
      B(2,I) = 0.0
      B(2,J) = SHP(2,LI)
      B(3,I) = 0.0
      B(3,J) = 0.0
      B(4,I) = B(2,J)
   80 B(4,J) = B(1,I)
C.....IN CASE OF PLANE STRAIN ANALYSIS DO NOT INCLUDE
C.....THE NORMAL STRAIN COMPONENT
      IF (IPLAX.EQ.0) GO TO 130
      DO 90 KI = 1,NNE
   90 XBAR = XBAR+SHP(3,KI)*XL(KI)
C.....EVALUATE THE HOOP STRAIN DISPLACEMENT RELATION
      IF (XBAR.GT.0.00000001) GO TO 110
C.....FOR THE CASE OF ZERO RADIUS EQUATE RADIAL TO HOOP STRAIN
      DO 100 KI = 1,NNE2
  100 B(3,KI) = B(1,KI)
      GO TO 130
C.....NON-ZERO RADIUS
  110 DUMA = 1./XBAR
      DO 120 KI = 1,NNE
      LH = 2*KI-1
  120 B(3,LH) = SHP(3,KI)*DUMA
C.....FORM THE PENALTY MATRIX
  130 IF (IPEN.EQ.0) GO TO 150
      DO 140 I = 1,4
      DO 140 J = 1,4
      D(I,J) = ALPHA
  140 IF (I.EQ.4.OR.J.EQ.4) D(I,J) = 0.0
      GO TO 160
C.....FORM THE STRESS-STRAIN MATRIX
  150 IF (NITER.EQ.0) EPSR = 1.0
      IF (NITER.EQ.0) TEPS(N) = 0.0
      IF (NITER.GT.0) CALL STINT (NNE,N,B,EPSR)
      LL = IMAT(N)
      CALL HARD (LL,TEPS(N),YYLD)
      DUM3 = 2.*YYLD/(3.*EPSR)
      IF (DUM3.GE.VRIG) DUM3 = VRIG
      D(1,1) = DUM3
      D(2,2) = DUM3
      D(3,3) = DUM3
      D(4,4) = DUM3/2.
C.....COMPUTE THE PRODUCT D*B
  160 DO 170 I = 1,4
      DO 170 J = 1,NNE2
      A(I,J) = 0.0
```

```
      DO 170 K = 1,4
  170 A(I,J) = A(I,J)+D(I,K)*B(K,J)
C.....COMPUTE (B**T *(D*B) AND ADD CONTRIBUTION TO ELEMENT STIFFNESS
      IF (IPLAX.EQ.0) XBAR = 1.0
      WT = XBAR*WG(L)*DETJAC
      DO 190 NROW = 1,NNE2
      DO 190 NCOL = NROW,NNE2
      OUM2 = 0.0
      DO 180 LI = 1,4
  180 OUM2 = OUM2+B(LI,NROW)*A(LI,NCOL)
      SE(NROW,NCOL) = SE(NROW,NCOL)+OUM2*WT
  190 CONTINUE
  200 CONTINUE
      IPEN = IPEN+1
      NINT = 1
      IF (IPEN.EQ.1) GO TO 40
C.....COMPLETE SE BY SYMMETRY.
      DO 210 K = 2,NNE2
      DO 210 L = 1,K
  210 SE(K,L) = SE(L,K)
      RETURN
C
C
 1000 FORMAT (//,"PROGRAM HAS HALTED IN SUBROUTINE QUAD2",//,"ELEMENT",I
     15,2X,"HAS ZERO OR NEGATIVE AREA")
 1010 FORMAT (1H ,"COORDINATES AT THE TIME OF ERROR",//)
 1020 FORMAT (1H ,I5,2F10.4)
      END

      SUBROUTINE PGAUSS (L,LINT,R,Z,W)
C
C.....GAUSS POINTS AND WEIGHTS FOR TWO DIMENSIONS
C
      REAL LR(9), LZ(9), LW(9), R(9), Z(9), W(9)
      DATA LR/-1.,1.,1.,-1.,0.,-1.,0.,-1.,0./
      DATA LZ/-1.,-1.,1.,1.,-1.,0.,1.,0.,0./
      DATA LW/4*25.,4*40.,64./
      LINT = L*L
      GO TO (10,20,40), L
C.....1X1 INTEGRATION
   10 R(1) = 0.
      Z(1) = 0.
      W(1) = 4.
      RETURN
C.....2X2 INTEGRATION
   20 G = 1./SQRT(3.)
      DO 30 I = 1,4
      R(I) = G*LR(I)
      Z(I) = G*LZ(I)
   30 W(I) = 1.
      RETURN
C....3X3 INTEGRATION
   40 G = SQRT(0.6)
      H = 1./81.
      DO 50 I = 1,9
      R(I) = G*LR(I)
      Z(I) = G*LZ(I)
   50 W(I) = H*LW(I)
      RETURN
      END

      SUBROUTINE SHAPE (SS,TT,XL,YL,SHP,DETJAC,NNE)
C
C.....   SHAPE FUNCTION SUBROUTINE FOR TWO DIMENSIONAL ELEMENTS
C
      REAL SHP(3,9), XL(4), YL(4), S(4), T(4), JAC(2,2)
      DATA S/-0.5,0.5,0.5,-0.5/,T/-0.5,-0.5,0.5,0.5/
C.....FORM 4 NODE QUADRILATERAL SHAPE FUNCTION
      DO 10 I = 1,4
      SHP(3,I) = (0.5+S(I)*SS)*(0.5+T(I)*TT)
      SHP(1,I) = S(I)*(0.5+T(I)*TT)
   10 SHP(2,I) = T(I)*(0.5+S(I)*SS)
      IF (NNE.EQ.2) RETURN
C.....FORM TRIANGLE BY ADDING THIRD AND FOURTH TOGETHER.
      DO 20 I = 1,3
   20 SHP(I,3) = SHP(I,3)+SHP(I,4)
C.....CONSTRUCT JACOBIAN, ITS INVERSE AND ITS DETERMINANT.
      DO 30 I = 1,2
      DO 30 J = 1,2
   30 JAC(I,J) = 0.0
      DO 40 K = 1,NNE
      JAC(1,1) = JAC(1,1)+SHP(1,K)*XL(K)
      JAC(1,2) = JAC(1,2)+SHP(1,K)*YL(K)
      JAC(2,1) = JAC(2,1)+SHP(2,K)*XL(K)
   40 JAC(2,2) = JAC(2,2)+SHP(2,K)*YL(K)
      DETJAC = JAC(1,1)*JAC(2,2)-JAC(1,2)*JAC(2,1)
      OUM1 = JAC(1,1)/DETJAC
      JAC(1,1) = JAC(2,2)/DETJAC
      JAC(2,1) = -JAC(2,1)/DETJAC
      JAC(1,2) = -JAC(1,2)/DETJAC
      JAC(2,2) = OUM1
C.....FORM GLOBAL DERIVATIVES
      DO 50 I = 1,NNE
      TP = SHP(1,I)*JAC(1,1)+SHP(2,I)*JAC(1,2)
      SHP(2,I) = SHP(1,I)*JAC(2,1)+SHP(2,I)*JAC(2,2)
   50 SHP(1,I) = TP
      RETURN
      END

      SUBROUTINE STINT (NNE,M,BA,EPSR)
C
C.....THIS SUBROUTINE CALCULATES THE STRAIN RATES AT THE GAUSS POINTS
C.....SO THAT THE ELEMENTAL STIFFNESS MATRIX CAN BE EVALUATED.
C
      COMMON /BLK1/ NP,NE,NB,NPC,NMAT,NEQ,NBAND,NITER,TITLE(8),NBF,NEDGE
      COMMON /BLK2/ CORD(297,2),NOP(260,4),IMAT(260),ELBAD(260,8)
      COMMON /BLK4/ STR(260,5),EPS(260,6),VEL(2,297),TEPS(260)
      DIMENSION BA(4,8), E(4), RA(8)
      NK = NNE
      DO 10 J = 1,NK
      KK = NOP(M,J)
      KI = (J-1)*2
      DO 10 JJ = 1,2
      IJ = JJ+KI
   10 RA(IJ) = VEL(JJ,KK)
      DO 20 KK = 1,4
      E(KK) = 0.0
      NNE2 = NNE*2
      DO 20 J = 1,NNE2
   20 E(KK) = E(KK)+BA(KK,J)*RA(J)
      EPSR = RBAR(E(1),E(2),E(3),E(4))
      RETURN
      END

      SUBROUTINE CONDE (N,U)
C
C.....THIS SUBROUTINE PERFORM THE MATRIX CONDENSATION WHEN
C.....THE VALUE OF A COMPONENT OF X IN AX=B IS SPECIFIED.
```

```
C
      COMMON /BLK1/ NP,NE,NB,NPC,NMAT,NEQ,NBAND,NITER,TITLE(8),NBF,NEDGE
      COMMON SK(594,30),R1(594),EST(50,60),FR(25),FZ(25),FPUR(50)
      DO 10 M = 2,NBAND
      KK = N+M-1
      IF (KK.GT.NEQ) GO TO 10
      R1(KK) = R1(KK)-SK(N,M)*U
   10 CONTINUE
      DO 20 M = 2,NBAND
      K = N-M+1
      IF (K.LE.0) GO TO 20
      R1(K) = R1(K)-SK(K,M)*U
      SK(K,M) = 0.
   20 SK(N,M) = 0.
      SK(N,1) = 1.
      R1(N) = U
      RETURN
      END

      SUBROUTINE BCMIX (N,THETA)
C
C.....SINCE UR=UZ*TAN(THETA) ALONG THE DIE,ACORRESPONDING CHANGE
C.....IS MADE IN THE STIFFNESS EQUATIONS FOR ROWS AND COLUMNS CORRESPOND
C.....TO THESE COMPONENTS...THEN THE EQUATIONS CONTAINING UR ARE ELIMINA
C
      COMMON /BLK1/ NP,NE,NB,NPC,NMAT,NEQ,NBAND,NITER,TITLE(8),NBF,NEDGE
      COMMON SK(594,30),R1(594),EST(50,60),FR(25),FZ(25),FPUR(50)
      COMMON /A/ VRIG,IPLAX,ALPHA,IHARD
      NZ = 2*N
      NR = NZ-1
      ALPA = 1./TAN(THETA)
      IF (IPLAX.EQ.1) ALPA = TAN(THETA)
      DO 10 M = 1,NBAND
   10 SK(NR,M) = SK(NR,M)*ALPA
      SK(NR,1) = SK(NR,1)*ALPA
      SK(NR,2) = SK(NR,2)*2.
      DO 20 M = 2,NBAND
      KR = NR-M+1
      IF (KR.LE.0) GO TO 30
   20 SK(KR,M) = SK(KR,M)*ALPA
   30 R1(NR) = R1(NR)*ALPA
      DO 50 M = 2,NBAND
      KZ = NZ-M+1
      IF (KZ.LE.0) GO TO 40
      SK(KZ,M) = SK(KZ,M)+SK(KZ,M-1)
   40 IF (M.EQ.NBAND) GO TO 50
      KZ = NZ+M-1
      IF (KZ.GT.NEQ) GO TO 50
      SK(NZ,M) = SK(NZ,M)+SK(NR,M+1)
   50 CONTINUE
      SK(NZ,1) = SK(NZ,1)+SK(NR,2)
      SK(NR,1) = 1.0
      DO 70 M = 2,NBAND
      KR = NR-M+1
      IF (KR.LE.0) GO TO 60
      SK(KR,M) = 0.
   60 SK(NR,M) = 0.
   70 CONTINUE
      R1(NZ) = R1(NZ)+R1(NR)
      R1(NR) = 0.
      RETURN
      END

      SUBROUTINE SOLVE
C
C.....THIS SUBROUTINE PERFORMS THE SOLUTION OF THE
C.....EQUATION SYSTEM AX=B,WHERE A IS A BANDED SYMMETRICAL MATRIX
C
      COMMON /BLK1/ NP,NE,NB,NPC,NMAT,NEQ,NBAND,NITER,TITLE(8),NBF,NEDGE
      COMMON /BLK3/ YIELD(4),NBC(65),NREST(65),NQ(40),R(40,2),XPRE(65),Y
     1PRE(65),NF(25)
      COMMON SK(594,30),R1(594),EST(50,60),FR(25),FZ(25),FPUR(50)
      COMMON /A/ VRIG,IPLAX,ALPHA,IHARD
C
C.....REDUCE MATRIX
C
      DO 50 N = 1,NEQ
      I = N
      DO 40 L = 2,NBAND
      I = I+1
      IF (SK(N,L)) 10,40,10
   10 C = SK(N,L)/SK(N,1)
      J = 0
      DO 30 K = L,NBAND
      J = J+1
      IF (SK(N,K)) 20,30,20
   20 SK(I,J) = SK(I,J)-C*SK(N,K)
   30 CONTINUE
      SK(N,L) = C
C
C
C.....AND LOAD VECTOR FOR EACH EQUATION.
      R1(I) = R1(I)-C*R1(N)
   40 CONTINUE
   50 R1(N) = R1(N)/SK(N,1)
C
C.....BACK SUBSTITUTION
C
      N = NEQ
   60 N = N-1
      IF (N) 100,100,70
   70 L = N
      DO 90 K = 2,NBAND
      L = L+1
      IF (SK(N,K)) 80,90,80
   80 R1(N) = R1(N)-SK(N,K)*R1(L)
   90 CONTINUE
      GO TO 60
  100 DO 110 I = 1,NB
      IZ = 2*NBC(I)
      IR = IZ-1
      IF (NREST(I).EQ.3) THETA = XPRE(I)*3.1415927/180.
      IF (NREST(I).EQ.3.AND.IPLAX.EQ.0) ALPA = 1./TAN(THETA)
      IF (NREST(I).EQ.3.AND.IPLAX.EQ.1) ALPA = TAN(THETA)
  110 IF (NREST(I).EQ.3) R1(IR) = R1(IZ)*ALPA
      RETURN
      END

      SUBROUTINE CFORC
      COMMON /BLK1/ NP,NE,NB,NPC,NMAT,NEQ,NBAND,NITER,TITLE(8),NBF,NEDGE
      COMMON /BLK2/ CORD(297,2),NOP(260,4),IMAT(260),ELOAD(260,8)
      COMMON /BLK3/ YIELD(4),NBC(65),NREST(65),NQ(40),R(40,2),XPRE(65),Y
     1PRE(65),NF(25)
      COMMON SK(594,30),R1(594),EST(50,60),FR(25),FZ(25),FPUR(50)
C
C.....THIS SUBROUTINE DETERMINES FORCES ON THE BOUNDARIES.
C
      IF (NBF.LE.0) GO TO 40
```

```
      NBAND2 = 2*NBAND-1
      DO 30 I = 1,NBF
      IR = 2*NF(I)-1
      IIZ = 2*I
      IIR = IIZ-1
      SUMR = 0.0
      SUMZ = 0.0
      DO 20 J = 1,NBAND2
      JR = IR+J-NBAND
      JZ = JR+1
      IF (JR.LE.0.OR.JR.GT.NEQ) GO TO 10
      SUMR = SUMR+EST(IIR,J)*R1(JR)
   10 IF (JZ.LE.0.OR.JZ.GT.NEQ) GO TO 20
      SUMZ = SUMZ+EST(IIZ,J)*R1(JZ)
   20 CONTINUE
      FR(I) = SUMR-FPUR(IIR)
      FZ(I) = SUMZ-FPUR(IIZ)
   30 CONTINUE
   40 RETURN
      END

      SUBROUTINE STRAIN
C
C.....THIS SUBROUTINE CALCULATES STRAIN RATES,STRESSES AND COORDINATES
C.....AT SAMPLING POINTS(CENTROIDS IN THE CASE OF BILINEAR ELEMENT.)
C
      COMMON /BLK1/ NP,NE,NB,NPC,NMAT,NEQ,NBAND,NITER,TITLE(8),NBF,NEDGE
      COMMON /BLK2/ CORD(297,2),NOP(260,4),IMAT(260),ELOAD(260,8)
      COMMON /BLK3/ YIELD(4),NBC(65),NREST(65),NQ(40),R(40,2),XPRE(65),Y
     1PRE(65),NF(25)
      COMMON /BLK4/ STR(260,5),EPS(260,6),VEL(2,297),TEPS(260)
      COMMON /A/ VRIG,IPLAX,ALPHA,IHARD
      DIMENSION SHP(3,9), SG(9), TG(9), WG(9), U(2,9)
      DIMENSION XL(9), YL(9), E(6)
      REWIND 1
      DO 100 N = 1,NE
      NNE = 4
      IF (NOP(N,4).EQ.0) NNE = 3
      DO 10 MM = 1,NNE
      XL(MM) = CORD(NOP(N,MM),1)
      YL(MM) = CORD(NOP(N,MM),2)
      U(1,MM) = VEL(1,NOP(N,MM))
   10 U(2,MM) = VEL(2,NOP(N,MM))
      L = 1
      CALL PGAUSS (L,LINT,SG,TG,WG)
      DO 90 JJ = 1,LINT
      DO 20 NN = 1,3
      DO 20 LL = 1,NNE
   20 SHP(NN,LL) = 0.0
C.....COMPUTE ELEMENT SHAPE FUNCTIONS.
      CALL SHAPE (SG(JJ),TG(JJ),XL,YL,SHP,DETJAC,NNE)
C.....COMPUTE CORDINATES AND STRAINS.
      DO 30 I = 1,6
   30 E(I) = 0.0
      XBAR = 0.0
      YBAR = 0.0
      DO 40 J = 1,NNE
      XBAR = XBAR+SHP(3,J)*XL(J)
   40 YBAR = YBAR+SHP(3,J)*YL(J)
      DO 50 J = 1,NNE
      E(1) = E(1)+SHP(1,J)*U(1,J)
      E(2) = E(2)+SHP(2,J)*U(2,J)
      E(3) = E(3)+SHP(3,J)/XBAR*U(1,J)
      IF (IPLAX.EQ.0) E(3) = 0.0
   50 E(4) = E(4)+SHP(1,J)*U(2,J)+SHP(2,J)*U(1,J)
      DO 60 J = 1,4
   60 EPS(N,J) = E(J)
      EPS(N,6) = RBAR(E(1),E(2),E(3),E(4))
      EPS(N,5) = E(1)+E(2)+E(3)
      CALL HARD (IMAT(N),TEPS(N),YYLD)
C.....CALCULATE STRESSES
      DO 70 KK = 1,4
   70 STR(N,KK) = EPS(N,KK)*2./3.*YYLD/EPS(N,6)
      STR(N,4) = STR(N,4)*0.5
      STR(N,5) = EPS(N,5)*ALPHA
      DO 80 KK = 1,3
      STR(N,KK) = STR(N,KK)+STR(N,5)
   80 IF (IPLAX.EQ.0) STR(N,3) = 0.0
C.....SAVE INFORMATION FOR LATER PUNCHING.
      WRITE (1,1000) XBAR,YBAR,EPS(N,1),EPS(N,2),EPS(N,3),EPS(N,4),EPS(N
     1,6)
      WRITE (1,1010) ((STR(N,I),I=1,5),TEPS(N))
   90 CONTINUE
  100 CONTINUE
      RETURN
C
C
 1000 FORMAT (2F10.5,5E12.5)
 1010 FORMAT (6E12.5)
      END

      SUBROUTINE FLOW (IPLOT)
C.....THIS SUBROUTINE FINDS THE FLOW LINES AND INTEGRATES
C.....ALONG THEM TO FIND THE EFFECTIVE STRAIN DISTRIBUTION.
      COMMON /BLK1/ NP,NE,NB,NPC,NMAT,NEQ,NBAND,NITER,TITLE(8),NBF,NEDGE
      COMMON /BLK2/ CORD(297,2),NOP(260,4),IMAT(260),ELOAD(260,8)
      COMMON /BLK4/ STR(260,5),EPS(260,6),VEL(2,297),TEPS(260)
      COMMON SK(594,30),R1(594),EST(50,60),FR(25),FZ(25),FPUR(50)
      COMMON /A/ VRIG,IPLAX,ALPHA,IHARD
      COMMON /B/ NTIMES,NDI,NDJ,NMAX,YSTART,YDIE,YEXIT,YMAX,RENTER,REXIT
     1,RCORE,STEP,NLIN,VSCAL
      DIMENSION RR(4), ZZ(4), URR(4), UZZ(4)
      DIMENSION X(13,30), AA(13,30), U(13,30), V(13,30), STRR(13,30), A(
     1260), B(260), Y(30), BB(30), XARB(13)
      DIMENSION XX(13,400), YY(13,400), EE(13,400), PX(402), PY(402)
      EQUIVALENCE (STR(1,1),X(1,1)), (STR(131,2),AA(1,1)), (STR(1,4),U(1
     1,1)), (STR(131,5),Y(1)), (STR(161,5),BB(1)), (STR(191,5),XARB(1))
      EQUIVALENCE (EPS(1,1),V(1,1)), (EPS(131,2),STRR(1,1)), (EPS(1,4),A
     1(1)), (EPS(1,5),B(1))
      EQUIVALENCE (SK(1,1),XX(1,1)), (SK(449,9),YY(1,1)), (SK(303,18),EE
     1(1,1)), (SK(157,27),PX(1)), (SK(559,27),PY(1))
      NIM1 = NDI-1
      NJM1 = NDJ-1
      IF (IPLAX.EQ.1) GO TO 20
      DO 10 I = 1,NP
      DUM1 = CORD(I,1)
      DUM2 = VEL(1,I)
      CORD(I,1) = CORD(I,2)
      CORD(I,2) = DUM1
      VEL(1,I) = VEL(2,I)
   10 VEL(2,I) = DUM2
C.....ARRANGE THE AVAILABLE INFORMATION IN PROPER FORM.
   20 K = 1
      L = 0
   30 L = L+1
      Y(L) = CORD(K,2)
      DO 40 I = 1,NIM1
      X(I,L) = CORD(K,1)
```

```
      U(I,L) = VEL(1,K)
      V(I,L) = VEL(2,K)
   40 K = K+1
      X(NDI,L) = X(NIM1,L)
      U(NDI,L) = U(NIM1,L)
      V(NDI,L) = V(NIM1,L)
      IF (K.LT.NP) GO TO 30
C.....DETERMINE COORDINATES OF THE CENTROIDS.
      DO 50 N = 1,NE
      I1 = NOP(N,1)
      I2 = NOP(N,2)
      I3 = NOP(N,3)
      I4 = NOP(N,4)
      A(N) = (CORD(I1,1)+CORD(I2,1)+CORD(I3,1)+CORD(I4,1))/4.
   50 B(N) = (CORD(I1,2)+CORD(I2,2)+CORD(I3,2)+CORD(I4,2))/4.
C.....ARRANGE THE NEWLY DETERMINED VALUES IN A PROPER FORM.
      K = 1
      L = 0
   60 L = L+1
      BB(L) = B(K)
      STRR(1,L) = EPS(K,6)
      DO 70 I = 2,NIM1
      AA(I,L) = A(K)
      STRR(I,L) = EPS(K,6)
   70 K = K+1
      AA(NDI,L) = RCORE
      IF (BB(L).LE.YDIE) AA(1,L) = RENTER
      IF (BB(L).LE.YDIE.OR.BB(L).GE.YEXIT) GO TO 90
      DO 80 KL = 1,NJM1
   80 IF (BB(L).GE.Y(KL).AND.BB(L).LE.Y(KL+1)) ML = KL
      TANTH = (X(1,ML+1)-X(1,ML))/(Y(ML+1)-Y(ML))
      RARB = X(1,ML)
      AA(1,L) = RARB+(BB(L)-Y(ML))*TANTH
      IF (TANTH.EQ.0.) AA(1,L) = REXIT
   90 IF (BB(L).GE.YEXIT) AA(1,L) = REXIT
      STRR(NDI,L) = EPS(K-1,6)
      IF (K.LT.NE) GO TO 60
C.....DETERMINE THE FLOW PATTERN
      DO 290 N = 1,NTIMES
C.....SET COORDINATES OF THE STARTING POINT
      XX(N,1) = CORD(N,1)
      YY(N,1) = YSTART
C
C.....DETERMINE THE LOCATION OF THE PRESENT COORDINATES OF
C.....THE POINT IN TERMS OF THE FOUR SURROUNDING POINTS.
      IFLAG = 0
      NCOUNT = 0
      MOLD = 1
      LOLD = 1
  100 NCOUNT = NCOUNT+1
      XXX = XX(N,NCOUNT)
      YYY = YY(N,NCOUNT)
      IF (N.EQ.1.AND.YYY.GE.YEXIT) GO TO 180
      IF (YYY.GE.YMAX) GO TO 180
      DO 110 I = MOLD,NJM1
  110 IF (YYY.GE.Y(I).AND.YYY.LE.Y(I+1)) M = I
      DO 120 I = 1,NDI
  120 XARB(I) = X(I,M)-(X(I,M)-X(I,M+1))*(YYY-Y(M))/(Y(M+1)-Y(M))
      DO 130 I = 1,NIM1
  130 IF (XXX.LE.XARB(I).AND.XXX.GE.XARB(I+1)) L = I
      IF (NCOUNT.EQ.1) GO TO 140
      IF (M.EQ.MOLD.AND.L.EQ.LOLD) GO TO 150
  140 RR(1) = X(L,M)
      RR(2) = X(L,M+1)
      RR(3) = X(L+1,M+1)
      RR(4) = X(L+1,M)
      ZZ(1) = Y(M)
      ZZ(2) = Y(M+1)
      ZZ(3) = ZZ(2)
      ZZ(4) = ZZ(1)
      URR(1) = U(L,M)
      URR(2) = U(L,M+1)
      URR(3) = U(L+1,M+1)
      URR(4) = U(L+1,M)
      UZZ(1) = V(L,M)
      UZZ(2) = V(L,M+1)
      UZZ(3) = V(L+1,M+1)
      UZZ(4) = V(L+1,M)
      GO TO 160
C.....THE POINT IS LOCATED IN THE SAME ELEMENT IT WAS IN THE LAST STEP
  150 IFLAG = 1
C.....DETERMINE U AND V AT THE POINT ON FLOW LINE
  160 CALL INTRPOL (RR,ZZ,URR,XXX,YYY,UU,IFLAG)
      IFLAG = 1
      CALL INTRPOL (RR,ZZ,UZZ,XXX,YYY,VV,IFLAG)
C.....DETERMINE THE NEXT LOCATION OF POINT ON FLOW LINE.
      XX(N,NCOUNT+1) = XXX+UU*STEP
      YY(N,NCOUNT+1) = YYY+VV*STEP
      LOLD = L
      MOLD = M
      IF (N.NE.1) GO TO 190
      IF (YY(N,NCOUNT+1).LT.YDIE) GO TO 190
      DO 170 KL = 1,NJM1
  170 IF (YY(N,NCOUNT+1).GE.Y(KL).AND.YY(N,NCOUNT+1).LE.Y(KL+1)) ML = KL
      TANTH = (X(N,ML+1)-X(N,ML))/(Y(ML+1)-Y(ML))
      RARB = X(N,ML)
      YARB = YY(N,NCOUNT+1)-Y(ML)
      XX(N,NCOUNT+1) = RARB+YARB*TANTH
      IF (TANTH.EQ.0.) XX(N,NCOUNT+1) = REXIT
C.....THE POINTS HAS GONE PAST THE DIE EXIT

      GO TO 190
  180 XX(N,NCOUNT+1) = XXX
      NOPI = N+(NDJ-1)*(NDI-1)
      YY(N,NCOUNT+1) = YYY+VEL(2,NOPI)*STEP
  190 IF (NCOUNT.LT.NMAX-1) GO TO 100
C.....DETERMINE THE VALUES OF EFFECTIVE STRAIN AT EACH
C.....POINT FOR ALL FLOW LINES.
      NCOUNT = 0
      EE(N,1) = 0.0
      MOLD = 1
      LOLD = 1
  200 NCOUNT = NCOUNT+1
      YYY = YY(N,NCOUNT)
      XXX = XX(N,NCOUNT)
      IF (YYY.GT.YEXIT) GO TO 270
C.....DETERMINE THE LOCATION OF FOUR SURROUNDING CENTROIDS.
      DO 210 IN = MOLD,NJM1
  210 IF (YYY.GE.BB(IN).AND.YYY.LE.BB(IN+1)) M = IN
      DO 220 IJ = 1,NDI
  220 XARB(IJ) = AA(IJ,M)-(AA(IJ,M)-AA(IJ,M+1))*(YYY-BB(M))/(BB(M+1)-BB(
     1M))
      DO 230 IK = 1,NIM1
  230 IF (XXX.LE.XARB(IK).AND.XXX.GE.(XARB(IK+1))) L = IK
      IF (NCOUNT.EQ.1) GO TO 240
      IF (M.EQ.MOLD.AND.L.EQ.LOLD) GO TO 250
C.....INTERPOLATE THE VALUES OF THE STRAIN RATES
  240 RR(1) = AA(L,M)
```

```
      RR(2) = AA(L,M+1)
      RR(3) = AA(L+1,M+1)
      RR(4) = AA(L+1,M)
      ZZ(1) = BB(M)
      ZZ(2) = BB(M+1)
      ZZ(3) = ZZ(2)
      ZZ(4) = ZZ(1)
      URR(1) = STRR(L,M)
      URR(2) = STRR(L,M+1)
      URR(3) = STRR(L+1,M+1)
      URR(4) = STRR(L+1,M)
      GO TO 260
  250 IFLAG = 1
  260 CALL INTRPOL (RR,ZZ,URR,XXX,YYY,ESTEP,IFLAG)
C.....ADD THE INTERPOLATED VALUES TO THE VALUES OF
C.....EFFECTIVE STRAIN AT THE PREVIOUS LOCATION.
      EE(N,NCOUNT+1) = EE(N,NCOUNT)+ESTEP*STEP
      LOLD = L
      MOLD = M
      GO TO 280
  270 EE(N,NCOUNT+1) = EE(N,NCOUNT)
  280 IF (NCOUNT.LT.NMAX-1) GO TO 200
  290 CONTINUE
C.....INTERPOLATE THE EFFECTIVE STRAIN DISTRIBUTION FOR
C.....ELEMENTS FROM VALUES OF EFFECTIVE STRAIN ALONG FLOW LINES
      DO 350 N = 1,NE
      IF (B(N).LT.YY(1,1)) GO TO 340
      DO 320 J = 2,NTIMES
      DO 300 I = 1,NMAX
      IF (B(N).GT.YY(J,I)) GO TO 300
      L = I
      GO TO 310
  300 CONTINUE
  310 IF (XX(J,L).GT.A(N)) GO TO 320
      K = J
      GO TO 330
  320 CONTINUE
  330 IFLAG = 0
      RR(1) = XX(K-1,L)
      RR(2) = XX(K-1,L-1)
      RR(3) = XX(K,L-1)
      RR(4) = XX(K,L)
      ZZ(1) = YY(K-1,L)
      ZZ(2) = YY(K-1,L-1)
      ZZ(3) = YY(K,L-1)
      ZZ(4) = YY(K,L)
      URR(1) = EE(K-1,L)
      URR(2) = EE(K-1,L-1)
      URR(3) = EE(K,L-1)
      URR(4) = EE(K,L)
      CALL INTRPOL (RR,ZZ,URR,A(N),B(N),TEPS(N),IFLAG)
      GO TO 350
  340 TEPS(N) = 0.0
  350 CONTINUE
C.....PLOT FLOW LINES AND GRID DISTORTION
      IF (IPLOT.EQ.0) GO TO 360
      CALL DRAW (PX,PY)
  360 IF (IPLAX.EQ.1) RETURN
      DO 370 I = 1,NP
      DUM1 = CORD(I,1)
      DUM2 = VEL(1,I)
      CORD(I,1) = CORD(I,2)
      CORD(I,2) = DUM1
      VEL(1,I) = VEL(2,I)
  370 VEL(2,I) = DUM2
      RETURN
      END


      SUBROUTINE INTRPOL (X,Y,U,XX,YY,UU,IFLAG)
C
C.....THIS SUBROUTINE INTERPOLATES THE VALUE OF UU AT (XX,YY)
C.....BY KNOWING THE VALUE OF U AT FOUR SURROUNDING POINTS.
C
      DIMENSION X(4), Y(4), U(4), A(4,4), COEF(4)
C.....DETERMINE THE MATRIX A, THE INVERSE OF THE INTERPOLATION MATRIX.
C.....IF IFLAG=1 THE MATRIX A IS ALREADY KNOWN
      IF (IFLAG.EQ.1) GO TO 10
      X1 = X(1)
      X2 = X(2)
      X3 = X(3)
      X4 = X(4)
      Y1 = Y(1)
      Y2 = Y(2)
      Y3 = Y(3)
      Y4 = Y(4)
      X12 = X1-X2
      X13 = X1-X3
      X14 = X1-X4
      X23 = X2-X3
      X24 = X2-X4
      X34 = X3-X4
      Y12 = Y1*Y2*X12
      Y13 = Y1*Y3*X13
      Y14 = Y1*Y4*X14
      Y23 = Y2*Y3*X23
      Y24 = Y2*Y4*X24
      Y34 = Y3*Y4*X34
      A(1,1) = X2*Y34-X3*Y24+X4*Y23
      A(1,2) = -X1*Y34+X3*Y14-X4*Y13
      A(1,3) = X1*Y24-X2*Y14+X4*Y12
      A(1,4) = -X1*Y23+X2*Y13-X3*Y12
      A(2,1) = -Y23+Y24-Y34
      A(2,2) = Y13-Y14+Y34
      A(2,3) = -Y12+Y14-Y24
      A(2,4) = Y12-Y13+Y23
      Z11 = Y1*X23
      Z12 = Y1*X24
      Z13 = Y1*X34
      Z21 = Y2*X13
      Z22 = Y2*X14
      Z23 = Y2*X34
      Z31 = Y3*X12
      Z32 = Y3*X1+
      Z33 = Y3*X24
      Z41 = Y4*X12
      Z42 = Y4*X13
      Z43 = Y4*X23
      A(3,1) = X2*Z23-X3*Z33+X4*Z43
      A(3,2) = -X1*Z13+X3*Z32-X4*Z42
      A(3,3) = X1*Z12-X2*Z22+X4*Z41
      A(3,4) = -X1*Z11+X2*Z21-X3*Z31
      A(4,1) = -Z23+Z33-Z43
      A(4,2) = Z13-Z32+Z42
      A(4,3) = -Z12+Z22-Z41
      A(4,4) = Z11-Z21+Z31
      DETER = A(1,1)+A(1,2)+A(1,3)+A(1,4)
   10 IFLAG = 0
```

```
      IF (DETER.EQ.0.) GO TO 40
      DO 30 J = 1,4
      COEF(J) = 0.0
      DO 20 I = 1,4
   20 COEF(J) = COEF(J)+A(J,I)*U(I)
   30 COEF(J) = COEF(J)/DETER
      UU = COEF(1)+COEF(2)*XX+COEF(3)*YY+COEF(4)*XX*YY
      RETURN
   40 UU = (U(1)*(YY-Y(2))+U(2)*(Y(1)-YY))/(Y(1)-Y(2))
      RETURN
      END

      SUBROUTINE DRAW (PX,PY)
C
C.....THIS SUBROUTINE PLOTS THE FLOW LINES AND
C.....GRID DISTORTION
      COMMON /BLK1/ NP,NE,NB,NPC,NMAT,NEQ,NBAND,NITER,TITLE(8),NBF,NEDGE
      COMMON /B/ NTIMES,NDI,NDJ,NMAX,YSTART,YDIE,YEXIT,YMAX,RENTER,REXIT
     1,RCORE,STEP,NLIN,VSCAL
      DIMENSION PX(402), PY(402)
      CALL START (2)
      CALL SYMBOL (2.0,1.0,0.15,TITLE,0.,80)
      CALL SYMBOL (3.0,0.7,0.15,10HFLOW LINES,0.,10)
      CALL PLOT (2.0,2.0,-3)
      DO 10 I = 1,NMAX
      PX(I) = 0.0
   10 PY(I) = 0.0
      PX(NMAX) = VSCAL
      PY(NMAX) = VSCAL
      CALL SCALE (PX,12.,NMAX,1)
      CALL SCALE (PY,12.,NMAX,1)
      XS = 1./PX(NMAX+2)
      YS = 1./PY(NMAX+2)
      XA = -PX(NMAX+1)/PX(NMAX+2)
      YA = -PY(NMAX+1)/PY(NMAX+2)
      CALL AXIS (0.,0.,6HZ-AXIS,-6,12.,0.,PX(NMAX+1),PX(NMAX+2))
      CALL AXIS (0.,0.,6HR-AXIS,6,12.,90.,PY(NMAX+1),PY(NMAX+2))
      DO 30 N = 1,NTIMES
      DO 20 I = 1,NMAX
      PX(I) = YY(N,I)
   20 PY(I) = XX(N,I)
      IF (N.EQ.1) CALL LINE (PX,PY,NMAX,1,0,1)
   30 IF (N.NE.1) CALL ARKIST (PX,PY,1,NMAX,10,XS,YS,XA,YA,2,1)
      CALL NEWPAGE
      CALL SYMBOL (2.0,1.0,0.15,TITLE,0.,80)
      CALL SYMBOL (3.0,0.7,0.15,15HGRID DISTORTION,0.,15)
      CALL PLOT (2.0,2.0,-3)
      CALL AXIS (0.,0.,6HZ-AXIS,-6,12.,0.,PX(NMAX+1),PX(NMAX+2))
      CALL AXIS (0.,0.,6HR-AXIS,6,12.,90.,PY(NMAX+1),PY(NMAX+2))
      DO 40 I = 1,NMAX
      PX(I) = YY(1,I)
      PY(I) = XX(1,I)
   40 CONTINUE
      CALL LINE (PX,PY,NMAX,1,0,1)
      DO 50 I = 1,NMAX
      PX(I) = YY(NTIMES,I)
   50 PY(I) = XX(NTIMES,I)
      CALL LINE (PX,PY,NMAX,1,0,1)
      PX(NTIMES+1) = PX(NMAX+1)
      PX(NTIMES+2) = PX(NMAX+2)
      PY(NTIMES+1) = PY(NMAX+1)
      PY(NTIMES+2) = PY(NMAX+2)
      DO 70 N = 1,NMAX
      IF (((N-1)/15)*15.NE.N-1) GO TO 70
      DO 60 I = 1,NTIMES
      PX(I) = YY(I,N)
   60 PY(I) = XX(I,N)
      CALL ARKIST (PX,PY,1,NTIMES,20,XS,YS,XA,YA,2,1)
   70 CONTINUE
      CALL ENPLOT
      RETURN
      END

      SUBROUTINE DOUT
      COMMON /BLK1/ NP,NE,NB,NPC,NMAT,NEQ,NBAND,NITER,TITLE(8),NBF,NEDGE
      COMMON /BLK2/ CORD(297,2),NOP(260,4),IMAT(260),ELOAD(260,8)
      COMMON /BLK3/ YIELD(4),NBC(65),NREST(65),NQ(40),R(40,2),XPRE(65),Y
     1PRE(65),NF(25)
      COMMON /BLK4/ STR(260,5),EPS(260,6),VEL(2,297),TEPS(260)
      COMMON SK(594,30),R1(594),EST(50,60),FR(25),FZ(25),FPUR(50)
      COMMON /A/ VRIG,IPLAX,ALPHA,IHARD
C...SAVE MESH DESCRIPTION FOR LATER PUNCHING..
      REWIND 4
      WRITE (4,1000) (N,(CORD(N,M),M=1,2),(VEL(M,N),M=1,2),N=1,NP)
      WRITE (4,1010) (N,(NOP(N,M),M=1,4),IMAT(N),N=1,NE)
      WRITE (6,1020) TITLE
C
C.....WRITE VELOCITY DISTRIBUTION
C
      WRITE (6,1030)
      IF (IPLAX.EQ.0) WRITE (6,1050) NITER
      IF (IPLAX.EQ.1) WRITE (6,1040) NITER
      WRITE (6,1060) (M,(VEL(J,M),J=1,2),(CORD(M,J),J=1,2),M=1,NP)
C.....WRITE STRAIN RATE AND STRESS DISTRIBUTION.
      WRITE (6,1070)
      IF (IPLAX.EQ.0) WRITE (6,1090)
      IF (IPLAX.EQ.1) WRITE (6,1080)
      WRITE (6,1070)
      WRITE (6,1100) (N,(EPS(N,J),J=1,6),TEPS(N),N=1,NE)
      WRITE (6,1110)
      IF (IPLAX.EQ.0) WRITE (6,1120)
      IF (IPLAX.EQ.1) WRITE (6,1130)
      WRITE (6,1110)
      WRITE (6,1140) (N,(STR(N,J),J=1,5),N=1,NE)
      WRITE (6,1110)
C
C.....WRITE FORCES AT NODES  IF DESIRED
C
      IF (NBF.LE.0) GO TO 10
      IF (IPLAX.EQ.0) WRITE (6,1150)
      IF (IPLAX.EQ.1) WRITE (6,1160)
      WRITE (6,1170) (NF(I),FR(I),FZ(I),I=1,NBF)
      WRITE (4,1170) (NF(I),FR(I),FZ(I),I=1,NBF)
   10 RETURN
C
C
 1000 FORMAT (I10,2F10.4,2E15.6)
 1010 FORMAT (6I5)
 1020 FORMAT (1H1,8A10)
 1030 FORMAT (///,15X,"VELOCITIES")
 1040 FORMAT (1H ,15X,"NUMBER OF ITERATIONS",I3,//,1H ,4X,"NODES",7X,"VE
     1LOC-R",8X,"VELOC-Z")
 1050 FORMAT (1H ,15X,"NUMBER OF ITERATIONS",I3,//,1H ,4X,"NODES",7X,"VE
     1LOC-X",8X,"VELOC-Y")
 1060 FORMAT (I10,2E15.6,5X,2F10.4)
 1070 FORMAT (1HO,120(1H*))
 1080 FORMAT (1HO,3X,"ELEMENTS",6X,"R-STRATE",7X,"Z-STRATE",7X,"O-STRATE
     1",6X,"RZ-STRATE",9X,"COMPRE",6X,"EF-STRATE",6X,"EF-STRAIN")
```

```
 1090 FORMAT (1HO,3X,"ELEMENTS",6X,"X-STRATE",7X,"Y-STRATE",7X,"Z-STRATE
     1",6X,"XY-STRATE",9X,"COMPRE",6X,"EF-STRATE",6X,"EF-STRAIN")
 1100 FORMAT (1H ,I10,7E15.4)
 1110 FORMAT (1HO,90(1H*))
 1120 FORMAT (1HO,3X,"ELEMENTS",6X,"X-STRESS",7X,"Y-STRESS",7X,"Z-STRESS
     1",6X,"XY-STRESS",5X,"HYD-STRESS")
 1130 FORMAT (1HO,3X,"ELEMENTS",6X,"R-STRESS",7X,"Z-STRESS",7X,"0-STRESS
     1",6X,"RZ-STRESS",5X,"HYD-STRESS")
 1140 FORMAT (1H ,I10,5E15.4)
 1150 FORMAT (1HO,"FORCES CALCULATED AT BOUNDARY NODES",///,5X,"NODES",5
     1X,"FORCE-X",3X,"FORCE-Y")
 1160 FORMAT (1HO,"FORCES CALCULATED AT BOUNDARY NODES",///,5X,"NODES",5
     1X,"FORCE-R",3X,"FORCE-Z")
 1170 FORMAT (1HO,I10,2X,2E10.3)
      END

      SUBROUTINE CONVER (NCONV)
      COMMON /BLK1/ NP,NE,NB,NPC,NMAT,NEQ,NBAND,NITER,TITLE(8),NBF,NEDGE
      COMMON /BLK4/ STR(260,5),EPS(260,6),VEL(2,297),TEPS(260)
      COMMON SK(594,30),R1(594),EST(50,60),FR(25),FZ(25),FPUR(50)
      DIMENSION RC(594)
      EQUIVALENCE (SK,RC)
C
C.....THIS SUBROUTINE CHECKS THE CONVERGENCE.
C
      NCONV = 0
      VCONV = 0.0
      IF (NITER.EQ.0) GO TO 30
      DO 10 N = 1,NP
      NZ = 2*N
      NR = NZ-1
      RC(NZ) = VEL(2,N)
   10 RC(NR) = VEL(1,N)
      ACONV1 = 0.
      ACONV2 = 0.
      DO 20 I = 1,NP
      IZ = I*2
      IR = IZ-1
      DVZ = R1(IZ)-RC(IZ)
      DVR = R1(IR)-RC(IR)
      ACONV2 = ACONV2+(DVR**2+DVZ**2)
      ACONV1 = ACONV1+(RC(IZ)**2+RC(IR)**2)
   20 CONTINUE
      VCONV = SQRT(ACONV2/ACONV1)
      IF (ABS(VCONV).LE.0.005) NCONV = 1
      WRITE (6,1000) NITER,VCONV
   30 DO 40 K = 1,NP
      DO 40 M = 1,2
      IC = (K-1)*2+M
   40 VEL(M,K) = R1(IC)
      RETURN
C
C
 1000 FORMAT (1HO,"NITER=",I2,"VCONV=",E10.4)
      END

      SUBROUTINE MODMES
      COMMON /BLK1/ NP,NE,NB,NPC,NMAT,NEQ,NBAND,NITER,TITLE(8),NBF,NEDGE
      COMMON /BLK2/ CORD(297,2),NOP(260,4),IMAT(260),ELOAD(260,8)
      COMMON /BLK4/ STR(260,5),EPS(260,6),VEL(2,297),TEPS(260)
      COMMON /A/ VRIG,IPLAX,ALPHA,IHARD
      COMMON /B/ NTIMES,NDI,NDJ,NMAX,YSTART,YDIE,YEXIT,YMAX,RENTER,REXIT
     1,RCORE,STEP,NLIN,VSCAL
C
C.....THIS SUBROUTINE MODIFIES THE MESH ACCORDING TO THE VELOCITIES
C
      IF (NITER.LT.5) RETURN
      IF (IPLAX.EQ.1) GO TO 20
      DO 10 I = 1,NP
      DUM1 = CORD(I,1)
      DUM2 = VEL(1,I)
      CORD(I,1) = CORD(I,2)
      VEL(1,I) = VEL(2,I)
      CORD(I,2) = DUM1
   10 VEL(2,I) = DUM2
   20 NIM1 = NDI-1
      NJM1 = NDJ-1
      DO 40 N = 2,NIM1
      NOPI = N
      DO 30 M = 1,NJM1
      NOPJ = NOPI+NIM1
      SLOPEI = VEL(1,NOPI)/VEL(2,NOPI)
      SLOPEJ = VEL(1,NOPJ)/VEL(2,NOPJ)
      ZETA = CORD(NOPJ,2)-CORD(NOPI,2)
      CORD(NOPJ,1) = CORD(NOPI,1)+0.5*ZETA*(SLOPEI+SLOPEJ)
   30 NOPI = NOPJ
   40 CONTINUE
      IF (IPLAX.EQ.1) RETURN
      DO 50 I = 1,NP
      DUM1 = CORD(I,1)
      DUM2 = VEL(1,I)
      CORD(I,1) = CORD(I,2)
      CORD(I,2) = DUM1
      VEL(1,I) = VEL(2,I)
   50 VEL(2,I) = DUM2
      RETURN
      END

      SUBROUTINE HARD (L,EFST,F1)
C
C.....THIS SUBROUTINE CALCULATES THE YIELD STRESS FROM A
C.....EQUATION OF THE FORM  A+B*X+C*X**2+D*X**3+E*X**4+
C                           F*X**5+G*X**6
C
      DIMENSION COEF(7)
      GO TO (10,20), L
C.....ALUMINIUM  (TONS/IN.IN)
   10 COEF(1) = 3.5182
      COEF(2) = 9.998
      COEF(3) = -9.6414
      COEF(4) = 6.0298
      COEF(5) = -1.8814
      COEF(6) = 0.2202
      COEF(7) = 0.0
      GO TO 30
C.....COPPER     (TONS/IN.IN)
   20 COEF(1) = 5.7168
      COEF(2) = 67.7022
      COEF(3) = -111.7871
      COEF(4) = 98.7455
      COEF(5) = -46.0875
      COEF(6) = 10.7608
      COEF(7) = -.9872
   30 F1 = COEF(1)
      XT = EFST
      DO 40 JJ = 2,7
      F1 = F1+COEF(JJ)*XT
      XT = XT*EFST
   40 CONTINUE
      RETURN
      END

      FUNCTION RBAR (RX,RY,RZ,RXY)
C.....THIS FUNCTION CALCULATES THE EFFECTIVE STRAIN RATE.
      S1 = RX*RX
      S2 = RY*RY
      S3 = RZ*RZ
      S4 = RXY*RXY
      RBAR = 2.*SQRT(3.*(S1+S2+S3)/2.+(3.*S4/4.))/3.
      RETURN
      END
```

PROGRAM 2

SOLUTION OF STEADY-STATE PROBLEMS (VELOCITY/PRESSURE)

```
      PROGRAM VELPRE (INPUT,OUTPUT,TAPE6=OUTPUT,TAPE5,TAPE4,TAPE1)
C ***************************************************************************
C * THIS PROGRAM HAS BEEN DESIGNED TO SOLVE STEADY-STATE PROBLEMS IN    *
C * METAL WORKING USING THE FINITE ELEMENT METHOD.                      *
C * THE MATERIAL IS ASSUMED TO BE RIGID-PLASTIC AND INCOMPRESSIBLE,THIS*
C * LATTER CONSTRAINT BEING INTRODUCED USING A LAGRANGE MULTIPLIER.     *
C * THE PROGRAM USES BILINEAR ISOPARAMETRIC ELEMENTS                    *
C ***************************************************************************
C       * WRITTEN BY LUIS A. PACHECO, ING. MEC., M.SC.(MANC) *
C              *IMPERIAL COLLEGE UNIVERSITY OF LONDON*
C                  *FINAL VERSION SUMMER 1978*
C       ***********************************************************
C
C
      COMMON /BLK1/ NP,NE,NB,NPC,NMAT,NEQ,NBAND,NITER,TITLE(18),NBF
      COMMON /BLK2/ CORD(234,2),NOP(204,4),IMAT(204)
      COMMON /A/ VRIG,IPLAX
C
C  READ NECESSARY INPUT INFORMATION
C
      CALL PRELIM
C
C   DETERMINE BANDWIDTH AND NUMBER OF EQUATIONS
C
      NEQ = NP*3
      J = 0
      DO 20 N = 1,NE
      DO 20 I = 1,4
      DO 10 L = 1,4
      KK = IABS(NOP(N,I)-NOP(N,L))
      IF (KK-J.LE.0) GO TO 10
      J = KK
   10 CONTINUE
   20 CONTINUE
      NBAND = 3*(J+1)
      VRIG = 1.E+09
      NLIN = 0
C
C   READ THE EXTERNAL LOADS IF ANY.FORM VECTOR LOAD
C
      NITER = 1
   30 CALL LOAD
C  FORM AND SOLVE THE EQUATION SYSTEM
C
      CALL FORMK
      CALL SOLVE
      CALL CONVER (NCONV)
      IF (NCONV.EQ.1) GO TO 40
      IF (NLIN.EQ.1) GO TO 40
      IF (NITER.EQ.12) GO TO 40
      NITER = NITER+1
      GO TO 30
C
C  CALCULATE FORCES AT BOUNDARY NODAL POINTS IF REQUIRED
C
   40 CALL CFORC
      CALL STRAIN
C
C  WRITE RESULTS
C
      CALL DOUT
      STOP
      END
```

```
      SUBROUTINE PRELIM
C
C  THIS SUBROUTINE READ AND PRINT THE NECESSARY INPUT INFORMATION
C
      COMMON /BLK1/ NP,NE,NB,NPC,NMAT,NEQ,NBAND,NITER,TITLE(18),NBF
      COMMON /BLK2/ CORD(234,2),NOP(204,4),IMAT(204)
      COMMON /BLK3/ YIELD(4),NBC(66),NREST(66),NQ(40),R(40,2),XPRE(66),Y
     1PRE(66),NF(25)
      COMMON /A/ VRIG,IPLAX
      COMMON /B/ INTF,NINTF(50)
C
C  READ TITLE AND CONTROL VARIABLES
C
      READ (5,1050) TITLE
      WRITE (6,1120) TITLE
      READ (5,1000) NP,NE,NB,NPC,NBF,NMAT,I1,IPLAX
      IF (IPLAX.EQ.0) WRITE (6,1070)
      IF (IPLAX.EQ.1) WRITE (6,1090)
      WRITE (6,1080) NP,NE,NB,NPC,NBF,NMAT,I1
C
C  READ MATERIAL INFORMATION
C
      READ (5,1100) (N,YIELD(N),L=1,NMAT)
      WRITE (6,1110)
      WRITE (6,1110)
      WRITE (6,1060) (N,YIELD(N),N=1,NMAT)
C
C  READ NODAL INFORMATION.
C
      READ (5,1010) (N,(CORD(N,M),M=1,2),L=1,NP)
C
C  READ ELEMENTS INFORMATION.
C
      READ (5,1020) (N,(NOP(N,M),M=1,4),IMAT(N),L=1,NE)
C
C  READ BOUNDARY CONDITIONS
C
      READ (5,1030) (NBC(I),NREST(I),XPRE(I),YPRE(I),I=1,NB)
      IF (NBF.EQ.0) GO TO 10
      READ (5,1040) (NF(I),I=1,NBF)
C
C  PRINT INPUT INFORMATION IF REQUIRED.
C
   10 IF (I1.EQ.0) GO TO 20
      WRITE (6,1140)
      WRITE (6,1010) (N,(CORD(N,M),M=1,2),N=1,NP)
      WRITE (6,1150)
      WRITE (6,1020) (N,(NOP(N,M),M=1,4),IMAT(N),N=1,NE)
   20 IF (NBF.EQ.0) GO TO 30
      WRITE (6,1170)
      WRITE (6,1130) (NF(I),I=1,NBF)
   30 WRITE (6,1160)
      WRITE (6,1030) (NBC(I),NREST(I),XPRE(I),YPRE(I),I=1,NB)
      RETURN
C
 1000 FORMAT (8I5)
 1010 FORMAT (I10,2F10.3)
 1020 FORMAT (6I5)
 1030 FORMAT (2I10,2F10.3)
 1040 FORMAT (16I5)
 1050 FORMAT (18A4)
 1060 FORMAT (1H ,I5,F15.4)
 1070 FORMAT (1HO,"PLANE STRAIN PROBLEM",/,1H ,20(1H*))
 1080 FORMAT (1HO,"NUMBER OF NODES=",I3,/,1H ,"NUMBER OF ELEMENTS=",I3,/
```

```
     1,1H ,"NUMBER OF NODES WITH BOUNDARY CONDITIONS=",I3,/,1H ,"NUMBER
     2OF LOADED NODES=",I3,/,1H ,"NUMBER OF NODES WHERE REACTIONS ARE CA
     3LCULATED=",I3,/,1H ,"NUMBER OF MATERIALS=",I3,/,1H ,"PRINT CONTROL
     4 VARIABLE(I1)=",I2)
 1090 FORMAT (1HO,"AXISYMMETRIC PROBLEM",/,1H ,20(1H*))
 1100 FORMAT (I5,F15.4)
 1110 FORMAT (1H ,2X,"MAT",3X,"YIELD POINT",/,1H ,9X,"(KG/CM++2)")
 1120 FORMAT (1H1,18A4)
 1130 FORMAT (1H ,20I5)
 1140 FORMAT (1HO,6X,"NODES",3X,"COORD X",3X,"COORD Y",/,1H ,14X,"(CMS)"
     1,5X,"(CMS)")
 1150 FORMAT (1HO,"ELEMENT",4X,"NODES",9X,"IMAT")
 1160 FORMAT (1HO,"BOUNDARY CONDITIONS",/,1H ,5X,"NODES",4X,"CONDITION",
     13X,"XPRE",5X,"YPRE")
 1170 FORMAT (1HO,"THE NODAL POINTS AT WHICH FORCE CALCULATIONS ARE DESI
     1RED")
 1180 FORMAT (1HO,"MATERIAL PROPERTIES")
      END
      SUBROUTINE LOAD
C
C  THIS SUBROUTINE FORM THE VECTOR LOAD R1.
C
      COMMON /BLK1/ NP,NE,NB,NPC,NMAT,NEQ,NBAND,NITER,TITLE(18),NBF
      COMMON /BLK3/ YIELD(4),NBC(66),NREST(66),NQ(40),R(40,2),XPRE(66),Y
     1PRE(66),NF(25)
      COMMON SK(468,39),R1(468),EST(50,78),FR(25),FZ(25),FPUR(50)
C
C  ZERO LOAD ARRAY.
C
      DO 10 J = 1,NEQ

   10 R1(J) = 0.0
      IF (NPC.EQ.0.AND.NITER.GT.1) RETURN
      IF (NPC.EQ.0) GO TO 50
      IF (NITER.GT.1) GO TO 30
      WRITE (6,1000)
      DO 20 N = 1,NPC
      READ (5,1010) NQ(N),(R(N,K),K=1,2)
      WRITE (6,1010) NQ(N),(R(N,K),K=1,2)
   20 CONTINUE
   30 DO 40 N = 1,NPC
      DO 40 K = 1,2
      IC = (NQ(N)-1)*3+K
   40 R1(IC) = R(N,K)+R1(IC)
      GO TO 60
   50 WRITE (6,1020)
   60 RETURN
C
 1000 FORMAT (1HO,"PRESCRIBED EXTERNAL LOADS",1HO,"NODES",3X,"FORCE-X",3
     1X,"FORCE-Y")
 1010 FORMAT (I5,2F10.3)
 1020 FORMAT (1HO,"NO EXTERNAL LOADS PRESCRIBED")
      END
      SUBROUTINE FORMK
C
C.....THIS SUBROUTINE FORMS THE OVERALL STIFFNESS MATRIX.
C
      COMMON /BLK1/ NP,NE,NB,NPC,NMAT,NEQ,NBAND,NITER,TITLE(18),NBF
      COMMON /BLK2/ CORD(234,2),NOP(204,4),IMAT(204)
      COMMON /BLK3/ YIELD(4),NBC(66),NREST(66),NQ(40),R(40,2),XPRE(66),Y
     1PRE(66),NF(25)
      COMMON SK(468,39),R1(468),EST(50,78),FR(25),FZ(25),FPUR(50)
      DIMENSION SE(12,12), ICODE(234)
C  INITIALIZE THE ARRAYS
      DO 10 I = 1,NP
   10 ICODE(I) = 0
      DO 20 N = 1,NEQ
      DO 20 M = 1,NBAND
   20 SK(N,M) = 0.0
C
C  THE PRESSURE VARIABLE IS ASSIGNED TO THE HIGHEST NUMBERED NODE
C
      DO 30 N = 1,NE
      MID = MAXO(NOP(N,1),NOP(N,2),NOP(N,3),NOP(N,4))
   30 ICODE(MID) = 1D
C
C  SCAN ELEMENTS
C
      NDF = 3
      DO 100 II = 1,NE
      CALL QUAD2 (SE,NITER,II)
C
C  FORM THE STIFFNESS MATRIX SK
C
C  FIRST ROWS
C
      DO 90 JJ = 1,4
      NROWB = (NOP(II,JJ)-1)*NDF
      IF (NROWB) 90,40,40
   40 DO 80 J = 1,NDF
      NROWB = NROWB+1
      I = (JJ-1)*NDF+J
C
C  THEN COLUMNS
C
      DO 70 KK = 1,4
      NCOLB = (NOP(II,KK)-1)*NDF
      DO 60 K = 1,NDF
      L = (KK-1)*NDF+K
      NCOL = NCOLB+K+1-NROWB
C
C  SKIP STORING IF BELOW BAND
C
      IF (NCOL) 60,60,50
   50 SK(NROWB,NCOL) = SK(NROWB,NCOL)+SE(I,L)
   60 CONTINUE
   70 CONTINUE
   80 CONTINUE
   90 CONTINUE
  100 CONTINUE
C
C  PREPARATION FOR FORCE CALCULATION
C  STORE THE ROWS OF SK WHICH ARE NECESSARY.
C
      IF (NBF.EQ.0) GO TO 160
      NBAND2 = 2*NBAND-1
      DO 110 I = 1,NBF
      IZ = 2*I
      IR = IZ-1
      DO 110 J = 1,NBAND2
      EST(IZ,J) = 0.0
  110 EST(IR,J) = 0.0
      DO 150 I = 1,NBF
      II = NF(I)
      IZ = 3*II-1
      IR = IZ-1
      IIZ = 2*I
      IIR = IIZ-1
```

```
      DO 120 J = NBAND,NBAND2
      JJ = J-NBAND+1
      EST(IIR,J) = SK(IR,JJ)
  120 EST(IIZ,J) = SK(IZ,JJ)
      DO 140 J = 1,NBAND
      NR = IR-J+1
      NZ = IZ-J+1
      JJ = NBAND-J+1
      IF (NR.LE.0) GO TO 130
      EST(IIR,JJ) = SK(NR,J)
  130 IF (NZ.LE.0) GO TO 140
      EST(IIZ,JJ) = SK(NZ,J)
  140 CONTINUE
      FPUR(IIR) = R1(IR)
  150 FPUR(IIZ) = R1(IZ)
C
C  INSERT DISPLACEMENT BOUNDARY CONDITIONS
C
  160 DO 170 N = 1,NB
      I = NBC(N)
      IR = 3*I-2
      IZ = IR+1
      NC = NREST(N)
C
C  CHECK IF THE X VELOCITY IS PRESCRIBED
C
      IF (NC.EQ.1.OR.NC.EQ.11) CALL CONDE (IR,XPRE(N))
C
C  CHECK IF THE Y VELOCITY IS PRESCRIBED
C
      IF (NC.EQ.2.OR.NC.EQ.11) CALL CONDE (IZ,YPRE(N))
C
C  CHECK IF THE POINT IS ALONG AN INCLINED BOUNDARY
C
      IF (NC.EQ.3) THETA = XPRE(N)*3.1415927/180.
      IF (NC.EQ.3) CALL BCMIX (I,THETA)
  170 CONTINUE
C
C.....CHECK THE POINTS WITH INFORMATION ABOUT THE MEAN STRESS.
C
      DO 180 N = 1,NP
      IC = ICODE(N)
      IP = 3*N
  180 IF (IC.NE.10) CALL CONDE (IP,0.)
      RETURN
      END
      SUBROUTINE QUAD2 (SE,NITER,N)
C
C.....THIS SUBROUTINE FORMS THE ELEMENTAL STIFFNESS MATRIX.
C
      COMMON /BLK2/ CORD(234,2),NOP(204,4),IMAT(204)
      COMMON /BLK3/ YIELD(4),NBC(66),NREST(66),NQ(40),R(40,2),XPRE(66),Y
     1PRE(66),NF(25)
      DIMENSION D(4,4), SE(12,12), A(4,8), XL(4), YL(4)
      REAL SEU(8,8), M(8), SEP(8)
      COMMON /A/ VRIG,IPLAX
      DIMENSION B(4,8), SHP(3,9), SG(9), WG(9), TG(9)
C.....INITIALIZE THE ARRAYS
      NNE = 4
      NNE2 = NNE*2
      DO 10 I = 1,4
      DO 10 J = 1,4
   10 D(I,J) = 0.0
      DO 20 I = 1,NNE2
      SEP(I) = 0.0
      DO 20 J = 1,NNE2
   20 SEU(I,J) = 0.0
      DO 30 I = 1,3
   30 M(I) = 1.0
      M(4) = 0.0
      DO 40 I = 1,12
      DO 40 J = 1,12
   40 SE(I,J) = 0.0
      DO 50 MM = 1,NNE
      XL(MM) = CORD(NOP(N,MM),1)
   50 YL(MM) = CORD(NOP(N,MM),2)
      NINT = 2
C.....COMPUTE GAUSS POINTS AND WEIGHT FACTORS
      CALL PGAUSS (NINT,LINT,SG,TG,WG)
C.....FORM STRAIN DISPLACEMENT MATRIX B.
      DO 170 L = 1,LINT
      XBAR = 0.0
      DO 60 NN = 1,3
      DO 60 LL = 1,NNE
   60 SHP(NN,LL) = 0.0
      CALL SHAPE (SG(L),TG(L),XL,YL,SHP,DETJAC,NNE)
      DO 70 LI = 1,NNE
      J = 2*LI
      I = J-1
      B(1,I) = SHP(1,LI)
      B(1,J) = 0.0
      B(2,I) = 0.0
      B(2,J) = SHP(2,LI)
      B(3,I) = 0.0
      B(3,J) = 0.0
      B(4,I) = B(2,J)
   70 B(4,J) = B(1,I)
C.....IN CASE OF PLANE STRAIN ANALYSIS DO NOT INCLUDE
C.....THE NORMAL STRAIN COMPONENT
      IF (IPLAX.EQ.0) GO TO 120
      DO 80 KI = 1,NNE
   80 XBAR = XBAR+SHP(3,KI)*XL(KI)
C.....EVALUATE THE HOOP STRAIN DISPLACEMENT RELATION
      IF (XBAR.GT.0.00000001) GO TO 100
C.....FOR THE CASE OF ZERO RADIUS EQUATE RADIAL TO HOOP STRAIN
      DO 90 KI = 1,NNE2
   90 B(3,KI) = B(1,KI)
      GO TO 120
C.....NON-ZERO RADIUS
  100 DUMA = 1./XBAR
      DO 110 KI = 1,NNE
      LH = 2*KI-1
  110 B(3,LH) = SHP(3,KI)*DUMA
C.....FORM THE STRESS-STRAIN MATRIX
  120 IF (NITER.EQ.1) EPSR = 1.0
      IF (NITER.GT.1) CALL STRA (NNE,N,B,EPSR)
      LL = IMAT(N)
      DUM3 = 2.*YIELD(LL)/(3.*EPSR)
      IF (DUM3.GE.VRIG) DUM3 = VRIG
      D(1,1) = DUM3
      D(2,2) = DUM3
      D(3,3) = DUM3
      D(4,4) = DUM3/2.
C.....COMPUTE THE PRODUCT D*B
      DO 130 I = 1,4
      DO 130 J = 1,NNE2
      A(I,J) = 0.0
      DO 130 K = 1,4
```

```
  130 A(I,J) = A(I,J)+D(I,K)*B(K,J)
C.....COMPUTE (B**T *(D*B) AND ADD CONTRIBUTION TO ELEMENT STIFFNESS
      IF (IPLAX.EQ.0) XBAR = 1.0
      WT = XBAR*WG(L)*DETJAC
C.....SEP IS PRESSURE STIFFNES MATRIX
      DO 140 I = 1,NNE2
      DO 140 J = 1,4
  140 SEP(I) = SEP(I)+M(J)*B(J,I)*WT
      DO 160 NROW = 1,NNE2
      DO 150 NCOL = NROW,NNE2
      DUM2 = 0.0
C.....SEU IS VELOCITY STIFFNESS MATRIX
      DO 150 LI = 1,4
  150 DUM2 = DUM2+B(LI,NROW)*A(LI,NCOL)
      SEU(NROW,NCOL) = SEU(NROW,NCOL)+DUM2*WT
  160 CONTINUE
  170 CONTINUE
C.....COMPLETE SE BY SYMMETRY.
      DO 180 K = 2,NNE2
      DO 180 L = 1,K
  180 SEU(K,L) = SEU(L,K)
C
C.....ASSEMBLE ELEMENTAL STIFFNESS FROM THE SEU AND SEP
C
      IXY2 = MAXO(NOP(N,1),NOP(N,2),NOP(N,3),NOP(N,4))
      DO 220 I = 1,NNE
      IF (NOP(N,I).NE.IXY2) GO TO 200
      IP = 3*I
      DO 190 J = 1,NNE
      IX = 3*J-2
      IIX = 2*J-1
      IY = 3*J-1
      IIY = 2*J
      SE(IX,IP) = SEP(IIX)
      SE(IY,IP) = SEP(IIY)
      SE(IP,IX) = SE(IX,IP)
  190 SE(IP,IY) = SE(IY,IP)
  200 LX = 3*I-2
      LY = LX+1
      LLX = 2*I-1
      LLY = LLX+1
      DO 210 K = 1,NNE
      KX = 3*K-2
      KY = KX+1
      KKX = 2*K-1
      KKY = KKX+1
      SE(LX,KX) = SEU(LLX,KKX)
      SE(LX,KY) = SEU(LLX,KKY)
      SE(LY,KX) = SEU(LLY,KKX)
  210 SE(LY,KY) = SEU(LLY,KKY)
  220 CONTINUE
      RETURN
      END
      SUBROUTINE PGAUSS (L,LINT,R,Z,W)
C
C.....GAUSS POINTS AND WEIGHTS FOR TWO DIMENSIONS
C
      REAL LR(9), LZ(9), LW(9), R(9), Z(9), W(9)
      DATA LR/-1.,1.,1.,-1.,0.,-1.,0.,-1.,0./
      DATA LZ/-1.,-1.,1.,1.,-1.,0.,1.,0.,0./
      DATA LW/4*25.,4*40.,64./
      LINT = L*L
      GO TO (10,20,40), L
C.....1X1 INTEGRATION
   10 R(1) = 0.
      Z(1) = 0.
      W(1) = 4.
      RETURN
C.....2X2 INTEGRATION
   20 G = 1./SQRT(3.)
      DO 30 I = 1,4
      R(I) = G*LR(I)
      Z(I) = G*LZ(I)
   30 W(I) = 1.
      RETURN
C....3X3 INTEGRATION
   40 G = SQRT(0.6)
      H = 1./81.
      DO 50 I = 1,9
      R(I) = G*LR(I)
      Z(I) = G*LZ(I)
   50 W(I) = H*LW(I)
      RETURN
      END
      SUBROUTINE SHAPE (SS,TT,XL,YL,SHP,DETJAC,NNE)
C
C     SHAPE FUNCTION SUBROUTINE FOR TWO DIMENSIONAL ELEMENTS
C
      REAL SHP(3,9), XL(4), YL(4), S(4), T(4), JAC(2,2)
      DATA S/-0.5,0.5,0.5,-0.5/,T/-0.5,-0.5,0.5,0.5/
C.....FORM 4 NODE QUADRILATERAL SHAPE FUNCTION
      DO 10 I = 1,4
      SHP(3,I) = (0.5+S(I)*SS)*(0.5+T(I)*TT)
      SHP(1,I) = S(I)*(0.5+T(I)*TT)
   10 SHP(2,I) = T(I)*(0.5+S(I)*SS)
C.....CONSTRUCT JACOBIAN, ITS INVERSE AND ITS DETERMINANT.
      DO 20 I = 1,2
      DO 20 J = 1,2
   20 JAC(I,J) = 0.D
      DO 30 K = 1,NNE
      JAC(1,1) = JAC(1,1)+SHP(1,K)*XL(K)
      JAC(1,2) = JAC(1,2)+SHP(1,K)*YL(K)
      JAC(2,1) = JAC(2,1)+SHP(2,K)*XL(K)
   30 JAC(2,2) = JAC(2,2)+SHP(2,K)*YL(K)
      DETJAC = JAC(1,1)*JAC(2,2)-JAC(1,2)*JAC(2,1)
      DUM1 = JAC(1,1)/DETJAC
      JAC(1,1) = JAC(2,2)/DETJAC
      JAC(2,1) = -JAC(2,1)/DETJAC
      JAC(1,2) = -JAC(1,2)/DETJAC
      JAC(2,2) = DUM1
C.....FORM GLOBAL DERIVATIVES
      DO 40 I = 1,NNE
      TP = SHP(1,I)*JAC(1,1)+SHP(2,I)*JAC(1,2)
      SHP(2,I) = SHP(1,I)*JAC(2,1)+SHP(2,I)*JAC(2,2)
   40 SHP(1,I) = TP
      RETURN
      END
      SUBROUTINE STRA (NNE,M,BA,EPSR)
C
C.....CALCULATE STRAIN RATES AT THE INTEGRATION POINTS.
C
      COMMON /BLK1/ NP,NE,NB,NPC,NMAT,NEQ,NBAND,NITER,TITLE(18),NBF
      COMMON /BLK2/ CORD(234,2),NOP(204,4),IMAT(204)
      COMMON /BLK4/ STR(204,6),EPS(204,6),VEL(2,234)
      DIMENSION BA(4,8), E(4), RA(8)
      NK = NNE
      DO 10 J = 1,NK
      KK = NOP(M,J)
```

```
      KI = (J-1)*2
      DO 10 JJ = 1,2
      IJ = JJ+KI
   10 RA(IJ) = VEL(JJ,KK)
      DO 20 KK = 1,4
      E(KK) = 0.0
      DO 20 J = 1,NNE*2
   20 E(KK) = E(KK)+BA(KK,J)*RA(J)
      EPSR = RBAR(E(1),E(2),E(3),E(4))
      RETURN
      END
      SUBROUTINE CONDE (N,U)
C
C  THIS SUBROUTINE PERFORM THE MATRIX CONDENSATION WHEN
C  THE VALUE OF A COMPONENT OF X IN AX=B IS SPECIFIED.
C
      COMMON /BLK1/ NP,NE,NB,NPC,NMAT,NEQ,NBAND,NITER,TITLE(18),NBF
      COMMON SK(468,39),R1(468),EST(50,78),FR(25),FZ(25),FPUR(50)
      DO 10 M = 2,NBAND
      KK = N+M-1
      IF (KK.GT.NEQ) GO TO 10
      R1(KK) = R1(KK)-SK(N,M)*U
   10 CONTINUE
      DO 20 M = 2,NBAND
      K = N-M+1
      IF (K.LE.0) GO TO 20
      R1(K) = R1(K)-SK(K,M)*U
      SK(K,M) = 0.
   20 SK(N,M) = 0.
      SK(N,1) = 1.
      R1(N) = U
      RETURN
      END
      SUBROUTINE BCMIX (N,THETA)
C
C  SINCE UR=UZ*TAN(THETA) ALONG THE DIE,ACORRESPONDING CHANGE
C  IS MADE IN THE STIFFNESS EQUATIONS FOR ROWS AND COLUMNS CORRESPONDING
C  TO THESE COMPONENTS..THEN THE EQUATIONS CONTAINING UR ARE ELIMINATED.
C
      COMMON /BLK1/ NP,NE,NB,NPC,NMAT,NEQ,NBAND,NITER,TITLE(18),NBF
      COMMON SK(468,39),R1(468),EST(50,78),FR(25),FZ(25),FPUR(50)
      COMMON /A/ VRIG,IPLAX
      NZ = 3*N-1
      NR = NZ-1
      ALPA = 1./TAN(THETA)
      IF (IPLAX.EQ.1) ALPA = TAN(THETA)
      DO 10 M = 1,NBAND
   10 SK(NR,M) = SK(NR,M)*ALPA
      SK(NR,1) = SK(NR,1)*ALPA
      SK(NR,2) = SK(NR,2)*2.
      DO 20 M = 2,NBAND
      KR = NR-M+1
      IF (KR.LE.0) GO TO 30
   20 SK(KR,M) = SK(KR,M)*ALPA
   30 R1(NR) = R1(NR)*ALPA
      DO 50 M = 2,NBAND
      KZ = NZ-M+1
      IF (KZ.LE.0) GO TO 40
      SK(KZ,M) = SK(KZ,M)+SK(KZ,M-1)
   40 IF (M.EQ.NBAND) GO TO 50
      KZ = NZ+M-1
      IF (KZ.GT.NEQ) GO TO 50
      SK(NZ,M) = SK(NZ,M)+SK(NR,M+1)
   50 CONTINUE
      SK(NZ,1) = SK(NZ,1)+SK(NR,2)
      SK(NR,1) = 1.0
      DO 70 M = 2,NBAND
      KR = NR-M+1
      IF (KR.LE.0) GO TO 60
      SK(KR,M) = 0.
   60 SK(NR,M) = 0.
   70 CONTINUE
      R1(NZ) = R1(NZ)+R1(NR)
      R1(NR) = 0.
      RETURN
      END
      SUBROUTINE SOLVE
C
C  THIS SUBROUTINE PERFORMS THE SOLUTION OF THE
C     EQUATION SYSTEM AX=B.
C
      COMMON /BLK1/ NP,NE,NB,NPC,NMAT,NEQ,NBAND,NITER,TITLE(18),NBF
      COMMON /BLK3/ YIELD(4),NBC(66),NREST(66),NQ(40),R(40,2),XPRE(66),Y
     1PRE(66),NF(25)
      COMMON SK(468,39),R1(468),EST(50,78),FR(25),FZ(25),FPUR(50)
      COMMON /A/ VRIG,IPLAX
C
C  REDUCE MATRIX
C
      DO 60 N = 1,NEQ
      IF (SK(N,1)) 10,60,10
   10 I = N
      DO 50 L = 2,NBAND
      I = I+1
      IF (SK(N,L)) 20,50,20
   20 C = SK(N,L)/SK(N,1)
      J = 0
      DO 40 K = L,NBAND
      J = J+1
      IF (SK(N,K)) 30,40,30
   30 SK(I,J) = SK(I,J)-C*SK(N,K)
   40 CONTINUE
      SK(N,L) = C
C
C
C  AND LOAD VECTOR FOR EACH EQUATION.
      R1(I) = R1(I)-C*R1(N)
   50 CONTINUE
      R1(N) = R1(N)/SK(N,1)
   60 CONTINUE
C
C  BACK SUBSTITUTION
C
      N = NEQ
   70 N = N-1
      IF (N) 110,110,80
   80 L = N
      DO 100 K = 2,NBAND
      L = L+1
      IF (SK(N,K)) 90,100,90
   90 R1(N) = R1(N)-SK(N,K)*R1(L)
  100 CONTINUE
      GO TO 70
  110 DO 120 I = 1,NB
      IZ = 3*NBC(I)-1
      IR = IZ-1
      IF (NREST(I).EQ.3) THETA = XPRE(I)*3.1415927/180.
      IF (NREST(I).EQ.3.AND.IPLAX.EQ.0) ALPA = 1./TAN(THETA)
```

```
      IF (NREST(I).EQ.3.AND.IPLAX.EQ.1) ALPA = TAN(THETA)
  120 IF (NREST(I).EQ.3) R1(IR) = R1(IZ)*ALPA
      RETURN
      END
      SUBROUTINE STRAIN
C
C.....THIS SUBROUTINE CALCULATES STRAIN RATES,STRESSES AND COORDINATES
C.....AT SAMPLING POINTS(CENTROIDS IN THE CASE OF BILINEAR ELEMENT.)
C
      COMMON /BLK1/ NP,NE,NB,NPC,NMAT,NEQ,NBAND,NITER,TITLE(18),NBF
      COMMON /BLK2/ CORD(234,2),NOP(204,4),IMAT(204)
      COMMON /BLK3/ YIELD(4),NBC(66),NREST(66),NQ(40),R(40,2),XPRE(66),Y
     1PRE(66),NF(25)
      COMMON /BLK4/ STR(204,6),EPS(204,6),VEL(2,234)
      COMMON /A/ VRIG,IPLAX
      COMMON SK(468,39),R1(468),EST(50,78),FR(25),FZ(25),FPUR(50)
      DIMENSION SHP(3,9), SG(9), TG(9), WG(9), U(2,9)
      DIMENSION XL(9), YL(9), E(6)
      REWIND 1
      DO 100 N = 1,NE
      NNE = 4
      IF (NOP(N,4).EQ.0) NNE = 3
      DO 10 MM = 1,NNE
      XL(MM) = CORD(NOP(N,MM),1)
      YL(MM) = CORD(NOP(N,MM),2)
      U(1,MM) = VEL(1,NOP(N,MM))
   10 U(2,MM) = VEL(2,NOP(N,MM))
      L = 1
      CALL PGAUSS (L,LINT,SG,TG,WG)
      DO 90 JJ = 1,LINT
      DO 20 NN = 1,3
      DO 20 LL = 1,NNE
   20 SHP(NN,LL) = 0.0
C.....COMPUTE ELEMENT SHAPE FUNCTIONS.
      CALL SHAPE (SG(JJ),TG(JJ),XL,YL,SHP,DETJAC,NNE)
C.....COMPUTE CORDINATES AND STRAINS.
      DO 30 I = 1,6
   30 E(I) = 0.0
      XBAR = 0.0
      YBAR = 0.0
      DO 40 J = 1,NNE
      XBAR = XBAR+SHP(3,J)*XL(J)
   40 YBAR = YBAR+SHP(3,J)*YL(J)
      DO 50 J = 1,NNE
      E(1) = E(1)+SHP(1,J)*U(1,J)
      E(2) = E(2)+SHP(2,J)*U(2,J)
      E(3) = E(3)+SHP(3,J)/XBAR*U(1,J)
      IF (IPLAX.EQ.0) E(3) = 0.0
   50 E(4) = E(4)+SHP(1,J)*U(2,J)+SHP(2,J)*U(1,J)
      DO 60 J = 1,4
   60 EPS(N,J) = E(J)
      EPS(N,6) = RBAR(E(1),E(2),E(3),E(4))
      EPS(N,5) = E(1)+E(2)+E(3)
      YYLD = YIELD(IMAT(N))
C.....CALCULATE STRESSES
      DO 70 KK = 1,4
   70 STR(N,KK) = EPS(N,KK)*2./3.*YYLD/EPS(N,6)
      STR(N,4) = STR(N,4)*0.5
      MID = MAXO(NOP(N,1),NOP(N,2),NOP(N,3),NOP(N,4))
      IP = 3*MID
      STR(N,5) = R1(IP)
      DO 80 KK = 1,3
      STR(N,KK) = STR(N,KK)+STR(N,5)
   80 IF (IPLAX.EQ.0) STR(N,3) = 0.0
C.....SAVE INFORMATION FOR LATER PUNCHING.
      WRITE (1,1000) XBAR,YBAR,EPS(N,1),EPS(N,2),EPS(N,3),EPS(N,4),EPS(N
     1,6)
      WRITE (1,1010) ((STR(N,I),I=1,5),TEPS(N))
   90 CONTINUE
  100 CONTINUE
      RETURN
C
C
C
 1000 FORMAT (2F10.5,5E12.5)
 1010 FORMAT (6E12.5)
      END
      SUBROUTINE DOUT
      COMMON /BLK1/ NP,NE,NB,NPC,NMAT,NEQ,NBAND,NITER,TITLE(18),NBF
      COMMON /BLK2/ CORD(234,2),NOP(204,4),IMAT(204)
      COMMON /BLK3/ YIELD(4),NBC(66),NREST(66),NQ(40),R(40,2),XPRE(66),Y
     1PRE(66),NF(25)
      COMMON /BLK4/ STR(204,5),EPS(204,6),VEL(2,234)
      COMMON SK(468,39),R1(468),EST(50,60),FR(25),FZ(25),FPUR(50)
      COMMON /A/ VRIG,IPLAX
C...SAVE MESH DESCRIPTION FOR LATER PUNCHING..
      REWIND 4
      WRITE (4,1000) (N,(CORD(N,M),M=1,2),(VEL(M,N),M=1,2),N=1,NP)
      WRITE (4,1010) (N,(NOP(N,M),M=1,4),IMAT(N),N=1,NE)
      WRITE (6,1020) TITLE
C
C.....WRITE VELOCITY DISTRIBUTION
C
      WRITE (6,1030)
      IF (IPLAX.EQ.0) WRITE (6,1050) NITER
      IF (IPLAX.EQ.1) WRITE (6,1040) NITER
      WRITE (6,1060) (M,(VEL(J,M),J=1,2),(CORD(M,J),J=1,2),M=1,NP)
C.....WRITE STRAIN RATE AND STRESS DISTRIBUTION.
      WRITE (6,1070)
      IF (IPLAX.EQ.0) WRITE (6,1090)
      IF (IPLAX.EQ.1) WRITE (6,1080)
      WRITE (6,1070)
      WRITE (6,1100) (N,(EPS(N,J),J=1,6),TEPS(N),N=1,NE)
      WRITE (6,1110)
      IF (IPLAX.EQ.0) WRITE (6,1120)
      IF (IPLAX.EQ.1) WRITE (6,1130)
      WRITE (6,1110)
      WRITE (6,1140) (N,(STR(N,J),J=1,5),N=1,NE)
      WRITE (6,1110)
C
C.....WRITE FORCES AT NODES  IF DESIRED
C
      IF (NBF.LE.0) GO TO 10
      IF (IPLAX.EQ.0) WRITE (6,1150)
      IF (IPLAX.EQ.1) WRITE (6,1160)
      WRITE (6,1170) (NF(I),FR(I),FZ(I),I=1,NBF)
      WRITE (4,1170) (NF(I),FR(I),FZ(I),I=1,NBF)
   10 RETURN
C
C
C
 1000 FORMAT (I10,2F10.4,2E15.6)
 1010 FORMAT (6I5)
 1020 FORMAT (1H1,8A10)
 1030 FORMAT (///,15X,"VELOCITIES")
 1040 FORMAT (1H ,15X,"NUMBER OF ITERATIONS",I3,//,1H ,4X,"NODES",7X,"VE
     1LOC-R",8X,"VELOC-Z")
 1050 FORMAT (1H ,15X,"NUMBER OF ITERATIONS",I3,//,1H ,4X,"NODES",7X,"VE
```

```
     1L0C-X",8X,"VEL0C-Y")
 1060 F0RMAT (I10,2E15.6,5X,2F10.4)
 1070 F0RMAT (1H0,120(1H*))
 1080 F0RMAT (1H0,3X,"ELEMENTS",6X,"R-STRATE",7X,"Z-STRATE",7X,"0-STRATE
     1",6X,"RZ-STRATE",9X,"C0MPRE",6X,"EF-STRATE",6X,"EF-STRAIN")
 1090 F0RMAT (1H0,3X,"ELEMENTS",6X,"X-STRATE",7X,"Y-STRATE",7X,"Z-STRATE
     1",6X,"XY-STRATE",9X,"C0MPRE",6X,"EF-STRATE",6X,"EF-STRAIN")
 1100 F0RMAT (1H ,I10,7E15.4)
 1110 F0RMAT (1H0,90(1H*))
 1120 F0RMAT (1H0,3X,"ELEMENTS",6X,"X-STRESS",7X,"Y-STRESS",7X,"Z-STRESS
     1",6X,"XY-STRESS",5X,"HYD-STRESS")
 1130 F0RMAT (1H0,3X,"ELEMENTS",6X,"R-STRESS",7X,"Z-STRESS",7X,"0-STRESS
     1",6X,"RZ-STRESS",5X,"HYD-STRESS")
 1140 F0RMAT (1H ,I10,5E15.4)
 1150 F0RMAT (1H0,"F0RCES CALCULATED AT B0UNDARY N0DES",///,5X,"N0DES",5
     1X,"F0RCE-X",3X,"F0RCE-Y")
 1160 F0RMAT (1H0,"F0RCES CALCULATED AT B0UNDARY N0DES",///,5X,"N0DES",5
     1X,"F0RCE-R",3X,"F0RCE-Z")
 1170 F0RMAT (1H0,I10,2X,2E10.3)
      END
      SUBR0UTINE CF0RC
      C0MM0N /BLK1/ NP,NE,NB,NPC,NMAT,NEQ,NBAND,NITER,TITLE(18),NBF
      C0MM0N /BLK3/ YIELD(4),NBC(66),NREST(66),NQ(40),R(40,2),XPRE(66),Y
     1PRE(66),NF(25)
      C0MM0N SK(468,39),R1(468),EST(50,78),FR(25),FZ(25),FPUR(50)
C
C  THIS SUBR0UTINE 0ETERMINES F0RCES 0N THE B0UN0ARIES.
C
      IF (NBF.LE.0) G0 T0 40
      NBAND2 = 2*NBAND-1
      00 30 I = 1,NBF
      IR = 3*NF(I)-2
      IIZ = 2*I
      IIR = IIZ-1
      SUMR = 0.0
      SUMZ = 0.0
      00 20 J = 1,NBAND2
      JR = IR+J-NBAND
      JZ = JR+1
      IF (JR.LE.0) G0 T0 10
      SUMR = SUMR+EST(IIR,J)*R1(JR)
   10 IF (JZ.LE.0) G0 T0 20
      SUMZ = SUMZ+EST(IIZ,J)*R1(JZ)
   20 C0NTINUE
      FR(I) = SUMR-FPUR(IIR)
      FZ(I) = SUMZ-FPUR(IIZ)
   30 C0NTINUE
   40 RETURN
      END
      SUBR0UTINE C0NVER (NC0NV)
      C0MM0N /BLK1/ NP,NE,NB,NPC,NMAT,NEQ,NBAND,NITER,TITLE(18),NBF
      C0MM0N /BLK2/ C0R0(234,2),N0P(204,4),IMAT(204)
      C0MM0N /BLK4/ STR(204,6),EPS(204,6),VEL(2,234)
      C0MM0N SK(468,39),R1(468),EST(50,78),FR(25),FZ(25),FPUR(50)
      C0MM0N /B/ INTF,NINTF(50)
      DIMENSI0N RC(648)
      EQUIVALENCE (SK,RC)
C
C  THIS SUBR0UTINE CHECKS THE C0NVERGENCE.
C
      NC0NV = 0
      IF (NITER.EQ.1) G0 T0 30
      00 10 N = 1,NP
      NZ = 3*N-1
      NR = NZ-1
      RC(NZ) = VEL(2,N)
   10 RC(NR) = VEL(1,N)
      AC0NV1 = 0.
      AC0NV2 = 0.
      00 20 I = 1,NP
      IZ = I*3-1
      IR = IZ-1
      DVZ = R1(IZ)-RC(IZ)
      DVR = R1(IR)-RC(IR)
      AC0NV2 = AC0NV2+(DVR**2+DVZ**2)
      AC0NV1 = AC0NV1+(RC(IZ)**2+RC(IR)**2)
   20 C0NTINUE
      VC0NV = SQRT(AC0NV2/AC0NV1)
      IF (ABS(VC0NV).LE.0.003) NC0NV = 1
      WRITE (6,1000) NITER,VC0NV
   30 00 40 K = 1,NP
      00 40 M = 1,2
      IC = (K-1)*3+M
   40 VEL(M,K) = R1(IC)
      RETURN
C
 1000 F0RMAT (1H0,"NITER=",I2,"VC0NV=",E10.4)
      END
      FUNCTI0N RBAR (RX,RY,RZ,RXY)
C  THIS FUNCTI0N CALCULATES THE EFFECTIVE STRAIN RATE
      S1 = RX*RX
      S2 = RY*RY
      S3 = RZ*RZ
      S4 = RXY*RXY
      RBAR = 2.*SQRT(3.*(S1+S2+S3)/2.+(3.*S4/4.))/3.
      RETURN
      END
```

PROGRAM 3

SOLUTION OF NON-STEADY STATE PROBLEMS
(PENALTY FUNCTION)

```
      PROGRAM INCRE (INPUT,OUTPUT,TAPE6=OUTPUT,TAPE5,TAPE4,TAPE62)
C*****************************************************************
C* THIS PROGRAM IS DESIGNED TO SOLVE NONSTEADY-STATE PROBLEMS IN ME- *
C* TAL FORMING USING THE FINITE ELEMENT METHOD.                     *
C* THE MATERIAL IS ASSUMED TO BE RIGID-PLASTIC AND INCOMPRESSIBLE,  *
C* THIS LATTER CONSTRAINT BEING INTRODUCED BY MEANS OF A PENALTY    *
C* FUNCTION.                                                        *
C* THE PROGRAM USES BILINEAR ISOPARAMETRIC ELEMENTS WITH REDUCED/SE- *
C* LECTIVE INTEGRATION.                                             *
C*****************************************************************
C          * WRITTEN BY LUIS A. PACHECO, ING.MEC., M.SC.*
C          *     IMPERIAL COLLEGE,UNIVERSITY OF LONDON  *
C          *     FINAL VERSION SUMMER 1979              *
C
C
      COMMON /BLK1/ NP,NE,NB,NPC,NMAT,NEQ,NBAND,NITER,TITLE(8),NBF
      COMMON /BLK2/ CORD(234,2),NOP(204,4),IMAT(204)
      COMMON /BLK5/ STR(204,6),EPS(204,6),VEL(2,234),TEPS(204)
      COMMON /A/ VRIG,IPLAX
      COMMON /B/ INTF,NINTF(50),NSTEP,STEP,ISTEP
C
C.....READ NECESSARY INPUT INFORMATION
C
      CALL START (2)
      CALL PRELIM
C
C.....CALCULATE BANDWIDTH AND NUMBER OF EQUATIONS.
C
      NEQ = NP*2
      J = 0
      DO 20 N = 1,NE
      DO 20 I = 1,4
      DO 10 L = 1,4
      KK = IABS(NOP(N,I)-NOP(N,L))
      IF (KK-J.LE.0) GO TO 10
      J = KK
   10 CONTINUE
   20 CONTINUE
      NBAND = 2*(J+1)
      NLIN = 0
      VRIG = 1.E+09
      ISTEP = 1
      DO 30 N = 1,NE
   30 TEPS(N) = 0.0
C
C.....READ THE EXTERNAL LOADS IF ANY.FORM VECTOR LOAD
C
      NITER = 0
   40 CALL LOAD
C.....FORM AND SOLVE THE EQUATION SYSTEM
C
      CALL FORMK
      CALL SOLVE
      CALL CONVER (NCONV)
      IF (NCONV.EQ.1) GO TO 50
      IF (NLIN.EQ.1) GO TO 50
      IF (NITER.EQ.12) GO TO 50
      NITER = NITER+1
      GO TO 40
C
C.....CALCULATE FORCES AT BOUNDARY NODAL POINTS IF REQUIRED
C
   50 CALL CFORC
      CALL STRAIN
C
C.....WRITE RESULTS
C
      CALL DOUT
      CALL MODMES
      IF (ISTEP.EQ.NSTEP) GO TO 60
      ISTEP = ISTEP+1
      NITER = 1
      GO TO 40
   60 CALL ENPLOT
      STOP
      END
      SUBROUTINE PRELIM
C
C.....THIS SUBROUTINE READ AND PRINT THE NECESSARY INPUT INFORMATION
C
      COMMON /BLK1/ NP,NE,NB,NPC,NMAT,NEQ,NBAND,NITER,TITLE(8),NBF
      COMMON /BLK2/ CORD(234,2),NOP(204,4),IMAT(204)
      COMMON /BLK3/ YIELD(4),NBC(60),NREST(60),NQ(40),R(40,2),XPRE(60),Y
     1PRE(60),NF(25)
      COMMON /A/ VRIG,IPLAX
      COMMON /B/ INTF,NINTF(50),NSTEP,STEP,ISTEP
C
C.....READ TITLE AND CONTROL VARIABLES.
C
      READ (5,1070) TITLE
      WRITE (6,1140) TITLE
      READ (5,1020) NP,NE,NB,NPC,NBF,NMAT,I1,IPLAX,INTF
      IF (IPLAX.EQ.0) WRITE (6,1090)
      IF (IPLAX.EQ.1) WRITE (6,1110)
      WRITE (6,1100) NP,NE,NB,NPC,NBF,NMAT,I1
      READ (5,1000) NSTEP,STEP
      WRITE (6,1010) NSTEP,STEP
C
C.....READ MATERIAL INFORMATION
C
      READ (5,1120) (N,YIELD(N),L=1,NMAT)
      WRITE (6,1210)
      WRITE (6,1130)
      WRITE (6,1080) (N,YIELD(N),N=1,NMAT)
C
C.....READ NODAL INFORMATION.
C
      READ (5,1030) (N,(CORD(N,M),M=1,2),L=1,NP)
C
C.....READ ELEMENTS INFORMATION.
C
      READ (5,1040) (N,(NOP(N,M),M=1,4),IMAT(N),L=1,NE)
C
C.....READ BOUNDARY CONDITIONS
C
      READ (5,1050) (NBC(I),NREST(I),XPRE(I),YPRE(I),I=1,NB)
      IF (INTF.EQ.0) GO TO 10
      READ (5,1060) (NINTF(I),I=1,INTF)
   10 IF (NBF.EQ.0) GO TO 20
      READ (5,1060) (NF(I),I=1,NBF)
C
C.....PRINT INPUT INFORMATION IF REQUIRED.
C
   20 IF (I1.EQ.0) GO TO 30
      WRITE (6,1160)
      WRITE (6,1030) (N,(CORD(N,M),M=1,2),N=1,NP)
      WRITE (6,1170)
      WRITE (6,1040) (N,(NOP(N,M),M=1,4),IMAT(N),N=1,NE)
```

```
   30 IF (INTF.EQ.0) GO TO 40
      WRITE (6,1200)
      WRITE (6,1150) (NINTF(I),I=1,INTF)
   40 IF (NBF.EQ.0) GO TO 50
      WRITE (6,1190)
      WRITE (6,1150) (NF(I),I=1,NBF)
   50 WRITE (6,1180)
      WRITE (6,1050) (NBC(I),NREST(I),XPRE(I),YPRE(I),I=1,NB)
      RETURN
C
 1000 FORMAT (I5,F10.3)
 1010 FORMAT (1HO,"NSTEP=",I3,2X,"INCREMENT=",E12.5)
 1020 FORMAT (9I5)
 1030 FORMAT (I10,2F10.4)
 1040 FORMAT (6I5)
 1050 FORMAT (2I10,2F10.3)
 1060 FORMAT (16I5)
 1070 FORMAT (8A10)
 1080 FORMAT (1H ,I5,F15.4)
 1090 FORMAT (1HO,"PLANE STRAIN PROBLEM",/,1H ,20(1H*))
 1100 FORMAT (1HO,"NUMBER OF NODES=",I3,/,1H ,"NUMBER OF ELEMENTS=",I3,/
     1,1H ,"NUMBER OF NODES WITH BOUNDARY CONDITIONS=",I3,/,1H ,"NUMBER
     2OF LOADED NODES=",I3,/,1H ,"NUMBER OF NODES WHERE REACTIONS ARE CA
     3LCULATED=",I3,/,1H ,"NUMBER OF MATERIALS=",I3,/,1H ,"PRINT CONTROL
     4 VARIABLE(I1)=",I2)
 1110 FORMAT (1HO,"AXISYMMETRIC PROBLEM",/,1H ,20(1H*))
 1120 FORMAT (I5,F15.4)
 1130 FORMAT (1H ,2X,"MAT",3X,"YIELD POINT")
 1140 FORMAT (1H1,8A10)
 1150 FORMAT (1H ,20I5)
 1160 FORMAT (1HO,6X,"NODES",3X,"COORD R",3X,"COORD Z")
 1170 FORMAT (1HO,"ELEMENT",4X,"NODES",9X,"IMAT")
 1180 FORMAT (1HO,"BOUNDARY CONDITIONS",/,1H ,5X,"NODES",4X,"CONDITION",
     13X,"XPRE",5X,"YPRE")
 1190 FORMAT (1HO,"THE NODAL POINTS AT WHICH FORCE CALCULATIONS ARE DESI
     1RED")
 1200 FORMAT (1HO,"THE NODAL POINTS AT THE FREE SURFACE")
 1210 FORMAT (1HO,"MATERIAL PROPERTIES")
      END
      SUBROUTINE LOAD
C
C.....THIS SUBROUTINE FORM THE VECTOR LOAD R1.
C
      COMMON /BLK1/ NP,NE,NB,NPC,NMAT,NEQ,NBAND,NITER,TITLE(8),NBF
      COMMON /BLK3/ YIELD(4),NBC(60),NREST(60),NQ(40),R(40,2),XPRE(60),Y
     1PRE(60),NF(25)
      COMMON SK(468,30),R1(468),EST(50,60),FR(25),FZ(25),FPUR(50)
C
C.....ZERO LOAD ARRAY.
C
      DO 10 J = 1,NEQ

   10 R1(J) = 0.0
      IF (NPC.EQ.0.AND.NITER.GT.0) RETURN
      IF (NPC.EQ.0) GO TO 50
      IF (NITER.GT.0) GO TO 30
      WRITE (6,1000)
      DO 20 N = 1,NPC
      READ (5,1010) NQ(N),(R(N,K),K=1,2)
      WRITE (6,1010) NQ(N),(R(N,K),K=1,2)
   20 CONTINUE
   30 DO 40 N = 1,NPC
      DO 40 K = 1,2
      IC = (NQ(N)-1)*2+K
   40 R1(IC) = R(N,K)+R1(IC)
      GO TO 60
   50 WRITE (6,1020)
   60 RETURN
C
 1000 FORMAT (1HO,"PRESCRIBED EXTERNAL LOADS",1HO,"NODES",3X,"FORCE-X",3
     1X,"FORCE-Y")
 1010 FORMAT (I5,2F10.3)
 1020 FORMAT (1HO,"NO EXTERNAL LOADS PRESCRIBED")
      END
      SUBROUTINE FORMK
C
C.....THIS SUBROUTINE FORMS THE OVERALL STIFFNESS MATRIX
C.....AND STORES IT IN A RECTANGULAR FORM.
C
      COMMON /BLK1/ NP,NE,NB,NPC,NMAT,NEQ,NBAND,NITER,TITLE(8),NBF
      COMMON /BLK2/ CORD(234,2),NOP(204,4),IMAT(204)
      COMMON /BLK3/ YIELD(4),NBC(60),NREST(60),NQ(40),R(40,2),XPRE(60),Y
     1PRE(60),NF(25)
      COMMON SK(468,30),R1(468),EST(50,60),FR(25),FZ(25),FPUR(50)
      DIMENSION SE(8,8)
C.....INITIALIZE THE ARRAYS
      DO 10 N = 1,NEQ
      DO 10 M = 1,NBAND
   10 SK(N,M) = 0.0
C
C.....SCAN ELEMENTS
C
      DO 80 II = 1,NE
      CALL QUAD2 (SE,II)
C
C.....FORM THE STIFFNESS MATRIX SK
C
C.....FIRST ROWS
C
      DO 70 JJ = 1,4
      NROWB = (NOP(II,JJ)-1)*2
      IF (NROWB) 70,20,20
   20 DO 60 J = 1,2
      NROWB = NROWB+1
      I = (JJ-1)*2+J
C
C.....THEN COLUMNS
C
      DO 50 KK = 1,4
      NCOLB = (NOP(II,KK)-1)*2
      DO 40 K = 1,2
      L = (KK-1)*2+K
      NCOL = NCOLB+K+1-NROWB
C
C.....SKIP STORING IF BELOW BAND
C
      IF (NCOL) 40,40,30
   30 SK(NROWB,NCOL) = SK(NROWB,NCOL)+SE(I,L)
   40 CONTINUE
   50 CONTINUE
   60 CONTINUE
   70 CONTINUE
   80 CONTINUE
C
C.....PREPARATION FOR FORCE CALCULATION
C.....STORE THE ROWS OF SK WHICH ARE NECESSARY.
C
      IF (NBF.EQ.0) GO TO 140
```

```
      NBAND2 = 2*NBAND-1
      DO 90 I = 1,NBF
      IZ = 2*I
      IR = IZ-1
      DO 90 J = 1,NBAND2
      EST(IZ,J) = 0.0
   90 EST(IR,J) = 0.0
      DO 130 I = 1,NBF
      II = NF(I)
      IZ = 2*II
      IR = IZ-1
      IIZ = 2*I
      IIR = IIZ-1
      DO 100 J = NBAND,NBAND2
      JJ = J-NBAND+1
      EST(IIR,J) = SK(IR,JJ)
  100 EST(IIZ,J) = SK(IZ,JJ)
      DO 120 J = 1,NBAND
      NR = IR-J+1
      NZ = IZ-J+1
      JJ = NBAND-J+1
      IF (NR.LE.0) GO TO 110
      EST(IIR,JJ) = SK(NR,J)
  110 IF (NZ.LE.0) GO TO 120
      EST(IIZ,JJ) = SK(NZ,J)
  120 CONTINUE
      FPUR(IIR) = R1(IR)
  130 FPUR(IIZ) = R1(IZ)
C
C.....INSERT DISPLACEMENT BOUNDARY CONDITIONS
C
  140 DO 150 N = 1,NB
      I = NBC(N)
      IR = 2*I-1
      IZ = IR+1
      NC = NREST(N)
C
C.....CHECK IF THE X VELOCITY IS PRESCRIBED
C
      IF (NC.EQ.1.OR.NC.EQ.11) CALL CONDE (IR,XPRE(N))
C
C.....CHECK IF THE Y VELOCITY IS PRESCRIBED
C
      IF (NC.EQ.2.OR.NC.EQ.11) CALL CONDE (IZ,YPRE(N))
C
C.....CHECK IF THE POINT IS ALONG AN INCLINED BOUNDARY
C
      IF (NC.EQ.3) THETA = XPRE(N)*3.1415927/180.
      IF (NC.EQ.3) CALL BCMIX (I,THETA)
  150 CONTINUE
      RETURN
      END
      SUBROUTINE QUAD2 (SE,IEL)
C
C.....THIS SUBROUTINE FORMS THE ELEMENTAL STIFFNESS MATRIX.
C
      COMMON /BLK1/ NP,NE,NB,NPC,NMAT,NEQ,NBAND,NITER,TITLE(8),NBF
      COMMON /BLK2/ CORD(234,2),NOP(204,4),IMAT(204)
      COMMON /BLK3/ YIELD(4),NBC(60),NREST(60),NQ(40),R(40,2),XPRE(60),Y
     1PRE(60),NF(25)
      COMMON /BLK5/ STR(204,6),EPS(204,6),VEL(2,234),TEPS(204)
      DIMENSION D(4,4), SE(8,8), A(4,8), XL(4), YL(4)
      COMMON /A/ VRIG,IPLAX
      DIMENSION B(4,8), SHP(3,9), SG(9), WG(9), TG(9)
C.....INITIALIZE THE ARRAYS
      N = IEL
      NNE = 4
      NNE2 = NNE*2
      DO 10 I = 1,4
      DO 10 J = 1,4
   10 D(I,J) = 0.0
      DO 20 I = 1,NNE2
      DO 20 J = 1,NNE2
   20 SE(I,J) = 0.0
      DO 30 MM = 1,NNE
      XL(MM) = CORD(NOP(N,MM),1)
   30 YL(MM) = CORD(NOP(N,MM),2)
      NINT = 2
      IPEN = 0
C.....COMPUTE GAUSS POINTS AND WEIGHT FACTORS
   40 CALL PGAUSS (NINT,LINT,SG,TG,WG)
C.....FORM STRAIN DISPLACEMENT MATRIX B.
      DO 200 L = 1,LINT
      XBAR = 0.0
      DO 50 NN = 1,3
      DO 50 LL = 1,NNE
   50 SHP(NN,LL) = 0.0
      CALL SHAPE (SG(L),TG(L),XL,YL,SHP,DETJAC,NNE)
      IF (DETJAC) 60,60,70
   60 WRITE (6,1000) N
      WRITE (6,1010)
      WRITE (6,1020) (LH,(CORD(LH,LT),LT=1,2),LH=1,NP)
      CALL DRAW
      CALL ENPLOT
      STOP
   70 DO 80 LI = 1,NNE
      J = 2*LI
      I = J-1
      B(1,I) = SHP(1,LI)
      B(1,J) = 0.0
      B(2,I) = 0.0
      B(2,J) = SHP(2,LI)
      B(3,I) = 0.0
      B(3,J) = 0.0
      B(4,I) = B(2,J)
   80 B(4,J) = B(1,I)
C.....IN CASE OF PLANE STRAIN ANALYSIS DO NOT INCLUDE
C.....THE NORMAL STRAIN COMPONENT
      IF (IPLAX.EQ.0) GO TO 130
      DO 90 KI = 1,NNE
   90 XBAR = XBAR+SHP(3,KI)*XL(KI)
C.....EVALUATE THE HOOP STRAIN DISPLACEMENT RELATION
      IF (XBAR.GT.0.00000001) GO TO 110
C.....FOR THE CASE OF ZERO RADIUS EQUATE RADIAL TO HOOP STRAIN
      DO 100 KI = 1,NNE2
  100 B(3,KI) = B(1,KI)
      GO TO 130
C.....NON-ZERO RADIUS
  110 DUMA = 1./XBAR
      DO 120 KI = 1,NNE
      LH = 2*KI-1
  120 B(3,LH) = SHP(3,KI)*DUMA
C.....FORM THE PENALTY MATRIX
  130 IF (IPEN.EQ.0) GO TO 150
      ALPHA = 10E+07
      DO 140 I = 1,4
      DO 140 J = 1,4
      D(I,J) = ALPHA
```

```
  140 IF (I.EQ.4.0R.J.EQ.4) D(I,J) = 0.0
      G0 T0 160
C.....F0RM THE STRESS-STRAIN MATRIX
  150 IF (NITER.EQ.0) EPSR = 1.0
      IF (NITER.GT.0) CALL STRA (NNE,N,B,EPSR)
      LL = IMAT(N)
      YYLD = YIELD(LL)
      DUM3 = 2.*YYLD/(3.*EPSR)
      IF (DUM3.GE.VRIG) DUM3 = VRIG
      D(1,1) = DUM3
      D(2,2) = DUM3
      D(3,3) = DUM3
      D(4,4) = DUM3/2.
C.....C0MPUTE THE PR0DUCT D*B
  160 D0 170 I = 1,4
      D0 170 J = 1,NNE2
      A(I,J) = 0.0
      D0 170 K = 1,4
  170 A(I,J) = A(I,J)+D(I,K)*B(K,J)
C.....C0MPUTE (B**T *(D*B) AND ADD C0NTRIBUTI0N T0 ELEMENT STIFFNESS
      IF (IPLAX.EQ.0) XBAR = 1.0
      WT = X3AR*WG(L)*DETJAC
      D0 190 NR0W = 1,NNE2
      D0 190 NC0L = NR0W,NNE2
      DUM2 = 0.0
      D0 180 LI = 1,4
  180 DUM2 = DUM2+B(LI,NR0W)*A(LI,NC0L)
      SE(NR0W,NC0L) = SE(NR0W,NC0L)+DUM2*WT
  190 C0NTINUE
  200 C0NTINUE
      IPEN = IPEN+1
      NINT = 1
      IF (IPEN.EQ.1) G0 T0 40
C.....C0MPLETE SE BY SYMMETRY.
      D0 210 K = 2,NNE2
      D0 210 L = 1,K
  210 SE(K,L) = SE(L,K)
      RETURN
C
 1000 F0RMAT (//,"PR0GRAM HAS HALTED IN SUBR0UTINE QUAD2",//,"ELEMENT",I
     15,2X,"HAS ZER0 0R NEGATIVE AREA")
 1010 F0RMAT (1H0,"C00RDINATES AT THE TIME 0F HALTING")
 1020 F0RMAT (1H ,I10,2F10.4)
      END
      SUBR0UTINE PGAUSS (L,LINT,R,Z,W)
C
C.....GAUSS P0INTS AND WEIGHTS F0R TW0 DIMENSI0NS
C
      REAL LR(9), LZ(9), LW(9), R(9), Z(9), W(9)
      DATA LR/-1.,1.,1.,-1.,0.,-1.,0.,-1.,0./
      DATA LZ/-1.,-1.,1.,1.,-1.,0.,1.,0.,0./
      DATA LW/4*25.,4*40.,64./
      LINT = L**L
      IF (L.EQ.1) G0 T0 10
      IF (L.EQ.2) G0 T0 20
      IF (L.EQ.3) G0 T0 40
C.....1X1 INTEGRATI0N
   10 R(1) = 0.
      Z(1) = 0.
      W(1) = 4.
      RETURN
C.....2X2 INTEGRATI0N
   20 G = 1./SQRT(3.)
      D0 30 I = 1,4
      R(I) = G*LR(I)
      Z(I) = G*LZ(I)
   30 W(I) = 1.
      RETURN
C....3X3 INTEGRATI0N
   40 G = SQRT(0.6)
      H = 1./81.
      D0 50 I = 1,9
      R(I) = G*LR(I)
      Z(I) = G*LZ(I)
   50 W(I) = H*LW(I)
      RETURN
      END
      SUBR0UTINE SHAPE (SS,TT,XL,YL,SHP,DETJAC,NNE)
C
C.....SHAPE FUNCTI0N SUBR0UTINE F0R TW0 DIMENSI0NAL ELEMENTS
C
      REAL SHP(3,9), XL(4), YL(4), S(4), T(4), JAC(2,2)
      DATA S/-0.5,0.5,0.5,-0.5/,T/-0.5,-0.5,0.5,0.5/
C.....F0RM 4 N0DE QUADRILATERAL SHAPE FUNCTI0N
      D0 10 I = 1,4
      SHP(3,I) = (0.5+S(I)*SS)*(0.5+T(I)*TT)
      SHP(1,I) = S(I)*(0.5+T(I)*TT)
   10 SHP(2,I) = T(I)*(0.5+S(I)*SS)
C.....C0NSTRUCT JAC0BIAN, ITS INVERSE AND ITS DETERMINANT.
      D0 20 I = 1,2
      D0 20 J = 1,2
   20 JAC(I,J) = 0.0
      D0 30 K = 1,NNE
      JAC(1,1) = JAC(1,1)+SHP(1,K)*XL(K)
      JAC(1,2) = JAC(1,2)+SHP(1,K)*YL(K)
      JAC(2,1) = JAC(2,1)+SHP(2,K)*XL(K)
   30 JAC(2,2) = JAC(2,2)+SHP(2,K)*YL(K)
      DETJAC = JAC(1,1)*JAC(2,2)-JAC(1,2)*JAC(2,1)
      IF (DETJAC.LE.0.) RETURN
      DUM1 = JAC(1,1)/DETJAC
      JAC(1,1) = JAC(2,2)/DETJAC
      JAC(2,1) = -JAC(2,1)/DETJAC
      JAC(1,2) = -JAC(1,2)/DETJAC
      JAC(2,2) = DUM1
C.....F0RM GL0BAL DERIVATIVES
      D0 40 I = 1,NNE
      TP = SHP(1,I)*JAC(1,1)+SHP(2,I)*JAC(1,2)
      SHP(2,I) = SHP(1,I)*JAC(2,1)+SHP(2,I)*JAC(2,2)
   40 SHP(1,I) = TP
      RETURN
      END
      SUBR0UTINE STRA (NNE,M,BA,EPSR)
C
C.....THIS SUBR0UTINE CALCULATES THE STRAINS AT THE GAUSS P0INTS
C
      C0MM0N /BLK1/ NP,NE,NB,NPC,NMAT,NEQ,NBAND,NITER,TITLE(8),NBF
      C0MM0N /BLK2/ C0RD(234,2),N0P(204,4),IMAT(204)
      C0MM0N /BLK5/ STR(204,6),EPS(204,6),VEL(2,234),TEPS(204)
      DIMENSI0N BA(4,8), E(4), RA(8)
      NK = NNE
      NK2 = NK*2
      D0 10 J = 1,NK
      KK = N0P(M,J)
      KI = (J-1)*2
      D0 10 JJ = 1,2
      IJ = JJ+KI
   10 RA(IJ) = VEL(JJ,KK)
      D0 20 KK = 1,4
```

```
      E(KK) = 0.0
      DO 20 J = 1,NK2
   20 E(KK) = E(KK)+BA(KK,J)*RA(J)
      EPSR = RBAR(E(1),E(2),E(3),E(4))
      RETURN
      END
      SUBROUTINE CONDE (N,U)
C
C.....THIS SUBROUTINE PERFORM THE MATRIX CONDENSATION WHEN
C.....THE VALUE OF A COMPONENT OF X IN AX=B IS SPECIFIED.
C
      COMMON /BLK1/ NP,NE,NB,NPC,NMAT,NEQ,NBAND,NITER,TITLE(8),NBF
      COMMON SK(468,30),R1(468),EST(50,60),FR(25),FZ(25),FPUR(50)
      DO 10 M = 2,NBAND
      KK = N+M-1
      IF (KK.GT.NEQ) GO TO 10
      R1(KK) = R1(KK)-SK(N,M)*U
   10 CONTINUE
      DO 20 M = 2,NBAND
      K = N-M+1
      IF (K.LE.0) GO TO 20
      R1(K) = R1(K)-SK(K,M)*U
      SK(K,M) = 0.
   20 SK(N,M) = 0.
      SK(N,1) = 1.
      R1(N) = U
      RETURN
      END
      SUBROUTINE BCMIX (N,THETA)
C
C.....SINCE UR=UZ*TAN(THETA) ALONG THE DIE,ACORRESPONDING CHANGE
C.....IS MADE IN THE STIFFNESS EQUATIONS FOR ROWS AND COLUMNS CORRESPODING
C.....TO THESE COMPONENTS.THEN THE EQUATIONS CONTAINING UR ARE ELIMINATED
C
      COMMON /BLK1/ NP,NE,NB,NPC,NMAT,NEQ,NBAND,NITER,TITLE(8),NBF
      COMMON SK(468,30),R1(468),EST(50,60),FR(25),FZ(25),FPUR(50)
      COMMON /A/ VRIG,IPLAX
      NZ = 2*N
      NR = NZ-1
      ALPA = 1./TAN(THETA)
      IF (IPLAX.EQ.1) ALPA = TAN(THETA)
      DO 10 M = 1,NBAND
   10 SK(NR,M) = SK(NR,M)*ALPA
      SK(NR,1) = SK(NR,1)*ALPA
      SK(NR,2) = SK(NR,2)*2.
      DO 20 M = 2,NBAND
      KR = NR-M+1
      IF (KR.LE.0) GO TO 30
   20 SK(KR,M) = SK(KR,M)*ALPA
   30 R1(NR) = R1(NR)*ALPA
      DO 50 M = 2,NBAND
      KZ = NZ-M+1
      IF (KZ.LE.0) GO TO 40
      SK(KZ,M) = SK(KZ,M)+SK(KZ,M-1)
   40 IF (M.EQ.NBAND) GO TO 50
      KZ = NZ+M-1
      IF (KZ.GT.NEQ) GO TO 50
      SK(NZ,M) = SK(NZ,M)+SK(NR,M+1)
   50 CONTINUE
      SK(NZ,1) = SK(NZ,1)+SK(NR,2)
      SK(NR,1) = 1.0
      DO 70 M = 2,NBAND
      KR = NR-M+1
      IF (KR.LE.0) GO TO 60
      SK(KR,M) = 0.
   60 SK(NR,M) = 0.
   70 CONTINUE
      R1(NZ) = R1(NZ)+R1(NR)
      R1(NR) = 0.
      RETURN
      END
      SUBROUTINE SOLVE
C
C.....THIS SUBROUTINE PERFORMS THE SOLUTION OF THE
C.....EQUATION SYSTEM AX=B.
C
      COMMON /BLK1/ NP,NE,NB,NPC,NMAT,NEQ,NBAND,NITER,TITLE(8),NBF
      COMMON /BLK3/ YIELD(4),NBC(60),NREST(60),NQ(40),R(40,2),XPRE(60),Y
     1PRE(60),NF(25)
      COMMON SK(468,30),R1(468),EST(50,60),FR(25),FZ(25),FPUR(50)
      COMMON /A/ VRIG,IPLAX
C
C.....REDUCE MATRIX
C
      DO 50 N = 1,NEQ
      I = N
      DO 40 L = 2,NBAND
      I = I+1
      IF (SK(N,L)) 10,40,10
   10 C = SK(N,L)/SK(N,1)
      J = 0
      DO 30 K = L,NBAND
      J = J+1
      IF (SK(N,K)) 20,30,20
   20 SK(I,J) = SK(I,J)-C*SK(N,K)
   30 CONTINUE
      SK(N,L) = C
C
C
C.....AND LOAD VECTOR FOR EACH EQUATION.
      R1(I) = R1(I)-C*R1(N)
   40 CONTINUE
   50 R1(N) = R1(N)/SK(N,1)
C
C.....BACK SUBSTITUTION
C
      N = NEQ
   60 N = N-1
      IF (N) 100,100,70
   70 L = N
      DO 90 K = 2,NBAND
      L = L+1
      IF (SK(N,K)) 80,90,80
   80 R1(N) = R1(N)-SK(N,K)*R1(L)
   90 CONTINUE
      GO TO 60
  100 DO 110 I = 1,NB
      IZ = 2*NBC(I)
      IR = IZ-1
      IF (NREST(I).EQ.3) THETA = XPRE(I)*3.1415927/180.
      IF (NREST(I).EQ.3.AND.IPLAX.EQ.0) ALPA = 1./TAN(THETA)
      IF (NREST(I).EQ.3.AND.IPLAX.EQ.1) ALPA = TAN(THETA)
  110 IF (NREST(I).EQ.3) R1(IR) = R1(IZ)*ALPA
      RETURN
      END
      SUBROUTINE CFORC
      COMMON /BLK1/ NP,NE,NB,NPC,NMAT,NEQ,NBAND,NITER,TITLE(8),NBF
      COMMON /BLK3/ YIELD(4),NBC(60),NREST(60),NQ(40),R(40,2),XPRE(60),Y
```

```
     1PRE(60),NF(25)
      COMMON SK(468,30),R1(468),EST(50,60),FR(25),FZ(25),FPUR(50)
C
C.....THIS SUBROUTINE DETERMINES FORCES ON THE BOUNDARIES.
C
      IF (NBF.LE.0) GO TO 50
      NBAND2 = 2*NBAND-1
      DO 40 I = 1,NBF
      IR = 2*NF(I)-1
      IIZ = 2*I
      IIR = IIZ-1
      SUMR = 0.0
      SUMZ = 0.0
      DO 30 J = 1,NBAND2
      JR = IR+J-NBAND
      JZ = JR+1
      IF (JR.GT.NEQ) GO TO 20
      IF (JR.LE.0) GO TO 10
      SUMR = SUMR+EST(IIR,J)*R1(JR)
   10 IF (JZ.LE.0) GO TO 30
   20 IF (JZ.GT.NEQ) GO TO 30
      SUMZ = SUMZ+EST(IIZ,J)*R1(JZ)
   30 CONTINUE
      FR(I) = SUMR-FPUR(IIR)
      FZ(I) = SUMZ-FPUR(IIZ)
   40 CONTINUE
   50 RETURN
      END
      SUBROUTINE STRAIN
C
C.....THIS SUBROUTINE CALCULATES STRAINS,STRESSES AND COORDINATES.
C
      COMMON /BLK1/ NP,NE,NB,NPC,NMAT,NEQ,NBAND,NITER,TITLE(8),NBF
      COMMON /BLK2/ CORD(234,2),NOP(204,4),IMAT(204)
      COMMON /BLK3/ YIELD(4),NBC(60),NREST(60),NQ(40),R(40,2),XPRE(60),Y
     1PRE(60),NF(25)
      COMMON /BLK5/ STR(204,6),EPS(204,6),VEL(2,234),TEPS(204)
      COMMON /A/ VRIG,IPLAX
      COMMON /B/ INTF,NINTF(50),NSTEP,STEP,ISTEP
      DIMENSION SHP(3,9), SG(9), TG(9), WG(9), U(2,9)
      DIMENSION XL(9), YL(9), E(6)
      NNE = 4
      DO 100 N = 1,NE
      DO 10 MM = 1,NNE
      XL(MM) = CORD(NOP(N,MM),1)
      YL(MM) = CORD(NOP(N,MM),2)
      U(1,MM) = VEL(1,NOP(N,MM))
   10 U(2,MM) = VEL(2,NOP(N,MM))
      L = 1
      CALL PGAUSS (L,LINT,SG,TG,WG)
      DO 20 NN = 1,3
      DO 20 LL = 1,NNE
   20 SHP(NN,LL) = 0.0
C.....COMPUTE ELEMENT SHAPE FUNCTIONS.
      CALL SHAPE (SG(L),TG(L),XL,YL,SHP,DETJAC,NNE)
C.....COMPUTE CORDINATES AND STRAINS.
      DO 30 I = 1,6
   30 E(I) = 0.0
      XBAR = 0.0
      YBAR = 0.0
      DO 40 J = 1,NNE
      XBAR = XBAR+SHP(3,J)*XL(J)
   40 YBAR = YBAR+SHP(3,J)*YL(J)
      DO 70 J = 1,NNE
      E(1) = E(1)+SHP(1,J)*U(1,J)
      E(2) = E(2)+SHP(2,J)*U(2,J)
C.....FOR THE CASE OF ZERO RADIUS EQUATE RADIAL TO HOOP STRAIN
      IF (XBAR.GT.0.0000001) GO TO 50
      E(3) = E(1)
      GO TO 60
   50 E(3) = E(3)+SHP(3,J)/XBAR*U(1,J)
   60 IF (IPLAX.EQ.0) E(3) = 0.0
   70 E(4) = E(4)+SHP(1,J)*U(2,J)+SHP(2,J)*U(1,J)
      DO 80 J = 1,4
   80 EPS(N,J) = E(J)
      EPS(N,6) = RBAR(E(1),E(2),E(3),E(4))
      EPS(N,5) = E(1)+E(2)+E(3)
      KK = IMAT(N)
      YYLD = YIELD(KK)
      DO 90 I = 1,4
      ALPHA = 10E+07
   90 STR(N,I) = 2.*YYLD/(3.*EPS(N,6))*EPS(N,I)+ALPHA*EPS(N,6)
      STR(N,5) = ALPHA*EPS(N,5)
      TEPS(N) = TEPS(N)+EPS(N,6)*STEP
  100 CONTINUE
      RETURN
      END
      SUBROUTINE DOUT
      COMMON /BLK1/ NP,NE,NB,NPC,NMAT,NEQ,NBAND,NITER,TITLE(8),NBF
      COMMON /BLK2/ CORD(234,2),NOP(204,4),IMAT(204)
      COMMON /BLK3/ YIELD(4),NBC(60),NREST(60),NQ(40),R(40,2),XPRE(60),Y
     1PRE(60),NF(25)
      COMMON /BLK5/ STR(204,6),EPS(204,6),VEL(2,234),TEPS(204)
      COMMON SK(468,30),R1(468),EST(50,60),FR(25),FZ(25),FPUR(50)
      COMMON /B/ INTF,NINTF(50),NSTEP,STEP,ISTEP
      REWIND 4
C.....PRINT NODAL POSITION FOR THIS STEP
      IF (ISTEP.EQ.1) GO TO 10
      IF (((ISTEP-1)/5)*5.NE.(ISTEP-1)) GO TO 20
   10 RED = FLOAT(ISTEP-1)*STEP*100.
      WRITE (6,1000) TITLE
      WRITE (6,1010) RED
      WRITE (6,1020)
      WRITE (6,1030)
      WRITE (6,1040) (N,(CORD(N,M),M=1,2),(VEL(M,N),M=1,2),N=1,NP)
      WRITE (6,1020)
C.....PLOT THE DEFORMED MESH
      IF (ISTEP.EQ.1.OR.((ISTEP-1)/5)*5.EQ.ISTEP-1) CALL DRAW
      WRITE (6,1050) NITER
C
C.....WRITE FORCES AT NODES  IF DESIRED
C
      IF (NBF.LE.0) GO TO 20
      WRITE (6,1060)
      WRITE (6,1070) (NF(I),FR(I),FZ(I),I=1,NBF)
      WRITE (4,1070) (NF(I),FR(I),FZ(I),I=1,NBF)
   20 CALL FOLD
      RETURN
C
 1000 FORMAT (1H1,8A10)
 1010 FORMAT (1H ,"NODAL COORDINATES AT",F6.2,"PERCENT REDUCTION",/,1H ,
     1 142(1H*))
 1020 FORMAT (1HO,100(1H-))
 1030 FORMAT (1HO,6X,"NODES",3X,"COORD-R",3X,"COORD-Z",20X,"VEL-R",5X,"V
     1EL-Z")
 1040 FORMAT (1H ,I10,2F10.4,2E12.5)
 1050 FORMAT (1H ,15X,"NUMBER OF ITERATIONS",I3)
 1060 FORMAT (1HO,"FORCES CALCULATED AT BOUNDARY NODES",///,5X,"NODES",5
```

```
     1X,"FORCE-X",3X,"FORCE-Y")
 1070 FORMAT (1HO,I10,2X,2E10.3)
      END
      SUBROUTINE DRAW
C.....THIS SUBROUTINE PLOTS THE DEFORMED MESH.
      COMMON /BLK1/ NP,NE,NB,NPC,NMAT,NEQ,NBAND,NITER,TITLE(8),NBF
      COMMON /BLK2/ CORD(234,2),NOP(204,4),IMAT(204)
      COMMON /BLK5/ STR(204,6),EPS(204,6),VEL(2,234),TEPS(204)
      COMMON /B/ INTF,NINTF(50),NSTEP,STEP,ISTEP
      DIMENSION X(20), Y(20)
      IF (ISTEP.GT.1) CALL NEWPAGE
      RED = FLOAT(ISTEP-1)*STEP*100.
      CALL SYMBOL (3.0,2.0,0.14,TITLE,0.0,80)
      CALL SYMBOL (3.0,1.6,0.14,57HDEFORMED MESH AND VELOCITY FIELD AT
     1   PERCENT REDUCTION,0.0,57)
      CALL NUMBER (8.1,1.6,0.14,RED,0.0,0)
      CALL PLOT (2.0,4.0,-3)
      DO 10 I = 1,5
      X(I) = 0.0
   10 Y(I) = 0.0
      X(5) = 1.2
      Y(5) = 1.2
      CALL SCALE (X,6.0,5,1)
      CALL SCALE (Y,6.0,5,1)
      CALL AXIS (0.0,0.0,6H -AXIS,-6,6.,0.0,X(6),X(7))
      CALL AXIS (0.0,0.0,6H -AXIS,6,6.,90.0,Y(6),Y(7))
      DO 30 N = 1,NE
      DO 20 J = 1,4
      X(J) = CORD(NOP(N,J),1)
   20 Y(J) = CORD(NOP(N,J),2)
      X(5) = CORD(NOP(N,1),1)
      Y(5) = CORD(NOP(N,1),2)
      CALL LINE (X,Y,5,1,0,1)
   30 CONTINUE
C.....CALCULATE SCALING FACTOR.......
      VMAX1 = VEL(2,1)
      DO 40 I = 2,NP
      DUMY = ABS(VEL(2,I))
      VMAX = AMAX1(VMAX1,DUMY)
      VMAX1 = VMAX
   40 CONTINUE
      VMAX1 = VMAX1+VMAX1*0.1
      SF = 0.05/VMAX1
      DO 50 I = 1,NP
      DO 50 J = 1,2
   50 VEL(J,I) = VEL(J,I)*SF
      Y(3) = Y(6)
      X(3) = X(6)
      X(4) = X(7)
      Y(4) = Y(7)
      CALL PLOT (7.5,0.0,-3)
      AL = 20.*3.14159/180.
      DO 70 I = 1,NP
      X(1) = CORD(I,1)
      Y(1) = CORD(I,2)
      X(2) = X(1)+VEL(1,I)
      Y(2) = Y(1)+VEL(2,I)
      CALL LINE (X,Y,2,1,0,1)
      PI = 3.14159
      IF (VEL(1,I).EQ.0..AND.VEL(2,I).EQ.0.) GO TO 70
      IF (VEL(1,I).EQ.0..AND.VEL(2,I).LT.0.) PHI = -PI/2.
      IF (VEL(1,I).EQ.0..AND.VEL(2,I).GT.0.) PHI = PI/2.
      IF (VEL(2,I).EQ.0..AND.VEL(1,I).GT.0.) PHI = 0.0
      IF (VEL(2,I).EQ.0..AND.VEL(1,I).LT.0.) PHI = PI
      IF (VEL(1,I).NE.0..AND.VEL(2,I).NE.0.) PHI = ATAN(VEL(2,I)/VEL(1,I
     1))
      IF (VEL(1,I).LT.0..AND.VEL(2,I).LT.0.) PHI = PHI+PI
      IF (VEL(1,I).LT.0..AND.VEL(2,I).GT.0.) PHI = PHI+PI
      VEL0 = SQRT(VEL(1,I)**2+VEL(2,I)**2)
      D = VEL0*0.2
      X(1) = X(2)
      Y(1) = Y(2)
      X(2) = X(1)-COS(PHI-AL)*D/COS(AL)
      Y(2) = Y(1)-SIN(PHI-AL)*D/COS(AL)
      CALL LINE (X,Y,2,1,0,1)
      X(2) = X(1)-COS(PHI+AL)*D/COS(AL)
      Y(2) = Y(1)-SIN(PHI+AL)*D/COS(AL)
      CALL LINE (X,Y,2,1,0,1)
      DO 60 J = 1,2
   60 VEL(J,I) = VEL(J,I)/SF
   70 CONTINUE
      RETURN
      END
      SUBROUTINE FOLD
C
C.....THIS SUBROUTINE CHECKS IF THE POINT IN THE FREE SURFACE
C.....IS FOLDING AND MODIFIES THE BOUNDARY CONDITIONS ACCORDINGLY.
C
      COMMON /BLK1/ NP,NE,NB,NPC,NMAT,NEQ,NBAND,NITER,TITLE(8),NBF
      COMMON /BLK2/ CORD(234,2),NOP(204,4),IMAT(204)
      COMMON /BLK3/ YIELD(4),NBC(60),NREST(60),NQ(40),R(40,2),XPRE(60),Y
     1PRE(60),NF(25)
      COMMON /BLK5/ STR(204,6),EPS(204,6),VEL(2,234),TEPS(204)
      COMMON /B/ INTF,NINTF(50),NSTEP,STEP,ISTEP
      IF (INTF.EQ.0) RETURN
      NRAD = NINTF(INTF)
      HEIGHT = CORD(NRAD,2)+VEL(2,NRAD)*STEP
      DO 40 I = 1,INTF
      DO 10 J = 1,NB
      IF (NINTF(I).EQ.NBC(J)) GO TO 40
   10 CONTINUE
      HEI = CORD(NINTF(I),2)+VEL(2,NINTF(I))*STEP
      IF (HEI.LT.HEIGHT) GO TO 20
      VEMOF = (HEIGHT-CORD(NINTF(I),2))/STEP
      FTES = VEMOF/VEL(2,NINTF(I))
      VEL(1,NINTF(I)) = VEL(1,NINTF(I))*FTES
      VEL(2,NINTF(I)) = VEL(2,NINTF(I))*FTES
      NB = NB+1
      NBC(NB) = NINTF(I)
      NREST(NB) = 11
      XPRE(NB) = 0.0
      YPRE(NB) = -0.75
      NBF = NBF+1
      NF(NBF) = NINTF(I)
      WRITE (6,1000) NINTF(I),ISTEP
   20 IF (HEI.GT.0.) GO TO 40
      VEMOF = -CORD(NINTF(I),2)/STEP
      FTES = VEMOF/VEL(2,NINTF(I))
      DO 30 J = 1,2
   30 VEL(J,NINTF(I)) = VEL(J,NINTF(I))*FTES
      NB = NB+1
      NBC(NB) = NINTF(I)
      NREST(NB) = 11
      XPRE(NB) = 0.
      YPRE(NB) = 0.
      WRITE (6,1000) NINTF(I),ISTEP
   40 CONTINUE
      RETURN
```

```
C
 1000 FORMAT (1H ,"NODE NO",I3,"HAS FOLDED AT STEP NO",I3)
      END
      SUBROUTINE CONVER (NCONV)
      COMMON /BLK1/ NP,NE,NB,NPC,NMAT,NEQ,NBAND,NITER,TITLE(8),NBF
      COMMON /BLK5/ STR(204,6),EPS(204,6),VEL(2,234),TEPS(204)
      COMMON SK(468,30),R1(468),EST(50,60),FR(25),FZ(25),FPUR(50)
      COMMON /B/ INTF,NINTF(50),NSTEP,STEP,ISTEP
      DIMENSION RC(468)
      EQUIVALENCE (SK,RC)
C
C.....THIS SUBROUTINE CHECKS THE CONVERGENCE.
C
      NCONV = 0
      IF (NITER.EQ.0) GO TO 30
      DO 10 N = 1,NP
      NZ = 2*N
      NR = NZ-1
      RC(NZ) = VEL(2,N)
   10 RC(NR) = VEL(1,N)
      ACONV1 = 0.
      ACONV2 = 0.
      DO 20 I = 1,NP
      IZ = I*2
      IR = IZ-1
      DVZ = R1(IZ)-RC(IZ)
      DVR = R1(IR)-RC(IR)
      ACONV2 = ACONV2+(DVR**2+DVZ**2)
      ACONV1 = ACONV1+(RC(IZ)**2+RC(IR)**2)
   20 CONTINUE
      VCONV = SQRT(ACONV2/ACONV1)
      IF (ABS(VCONV).LE.0.001) NCONV = 1
      WRITE (6,1000) NITER,VCONV
   30 DO 40 K = 1,NP
      DO 40 M = 1,2
      IC = (K-1)*2+M
   40 VEL(M,K) = R1(IC)
      RETURN
C
 1000 FORMAT (1HO,"NITER=",I2,"VCONV=",E10.4)
      END
      SUBROUTINE MODMES
      COMMON /BLK1/ NP,NE,NB,NPC,NMAT,NEQ,NBAND,NITER,TITLE(8),NBF
      COMMON /BLK2/ CORD(234,2),NOP(204,4),IMAT(204)
      COMMON /BLK3/ YIELD(4),NBC(60),NREST(60),NQ(40),R(40,2),XPRE(60),Y
     1PRE(60),NF(25)
      COMMON /BLK5/ STR(204,6),EPS(204,6),VEL(2,234),TEPS(204)
      COMMON /B/ INTF,NINTF(50),NSTEP,STEP,ISTEP
C.....MODIFY COORDINATES
      DO 10 I = 1,NP
      DO 10 J = 1,2
   10 CORD(I,J) = CORD(I,J)+VEL(J,I)*STEP
      RETURN
      END
      FUNCTION RBAR (RX,RY,RZ,RXY)
C
C.....CALCULATE EFFECTIVE STRAIN RATE.
C
      S1 = RX*RX
      S2 = RY*RY
      S3 = RZ*RZ
      S4 = RXY*RXY
      RBAR = 2.*SQRT(3.*(S1+S2+S3)/2.+(3.*S4/4.))/3.
      RETURN
```